Investigations on sensorial properties of Indian Black teas using Impedance based techniques

A thesis submitted in fulfilment of the requirement for the award of the degree of

DOCTOR OF PHILOSOPHY

IN

BIOTECHNOLOGY

Mopsy Dhiman

(Reg. No. 900900004)

Department of Biotechnology and Environmental Sciences,

Thapar University, Patiala –147004

Punjab (India)

Aug, 2013

DECLARATION

I hereby declare that the work which is being presented in this thesis "**Investigations on sensorial properties of Indian Black teas using Impedance based techniques**" submitted by me for the award of the degree of **Doctor of Philosophy** in the Department of Biotechnology and Environmental Sciences, Thapar University, Patiala, is true and original record of my own independent and original research work carried out under the supervision of **Dr. M. L. Singla**, Ex- Scientist 'G', CSIO, Chandigarh; **Dr. Abhijit Ganguli**, Associate Professor, Department of Biotechnology and Environmental Sciences, Thapar University, Patiala, and **Dr. Pawan Kapur**, Ex-Director, CSIO, Chandigarh. The matter embodied in this thesis has not been submitted in part or full to any other university or institute for the award of any degree in India or abroad.

Mopsy Dhiman

CERTIFICATE

This is to certify that the thesis entitled "Quality analysis of Indian Black tea using Impedometric techniques" submitted by Miss Mopsy Dhiman in the fulfilment of the requirement for the award of the degree of **Doctor of Philosophy** in the Department of Biotechnology and Environmental Sciences, Thapar University, Patiala, is a record of candidate's own work carried out by her under our supervision and guidance. The matter embodied in this thesis has not been submitted in part or full to any other University or Institute for the award of any degree.

Attestation by Supervisors

(Dr M. L. Singla)	**(Dr A. Ganguli)**	**(Dr Pawan Kapur)**
Ex-Scientist 'G'	Associate Professor	Ex-Director
Materials Research Division	DBTES, Thapar University	Distinguished Emeritus Professor
Central Scientific Instruments Division C	Patiala- 147004	CSIO, Sec- 30
Chandigarh- 160030	INDIA	Chandigarh- 160030
INDIA		INDIA

ACKNOWLEDGMENTS

First and foremost I pay my heartfelt thanks to the great almighty whose blessings provided me the vigorous passion, uninterrupted strength and indispensable patience needed to begin my Research work and end it successfully.

"With the Grace of All Mighty seed of thought flourished into sapling

In deed God and Guide work hand in hand".

I would like to take this opportunity to thank many people who have helped and encouraged me throughout this study. It is a pleasant aspect that I have now the opportunity to express my gratitude to all of them. With utmost indebtedness and unbound gratitude I would like to express my deep respect to my mentor **Dr M. L. Singla,** Ex-Scientist 'G', Materials Research Division, Central Scientific Instruments Organisation, Chandigarh, for his able & invaluable guidance & persistent encouragement advice, constructive criticism and incessant encouragement from the very early stage of this research as well as offering me extraordinary experiences throughout the work. I am extremely indebted to him for the scientific attitude he has installed in me which will definitely stand in all future endeavours.

I am also greatly indebted to my supervisors, **Dr. Abhijit Ganguli,** Associate Professor, Thapar University, Patiala and **Dr Pawan Kapur**, Ex- Director, Central Scientific Instruments Organisation, Chandigarh, for their kind guidance and technical advice in every aspect of this thesis. My gratitude to them for their invaluable support and guidance during my research work can never be fully expressed.

I wish to express my sincere gratitude to **Dr. Amod Kumar**, Sceintist 'G', Central Scientific Instruments Organisation, Chandigarh who introduced me to this fascinating world of research and for invaluable guidance.

I am thankful to my PhD committee members and **Dr. Susheel Mittal**, Senior Professor, School of Chemistry and Biochemistry, Thapar University, Patiala, for their constructive comments and regularly ensuring the progress of my research work.

I wish to express my thanks to **Prof. K. K. Raina,** Director, Thapar University, for providing facilities for accomplishment of this Research work. I gratefully acknowledge to **Dr. P. K. Bajpai,** Dean (Research and Sponsored Projects), Thapar University, Patiala, for their encouragement and support during my research work in the University.

I am heartily thankful to **Dr. Dinesh Goyal,** Professor and Head and ex-head **Dr. M. Sudhakara Reddy,** Department of Biotechnology and Environmental Sciences, Thapar University, Patiala, for their valuable suggestions during my Research work and also for providing me the necessary facilities for the completion of this Research work. I am thankful to the office and laboratory staff of Department of Biotechnology and Environmental for all the cooperation.

I am also thankful **Dr. Moushumi Ghosh,** Associate Professor, Department of Biotechnology and Environmental Sciences and all the faculty members of School of Biotechnology and Environmental Sciences for their support.

I am profoundly thankful to **Dr. Ashu Gulati,** Senior Scientist at IHBT, Palampur and **Dr Rajesh Khanna,** Head and Associate Professor, Electronics and Communications Department, Thapar University, for providing facilities for accomplishment of this Research work.

I am especially indebted to **Dr. H. P. Kayath, Dr. Amitava Das, Dr. Gursharan Singh** and **Dr. Ashish Dhir** for their help, constant encouragement, love and support. I feel lacuna of words to express my gratefulness and indebtedness to all my friends especially for their help, support and understanding. I express my regards and gratitude to labmates and friends **Dr. Richu, Seema, Ms. Gurpreet Khaira, Ms. Taranpreet, Ms. Gaatha Sharma, Dr Sajeela Awasthi, Ms. Prerna Bhardwaj, Ms. Anupma Sharma, Mr. Manish Jharwal, Ms. Suman Singh, Mr. Mrinmoy Misra, Ms. Pooja Sharma, Mr. Hari, Mr. Anil, Ms. Pandey, Mr. Amol Bhondekar, Ms. Shweta Arora, Mr. Rajender Shounda, Mr. Satish Kumar, Mr. Robin Joshi, Mr. Sohan, Mr. R. D. Deol** and all other research scholars, for the stimulating discussions, for providing keen interest, unfailing support, inspiration, critical observations and ingenuous suggestions, for always being supportive and caring for me. I am especially indebted to for their help, constant encouragement, love and support. Life at Thapar University, Patiala and CSIO, Chandigarh has been enjoyable with friends and I thank them all for their great company.

I would like to individually thank my best pals **Avinash Kundal, Arun Jarower, Manish Nischal, Dr Sanjeev Kumar and Rohit Yadav** who have been an indispensable part of my life's journey, providing unmatched support and motivation.

I owe my deepest gratitude and benevolence to my family. I dedicate this thesis to my loving parents **Sh. C.S.Dhiman** and **Smt. Nirmal Dhiman**, to whom I owe my life and if it wasn't for their constant support, unconditional love and encouragement, I would not have been what I am today. My loving brothers **Saurabh Dhiman** and **Gaurav Dhiman** deserve special mention for their inseparable support and prayers. I must mention that it would have been an uphill task for

me to accomplish what little work I have done, I indebt emotional, psychological, and intellectual support, endless unconditional love, consistent motivation, and care from my family members. The heavenly grace of almighty have defined and given meaning to my existence. But also it is the support of my parents, without which I would not have been able to complete this research work.

Last but not the least, I shall remain thankfully indebtness to all those learned souls known and unknown hands that directly or indirectly motivated me to achieve my goals and enlightened me with the touch of their knowledge and constant encouragement Finally, I would like to thank unsaid who was important to the successful realization of thesis, as well as expressing my apology that I could not mention personally one by one.

Date: 19.02.2014

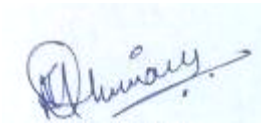

(Mopsy Dhiman)

LIST OF PUBLICATIONS

1. M. Dhiman, P. Kapur, A. Ganguli, and M. L. Singla, "Behavior of Metal and Emeraldine Salt for Detection of Threshold Level of Sucrose and Citric Acid in Impedance Mode", **Sensors Letters**, 10, pp.1-7 (2012).

2. M. Dhiman, P. Kapur, A. Ganguli, and M. L. Singla, "Impedance Study of Tea with Added Taste Compounds Using Conducting Polymer and Metal Electrodes", **Journal of Nanoscience and Nanotechnology,** 12 pp. 1-6 (2012).

3. M. Dhiman, R. Joshi, A. Gulati, P. Kapur, A. Ganguli, and M. L. Singla, "Interpretation of Indian Orthodox Tea Using Multi-Sensing Impedometric Technique", **Journal of Nanoscience and Nanotechnology**, 13 pp. 1-6 (2013).

4. A. P. Bhondekar, M. Dhiman, A. Sharma , A. Bhakta , A. Ganguli , S. S. Bari, R. Vig, P. Kapur, and M. L. Singla, A Novel iTongue For Indian Black Tea Discrimination", **Sensors & Actuators: B. Chemical,** 148 pp. 601-609 (2010)**.**

PARTICIPATION IN CONFERENCES

1. Mopsy Dhiman, Abhijit Ganguli, Amol Bhondekar, Pawan Kapur, M. L. Singla, Multisensor AC Impedance Spectroscopy Based Classification of Indian Black Tea, APA-09, IIT Delhi, India (Dec 17-20, 2009).

2. Mopsy Dhiman, Abhijit Ganguli, Pawan Kapur, M. L. Singla, A.C. impedance classification of Indian black tea using conducting polymer electrode Poster presentation in International Conference PSE-10 held at PU, Chandigarh, India, on (Nov 26-27, 2010).

3. Mopsy Dhiman, Pawan Kapur, Abhijit Ganguli, M. L. Singla, Analysis of basic tastants using impedance tongue, NSI-37, Central Scientific Instruments Organization Chandigarh (Oct 30-Nov 1, 2012).

4. Mopsy Dhiman, M.L.Singla, Pawan Kapur, Abhijit Ganguli, Multi electrode set up for classification of Indian black tea, NSI-37 Advances in Polymer Science and Technology (APST-2010), N. I. T. Hamirpur (H.P) (Oct 22-24, 2010) .

CONTENTS

LIST OF TABLES

LIST OF FIGURES

LIST OF ABBREVIATIONS

AA	Antioxidant activity
AC	Alternating Current
Ag	Silver
Au	Gold
CAF	Caffiene
CAT	Catechin
ccp	Cubic Close Packed
CE	capillary electrophoresis
COD	Chemical oxygen demand
CTC	Cut Tear Curl
CV	Cyclic Voltammetry
DI	De Ionized
DSC	Differential Scanning Calorimetry
EC	Epicatechin
ECG	Epicatechin gallate
EGC	Epigallocatechin
EGCG	Epigallocatechin gallate
fcc	Face-Centred Cubic
FIA	Flow injection analysis
FTIR	Fourier transform infra red
GA	Gallic Acid

GC	Glassy Carbon
HIV	Human immunodeficiency virus
HPLC	High performance liquid chromatography
ITO	Indium Tin Oxide
K1-K12	Kangra tea samples procured from IHBT, Palampur, Himachal Pradesh, India, processed at different intervals of the year.
LAPV	Large amplitude pulsed voltammetry
MAE	Microwave Assisted Extraction
MLAPV	Multifrequency large amplitude pulse voltammetry
OTCM	One time constant model
PANI	Polyaniline
PCA	Principal Component Analysis
PLE	Pressurized Liquid Extraction
PLS	Partial least square
PPY	Polypyrrole
Pt	Platinum
PTS	p-tolune sulphonic acid
PVC	Polyvinylchloride
PVPP	Polyvinylpolypyrrolidone
SAPV	Small amplitude pulsed voltammetry
SCE	Saturated Calomel Electrode
SIA	Sequential injection analysis
SV	Stripping voltammetry
TF	Theaflavins
TGA	Thermo gravimetric analysis

TR	Thearubigins
UPLC	Ultra performance liquid chromatography
UV-VIS	Ultra violet visible
XRD	X-ray Diffraction

LIST OF SYMBOLS

A Area of the electrode
F Faradays constant
Hz Hertz

KHz Kilo Hertz
L Length
M Molar
mm Milli m
nM Nano Molar

R gas constant
S/cm Siemens/Centimeter
T Temperature
V Volume

i_0 Exchange current density
η Overpotential

w/v Weight/Volume

α reaction order
µl Microlitre

µm Micro meter
µM Micro Molar

CHAPTER 1

INTRODUCTION

1. Introduction

Tea is one of the most popular drinks due to its pleasant taste and perceived health effects. Although health benefits have been attributed to tea consumption since the beginning of its history, scientific investigation of this beverage and its constituents has been under way for about 30 years.

1.1 Origin and History of Tea

Tea, the beverage, is the second most widely consumed drink in the world, exceeded only by water. In many cases today, as in ancient times, tea is safer to drink than water because it is boiled first, killing any disease-carrying bacteria.

The discovery of tea in China can be traced back to the ancient time of Holy Farmer, who was thought as the God of Farming and Medicine. It is said that one day he got poisoned 72 times when gathering and tasting herbs on a mountain. Later he found a plant (tea) and brewed the leaves in a pottery tripod and drank the liquid. As a result, the toxins in his body disappeared. Since then, tea was treated as a precious medicine and later a vegetable and was specially used as a magical drink among a group of high-level scholars in the Han Dynasty (206B.C.-A.D.220). However, it was not until the Tang Dynasty (618-907) did the real Chinese tea culture, including tea art, the tea ceremony and a complete expression of cultural philosophy

come into being. In the Tang Dynasty, the tea plant was cultivated in 42 prefectures of China, and the habit of drinking tea had filtered into the daily life of people of all social ranks and classes [1].

Its first use is believed to be about 5,000 years back and has remained popular as the most pleasurable and efficacious beverage in the world for medical properties [2]. The most commonly recognized varieties of *Camellia sinensis* used for tea are *C. sinensis var. sinensis* (China bush or Chinese Tea) and C. *sinensis var. assamica* (Assam bush or Assam Tea) [3]. China and Assam tea differ in quality and morphological features. As far as the Western tea trade is concerned, Assams have been regarded as producing the best fermented tea. Most sources, and Legends, acknowledge the Chinese Emperor Shen Nung (28th century B.C.) with the discovery of tea. The tea plant originated in South-East Asia, believably in the region incorporating sources and high valleys of the Brahmaputra, the Irrawaddy, the Salween and the Mekong rivers at the border separating India, Burma and China. The camellia leaves are familiar to Chinese, which they used as a part of medicinal compounds and in vegetable relishes. But, the leaves had never been considered an ingredient of a hot, refreshing drink until the emperor's discovery.

The cultivation of tea plant in other countries was started at different time historically. Introduction of the first cultivation to various countries was Indonesia in 1684, India in 1780, Russia in 1833, Sri Lanka in 1839, Malawi in 1875, Iran in 1900, Kenya in 1903, and Turkey and Argentina in 1924. Tea became a popular beverage served in numerous tea houses in London in the late 17th century.

1.2 Botany of Tea Plant

Tea grows in to a small tree about 10 m high with a conical shape, when left unpruned. It is pruned to form a hedge of convenient height for hand plucking or machine harvesting in cultivation. In tropical countries much of the tea produced is grown on steep hillsides at high elevations [4].

The tea shrub is a perennial evergreen plant. Tea comes under the Theaceae family and the Camellia species (Camellia sinensis). Indeed, in addition to the previous two types of varieties there are other varieties. Tea varieties differ in the height of the tea bush, characteristics of their leaves and the number of stems. On branches leaves are produced alternatively, which originate in the leaf axils lower in the canopy having a finely serrated margin. All tea leaves are somewhat shiny and they contain thickened stone cells (scleroids) and glabrous, these are important in the tea-trade because their presence in made tea determine its quality. Leaf growth is of central importance because the leaves provide the yield, with the tea crops. Tea flushes at regular frequency which is not strongly related to climatic changes, though the quantity of leaf produced at flush is highly affected by temperature and rainfall as well as by nutrition. The frequency of plucking depends on the growth rates and flushing; it will vary from one to two weeks in tropics, during the period of flushing. For quality of tea, in general, two leaves and a bud are the ones to be plucked [5]. For continued production, it is very important not to pluck the mature leaves below this; these are called maintenance leaves [6].

1.3 Soil and Climate for Tea Growth

Soil and climate characteristics are the most important ecological factors in growing tea. The variety of the tea plant is also another factor in growing tea. The Assam variety is less hardy than the China variety, for instance, which can tolerate a lower temperature or longer dry season. Under a variety of climate conditions it grows from the humid tropical lowlands to regions of high latitudes in Japan and Russia. Tea leaves are harvested all year around in tropical countries. Harvesting is seasonal in temperate countries. There are many different kinds of products of different quality arising from different cultivation practices, growing conditions and processing methods. For the quality of the black tea leaves and the growth of the tea plant application of fertilizer is also important [7].

For instance, an increase in the potassium application rate increases the amino acid content and polyphenol of the tea. The depletion of the organic matter status of the soil results from the failure to apply fertilizer [8].

1.4 Tea harvesting and processing

The processing method for tea varies, according to the kind of tea desired- white, green, oolong, or black. Every tea master, just like every wine master, has a unique way of creating a special product, but in general, the same basic steps are performed to make leaves into tea. For making tea, every step is not required making tea, for example, black tea involves every stage, while white tea involves only a few.

Once the buds and leaves are plucked, they are brought in from the field within two to three hours for the finest quality tea. If the picked leaves are bruised, left unattended for too long, or allowed to get too warm, the cell walls in the leaf break down and oxidation begins, resulting in an unpleasant, bitter flavour. The taste of tea depends very much on the methods of tea processing. Tea is traditionally classified based on the degree or period of "fermentation" the leaves have undergone. The freshly plucked leaves may undergo one or more of the following processes which is called as an orthodox method of tea processing.

Fig.1.1: Tea leaves plucking process

Tea harvesting is a laborious task that requires some training in order to yield the best results. When plucking the leaves for a high quality tea, they pluck the bud and the second and third leaves only. This is called fine plucking (this is known as "Orthodox" method). Another factor in the picking of young leaves is called a "flush." This is when there is a sprouting of new buds and leaves on a plant. These fresh young leaves and buds are then picked. Here is a general guideline of steps taken in processing tea leaves: Once the tea leaves are collected in baskets they are taken to the factory to be processed. The processing steps taken will depend

on the type of tea desired. Common processing terms are withering, rolling, fermentation, and drying or firing.

1.5 Tea Processing

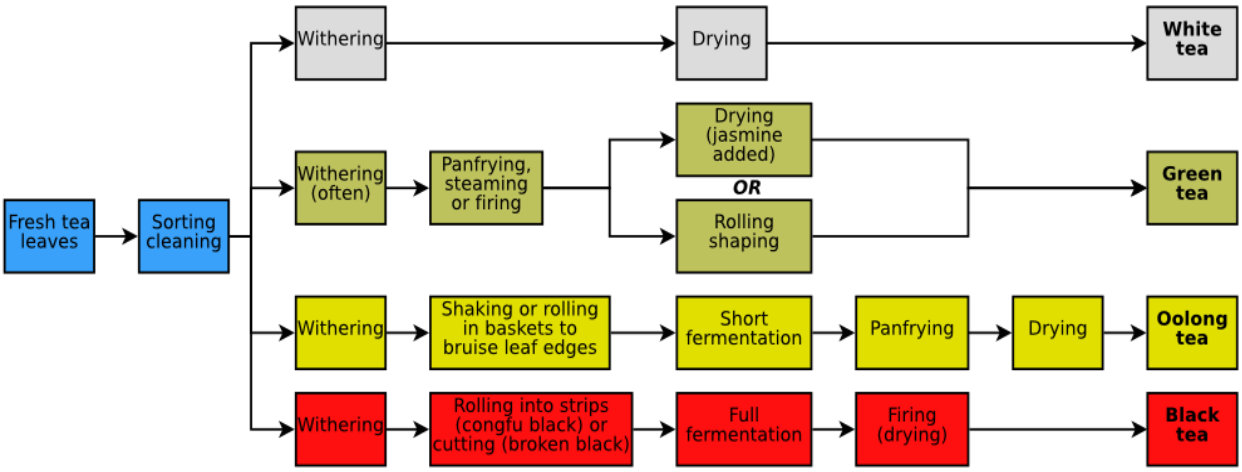

Fig. 1.2: Tea (Camellia sinensis) processing chart

1.5.1 Withering

It is a procedure which brings about physical and chemical changes in the shoots to produce quality, apart from conditioning the flush for rolling by reducing turgor, weight and volume. Previously the flush used to be withered under the sun. Now this process is generally achieved either by thinly spreading the flush on mats, or in thick layers in troughs for 8-18 hours depending on the condition of the leaves.

Fig. 1.3: Process of Withering

1.5.2 **Rolling**

From the withering racks, the leaves are now twisted and rolled so that the leaf cells are broken up. Sometimes shaking is done as well. Oils are released with this rolling process that gives the tea its distinctive aroma. The leaves can be rolled with machinery or by hand. The juices that are released remain on the leaf; a chemical change will occur shortly.

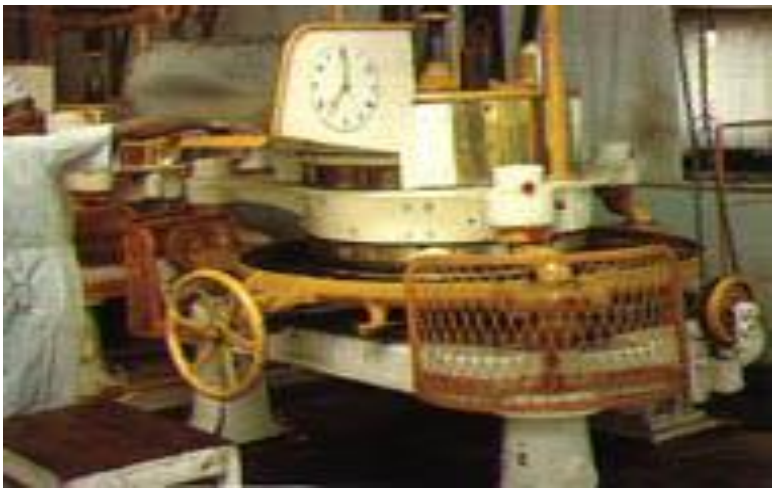

Fig. 1.4: Process of Rolling

1.5.3 Fermentation

It is the process of oxidation of leaves. The mechanical aspect involves spreading out of the leaves macerated by rolling a layer 5-8 cm thick, for 45 minutes to 3 hours, depending on the quality of the leaves. Fermenting machines make the process continuous, that is, every unit of macerated leaf has to be spread out for individual treatment.

Fig. 1.5: Process of Tea fermentation

1.5.4 Firing

The leaves are dried and the fermentation process is retarded. In this stage, the leaves move through hot air chambers to stabilize the leaves and lock in the flavour.

Fig. 1.6: Process of firing of tea leaves

1.5.5 Grading

The tea will be packed after sorting, consisting of extracting the fibres with the aid of winnowing machines and grading the tea by volumetric weight and size. This is the final stage before longer leaves, such as orange pekoes, are used for loose tea. The left-over fannings and dust leaves are used for tea bags

Fig. 1.7: Process of grading

1.6: Types of Tea

Several major categories of tea are there which are distinguished by different processing methods and, consequently, different concentrations of the chemical components in tea. Prior to further heating and processing depending on the degree of fermentation tea are categorized in to three major varieties: Green tea, Oolong tea and Black tea. An enzymatic oxidation of polyphenols is involved in the fermentation process, leading to the formation of chemical compounds which generates the colour and aroma of black tea.

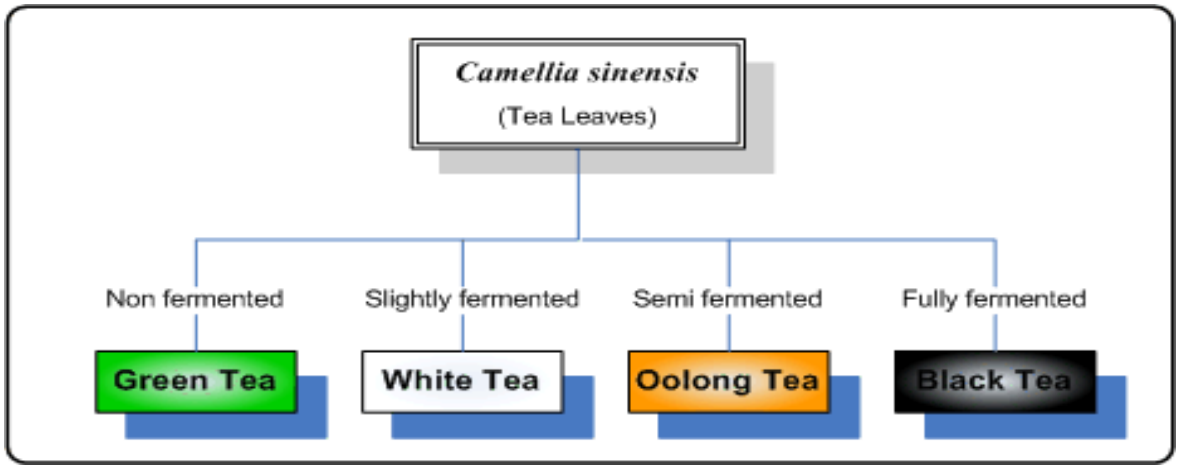

Fig. 1.8: Types of tea

1.6.1 Black tea

The Black tea process goes through the most stages. Once the leaves are picked, they are left to wither for several hours. After the leaves are rolled, oils from the leaves are brought to the surface. These aromatic oils aid in the oxidation process, which last for several hours. The last step consists of placing the leaves in an oven with temperatures reaching up to 200 degrees Fahrenheit. When the leaves are 80 percent dry, the leaves complete their drying over wood fires. The resulting product is brownish (sometimes black) in color and is sorted accordingly to size, the larger grade is considered "leaf grade," and smaller "broken grade" are usually

used for tea bags. As compared to green tea and oolong tea, black tea brings a difference in the colour, aroma and chemical composition of the tea leaf, giving 20% of caffeine in a cup of coffee [9].

1.6.2 Oolong tea

Oolong goes through a similar process that black tea goes through. The first two steps are withering and rolling. Instead of rolling, sometimes shaking is done to bruise the outer edges of the leaves. The oxidation period for oolong is half that of black tea. Once the veins become clear and the edges of the leaves become reddish brown, while the centre remains green, the oxidation process is stopped by firing. For oolong tea, the leaves are heated at a higher temperature so that they can be kept longer, due to the lower resulting water content. The chemical composition of Oolong tea is in between the black tea and the green tea.

1.6.3 Green Tea

The process for making green tea is the shortest. Withering is done first, but this step might be omitted. Rolling the leaves to break the membranes for oxidation is skipped, hence the oxidation process is also skipped. After withering, the leaves are pan fried or fired to prevent oxidation from occurring. The last step is to roll the leaves and dry them one last time for its final shape. The green tea leaves usually remain green.

There are other two types of tea in fact; the white and yellow tea regarded as two subclasses of green tea, due to differences in processing, variety, traditional and geographical distributions**.**

1.6.4 White Tea

White tea is the purest and least processed of all tea. This loose leaf tea has very little caffeine and brews a light brown colour and flavour. White tea also contains healthy antioxidants and is the best for skin and complexion.

1.6.5 Yellow tea

The yellow tea is a specially processed tea similar to green tea but slower with a drying phase, where the damp tea leaves are allowed to sit and yellow. The tea has generally a very yellow-green appearance and a smell different from both white and green tea.

1.6.6 CTC tea

CTC tea, called an unorthodox tea, takes its name from the mechanical "crush, tear, and curl" process used to get cheap, uniform, but inferior tea. Tea derived from this process is generally used for blends or tea bags, and it brews quickly, in two to three minutes. The CTC market is very strong; some estimates that more than 80% of India's tea production is CTC.

1.6.7 The different Grades of tea

Despite more or less intense sifting, bulk obtained after drying are still heterogeneous. Tea ranges in size from that of a speck of dust to a leaf approximately 4 cm long and 1cm wide. The fractions are to be brought to the desired forms and sizes with adequate uniformity and cleanliness conforming to trade requirement. Tea is, therefore, sorted into pieces of roughly equal size and to remove fibre and stalk in the tea. The electrostatically charged rollers are

used to remove stalk and fibre, which attract the stalk and fibre preferentially. Four main sizes of tea are produced, namely, Whole Leaf Grades, Brokens, Fannings and Dusts. Within each of these sections tea is further split up into grades of varying qualities.

1.6.7.1 Whole leaf

Whole Leaf grades are the largest sizes produced and depending on the actual grade within the section may range from a long and wiry stem, 1cm to 2 cm in length, to a round and knobby twisted leaf similar in size and shape to that of a small garden pea.

1.6.7.2 Broken grades

Broken grades consist of smaller than the Whole Leaf grades, are generally about 1cm in length and are largely made up of leaf as opposed to stem.

1.6.7.3 Fannings Grades

Fannings grades are smaller still and sizes of more than 1/8 of an inch are rare. Fannings contain small parts of the leaf, which have broken off either during rolling or sorting.

1.6.7.4 Dust grades

Dust grades are self-explanatory regarding size.

1.7 Economic Importance of Tea

As stated in a Chinese document published in 347 A.D, people in Southwest China used tea for paying tribute to the Chinese emperors as early as 1066 B. C. In the essay "Tong Yue", written by a country landlord Wang Bao and published in 59 B.C., there mentioned the making and sale of tea. It showed that tea was commercially available in the local country market, suggesting that tea processing and marketing as early as 59 B.C. in Southwest China. The second most consumed beverage in the world is tea with an estimated 18-20 billion cups consumed daily. The principal tea produced and consumed in the world are black and green tea, with small amount of other types. Black tea represents approximately 78% of total consumed tea in the world, whereas green tea accounts for approximately 20%. India, China, Sri Lanka, and Kenya, are the major producers of tea while the major consumers are India, China, Turkey, and Japan.

The world production and consumption of tea has increased steadily with occasional fluctuation during the 1990s. With unique horticultural and processing methods Camellia sinensis has become a very important agricultural and commercial product. For instance, the leading export crop is tea in Kenya, which places Kenya to be the third largest producer of black tea after India and Srilanka and large amount of money is earned. Tea is regularly exported from Ethiopia to different countries nowadays

1.8 Health Benefits of Tea

It has been scientifically established that tea offers several health benefits to the consumer. Most of the health benefits of the tea are associated with the antioxidant properties of polyphenols called "flavanoids". While much of the research on flavanoids has been done with Green tea, Black tea too contains about the same amount of flavanoids as Green tea. The major difference between Green tea and Black tea is the fact that Green tea has more simple flavanoids called catechins as compared to Black tea, which contains more complex flavanoids called theaflavins and thearubigins. The black tea components have many health benefits to humans. Animal studies and epidemiological studies suggest that tea is protective against certain cancers, neurodegenerative diseases, and cardiovascular diseases [10].

The oxidization process modifies the type of flavonoid and antioxidant activity is similar in both green tea and black tea. Tea has been also used in folk medicine for headaches, pain, digestion, diuretics, enhancement of immune defence, body aches and detoxification, as an energizer to prolong life [11].

1.9 Antioxidative properties of tea

A free radical is an atom, molecule, or compound that is highly unstable because of its atomic or molecular structure (i.e., the distribution of electrons within the molecule). As a result, free radicals are very reactive as they attempt to pair up with other molecules, atoms, or even individual electrons to create a stable compound. These free radicals, unless removed, can cause immense damage to the DNA and other units of the cell. Under normal circumstances, the body is equipped to eliminate the free radicals by itself mainly through the presence of an enzyme called Super Oxide

Dismutase. However, when exposed to harmful conditions such as excessive UV exposure, exposure to smoke or pollution, the number of free radicals produced increases dramatically, which can be harmful to the body.

1.10 The Chemical Composition of Tea

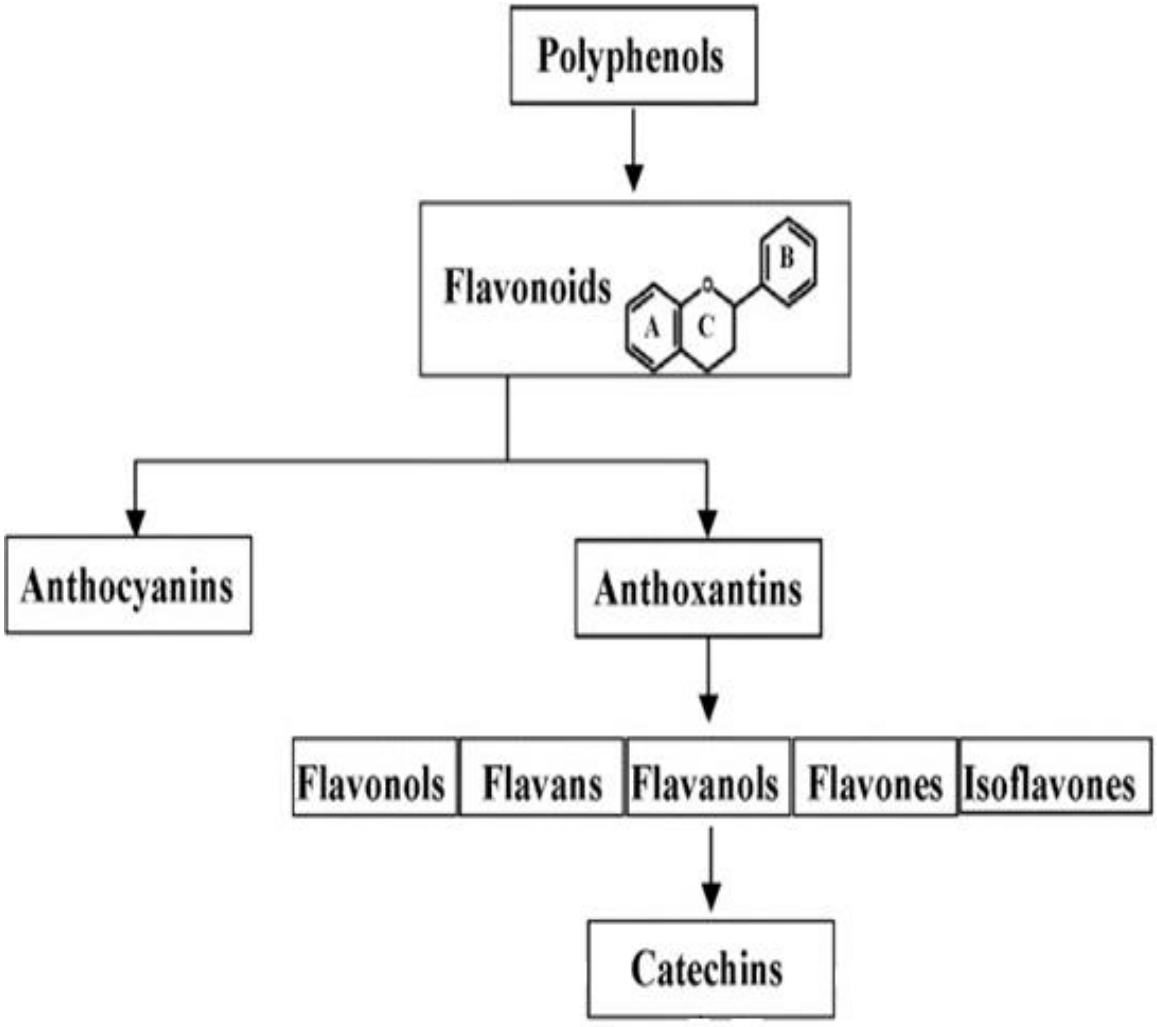

Fig. 1.9: Chemical compounds of tea

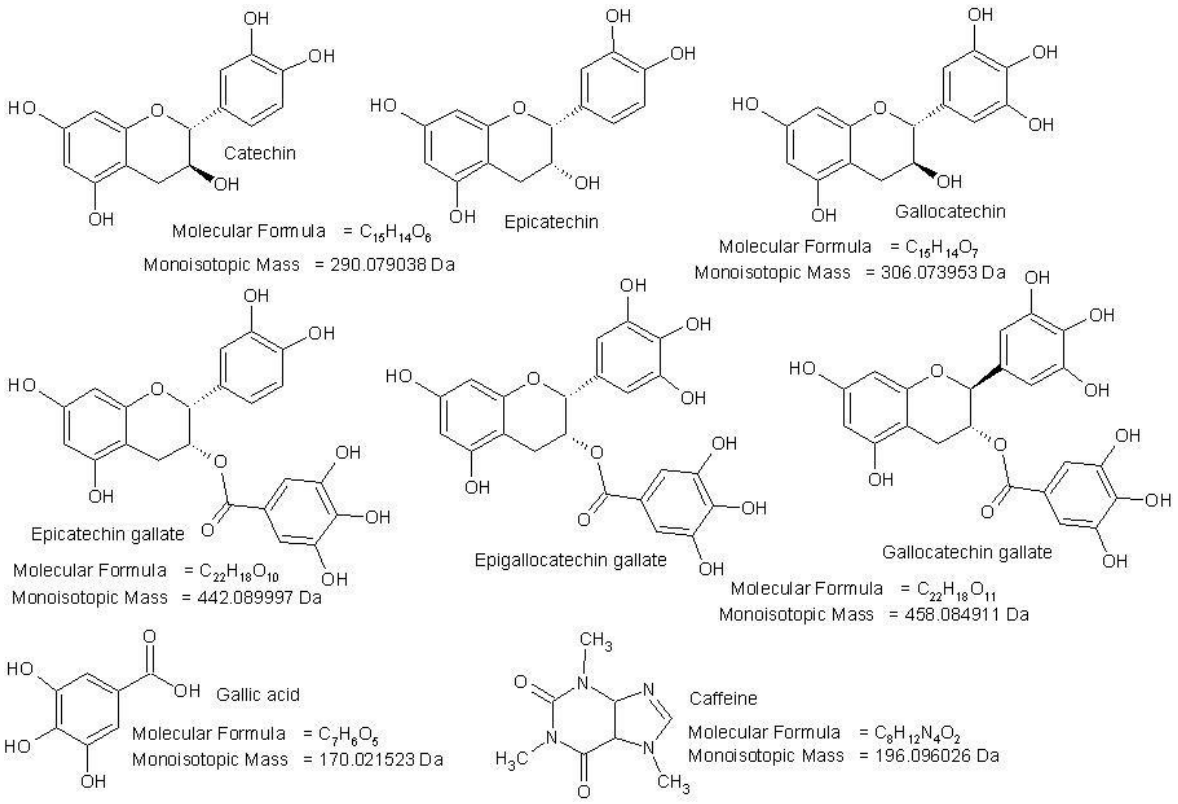

Fig. 1.10: Structures of some biologically active compounds in tea

Depending on different parameters such as the variety of leaf, growing environment, application of fertilizers, manufacturing, particle size of ground tea leaves and infusion preparation the chemical composition of tea may vary. The tea leaves consists of many compounds, such as polysaccharides, volatile oils, vitamins, minerals, purines, alkaloids (eg. caffeine) and polyphenols (catechins and flavonoids). Whereas, all three types of tea have free radical capturing (antioxidising) and antibacterial activities and when the tea becomes darker the efficacy decreases substantially which results due to lower contents of anti-oxidising polyphenols remaining in the leaves.

1.10.1 Flavonoids (polyphenols)

Proven medicinal properties include anti-inflammatory, anti-allergic, antibacterial, antioxidant and antiviral effects and also have the ability to strengthen veins and decrease their permeability. It is widely believed that the antioxidising effects of both black and green varieties are reduced when taken with milk, which is thought to be due to the effective binding of flavonoids by proteins [12].

According to a recent ex vivo study the flavonols are absorbed from tea and their bioavailability is not affected by milk [13].

1.10.2 Tea tannins - called catechins (polyphenols)

Seems to be the most potent therapeutic plant-derived chemicals, aside from their antioxidant and antiseptic properties, they are able to form complexes with other molecules, hence detoxifying the system. Catechins include gallocatechin, epicatechin (EC), epigallocatechin (EGC), epicatechin gallate (EGC) and epigallocatechin gallate (EGCG). Catechins make up approximately one-quarter of fresh dried green tea leaves, among which 60% is comprised of EGCG.

1.10.3 Vitamin C

Du Toit et al., in their recent studies stated that the Black, Green and Oolong tea are all extremely good sources of vitamin C [14].

They stated that one or two cups a day provide the equivalent of three glasses of orange juice or two capsules.

The chemical entities in tea that are generally believed to cause variations in colour and bitterness are mainly the theaflavins (3-6%) and thearubigins (12-18%) of tea solids by weight, respectively. The quantities of each theaflavins and thearubigins, and the ratio of their quantities, both are said to determine the colour characteristics of the tea beverage (tea infusion). For example, a tea with a low level of thearubigins and a high level of theaflavins would tend to give a beverage with a high degree of briskness and a yellow-orange colour. Whereas, a tea with low level of theaflavins and high level of thearubigins would be expected to give a tea infusion with a brown colour and little briskness (a soft tea). An optimum level of each of these chemical groups in a tea may give a tea infusion with a rosy color and appropriate briskness. [15].

Compound	**Description**	**Reaction**	**Health effects**	**Mostly found tea type**
Polyphenol	**Antioxidant**	**Taste**	**Antiviral and antibacterial properties, anti-cholesterolemic**	**Green**
Vitamins	**A (carotene) B (B1,B2, B6,Niacin and Folic acid)**	**Colour**		**Black**

Theaflavin, thearubigins	**Antioxidant**	**Colour and taste**	**Have effects against infection, strengthen human circulatory system, Capillary walls, stroke prevention**	**Black**
Minerals	**Zinc, magnesium, potassium and calcium**	**Colour and taste**	**Boosts immune system, helps prevent cancer and blindness in old age and fights cold, Zinc also helps maintain our senses smell, taste and vision. Important in fighting osteoporosis, high blood pressure, high cholesterol and arthiritis.**	
Tea fibre				
Amino acids		**Taste**	**Tranquilizing effect on the brain for anti-stress.**	**Black**
Carbohydrates				
Caffiene		**Taste**	**Mental clarity and awakeness, excessive amounts are harmful.**	**Black**
Lipid				

Table 1.1: Chemical composition of tea in tabulate form

1.10.4 Theaflavin and thearubigins

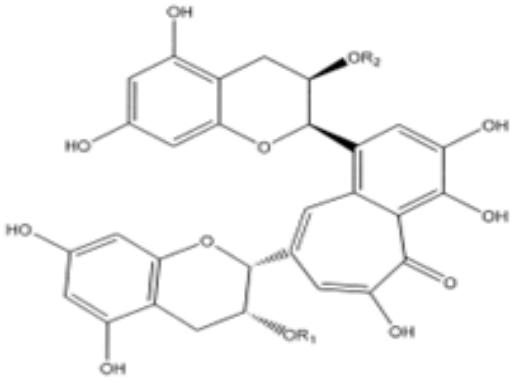

		R1	R2
Theaflavin	TF	H	H
Theaflavin 3-gallate	TF3G	Gallate	H
Theaflavin3'-gallate	TF3'G	H	Gallate
Theaflavin3,3 'gallate	TFDG	Gallate	Gallate

Fig. 1.11: Structure of theaflavins

During fermentation, the characteristic black tea polyphenols, theaflavins and thearubigins, are generated. Four major theaflavins have been identified from black tea, including theaflavin, theaflavin-3-gallate, theaflavin-3'-gallate, and theaflavin-3,3-digallate (Fig.1.11) [16] .Thearubigin is known as a heterogeneous mixture of pigment.

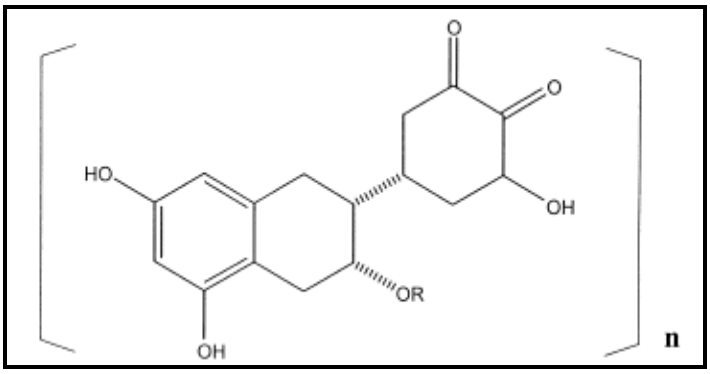

Fig. 1.12: Structure of thearubigins

Thearubigins are polymeric polyphenols that are formed during the enzymatic oxidation (called fermentation by the tea trade) of tea leaves. Thearubigins are red in colour. Therefore,

black (fully oxidized) tea gives reddish liquor while a green or white tea gives a much clearer one. The colour of black tea, however, is affected by many other factors as well.

1.11 Geographical distribution of tea in India

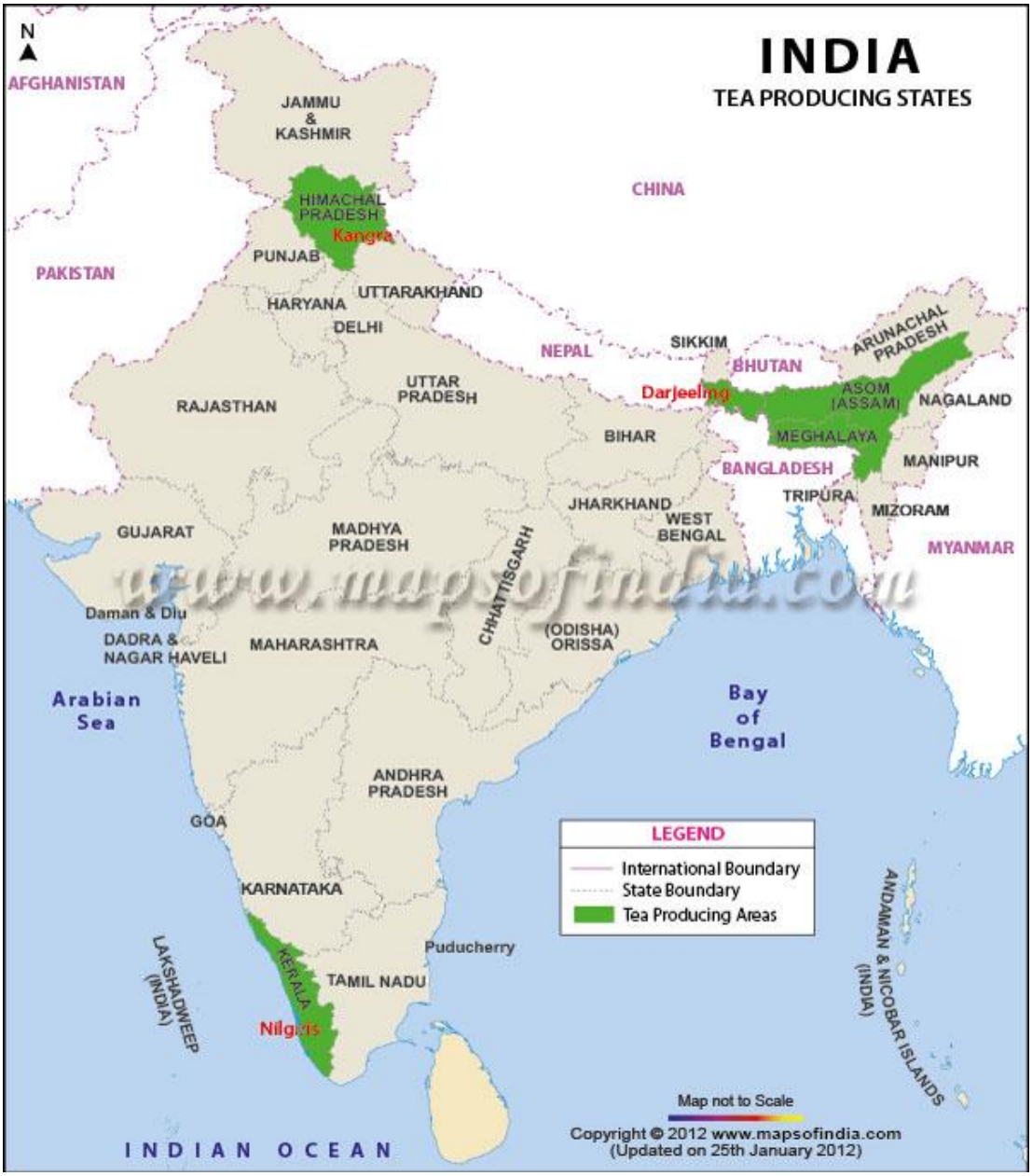

Fig. 1.13: Geographical distribution of tea in India

Indian Tea Industry is about 172 years old. In 1823 Robert Bruce observed tea plants growing wild in upper Brahmaputra Valley.

The first Indian tea from Assam was sent to United Kingdom for Public Sale. Then later it extended to other parts of country between 50's and 60's of the last century.

Tea plantations are mainly located in rural hills and backward areas of Northern Eastern and Southern states. The major tea growing areas in India are concentrated in Assam, West Bengal, Tamilnadu and Kerala. The other areas growing tea to the extent is Karnataka, Tripura, Himachal Pradesh, Uttaranchal, Arunachal Pradesh, Manipur, Sikkim, Nagaland, Meghalaya, Mizoram and Bihar. In India Tea is indigenous and is an area where the country can take a lot of pride. It is mainly due to its pre-eminence as a foreign exchange earner and its contributions to the country's gross national product.

India has emerged as world leader in all aspects of tea production, consumption and export mainly because it accounts for 31% of global production. For last 150 years perhaps the Tea Industry is the only one where India has retained its leadership. The range of tea offered by India - from the original Orthodox to CTC and Green Tea, from the aroma and flavour of Darjeeling Tea to the strong Assam and Nilgiri Tea- remains unparalleled in the world.

1.12 Tea Quality Assessment techniques

Various analytical tools have been reported for estimation of tea quality in terms of colour, tone strength, briskness, astringency and other characteristics attributed to Theaflavins and other factors. In the past few years, tea quality had been assessed using different analytical tools such as, high-performance liquid chromatography [17] , gas chromatography [18], capillary electrophoresis [19], plasma atomic emission spectrometry [20], electronic tongue and lipid membrane taste sensors [21-24].

However, these techniques are complex and have certain limitations and not widely used commercially due to high cost and requirement of skilled personnel and laboratory setup. At present, the assessment of the tea quality is commonly made by sensory evaluation from tea experts, but this is unfortunately susceptible to influence of the environment and subjectivity. To make the evaluation more efficient and objective, several tea experts are usually summoned to assess the tea quality [25]. Thus both for the customers and the tea industry, developing technologies to objectively assess tea quality using a low-cost instrument and discriminate between different tea types is highly desired.

Electronic sensor technology is an application of multi-sensor system which is applied particularly to analyze liquid phase foodstuffs, and had started finding applications in the last decade. Different tasks such as discrimination, classification, quality control and process monitoring have been successfully performed using electronic sensors. The low cost, easy-to-handle measurement set-up and rapidness are the advantages over the well-established analytical methods such as liquid chromatography and spectroscopy.

The main principle used in electronic sensor devices is the application of the array of non-specific chemical sensors with wide sensitivity toward several components. Therefore, the electronic sensor output contains the overlapped information about the sample due to cross-sensitivity of sensors. Several outputs can be derived from this overlapped information with the help of multivariate data analysis. Electronic sensor coupled with multivariate data analysis has proved to be a powerful analytical tool applied widely in foodstuff and beverage. In recent years, intensive studies have been carried out regarding the sensory activity of the individual components of food and alcoholic beverage odours, and the dependence between the odour and the chemical composition of the volatile fraction of these products. The majority of the accomplishments within this area can be attributed to the combination of gas chromatography with olfactometric detection [26].

Testing and developing food uses the results from sensory experiments in which products are systematically presented to people, trained panellists, or random consumers, who score them in various ways. The understanding of the aroma profile will help technologists to enhance the sensory quality of this beverage [27].

The taste sensors introduced by Toko [28] are composed of eight lipid/polymer membranes, and are claimed to be applicable for the qualitative discrimination of mineral waters, beverages (beers and shake), and foodstuffs (tomatoes, sake mash, soybean paste, etc.). These taste sensors have been demonstrated to be useful for the quantitative taste representation. Since 2000, electronic sensors has been attempted to classify different tea categories. The

influence of different applied waveforms on discrimination ability between green and black tea by means of pulse voltametric electronic sensor has also been investigated [29].

An application of disposable all-solid-state potentiometric electronic sensor micro-system for the discrimination of Korean green tea was reported [30- 31]. State of the art in the field of Electronic and Bioelectronic Tongues – Towards the Analysis of Wines was reported by Zeravik et al. [32]

The above mentioned studies show that the electronic sensor technique can be employed for tea classification, but no discussion has been undertaken in these studies regarding the classification results obtained by different pattern recognition methods and even an independent sample set was not used in these studies to test the robustness of the identification models. Moreover, a very few studies on the application of electronic sensor technology for the identification of the tea grade level have been reported till date in literature.

In view of the above, this work proposes to employ the electronic sensor based on AC impedance technique for identifying different grades of black tea coupled with pattern recognition through actual sensorial analysis of tea as well as other preformulated and commercially available beverages.

1.13 AC Impedance technique

Electrochemical impedance (also known as AC impedance or the electrochemical impedance) is an electrochemical technique that has gained wide acceptance for quality control, product development and sensory evaluation food technology applications, food quality assurance, corrosion research etc.

AC impedance applications have become a very useful tool in the field of metal packaging with the base materials steel and aluminium, aiming to enhance the corrosion stability and to minimize metal migration into food.

There are few reports available detailing the impact of artificial processes such as commonly-used food processing techniques on the electrical impedance characteristics of fruits and vegetables. The use of AC impedance analysis would provide a new approach to the evaluation of the freshness or quality of processed agricultural products [33]. Main applications are foreseen as the replacement of long-term storage tests to establish the compatibility of food and package material and to work out the specific influence of individual food components [34]. The technique itself is conceptually rather simple [35].

Low amplitude alternating potential (or current) wave is imposed on top of a DC potential (often the corrosion potential with zero imposed current). The frequency is varied from as high as 10^5 Hertz to as low as about 10^{-3} Hertz in one experiment in a set number (often between 5 and 10) steps per decade of frequency [36]. Varying frequency from low to high frequency is also possible. Dividing the input voltage by the output current furnishes the

impedance. The variation in impedance values which are also related with the working surface (electrode) is used for the interpretation [37].

For this purpose, metal electrodes, Glassy Carbon electrode standard configuration has been used while two electrodes of conducting polymers have been in house fabricated. The brief introduction of conducting polymers is given below.

1.14 Conducting polymers

Electronically conducting polymers possess a variety of properties related to their electrochemical behaviour and are therefore active materials whose properties can be altered as a function of their electrochemical potential. The importance and potential impact of this new class of material was recognized by the world scientific community when Hideki Shirakawa, Alan J. Heeger and Alan G. MacDiarmid were awarded the Nobel Prize in Chemistry in 2000 for their research in this field [38-39].

Although these materials are known as new materials in terms of their properties, the first work describing the synthesis of a conducting polymer was published in the nineteenth century. At that time 'aniline black' was obtained as the product of oxidation of aniline, however, its electronic properties were not established [40].

The conducting polymers may be divided into three categories:

1. Redox polymer.

2. Ion conducting polymer.

3. Inherently conducting polymers.

Ionically conducting polymers (polymer/salt electrolytes) are of great interest because they exhibit ionic conductivity in a flexible but solid membrane. Ionic conductivity is different than the electronic conductivity of metals and conjugated conducting polymers, since current is carried through the movements of ions. They have been critical to the development of devices such as all-solid-state lithium batteries.

In 'conjugated conducting polymers', the redox sites are delocalized over a conjugated π system, however, 'redox polymers' have localized redox sites. The redox polymers are well known to transport electrons by hopping or self-exchange between donor and acceptor sites. The redox conductivity is comparatively lower than that of conjugated conducting polymers, likely due to slow electron transport to from the redox centre [41].

An organic polymer that possesses the electrical and optical properties of a metal while retaining its mechanical properties and processability, is termed as an 'intrinsically conducting polymer' (ICP). These properties are intrinsic to the 'doped' form of the polymer. The conductivity of ICPs lies above that of insulators and extends well into the region of common metals; therefore, they are often referred to as 'synthetic metals'. The common feature of most ICPs is the presence of alternating single and double bonds along the polymer chain, which enable the delocalization or mobility of charge along the polymer backbone. The conductivity is thus assigned to the delocalization of π-bonded electrons over the polymeric backbone, exhibiting unusual electronic properties, such as low energy optical transitions, low ionization potentials and high electron affinities of the many interesting conducting polymers that have been developed over the past 30 years, such as polyaniline/ polypyrrole/ polythiophenes/polyphenylene and poly (*p)* phenylene vinylene have attracted the most attention. In order to make conjugated polymers electronically conductive, it is necessary to

introduce mobile carriers into the conjugated system; this is achieved by oxidation or reduction reactions and the insertion of counter ions (called 'doping').

During the doping process, an organic polymer, either an insulator or semiconductor having small conductivity, typically in the range of 10^{-10} to 10^{-5} S/cm, is converted to a polymer which is in a 'metallic' conducting regime (1 -10^4 S/cm).

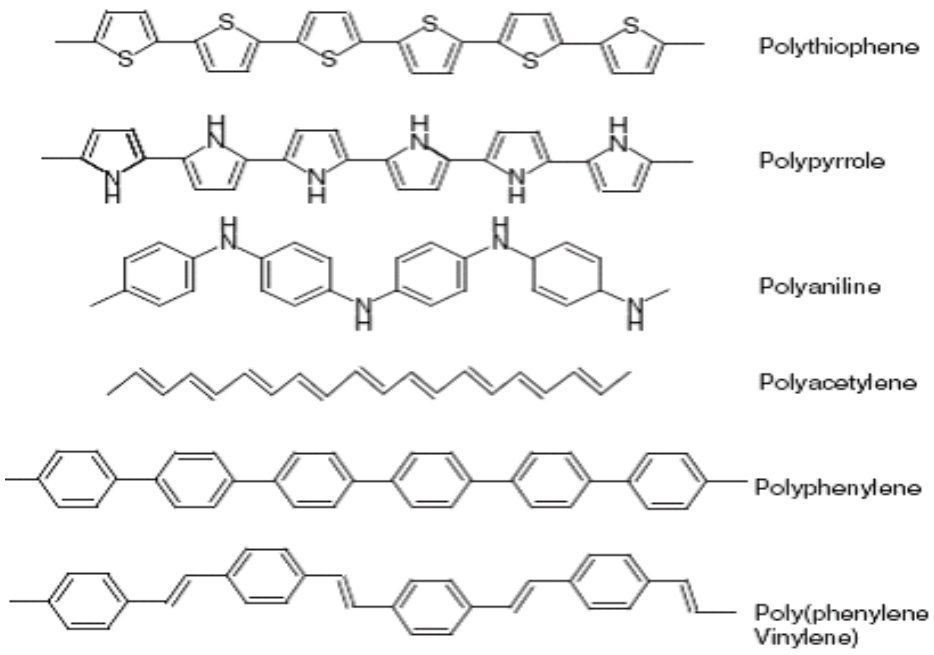

Fig.1.14: Structure of conjugated polymers

The highest value reported to date has been obtained in iodine-doped polyacetylene (>10^5 S/cm) and the predicted theoretical limit is about 2×10^7, more than an order of magnitude higher than that of copper. Conductivity of other conjugated polymers reaches up to 10^3 S/cm [42].

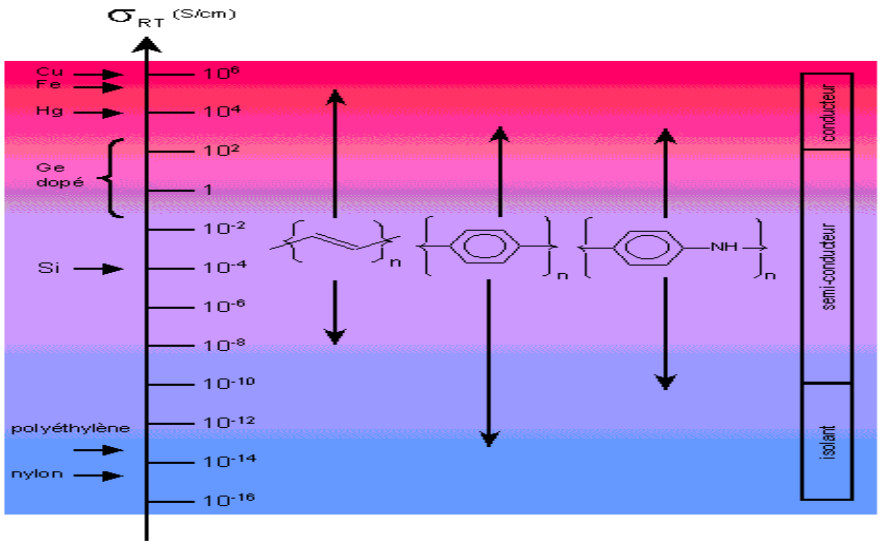

Figure 1.15: Conductivity range of different materials

Conducting polymers are unusual in that they do not conduct electrons *via* the same mechanisms used to describe classical semiconductors and hence their electronic properties cannot be explained well by standard band theory. The electronic conductivity of conducting polymers results from mobile charge carriers introduced into the conjugated π-system through doping. To explain the electronic phenomena in these organic conducting polymers, new concepts including solitons, polarons and bipolarons have been proposed by solid-state physicists. The electronic structures of π-conjugated polymers with degenerate and nondegenerate ground states are different. In π-conjugated polymers with degenerate ground states, applications are important and dominant charge storage species. Polyacetylene, (CH)*x*, is the only known polymer with a degenerate ground state due to its access to two possible configurations as shown in Figure 1.16. The two structures differ from each other by the exchange of the carbon–carbon single and double bonds. While polyacetylene can exist in two

isomeric forms: cis and trans, the trans-acetylene is thermodynamically more stable [43].

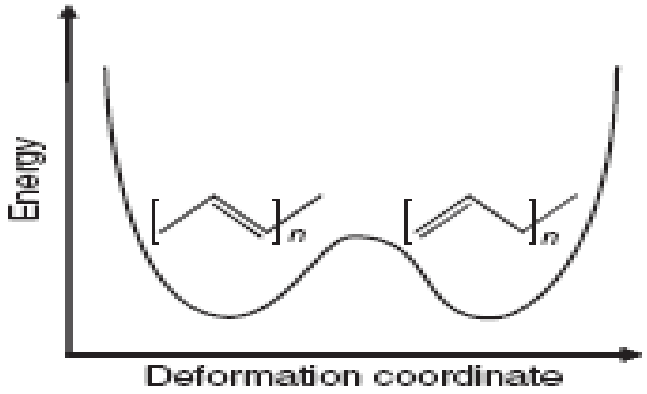

Fig.1.16: Energetically equivalent forms of degenerate polyacetylene

Oxidative (p-type) doping of polyacetylene involves the chemical or anodic oxidation of the polymer to produce carbonium cations and radicals with simultaneous insertion of an appropriate number of anions between the polymer chains that neutralize the charge as shown in Fig.1.17 [44]. Two radicals can then recombine to give a spinless dication referred to as a positive soliton, which can act as the charge carrier [45].

Each soliton constitutes a boundary which separates domains that differ in the phase of their π-bonds. In solid-state physics a charge associated with a boundary or domain wall is called a soliton, because it has the properties of a solitary wave that can move without deformation and dissipation [46].

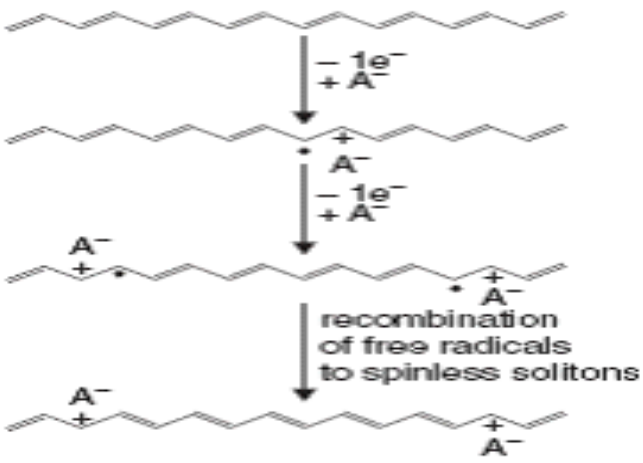

Fig.1.17: p-type doping in polyacetylene

The π-conjugated systems based on aromatic rings, such as polythiophene, polypyrrole, polyaniline, polyparaphenylene and their derivatives have non-degenerate ground states. In these polymers, the ground-state degeneracy is weakly lifted so that polarons and bipolarons (confined soliton pairs) are the important and dominant charge storage configurations.

1.15 Data Analysis using chemometric technique Principal Component Analysis

Classification of tea from electronic sensor data is complex primarily due to the fact the data set obtained is small compared to other applications of classification. As a first step, exploratory data analysis has been performed using principal component analysis (PCA) to identify underlying clusters in the electronic sensor signatures. PCA is a statistical technique for the reduction of input data dimension and is largely used for feature extraction. It captures the relevant information in a set of input data providing a lower dimension, but informative representation of the original data. It sequentially creates a set of principal components from the original data. The first principal component (PC1) maps the maximum variance and

information of the input data followed by the other principal components (PC2, PC3 and so on) in descending order of the variance. Generally a good discrimination is mapped by the first two principal components i.e. PC1 and PC2 [47-49].

1.16 Gap in Current Studies

Various methods based on techniques like potentiometry, voltametry and conductivity has been generally employed for the quantification of the some of the parameters of ready tea for quality classification. However each method has some limitation in terms of either lower in sensitivity or tedious procedures for sample preparation/handling and use of number of costly instrumentation/data interpretation. Therefore further research in this field is required in terms of development of new and more efficient sensors and techniques. A method involving AC Impedance technique based on a multi sensor response (non specific) has been proposed for the classification of different types of Indian black tea. The AC Impedance method is used to record the impedance plots or the part of it (possibly at only one or more frequencies) for qualitative and quantitative analysis. The samples which are measured are often complex matrices, and certainly non-ideal, so that the filming of simple equivalent circuits to the experimental data is not easy or obvious. The data has been obtained in the form of Nyquist and Bode plots to get various parameters like real impedance, virtual impedance, resistance and others. The bulk data has been analyzed using chemometric methods in which PCA has deployed as main tool in our studies. The pattern generated will be able to classify the tea liquor and behaviour how these tastants behave which has been computed with the known data available with tea tastes or from the existing literature.

1.17 Objectives of the present study

To study the response of 6 different sensing/working electrodes for various tea liquors/DI water in impedance mode & to generate a specific pattern.

1. Develop conducting polymer sensors of Polyaniline and Polypyrrole adding different dopants and their characterization.
2. To make an array of sensors of Metal Electrode, Glassy Carbon and Conducting Polymer.
3. To conduct AC Impedance Studies using this array of Sensors.
4. To find significant sensorial parameter using PCA.
5. Validation of Impedance based output with conventional Sensorial Analysis.

CHAPTER 2

LITERATURE REVIEW

2.1 Monitoring of food/beverage quality in research

Black teas mostly come from plantations in Africa, India, Sri Lanka and Indonesia. Black tea represents approximately 72% of total consumed tea in the world and consumed primarily in Western countries and in some Asian countries**.** Black and green teas both contain similar amount of flavonoids, they differ in their chemical structure. Green teas contain more of the simple flavonoids called catechins, while the oxidisation that the leaves undergo to make black tea converts these simple flavonoids to the more complex varieties called theaflavins and thearubigins; the principle component profile is depicted in Table 2.1.

Table 2.1 – Principle components of black tea

Tea Biochemicals	**Black Tea** (% weight of extract solids)
Catechins	3-10
Theaflavins	3-6
Thearubigens	12-18
Flavonols	6-8
Phenolic acids and depsides	10-12
Amino acids	13-15
Methylxanthines	8-11
Carbohydrates	15
Protein	1

Moisture containing minerals	10
Volatiles	<0.1

Black tea leaves are oxidized the longest during processing, while oolong tea leaves are partially oxidized and green tea leaves are minimally oxidized. Enzyme initiated oxidation and hydrolysis reactions during processing convert some GTCs and gallic acid to by-products including theaf1avins, theaflavic acids, theaflavin gallates, bis f1avanols and thearubigins. These chemical by-products created during processing account for red, orange and brown pigments in black and oolong teas, and also contribute to the color, f1avor and aroma nutritional composition of the infusions has been documented by Francis, Caballero et al., and Graham [50-52].

The two leaves and bud are processed to give tea beverage. The main constituents, catechins constitute up to 30% on a dry weight basis. The main compounds present in the tea leaves are (-)-epigallocatechin (EGC), (-)-epigallocatechin -3-gallate (EGCG), (-)-epicatechin(EC), (-)-epicatechin gallate (ECG), (+)-gallocatechin gallate(GCG), (+)-gallocatechin(GC), and (+)-catechin(C)[1.]Green tea catechins are structurally primarily flavanols [53].

A major alkaloid caffeine 1, 3, 7-trimethylxanthine an ingredient in ***Camellia sinesis,*** **thea sinesis,** ***coffee arabica***, to which their CNS stimulation is attributed. The pharmacological effect of caffeine can be noticed when it is consumed in the form of herbal extract. Caffeine is one of the common ingredients in many painkillers and antimigraine pharmaceuticals [54]. The other alkaloids include theobromine and theophylline, account for 4% of its dry weight. There are many phenolic acids such as gallic acids and characteristic amino acids such as threoanine. These natural products shows antioxidant activity [55-57] and exhibit numerous

potentially beneficial medicinal properties including inhibition of carcinogenesis, tumorigensis and mutagenesis as well as the inhibition of tumour growth and metastasis. These bioflavanoids have antibacterial and anti-allergic properties in addition, and have been demonstrated to induce apoptosis in human leukemia cells, inhibit human immunodeficiency virus (HIV) reverse transcriptase and inhibit platelet aggregation.

A broad range of extraction technique (percolation, maceration, digestion, soxhlet extraction, extraction under reflux, steam distillation etc) are currently used for the extraction of polyphenols from tea leaves and caffeine. Different solvents like water, ethanol, ethyl acetate, and methanol are used for extraction. Recently other techniques such as Pressurized Liquid Extraction (PLE), Magnetic Stirring [58], Ultrasound Assisted Extraction and Microwave Assisted Extraction (MAE) have been used [59].

MAE is used for extraction of catechins. Microwave Assisted Extraction is used for thermolabile constituents and it has high and fast extraction ability with less solvent consumption which is based on the basic principle of microwave energy for extraction [60]. Microwave assisted extraction of tea caffeine and tea polyphenols from tea leaves has been carried out. The tea poyphenols i.e. catechin and caffeine isolated are analyzed using different UV/ colourimetric/chromatographic [61], techniques [62-65]. Both catechins and caffeine can be simulataneously analysed also [66]. Analysis of catechins, gallic acid, strictinin and purine alkaloids in green tea by using catechol as an internal standard has been studied by Mizukami et al. [67]

Liu et al studied Quantitative analysis of acrylamide in tea by liquid chromatography coupled with electrospray ionization tandem mass spectrometry [68]. Horie et al., reported the

Analysis of tea components by high-performance liquid chromatography and high-performance capillary electrophoresis [69]. Separation of catechins and methylxanthines in tea samples by capillary electrochromatography has been reported by Uvsal et al [70]. Zuo et al., reported the simultaneous determination of catechins, caffeine and gallic acids in green, Oolong, black and pu-erh teas using HPLC with a photodiode array detector [71]. Syu et al., has reported the determination of theanine, GABA, and other amino acids in green, oolong, black, and Pu-erh teas with dabsylation and high-performance liquid chromatography [72].

Determination of catechin isomers in human plasma subsequent to green tea ingestion using chiral capillary electrophoresis with a high-sensitivity cell has been carried out by Deia Abd el-Hady et al. [73] Simple and rapid UV spectrophotometry of caffeine in tea coupled with sample pre-treatment using a cartridge column filled with polyvinylpolypyrrolidone (PVPP) has been reported by Yamauchi et al. [74] Quasi-flow injection analysis for rapid determination of caffeine in tea using the sample pre-treatment method with a cartridge column filled with polyvinylpolypyrrolidone has been carried by Yamauchi et al. [75]

Rapid analysis of methylated xanthines in teas by an improved high-performance liquid chromatographic method using a polyvinylpolypyrroridone pre-column has been carried by Nakakuki et al. [76] Due to its pharmacological importance and application in the food industry Routine quality control methods have recently become very important for determining tea quality. Several studies using capillary electrophoresis have been reported in the literature determining tea catechins and tea alkaloids separately [77-79] and HPLC following either isocratic or gradient elution methods [80, 81].

The HPLC methods developed employ complex mobile phases, and the separation methods either separate the tea catechins or xanthine alkaloids. The utilization of capillary electrophoresis in routine analysis is limited as capillary electrophoresis being highly precise. Khokhar et al., studied the levels of total phenols, catechins and caffeine in commonly consumed teas in United Kingdom [82].

Lin et al., studied the determination of tea polyphenols and caffeine in tea flowers (Camellia sinensis) and their hydroxyl radical scavenging and nitric oxide suppressing effects [83]. Rawat et al., reported Characterization of volatile components of Kangra orthodox black tea by gas chromatography–mass spectrometry [84]. Electronic sensor or taste sensor is a device which has three principal components, sensory array, the equipment of emitting and receiving signals, and pattern recognition. Based on potential, impedance methods, and voltammetry, in the recent years, three types of devices called electronic sensor, or taste sensors, had been developed. Based on potential the gustatory sensors were first presented by Iiyama et al. [85]

It is composed of several kinds of lipids/polyvinylchloride (PVC) membranes for transforming the information of taste quality like sweetness, saltiness, etc., into electrical signals. Vlasov et al., [86] presented another type of potential taste sensors designed by several non-specific sensors based on chalcogenide glasses as transducer. Based on impedance spectroscopy described by Riul and coworkers the second electronic sensors was presented in which the sensors were built by supramolecular thin films of conducting polymers with lipid-like material and were analyzed using impedance technique. Designed by Winquist et al., the third one based on the principle of voltammetery was presented, consisting of several metallic electrodes (platinum, gold, palladium, iridium, rhenium, and rhodium) as

working electrode (Ag/AgCl as reference electrode and stainless steel electrode as counter electrode for standard three cell electrode systems).

2.2 Electronic sensor basic Principle

The agreed definition of an "electronic sensor," as defined by significant research groups working in this area can be summarized as "an analytical instrument comprising an array of non-specific, poorly selective chemical sensors with partial specificity (cross sensitivity) to different compounds in a solution, coupled to an appropriate chemometric tool for data processing,".

The main components of an electronic taste-sensing system are; a number of different sensor types attached to arm, a sample table, an amplifier, and a monitor for data recording. Fig. 2.1 shows a basic principle of electrochemical sensing system. The principle for the electronic sensor is to combine signals from specific, non-specific and overlapping sensors with pattern recognition. The obtained data can be evaluated further on the basis of already existing matrix of sensor responses which can be compared with already existing taste signatures. Potentiometry is the most applied principle. Electrochemical concepts of electronic sensor are dealt here under.

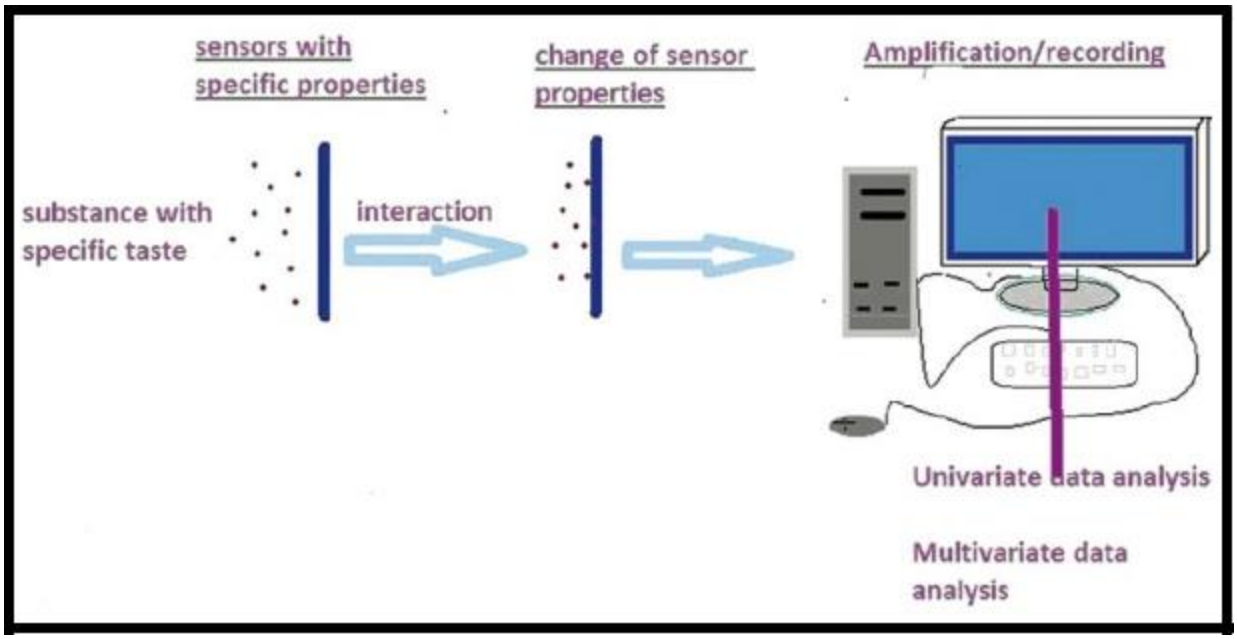

Fig. 2.1: Basic principle of electronic taste sensing system (courtesy: http://www.ncbi.nlm.nih.gov/pmc/articles/PMC3312724/)

2.3 Trends in Electrochemistry

An array of nonspecific or low-selective sensors is used for electronic sensor study in order to produce signals during analysis of samples. In 1943 the idea of reproducing artificially the human response to external stimuli was first published [87]. Based on neural computing, this concept has been extended to build an "electronic brain" and artificial intelligence. "Electronic nose" was the first analytical tool of these concepts (1982) [88] used for analysis of gases. Introduced in 1995 "Electronic sensor," [89] is considered as a promising device in quantitative and qualitative analysis of multi-component matrices.

In literature, electronic sensor is defined as "Taste sensor or electronic sensor is an analytical tool including an array of non-specific, low selective chemical sensors with partial specificity

(cross-sensitivity) to different components in solution accompanied by an appropriate method of pattern recognition and/or multivariate calibration for the data-processing". The development of electronic sensors has increased during the last decade and today a number of sensors called taste sensors/electronic sensors exist. Different research groups have developed them and are focused on specific application areas ranging from taste- and quality analysis to environmental monitoring [90, 91]. The other applications of electronic sensor include analysis of taste and aging processes in beverages. For example, Winquist et al., has worked with fruit juices [92] and milk [93] and Legin et al., worked on mineral water [94].

Ivarsson et al., have utilized tea and wine in his study [95], Legin et al., used their study for quality analysis of mineral water and de Sousa used his studies for red wines and water readings [96]. Also flesh food has been studied by Legin et al. [97]. Most electronic sensors use some electrochemical method, typically voltammetry or potentiometry.

2.4 General applications and developments

Early in 1997 Winquist et al., described the first voltammetric electronic sensor, consisted of a double working electrode (platinum and gold), an auxiliary and a reference electrode onto which both large amplitude pulsed voltammetry (LAPV) and small amplitude pulsed voltammetry (SAPV) were applied. In different trails samples of milk, different juices and phosphate buffer were studied and further PCA study performed on the data showed good separation between the samples [98].

The voltammetric electronic sensor was further developed, after this first set-up. A common configuration consisting of five working electrodes (iridium, palladium, gold, rhodium and platinum), a reference electrode and an auxiliary electrode of stainless steel were used. In a dental material in stainless steel tubing the working electrodes were embedded. The wires from the working electrode were connected via a relay box to a potentiostat and a monitor. Different types of pulsed voltammetry, LAPV, SAPV and staircase have been applied. Söderström et al., used voltammetric electronic sensor to study the milk deterioration due to microbial growth and correlated with colony forming units [99].

Ivarrson et al., reported that various types of teas could be separated [100], as well as different detergents could be separated [101]. For monitoring of drinking water quality the voltammetric electronic sensor has also been used, and a review has been published by Krantz-Rülcker et al. [102]. To discriminate between red wines aged in oak barrels and red wine matured in steel tanks in contact with oak wood chips a voltammetric electronic sensor was used by Apetrei et al. [103]. The wine quality was also determined using conventional analytical methods by Parra et al. In another study, it was possible to detect fraudulent red wines successfully, obtained by adding a range of forbidden adulterants to red wine samples [104].

Studies were performed on the amino acids, tryptophan, cysteine and tyrosine, with applications on direct measurement of these amino acids in animal feed samples [105, 106]. A novel electrochemical method using multifrequency large amplitude pulse voltammetry (MLAPV) for electronic sensor (comprised three individual frequency segments, 1 Hz, 10 Hz

and 100 Hz) [107] . For standard three-electrode systems the electronic sensor was based on several metallic working electrodes, such as platinum, gold, titanium, nickel, palladium, a Ag/AgCl reference electrode and a pillar platinum electrode as counter electrode. At different frequency segments six Chinese spirits and seven Longjing teas were successfully discriminated. Martina et al., demonstrated the usefulness of modified electrodes in a system with two traditional Au and Pt electrodes and the third was modified with poly (3,4-ethylenedioxythiophene) conducting polymer [108].

A Chinese yellow wine classification method was described by Wu et al., based on chemometric analysis of voltammograms from a copper electrode in strong alkaline solution [109], in which six Chinese wine samples could be classified. Also the quality of information will increase if the number of information sources is increased, demonstrated by the hybrid electronic sensor by Winquist at al., [110] based on the combination of the measurement techniques conductivity, potentiometry and voltammetry used for classification of different types of fermented milk. The system with these sensors consisted of ion selective electrodes for pH, carbon dioxide and chloride ion, a voltammetric electronic sensor and a conductivity meter. Multivariate data analysis based on PCA and an artificial neural net was carried out for the data obtained from the measurement.

Using information obtained individually from either the electronic sensor or conductivity meter, or from the ion selective electrode, all but two of the fermented milk samples could be separated, but when merging all sensor data, all six different types of fermented milks could be clearly separated. Also, in the PCA, the composition of the microorganisms of the different fermentations was reflected.

An integrated electronic sensor device was developed by Men et al. [111], with a multiple light-addressable potentiometric sensor (MLAPS) and two groups of electrodes. The chalcogenide thin film based MLAPS were used for simultaneous detection of Fe (III) and Cr (VI) while the electrodes detect other heavy metals using stripping voltammetry (SV). Applications include detection of heavy metal in seawater or wastewater. Based on flow injection analysis (FIA) the voltammetric electronic sensor has also been used in measurement system by Winquist et al. [112].

Hence, a reference solution was continuously pumped through a cell with the electronic sensor, and test samples were injected into the flow stream. For classification of different orange juices the set-up was also used. For characterization and prediction of conductivity, pH and chemical oxygen demand (COD) of waste water coming from the paper mill industries this system has also been used by Gutes et al. [113]. Gutes et al. described a system based on sequential injection analysis (SIA), [114, 115], based on three different enzymatic glucose oxidase electrodes and metallic catalysts electrodes, which was used for simultaneous determination of ascorbic acid and glucose. For the quantification of ascorbic acid, uric acid and paracetamol, a similar sequential injection analysis system based on 3 working electrodes, gold, platinum, and epoxy-graphite disks were used. Based on pulsed voltammetry a miniaturized electronic sensor, has also been developed, consisting of three types of working electrodes namely platinum, gold and rhodium inserted in a platinum tube, behaving as a counter electrode. The dimensions of miniaturized electronic sensor are 2 mm diameter and 4

mm length and initial experiments on this were performed for the determination of trace amount of lead and cadmium in the μM range.

Using either potentiometric or amperometric electrodes, fouling is a general problem. If the sample measured is relatively clean/transparent, such as drinking water, no problem occurs, but for the measurements of more complex media, such as process water from the paper and pulp industry or milk, fouling of the electrode surfaces can be noticed, which in turn causes drift and eventually loss of sensitivity. As a result, electrodes must be cleaned and calibrated regularly, which especially for the process industry is time consuming and expensive. This is one main reason why potentiometric and amperometric electrodes are not so frequently used. Another way to overcome this problem is to wash the electrode within the measurement cycles, an example of this is to use the voltammetric electronic sensor in a dishing and washing machine and the other way is polishing of the electrode surface regularly.

Therefore Olsson et al., designed self polishing voltammetric electronic sensors, either polishing the electrode surface continuously or at regular time intervals and stated drawback was rectified [116].

A self cleaning voltammetric electronic sensor is completely maintenance free, since a new surface is regularly created. Measurements of e.g. heavy metals can be made extremely sensitive when combining the electronic sensor with stripping voltammetry. Thus, the concentration of cadmium could be determined down to a concentration of 1μg/L

(corresponding to 9nM). Also equipped with a self polishing unit this measurement procedure has been automatized in a flow injection analysis configuration. Cadmium concentrations have been determined in soil and flour samples with this system. Rodriguez-Mendez et al., has recently revised the state of the art of the electrochemical sensors [117], with a special attention to two families of compounds, the phthalocyanines and the conducting polymers. Jain et al worked on Growth *and* characterization *of* transparent conducting nanostructured zinc indium oxide thin films [118]. Joshi et al., studied in vitro cytotoxicity, antimicrobial, and metal-chelating activity of triterpene saponins from tea seed grown in Kangra valley, India. [119]. Kohli et al., worked on Impedance of a goat eye lens [120]. Singh et al., worked on electrochemical synthesis of conducting polymers for application in catechin electrochemical biosensor [121]. Kehwar T S., studied analytical approach to estimate normal tissue complication probability using best fit of normal tissue tolerance doses into the NTCP equation of the linear quadratic model [122].

2.5 Applications of Electronic sensor

Electronic sensor is specially designed for taste analysis in R and D, food product Development, food process improvement applications, and formulation. In various industrial areas it has got several applications like food and beverage sector, pharmaceutical industry, etc. **Electronic sensor** can be used for analyzing human urine for the detection of urinary system dysfunction and creatinine levels [123], evaluating wine for taste and flavour [124], by using porphyrin-based potentiometric electronic sensor Detection of alcohols in beverages can be studied [125]. Analyzing flavour ageing in beverages (for instant fruit juice, alcoholic or

non-alcoholic drinks, flavoured milk, in quantifying bitterness or spicy levels of drinks or dissolved compounds, used in quantifying taste-masking efficiency of pharmaceuticals (tablets, syrups, powders, capsules, etc.). Electronic sensor can be used to analyze stability of medicines regarding taste, as benchmark the target products, in differentiating the different kinds of mineral water based on hardness of water [126].

Differentiating varieties of tomato by measuring crushed tomatoes [127], also used in discriminating fresh from spoiled milk [128]. Differentiating different brands of coffee of different origin [129], in monitoring agriculture and industrial pollution of air and water, in identification of toxic substances, quantifying taste and foodstuff recognition, monitoring environment with respect to water, metal ions, endotoxins, pesticides, characterize amino acids like L-isoleucine, L-leucine, and L-phenylalanine [130]. To study sweet taste evaluation with lipid/polymer membrane [131], measure solid food [132], detect trace amounts of organic substances [133], and evaluate taste of crude drugs and Kampo Formula [134]. Bhondekar et al., reported the quality analysis of Indian black tea using itongue [135]. Joshi and Singh worked on principles and objectives of Biotechnology [136].

CHAPTER 3

MATERIAL AND METHODS

This section of thesis deals with the details of the various experiments which have been carried out. Various techniques used to characterize the material are also discussed. Chemicals and equipments which are used during experiment are also described in this chapter.

3.1: Chemicals/ Biochemicals used

All the chemicals/bio chemicals used were of higher analytical grade/purity and purchased from Sigma Aldrich (St. Louis, MO, USA) unless otherwise specified.

During this study the chemicals/materials were used for fabrication of working electrode and Impedometric studies of tea and tastants was carried out. HPLC studies were also carried out as required to identify various compounds. The detailed list of chemicals/materials with their composition has been presented in appendix I.

3.2: Impedance study

3.2.1 Impedance fundamentals

Electrochemical impedance is usually measured by applying an AC potential to an electrochemical cell and then measuring the current through the cell. In quantitative terms, it is the complex ratio of the voltage to the current in an alternating current (AC) circuit. Impedance extends the concept of resistance to AC circuits, and possesses both magnitude

and phase, unlike resistance, which has only magnitude. This study relates to Impedometric measurement on varieties of tea liquor or beverages.

3.2.2 Impedance analysis in electrochemistry

In this study a small potential across a cell or sample is created; this potential is different from equilibrium state value, there is an over potential of η. An additional advantage of impedance over amperometric analysis is that the potential is only perturbing so concentration change in the sample or cell is minimized.

The potential selected in our studies was 5 mV-10 mV. However, the perturbing voltage changes in a cyclic sinusoidal manner, so time averaged over potential is zero. Because the voltage changes in such cyclic manner, we say that the induced current alternates and hence the term AC current. The analogies between electrochemical cell and electrical circuit made of resistors and capacitors assembled in order to mimic the current-voltage behaviour of a cell. The elements which behave resistor/capacitors are bulk solutions, double layer, electrode surface, electrode or any other plane.

According to Ohm's law: Applying a constant voltage V, across a resistance R induces a constant current I. V=IR. In a similar way application of sinusoidally varying potential across electrochemical cell induces AC.

$V=V_o e^{iwt}$ and $I= I_o e^{iwt}$

The impedance Z is defined as the ratio of the complex voltage and current amplitudes:

$$Z = \frac{\hat{V_0}}{\hat{I_0}} = \frac{V_0}{I_0} e^{i\phi}.$$

The complex voltage V and current I, thus obey the linear relation V = IZ, which is a complex generalization of Ohm's law, V = IR. Z has unit of Ohms, just like DC= Resistance.

The complex impedance Z= Z'+Z*

Where Z' is real resistance and Z* is capacitance. The plot between Z' and Z* is called Nyquist plot or impedance plot under selected frequency range. Z' is measured in the frequency range of 10^{-2} to 10^{6} Hz. In impedance analysis equivalent circuit, where in a cell its planes, layers and phases are considered as electrical elements. The arrangement of these components is as follows,

Cdl- The double layer consists of ions juxtaposed with electrode.

Rct- Resistance to charge transfer. The moment of electron is activated that is requiring energy or moment is restricted by the resistance rct. Warburg impedance relates to diffusion.

3.3: Electrochemical Impedance Analysis

Electrochemical Impedance analysis is an ac impedance methods have seen tremendous increase in popularity in recent years. Initially applied to the determination of the double-layer capacitance [137-140] and in ac polarography [141-143] they are now applied to the characterization of electrode processes and complex interfaces. EIS studies the system response to the application of a periodic small amplitude ac signal. These measurements are carried out at different ac frequencies and, thus, the name impedance spectroscopy was later adopted. Analysis of the system response contains information about the interface, its

structure and reactions taking place there. EIS is now described in the general books on electrochemistry, [144-153] specific books [154, 155].

3.3.1: Electrical circuit elements

Most of the circuit elements such as resistors, capacitors and inductors, the element in this model have the basis of the physical electrochemistry of the system. As an example, most of the resistors are the cell solution resistors. Some of the components are tabulated below:

Table 3.1: Circuit elements in electrochemistry

Component	Current Vs. Voltage	Impedance
Resistor	E= IR	Z = R
Inductor	E = L di/dt	Z = jωL
Capacitor	I = C dE/dt	Z = 1/jωC

The impedance of a resistor is independent of frequency and has no imaginary component. With only a real impedance component, the current through a resistor stays in phase with the voltage across the resistor. The impedance of an inductor increases as frequency increases. Inductors have only an imaginary impedance component. As a result, the current through an inductor is phase shifted -90 degrees with respect to the voltage.

The impedance versus frequency behavior of a capacitor is opposite to that of an inductor. A capacitor's impedance decreases as the frequency is raised. Capacitors also have only an imaginary impedance component. The current through a capacitor is phase shifted 90 degrees with respect to the voltage [156, 157].

3.4: Physical Electrochemistry and Equivalent Circuit Elements

3.4.1: Electrolyte Resistance

Solution resistance is often a significant factor in the impedance of an electrochemical cell where the solution resistance between the working and reference electrode is important. The resistance of solution depends on the ionic concentration, type of ions, temperature, and the geometry of the electrode.

$R = \rho l / A$ where ρ is the solution resistivity

A= Area of the electrode

l= length

However, exact resistance of the solution is not possible to calculate hence we calculate using EIS model [158, 159].

3.4.2: Double layer capacitance

An electrical double layer exists on the interface between an electrode and surrounding solution. The double layer is formed as ions/molecules from the solution, stick on the electrode surface. The charged electrode is separated from the charged ions. This separation is of the order of angstroms. Charge is separated by an insulator or a capacitor. The values of the double layer capacitor depends upon electrode potential, temperature, solution strength, types of ion, coating of a layer on an electrode surface, electrode roughness, impurity and adsorption etc.

3.4.3: Polarization resistance

When the plot of an electrode is forced away from its value at an open circuit is referred as potential of the electrode. It causes current to flow the electrochemical reactions that occur at the electrode surface. The open circuit potential is controlled by the equilibrium between 2 electrode potential at cathode and anode.

Mixed potential control occurs when the electrode is not corroding (this is Rp) so the term used is the potential resistance named as Rp. Rct is the charge transfer resistance; in this case, a single reaction equilibrium process is employed.

$$Me \Leftrightarrow Me^{n+} + ne^{-}$$

In the forward reaction, electron enters the metal and a metal ion diffuses into electrolyte, charge is being transferred. This charge transfer reaction has a certain speed. The speed depends on the kind of reaction, the temperature, the concentration of the reactants.

The general relation between the potential and the current (which is directly related with the amount of electrons and so the charge transfer via Faradays law) is:

$$i = i_0 \left[\frac{C_O}{C_O^*} e^{\left(\frac{\alpha n F \eta}{RT}\right)} - \frac{C_R}{C_R^*} e^{\frac{-(1-\alpha) n F \eta}{RT}} \right]$$

With, i_0 = exchange current density

C_O = concentration of oxidant at the electrode surface

C_O^* = concentration of oxidant in the bulk

C_R = concentration of reductant at the electrode surface

η= overpotential (Eapp – Eoc)

F = Faradays constant

T = temperature (K)

R = gas constant

α= reaction order

n = number of electrons involved

When the over potential η, is very small and the electrochemical system is at equilibrium, the expression for the charge transfer resistance is:

$$R_{ct} = \frac{RT}{nFi_0}$$

Where;

η= no. of electrons transferred

i_0= exchange current density

3.4.4: Diffusion

Diffusion also creates impedance called Warburg impedance. The impedance depends on the frequency of the potential perturbation. At high frequency, Warburg impedance is small, since; diffusing reactant does not have to move very far. At low frequencies, the reactant has to diffuse further, increasing Warburg impedance. On Nyquist plot Warburg impedance appears as a diagonal line with a slope of 45 degrees. On Bode plot the Warburg impedance

exhibits a phase shift of 45 degree; the Warburg impedance is only valid if diffusion layer has infinite thickness [160-162].

3. 5: Common Equivalent Circuit Models

3.5.1: Cole-Cole Plots: Impedance Plots in the Complex Plane

When we plot the real and imaginary components of impedance in the complex plane (Argand diagram), we obtain a semicircle or partial semicircle for each parallel RC Voigt network:

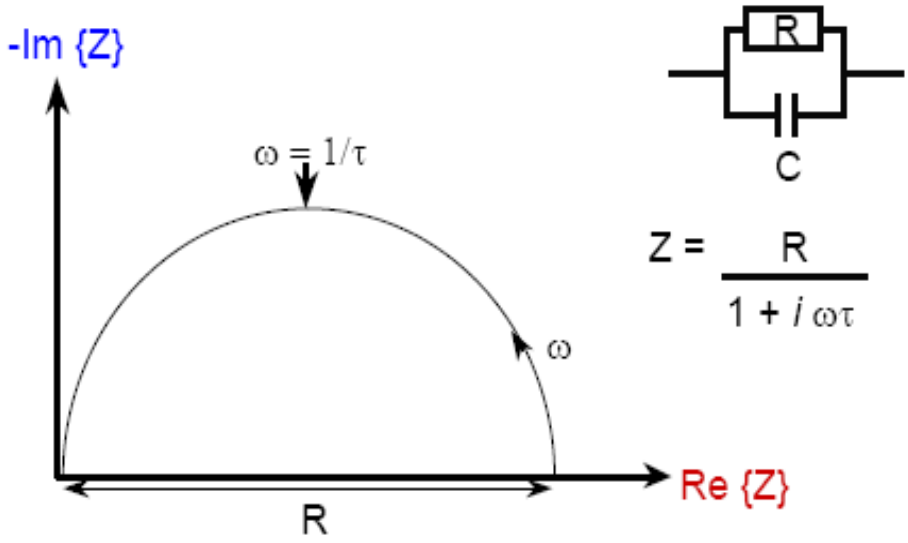

Fig. 3.1: Argand diagram

The diameter corresponds to the resistance R. The frequency at the 90° position corresponds to 1/t = 1/RC

3.5.2: Randle's Cell

The Randle's cell is one of the simplest and most common cell models. It includes a solution resistance, a double layer capacitor and a charge transfer or polarization resistance. In addition to being a useful model in its own right, the Randle's cell model is often the starting point for other more complex models.The equivalent circuit for the Randle's cell is shown in the Fig. 3.2. The double layer capacity is in parallel with the impedance due to the charge transfer reaction.

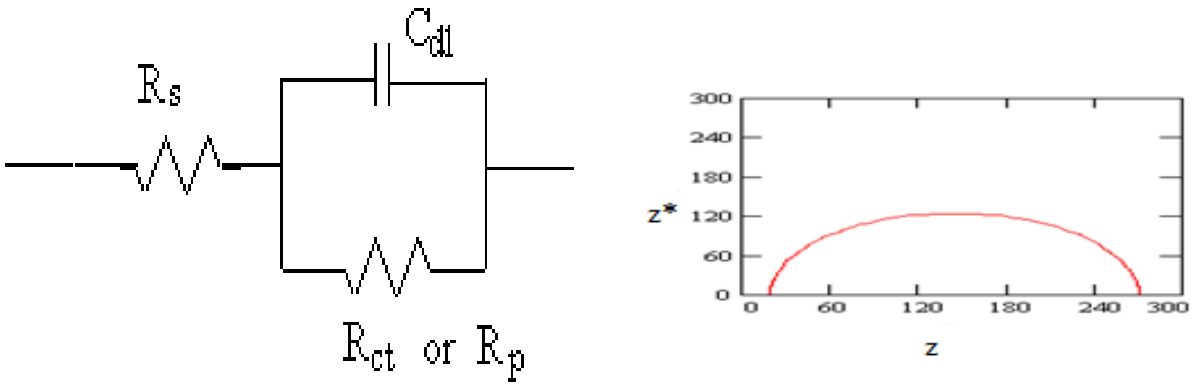

Fig. 3.2: Randle's equivalent circuit

The Nyquist plot for a Randle's cell is always a semicircle. The solution resistance can be found by reading the real axis value at the high frequency intercept. This is the intercept near the origin of the plot [163].

The real axis value at the other (low frequency) intercept is the sum of the polarization resistance and the solution resistance. The diameter of the semicircle is therefore equal to the polarization resistance.

3.5.3: Analyzing Circuits

Using the various Cole-Cole/Nyquist plots one can calculate values of the elements of the equivalent circuit for any applied bias voltage in a wide range.

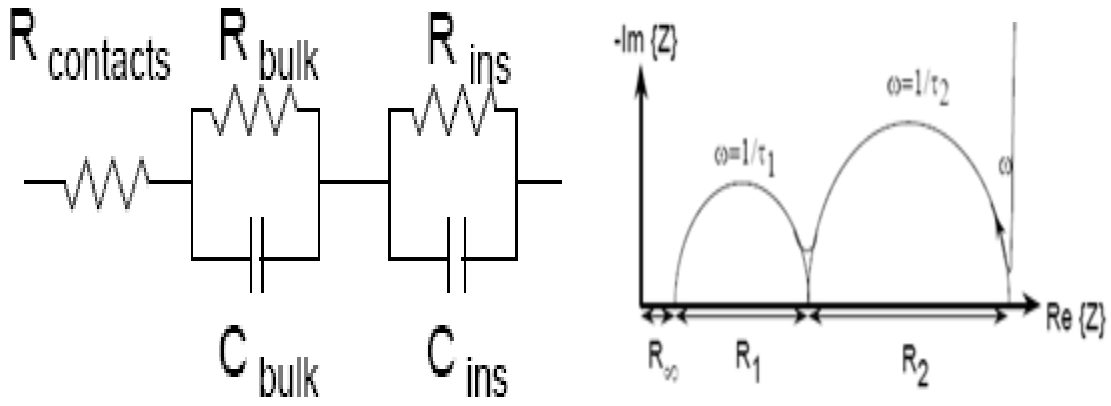

Fig. 3.3: Representation of equivalent circuit

The field distribution in the layers of the device (potential divider) and the relative widths of the layers, since C ~ 1/d

3.6: Data Representation

Once the raw data of experiment have been obtained, it is important to extract characteristic parameters to analyse the system properties. There are a few ways the data can be plotted, such as the Nyquist and Bode plane plotting. This section describes the several methods used to present data graphically [164].

3.6.1: Nyquist Plot

Application of an electrical perturbation (current, potential) to an electrical circuit causes the appearance of a response. The Nyquist Plot is named after Harry Nyquist. It is also known as the complex plane, which generally plots the negative of the imaginary part of impedance against the real part of impedance.

$$Z = \frac{E}{I} = Z_0 \exp(i\phi) = Z_0(\cos\phi + i\sin\phi)$$

In the equation above, the expression for Z (ω) is composed of a **real and an imaginary part**. If the real part is plotted on the X axis and the imaginary part on the Y axis of a chart, we get a "**Nyquist plot**". In this plot the y-axis is negative and that each point on the Nyquist plot is the impedance Z at specific frequency. On the Nyquist plot the impedance can be represented as a vector of length |Z|. The angle between this vector and the x-axis is Φ.

Low frequency data are on the right side of the plot and higher frequencies are on the left. This is true for EIS data where impedance usually falls as frequency rises (this is not true of all circuits). The Nyquist plot results from the RC circuit. The semicircle is characteristic of a single "time constant". Electrochemical Impedance plots often contain several time constants. Often only a portion of one or more of their semicircles is seen [165,166].

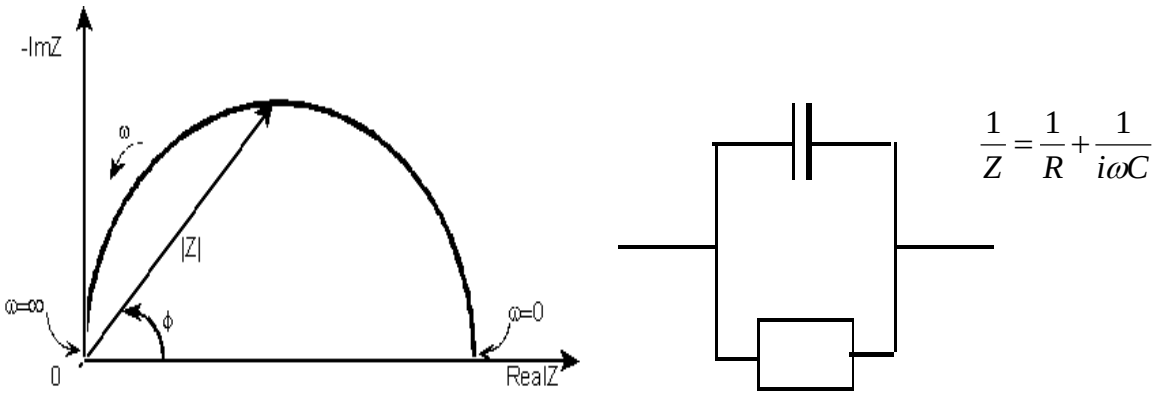

Fig. 3.4: Nyquist plot with impedance vector

Interpretation from Nyquist plot for any cell

1. Offset on real axis (Ohmic resistance).
2. Semi circular arc, due to moment of ions through the electrolyte layer and related R & C elements.
3. Movement of electrons across the electrical double layer, Rc element is made up of Rct & Cdl (If two semicircles are there).
4. Near vertical spike, built up of charge at the electrode-electrolyte interface. This is called capacitor.

3.6.2: Bode Plot

The Bode plot named after Hendrik Wade Bode consists of two subplots, the Bode magnitude plot and the Bode phase plot respectively. A Bode magnitude plot is a graph of log magnitude against log frequency. A Bode phase plot is a graph of phase against log frequency, which usually used in conjunction with the magnitude plot.

$$\frac{1}{Z} = \frac{1}{R} + \frac{1}{i\omega C}$$

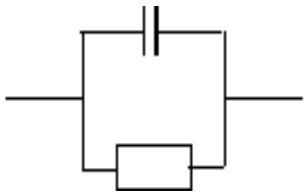

The impedance is plotted with log frequency on the x-axis and both the absolute value of the impedance ($|Z| = Z_0$) and phase-shift on the y-axis. Unlike the Nyquist plot, the Bode plot explicitly shows frequency information.

An example of the Bode plot is given in Fig. 3.5 and the curves were drawn by Z-view software. Fig. 3.5 (A) is the Bode magnitude plot, and Fig. 3.5 (B) is the Bode phase plot.

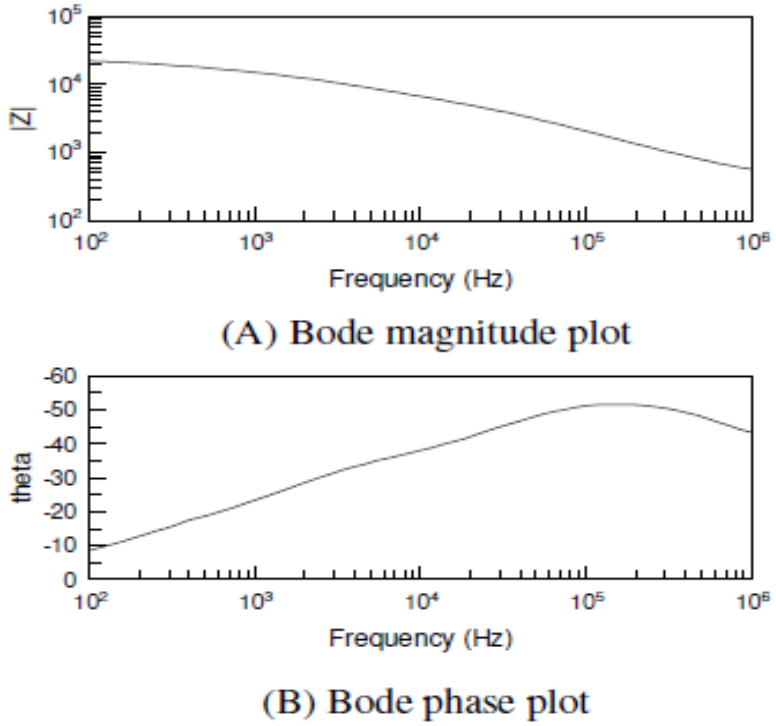

Fig. 3.5: Representation of Bode Plot

3.7: Data Analysis

Impedance data is multidimensional because of the frequency variation, concentration changes; electrode surface contains a wealth of independent information related to impedance and its surroundings. An independent assumption is that excitation voltage is kept quite low.

3.7.1: Chemometrics

Impedance data contains a large amount of highly correlated data due to experimental conduction and reaction cell. Multivariate data analysis tools such as principal component analysis (PCA), partial least square (PLS) regression have proved to be powerful tool for mathematical extraction of the dominant latent data structure. Chemometry has been defined as a chemical discipline that uses mathematical statistics and formal logic to design or select optimal experimental procedures, to provide maximum relevant chemical/physical information by analysing the data. Multivariate so called latent variable methods are more robust, forwards peak shift than uni-variate methods, because multivariate methods use areas under whole curves [167].

3.7.2: Principal Component Analysis (PCA)

Principal component analysis is central to the study of multivariate data. Although one of the earliest multivariate techniques, Principal component analysis (PCA) involves a mathematical procedure that transforms a number of (possibly) correlated variables into a (smaller) number of uncorrelated variables called principal components. The first principal component accounts for as much of the variability in the data as possible, and each succeeding component accounts for as much of the remaining variability as possible.

Tea tasting is a highly specialized job and calls for multidimensional sensory capabilities like finer senses of taste and smell, experienced analytical skill, and ultrasensitive classification ability. It is a way of identifying patterns in data, and expressing the data in such a way as to highlight their similarities and differences. Since patterns in data can be hard to find in data of high dimension, where the luxury of graphical representation is not available, PCA is a powerful tool for analysing data. The other main advantage of PCA is that once we have found these patterns in the data, and we compress the data, i.e. by reducing the number of dimensions, without much loss of information. In view of the capability of neural networks to learn input–output relation from a training data set, the neural networks have been the favoured choice for the researchers of electronic olfaction [168, 169].

3.8: Electrochemical system and electrodes

Electrochemical workstation: Electrochemical analysis is an analytical tool which provides the analytical methodology. These methods may be potentiometric with zero current or amperometric where current response is with perturbation potential. It relates to electrode potential or concentration which follows EMF measurements.

Usually **q=it**

Where q is charge flowing in coulombs

i= current in 1 ampere

t= 1 second

Oxidant + ne- $\longrightarrow$ Reductant

Redox Potential:

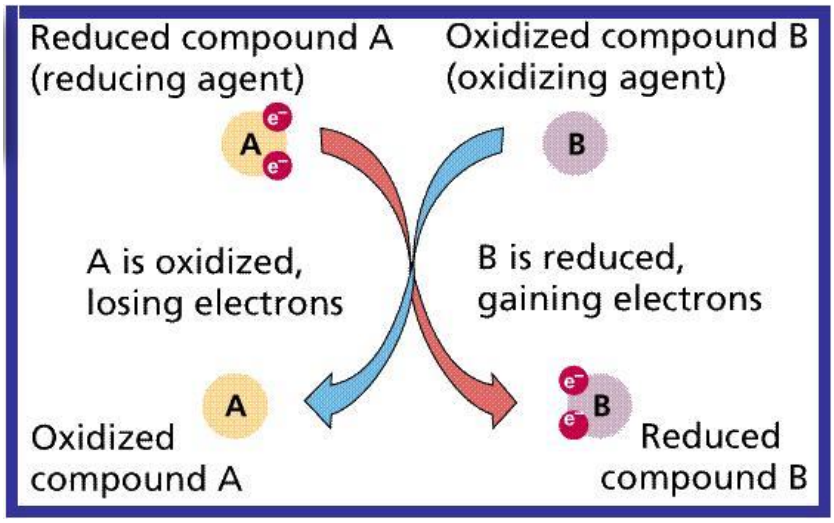

Fig. 3.6: Redox potential of healthy aquarium

Oxidant + ne^- ⟶ Reductant

Nernst equation represents:

$$E = E^\circ + \frac{RT}{nF} \ln \frac{a\ redn}{a\ oxid}$$

$$E = E^\circ + \frac{RT}{nF} \ln\ [Q]$$

Where Q is reaction quotient,

Putting the value of RT and F,

$$E = E^\circ + \frac{0.0591\ V}{n} \log \frac{a\ redn}{a\ oxid}$$

E= Cell potential of the cell,

E°= Standard potential of cell at 25 °C and 1 atmosphere,

T= Temperature in Kelvin,

n= Number of electron exchange in electrochemical reaction,

R= Gas constant and is equal to 8.31447 J mol^{-1} k^{-1},

F= Faraday's constant and equal to 9.6485 x 10^4 C where J/C is equal to volt.

3.9: Electrochemical workstation configuration

To carry out this study a sample cell with measuring system is used; electrochemical system (CH instruments USA, Texas). It's a three cell electrode set up used for studying impedance behaviour of tea solutions using electrochemical workstation 660C (Austin, TX, USA) and impedance studies were performed over the frequency range1 Hz to 100 KHz. Fig. 3.7 shows the experimental setup of electrochemical workstation. All impedance measurements were carried out at 25 ºC. The working electrodes for measurements were selected manually using a wire jumper arrangement. The data was recorded and displayed by the software provided with the electrochemical workstation which communicates with a personal computer using a RS232 link. Platinum (Pt), Gold (Au), Silver (Ag), Glassy Carbon (GC), polyaniline (PANI) and polypyrrole (PPY) were used as working electrodes. Pt wire and Ag/AgCl (4M KCl) were used as counter and reference electrodes respectively. Five readings per sample were taken and their mean was used for further analysis [170].

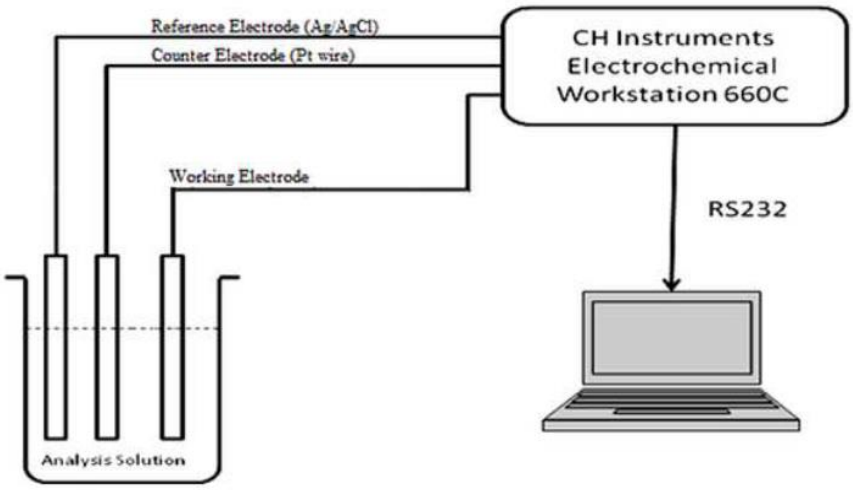

Fig. 3.7: Experimental setup of electrochemical workstation

3.9.1: Electrodes used

3.9.2: Working electrodes

The working electrode is the electrode in an electrochemical system on which the reaction of interest is occurring. The working electrode is often used in conjunction with an auxiliary electrode, and a reference electrode in a three electrode system.

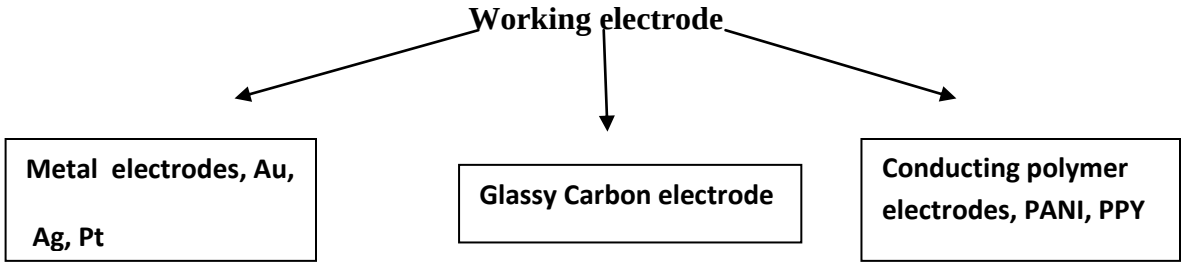

3.9.2.1: Metal electrodes

Pt, Au, Ag, GC working electrodes supplied by CHI was used throughout the study. The geometry along with its dimensions is given in the Fig. 3.8. .Fig. 3.9 shows the geometry of Pt, Au, Ag and GC electrodes.

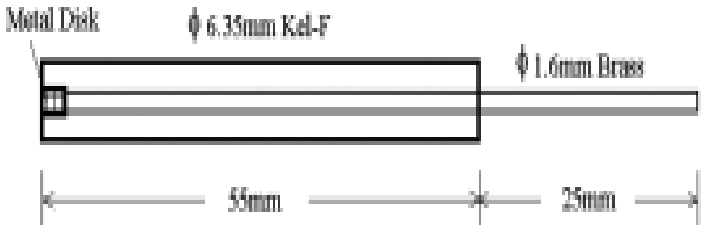

Fig. 3.8: Dimensions of Metal electrode

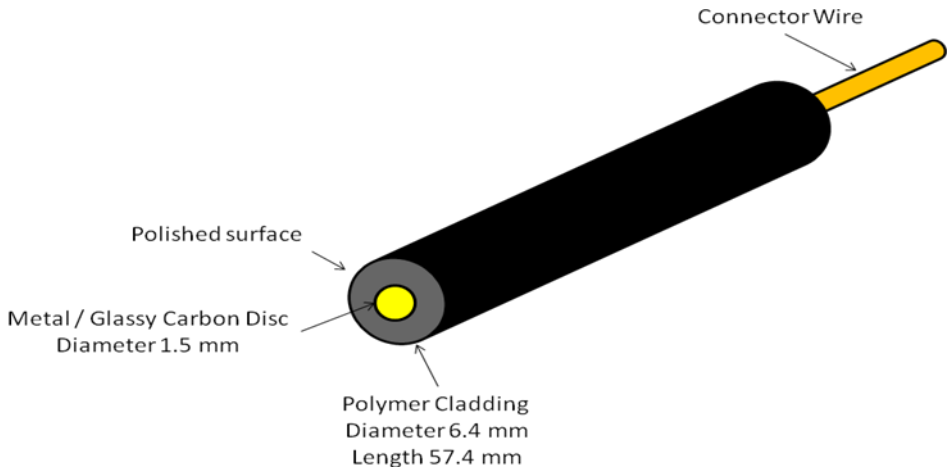

Fig. 3.9: Geometry of the Pt, Au, Ag and GC electrodes

3.9.2.2: Glassy Carbon

GC working electrode was used for impedance response of tea liquor/tastants supplied by CHI. Owing to its physical and chemical properties; glassy carbon has become an interesting and widely applied electrode material. It exhibits a rather low oxidation rate and a high chemical inertness which, together with very small pore sizes and a small gas and liquid permeability, make glassy carbon a convenient inert electrode [171]. This electrode possesses the similar geometry as that of other metal electrodes used in this study.

3.9.2.3: Polishing of metal electrodes

Pt, Au, Ag and GC working electrodes were polished with alumina powder of particle size of 1.0, 0.3, and 0.05 μm stepwise to get smooth surface. Each electrode was washed well with DI water. The working electrodes for measurements were selected manually using a wire jumper arrangement. The data was recorded and displayed by the software provided with the electrochemical workstation which communicates with a personal computer using a RS232 link. Pt, Au, Ag, GC, PANI and PPY were used as working electrodes [172].

3.9.2.4: Conducting polymer electrodes

PANI and PPY electrodes were used as conducting polymer working electrodes. Both these electrodes were fabricated in house. Fig. 3.10 shows the geometry of the PANI and PPY electrodes.

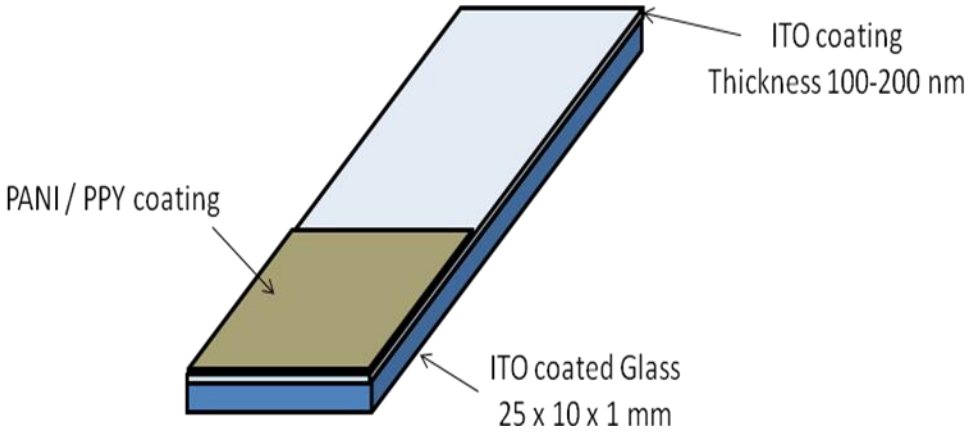

Fig. 3.10: Geometry of the PANI and PPY electrodes

3.9.2.4.1: Polyaniline

Two electrodes have been fabricated from the conducting polymers of PANI and PPY. PANI is important material which has been utilized in the applications of batteries, electronics, corrosion resistance and biosensors. It is promising material for the electronic devices such as diodes, transducers and sensors because of change in conductivity under applied potential. The conductivity depends upon many factors including molecular weight, temperature, humidity, counter doping, oxidation states and proton doping. Although all these parameters affects the conductivity but primarily depends upon oxidation state and proton doping.

PANI can exist in fully reduced state called leuco emarlidine, half oxidized half reduced called emarlidine and fully oxidized is called pernigraniline. Numerous studies show the influence of pH on the conductivity of emarlidine which is most stable form of PANI to be used for the fabrication of devices. Acid doping or the solution in which it is synthesized; the pH is maintained 2-2.5 gives rise to most conducting stage of PANI. PANI can interact with

other novel metals like Au, Ag, Pt and Ruthenium to work for chemical catalysis and sensing interaction.

3.9.2.4.2: Synthesis of PANI

PANI can be synthesized by variety of methods like chemical, electrochemical, gas phase plasma etc. The most common method is synthesis of PANI by direct chemical oxidation of aniline in presence of a suitable oxidant. In our studies we have used ammonium persulphate and hydrogen peroxide as oxidant.

Electrochemical synthesis produces only small quantities; however it is useful as the synthesis occur under controlled condition such as applied potential, so quality of polymer is moderate in the form of thin film on the conducting surface like ITO (Indium Tin Oxide).

In chemical synthesis adding suitable dopant, applied potential, reaction time and the area of electrode surface almost uniform thickness can be achieved which we have done in our studies.

PANI has been grown on ITO surface in acidic solution which acts as a electrolyte. The solutions chosen are HCl, H_2SO_4 and $HClO_4$ to have the dopant of chloride ion, sulphate and perchlorate ion. Each of the electrode behaviour was studied through cyclic voltammetry (CV) and conductance values. The current density in CV is usually between 1-5 mA/cm to ensure sufficient rate of reaction with a pre-set time. Finally, a CV is utilized to study the PANI characteristics. The conductance value varies between 10 s/cm to 10^{-2} s/cm, depending upon the dopant added when emeraldine is in conducting state.

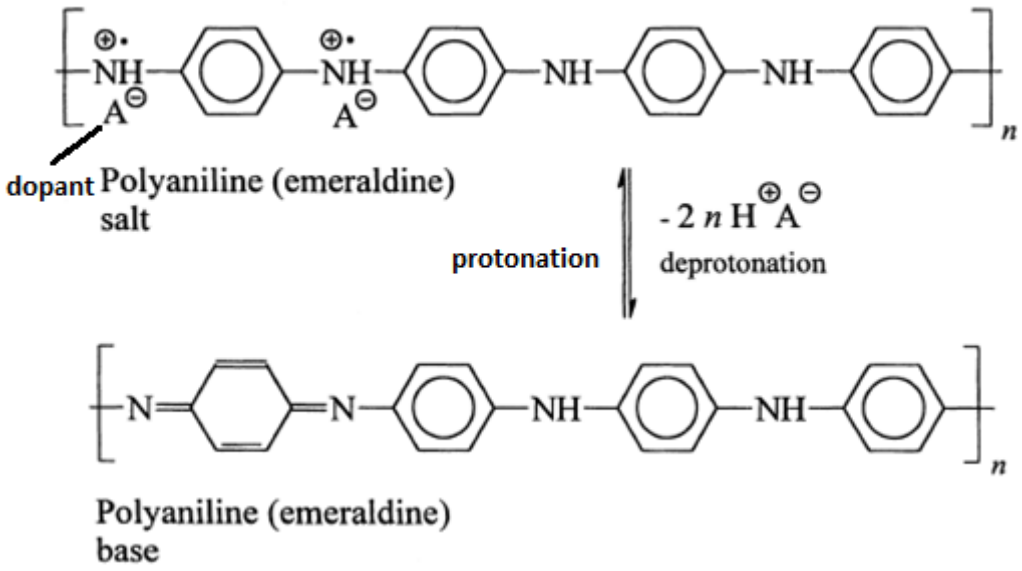

Fig. 3.11: Polyaniline (emeraldine) salt is de-protonated in the alkaline medium to polyaniline (emeraldine) base. A^- is an arbitrary anion e.g. chloride.

3.9.2.4.3: Electrochemical synthesis of PANI with different dopants

Indium tin oxide (ITO or tin-doped indium oxide) is 90% In_2O_3, 10% SnO_2 by weight. It is transparent and colourless in thin layers while in bulk form it is yellowish to grey. In the infrared region of the spectrum it acts as a metal-like mirror. Indium tin oxide is one of the most widely used transparent conducting oxides because of its two chief properties, its electrical conductivity and optical transparency, as well as the ease with which it can be deposited as a thin film.

3.9.2.4.4: Electro polymerization of PANI in H_2SO_4 electrolyte solution

An ITO coated glass of dimensions 2.5 cm x 1 cm x 0.1 cm was used to deposit conducting polymer film on 0.8 cm^2 area. The conducting polymer films were deposited by electro-polymerization (potentiometric method) from their respective monomers in a glass cell with standard three electrode setup [ITO coated glass as working electrode, Pt wire as counter electrode and saturated calomel electrode (SCE) as reference electrode] at room temperature [22]. PANI film was grown potentiostatically applying +1.2V potential for 2 min in 10 ml aqueous solution of H_2SO_4 (1 M) and 450 µl of aniline monomer. Each film was washed 2-3 times with DI water. After drying; these electrodes were stored in vacuum desiccator before and after their use. In this manner, nearly 100 films were grown for further studies keeping all reaction parameters constant, to characterize PANI it was also chemically synthesized. Similarly electrodeposition was carried in 1M HCl and $HClO_4$ to make the dopant of Cl^- ion and percholrate ions.

3.9.2.4.5: Chemical synthesis of PANI

In a typical experiment, 5 ml of aniline monomer was added to 100 ml of 2 M HCl solution in glass beaker and ice cooled (A solution). To another beaker 5 gm of $(NH_4)_2S_2O_8$ (ammonium persulphate) was dissolved in 20 ml of DI water and also ice cooled (B solution). This solution was added to A solution drop wise with constant stirring till green precipitation occurs. The solution was allowed to be stirred about one hour while maintaining it at ice cool temperature. The solution was allowed to stand overnight (20 hrs) for complete polymerization.

The green colour residue was separated from the reaction product by vacuum filtration, washed with DI water till the residue becomes free from acid. This residue was treated with 50 ml of 1N ammonium hydroxide solution and allowed to stand for another over night. The blue coloured residue which is emeraldine base was separated by filtration followed by washing with DI water. It was again treated with 50 ml of 0.1N HCl solution to convert it into emeraldine salt. This green powder was used for further studies to characterize the PANI for morphology, UV-Vis spectroscopy, thermal analysis, FTIR and structural properties.

However, electrode with deposited of film of emeraldine (PANI) has been used to characterize impedance behaviour of tea sample with Cl^- anion as dopant. The films produced with Cl^- anoin dopant seems to be stable, compact, uniform in thickness and reproducible conductance values.

3.9.2.4.6: Polypyrrole

Polypyrrole (PPY) is a type of organic polymer formed from by polymerization of pyrrole monomer. Fig. 3.12 shows the formation and polymerization of pyrrole radical cation.

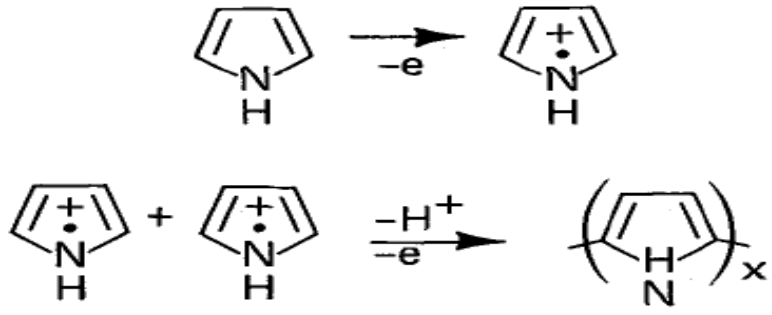

Fig. 3.12: Formation and polymerization of pyrrole radical cation and chain reaction

Chain propagation continues by reaction of the oligomer radical cation primarily with the radical cation of the monomer, which is present in high concentration in the region of the anode. As the chain grows the pyrrole oligomer becomes insoluble and eventually precipitates out on the electrode, where the chain can continue to grow until the oligomer radical cation becomes too unreactive or until it becomes prevented from reacting by steric reasons.

3.9.2.4.7: Electrochemical synthesis of PPY with different dopants

An ITO coated glass of dimensions 2.5 cm x 1 cm x 0.1 cm was used to deposit PPY film on 0.8 cm^2 area. The PPY films were deposited by electro-polymerization from pyrrole monomer in a glass cell with standard three electrode setup [ITO coated glass as working electrode, Pt wire as counter electrode and saturated calomel electrode (SCE) as reference electrode] at room temperature [172]. In this study, PPY films were grown potentiostatically applying +1V potential for 1 min in 10 ml aqueous solution of $K_4[Fe(CN)_6]$ (0.422 g) with 129 µl of pyrrole monomer for each film. Each film was washed 2-3 times with DI water. After drying these electrodes were stored in vacuum desiccators before and after their use. The PPY doped with [Fe $(CN)_6$] anions. However, in other studies synthesis was also carried out in presence of $FeCl_3$ to make Cl- ions as dopants.

3.9.2.4.8: Chemical synthesis of PPY

2 ml of distilled pyrrole was mixed in 50 ml of distilled water taken in the round bottom flask and well stirred. 9.74 g $FeCl_3.6H_2O$ dissolved in 50 ml distilled water taken and added to this

solution in the round bottom flask at 25 ºC. The reaction mixture was stirred for 24 hours with magnetic stirring, which results in the formation of the black precipitates. The resulting black precipitates were filtered with the vacuum filtration assembly and residue was washed with the distilled water 5 to 6 times and finally with ethanol. The polypyrrole so obtained was soft black powder, dried in the oven at 50^0C and stored in desiccators to avoid moisture. Similarly synthesis was carried in presence of K_4 [Fe (CN_6)] to have ferrocyanide doping.

3.9.2.5 Characterization of PANI

3.9.2.5.1: TGA/DSC- Thermal Analysis instrument (TGA-DSC)

TA Instruments Q600 Sdt, Banglore, India was used to study TGA-DSC [Differential Scanning Calorimetry (DSC) & Thermo gravimetric analysis (TGA)]. This system works from ambient to 1500ºC temperature.

In the present study both PANI and PPY were characterized for thermal analysis in nitrogen atmosphere with temperature gradient 5 degree/min in the selected temperature range from ambient to 1000ºC.

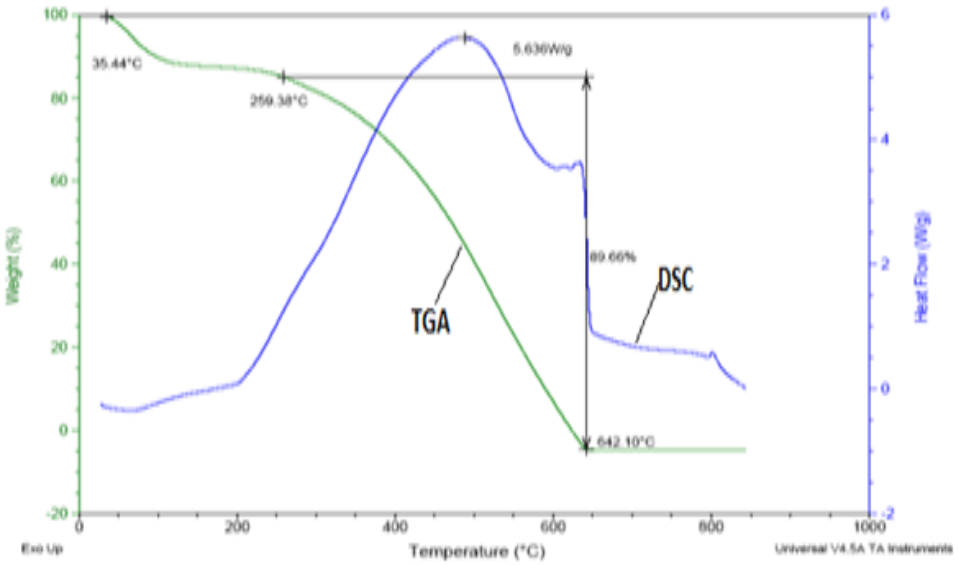

Fig. 3.13: TGA of PANI

In TGA studies of PANI, Fig. 3.13 shows about 5% loss of water at about 100-120ºC and then slow degradation of the polymer which completes at about 640ºC with no residue. The results are in agreement to the earlier reported studies (Voltammetric determination of citric acid and quinine hydrochloride using polypyrrole-pentacyanonitrosylferrate/platinum electrode [173]

This study shows that the material is stable at ambient temperature and works as a stable film for sensing behavior.

3.9.2.5.2 FTIR of PANI

Fourier transform infra red spectroscopy is performed using Perkin Elmer spectrum RX-1 system from Mumbai, India to determine the chemical composition of pristine PANI. FTIR spectroscopy has been used to qualitatively evaluate changes in functional group including benzoid, quinoid, amine and imine moieties in PANI.

FTIR spectra have been studied using Perkin Elmer RX-1 FTIR spectrophotometer in the range 500 cm^{-1} to 3500 cm^{-1}. PANI was dispersed in KBr solution to make FTIR studies.

Fig. 3.14 shows the FTIR spectra of PANI. Characteristic benzoid and quinoid bands of PANI are observed at 1472.4 and 1559.8 cm respectively [174].

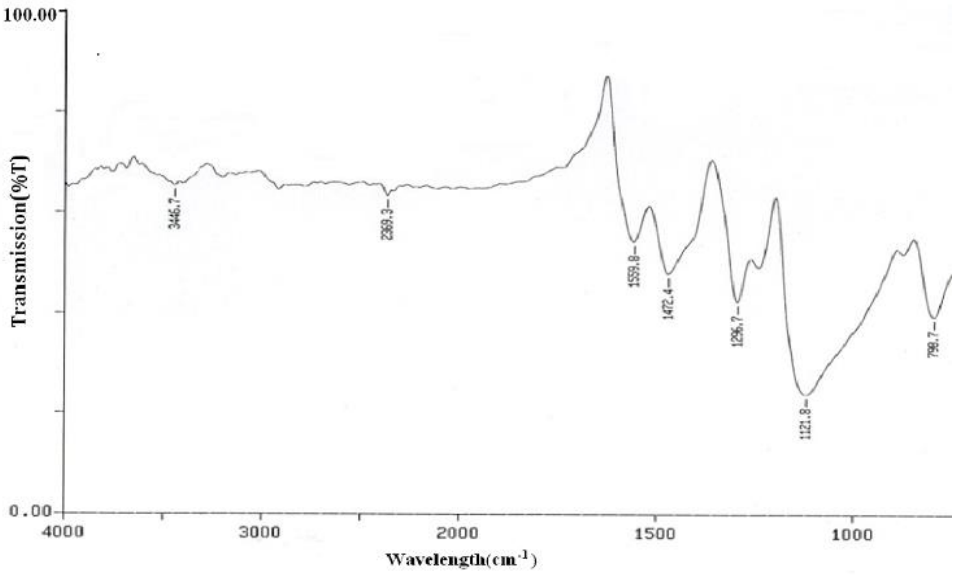

Fig. 3.14: FTIR of PANI

The band at 1472 is attributed to the aromatic C-C stretching vibration. The band at 1559 is attributed to the conjugated C=C stretching of quinoid unit. The characteristic band of benzoid and quinoid are used to qualitatively, based upon the intensity of the bands. C-N stretching vibration was observed at 1296.7 cm^{-1} and C=N stretching was seen at 1121.8 cm^{-1}, which is also in agreement to the already reported results. C-H bending was seen around 798.7 cm^{-1}. Peak at 3446.7 is due to the moisture. The results are in agreement to the already data [175].

3.9.2.5.3 UV-VIS Spectroscopy

UV-VIS (UV- visible) spectra of synthesized PANI was recorded using Perkin Elmer (Lambda 35) spectrophotometer from Mumbai, India in which quartz cuvette was used to

hold the liquor sample with path length of 1 cm.

Fig. 3.15 represents UV-VIS spectra of PANI. The polymer was dispersed in DMSO to make a clear solution. The UV-VIS spectra major absorption peak from 280-350 nm due to π-π transition and another peak were observed at 430-440 nm due to polaron transitions and a broad peak of 600-800 is from transition of benzoid.

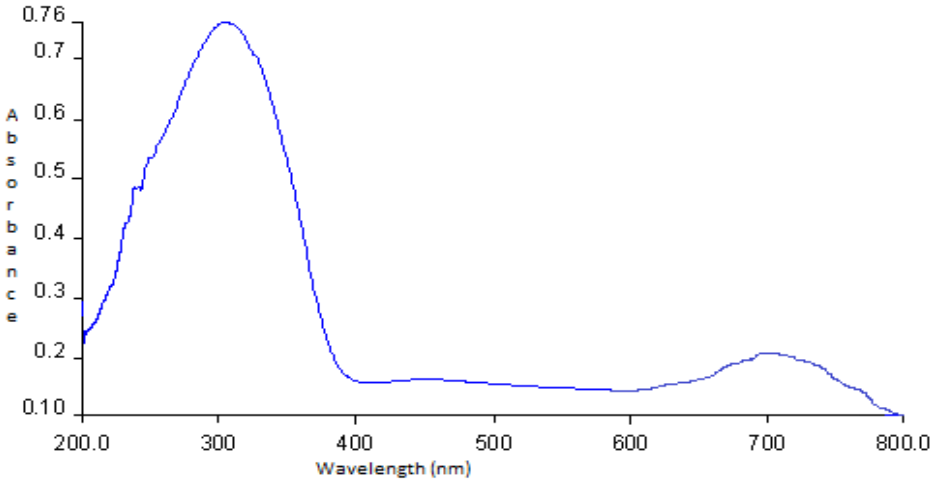

Fig. 3.15: UV-VIS spectra of PANI

3.9.2.5.4 X-ray Diffraction (XRD)

XRD pattern were recorded with a X'pert panalytical diffractometer from Delhi, India using Cu (Kα) radiation (λ= 1.5406 Å) at room temperature. This technique is based on the Braggs law of diffraction.

Fig. 3.16 shows the XRD pattern of PANI. The XRD pattern shows that the polymer is amorphous with a broad peak between 20-25ºC which is in agreement to the already reported studies [176]. Based on this further methodology was developed.

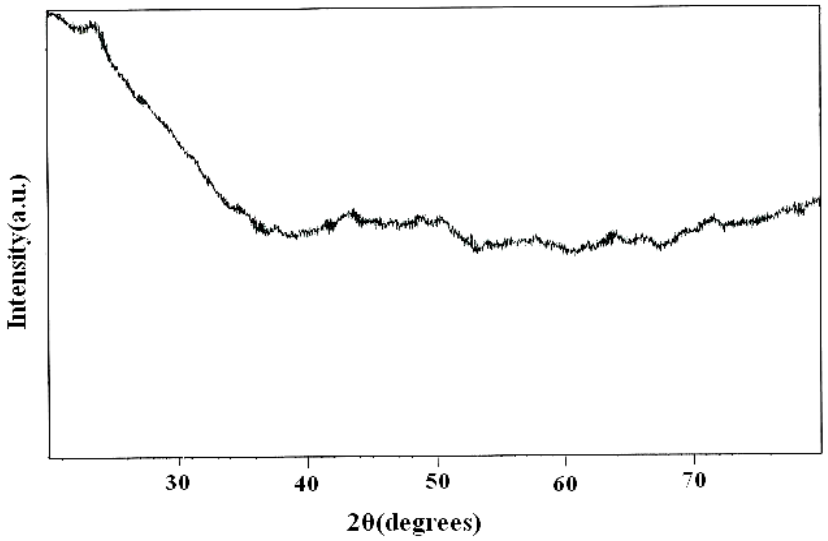

Fig. 3.16: XRD pattern of PANI

3.9.2.5.5 Cyclic Voltammetry (CV) of PANI

Cyclic voltammetry is a method for investigating the electro chemical behaviour of a system. It was first reported in 1938 and described theoretically by Randles [177]. In this technique current flowing between the electrode of interest (whose potential is monitored with respect to a reference electrode) and a counter electrode is measured under the control of a potentiostat. The voltammogram determines the potentials at which different electrochemical processes occur. The working electrode is subjected to a triangular potential sweep, whereby the

potential rises from a start value Ei to a final value Ef then returns back to the start potential at a constant potential sweep rate. The sweep rate applied can vary from a few millivolts per second to a hundred volts per second. The current measured during this process is often normalised to the electrode surface area and referred to as the current density. The current density is then plotted against the applied potential, and the result is referred to as a cyclic voltammogram. A peak in the measured current is seen at a potential that is characteristic of any electrode reaction taking place. The peak width and height for a particular process may depend on the sweep rate, electrolyte concentration and the electrode material [178, 179].

Cyclic voltammetry makes possible the elucidation of the kinetics of electrochemical reactions taking place at electrode surfaces [180,181]. In a typical voltammogram, there can be several peaks. From the sweep-rate dependence of the peak amplitudes, widths and potentials of the peaks observed in the voltammogram, it is possible to investigate the role of adsorption, diffusion, and coupled homogeneous chemical reaction mechanisms [182].

CV has been carried for both PANI and PPY in 3 cell electrode compartment of electrochemical workstation on CH instruments (Model 600C). Growth of PPY film on ITO is shown in Fig. 3.17 below keeping 0.V, 0.2V, 0.3V, 0.4V, 0.5V, 0.6V, 0.7V, 0.8V, 0.9V and 1.0 V potential.

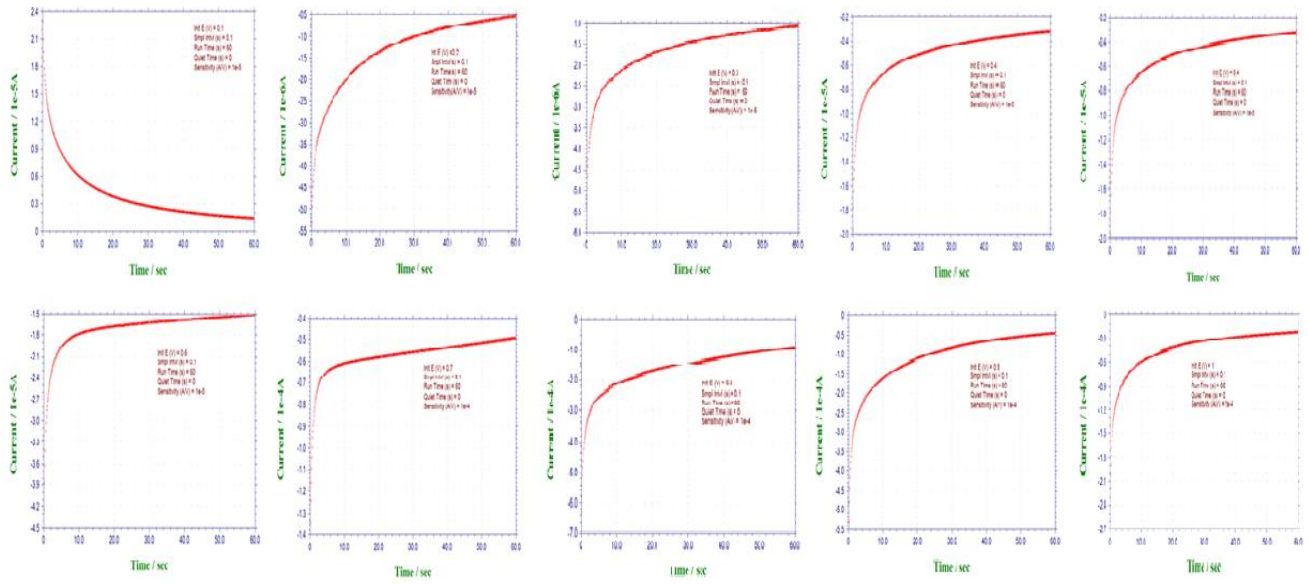

Fig. 3.17: Growth of PPY shown in 0.1 V to 1.0 V using CV

Fig. 3.18 shows the CV of PANI doped with with Cl- ions. CV has been carried for PANI doped with Cl^- ions at various scan rates at 0.1 V/s, 0.02, 0.3 and 0.02 V/s.

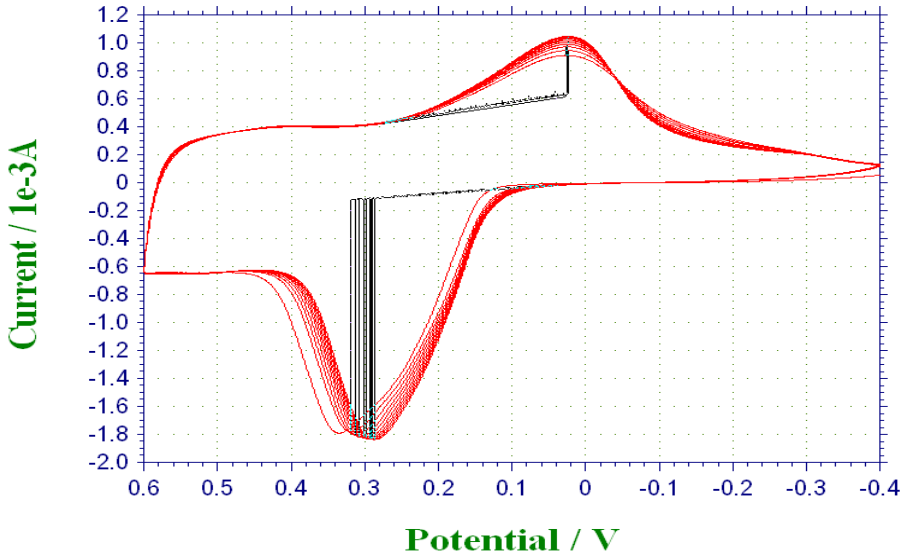

Fig. 3.18: CV of PANI doped with with Cl^- ions

Each experiment was repeated 5 times and the results are mean of the 5 observations. Reproducible C.V's were observed for PANI doped with HCl and PPY doped with para toluene sulphonic acid. Hence all sensing surface fabricated from monomer in a 3- electrode set-up, keeping the surface area of the working electrode, monomer concentration, electropolymerization time and potential scan was kept constant throughout the studies in view of almost same film thickness, optical behaviour and conductance levels.

3.9.2.6: Characterization of PPY

Electrochemical properties of polypyrrole films have been studied using cyclic voltammetry at different scan rates and at different voltage.

CV of Polypyrrole films prepared in NaCl, KCl, HCl and p-tolune sulphonic acid was recorded and is shown in figure Fig. 3.19.

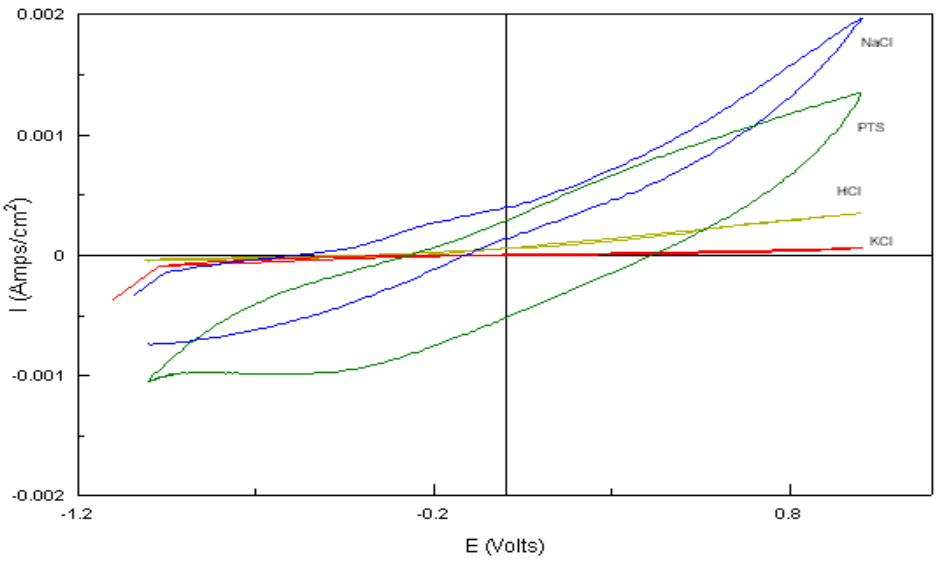

Fig. 3.19: CV of PPY using NaCl, PTS, HCl, KCl

It can been seen from Fig. 3.19, film prepared in 0.1 M p-tolune sulphonic acid showed much better electrochemical response as compared to prepared in other electrolytes. CV of ITO/PPY electrode was recorded in 0.1 M KCl and 0.1 M p-tolune sulphonic acid at scan rate of 100, 70 and 50 mV/s. Fig. 3.20 shows CV of PPY at different scan rates using PTS and Fig. 3.21 gives CV of PPY at different scan rates using KCl.

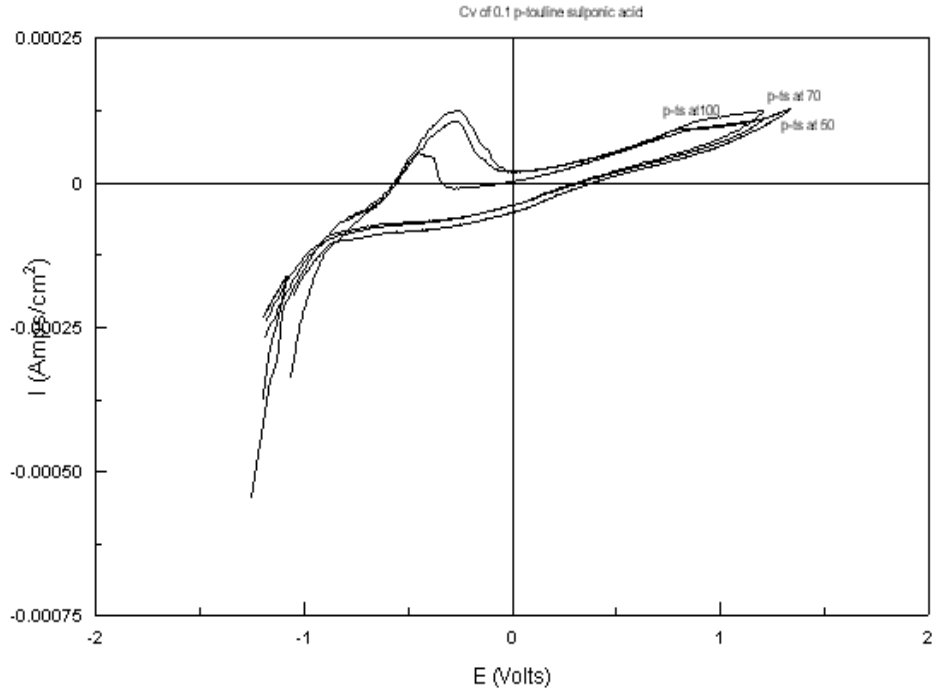

Fig. 3.20: CV of PPY at different scan rates using PTS

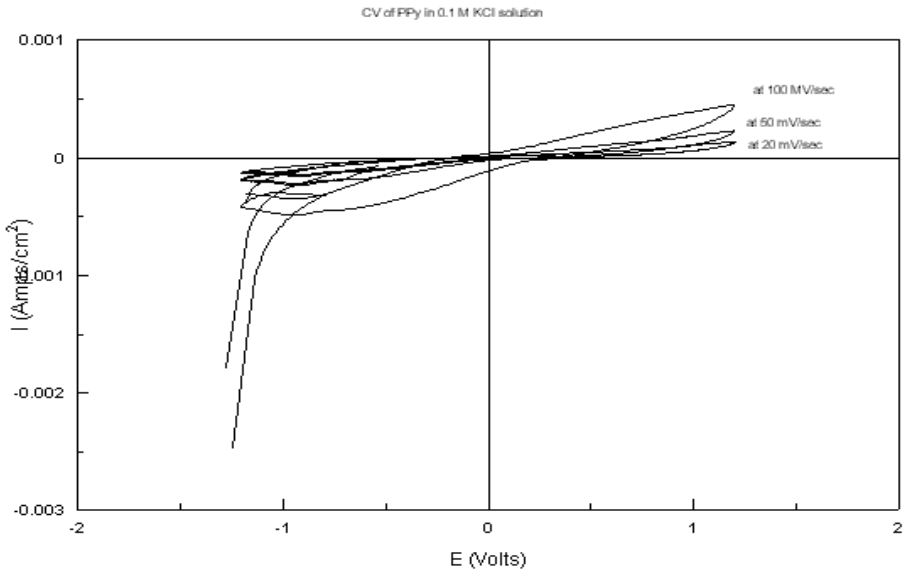

Fig. 3.21: CV of PPY at different scan rates using KCl

In both KCl and p-toluene sulphonic acid, current increased with increase in scan rate. However, polymer films prepared in p-toluene sulphonic acid showed much better response in terms of defined peak at about -0.3V.

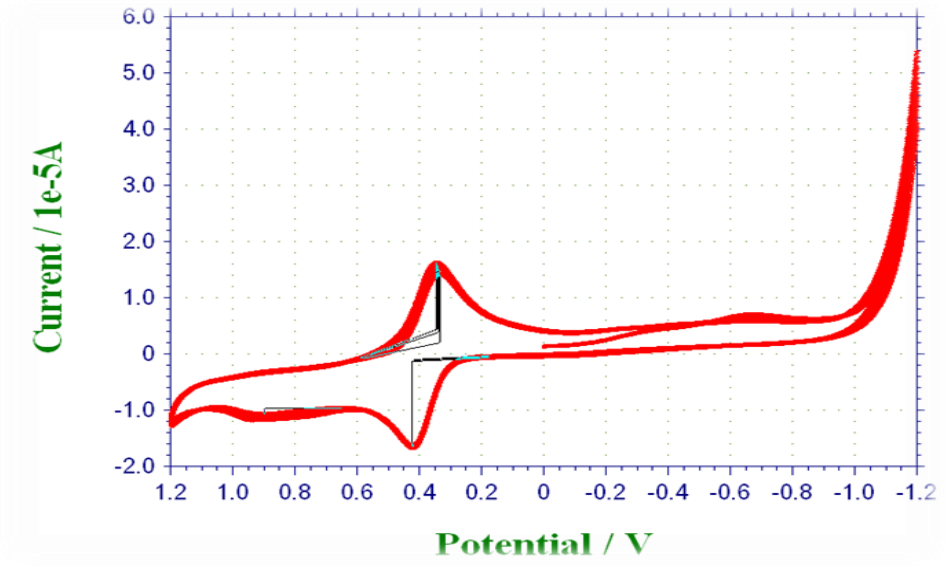

Fig. 3.22: CV of PPY doped with $K_4[Fe(CN)_6]$

CV for PPY doped with $K_4[Fe(CN)_6]$ is given in Fig. 3.22 at various scan rates i.e. 0.1, 0.4, 0.8 and 0.3 V/s. The upper peak represents oxidation whereas lower peak corresponds to reduction.

3.9.2.6.1: TGA of PPY

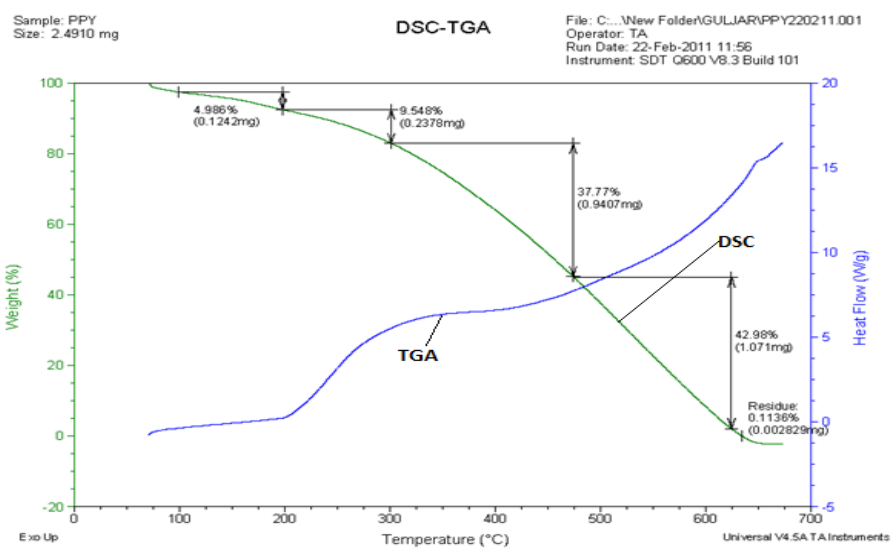

Fig. 3.23: TGA-DSC of PPY

Around 5% loss of water at about 100-125ºC can be seen in Fig. 3.23 followed by a slow degradation of the polymer which completes at about 680ºC with no residue. The results are in agreement to the earlier reported studies [183].

The material is stable at ambient temperature and works as a stable film for sensing behavior is shown in this study.

3.9.2.6.2: FTIR of PPY

Fig. 3.24 shows the FTIR spectra of PPY. Characteristic benzoid and quinoid bands of PPY are observed at 1465 and 1546.2 cm respectively [184].

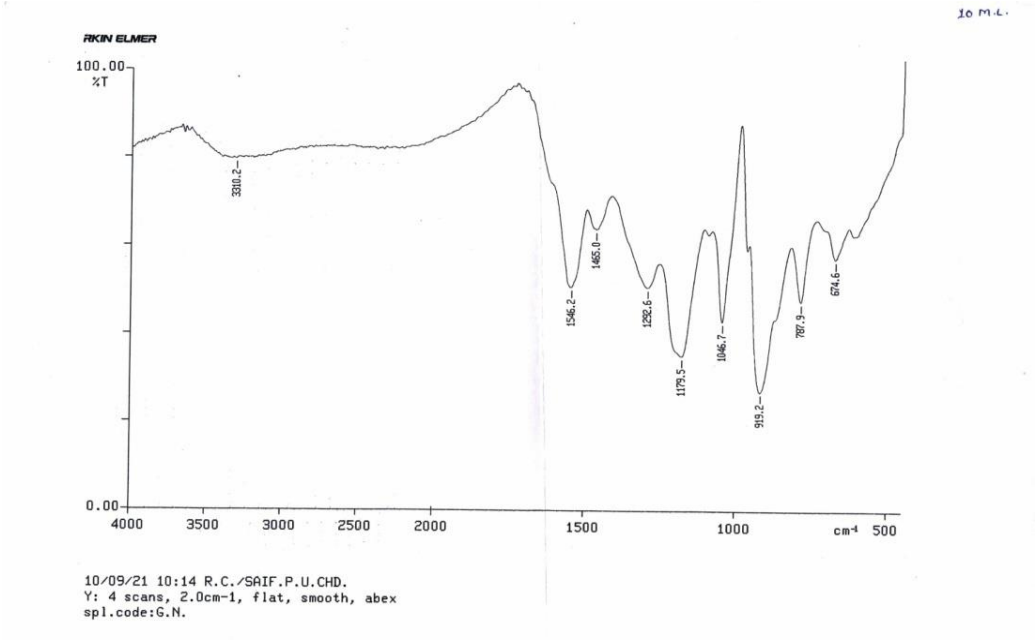

Fig.3.24: FTIR spectra of PPY

The band at 1465 is attributed to the aromatic C-C stretching vibration. The band at 1546.2 is attributed to the conjugated C=C stretching of quinoid unit. The characteristic band of benzoid and quinoid are used to qualitatively based upon the intensity of the bands. C-N stretching vibration was observed at 1292.6 cm^{-1} and C=N stretching was seen at 1179.5cm^{-1}, which is also in agreement to the already reported results. C-H bending was seen around 787.9 cm^{-1}. The results are in agreement to the already data [185].

3.10: High Performance Liquid Chromatography (HPLC) method

Antioxidants and phenolic constituents are widely present in tea. Compounds which are antioxidants by virtue of their ability to act as reductants in solution tend to be easily oxidized (loss of electrons). Sensitive and selective liquid chromatography methods are used for determining many of these compounds in extracts.

3.10.1 **High-Performance Liquid Chromatography (HPLC)**

High Performance Liquid Chromatography (HPLC) was developed in the late 1960s and early 1970s. Today it is widely applied for separations and purifications in a variety of areas including pharmaceuticals, biotechnology, environmental, polymer and food industries. HPLC is accomplished by injection of a small amount of liquid sample into a moving stream of liquid (called the mobile phase) that passes through a column packed with particles of stationary phase. Separation of a mixture into its components depends on different degrees of retention of each component in the column. The extent to which a component is retained in the column is determined by its partitioning between the liquid mobile phase and the stationary phase.

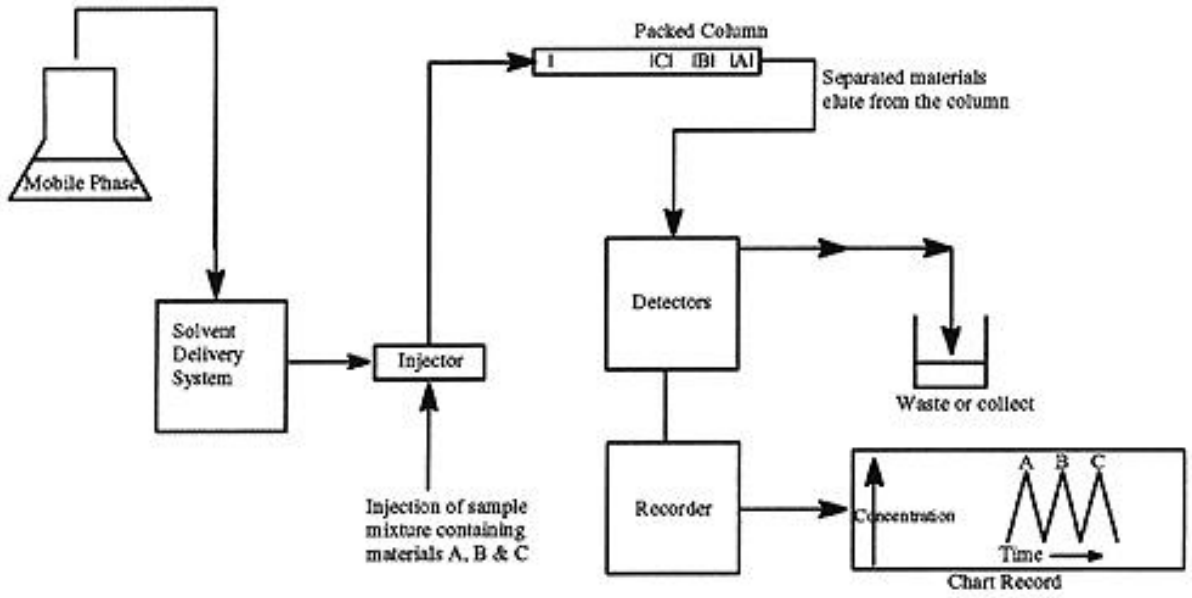

Fig. 3.25: Block diagram of HPLC system

In HPLC this partitioning is affected by the relative solute/stationary phase and solute/mobile phase interactions. An automatic injector providing reproducible injection volume is extremely beneficial, and is standard on modern commercial systems.

3.10.2: **Normal–phase chromatography**

In normal phase chromatography, mobile phase is non-polar like hexane, chloroform, pentane and stationary phase is polar.

3.10.3: **Reverse-phase chromatography**

In reverse phase chromatography, mobile phase is polar like methanol, water, acetonitrile and stationary phase is non-polar.

3.10.4: **HPLC detectors**

These detectors are designed to have certain properties like

♦ Being inert (non-reactive) to the samples injected and the mobile phases passing through.

♦ Preferably non-destructive to the sample.

♦ Produce quick and quantitative response.

♦ Produce uniform, reliable and reproducible detection and analytic data.

♦ Compatible for all types of compounds under testing.

♦ Should have good sensitivity .i.e able to detect compounds at very low concentration in the ranges below micro-grams, nano-grams etc. as the sample quantity may be lower in many cases.

3.10.4.1: **UV detectors**

These detector systems work on the spectroscopy principle. The sample detection depends on absorption of UV ray energy by the sample. The equipment comprises of accessories in order as UV source, grating (for light defraction), sample passing through a tubing exposed to rays, photo cell, charge conductor etc.

3.10.4.2: **PDA detectors**

These are detectors which follow **principle similar to UV detectors** but the range of detection extends from UV, visible and to some extent to IR region. Thus the advantages are **higher sensitivity** and measure the **entire absorption range** i.e. it gives scan of entire spectrum.

3.10.4.3: HPLC Fluorescence detector

In this detector the fluorescence rays emitted by sample after absorbing incident light is measured as a function of quality and quantity of the sample.

The equipment comprises of accessories in order as light source, sample passing through a tubing exposed to rays, grating (for light defraction), photo cell, charge conductor etc.

Xenon arc lamp is used to produce light for excitation of sample molecules. These light rays excite the sample molecules. These excited molecules emit florescence, which pass through gratings. These gratings pass the florescence at specific wavelength to photo cell which is recorded.

3.10.4.4: **Light Scattering Detectors**

Light scattering detectors are useful for detection of high molecular weight molecules. After removal of mobile phase by passing through a heated zone the solute molecules are detected by light scattering depending on molecular sizes.

3.10.5: **Principle of HPLC**

HPLC separates mixture of compounds on the basis of polarity. {Polarity refers to: the greater the difference in electron affinity i.e. electronegativity between atoms in a covalent bond, the more polar the bond. Partial negative charges are found on the most electronegative atoms, the others are partially positive. Negative electrostatic potential corresponds to: partial negative charges, Positive electrostatic potential corresponds to : partial positive charges.} It is used to analyze, identify, purify and quantify compounds.

3.10.6: **Compounds Identification using HPLC**

Identification of compounds by HPLC is a crucial part of any HPLC assay. In order to identify any compound by HPLC a detector must first be selected. Once the detector is selected and is set to optimal detection settings, a separation assay must be developed. The parameters of this assay should be such that a clean peak of the known sample is observed from the chromatograph. The identifying peak should have a reasonable retention time and should be well separated from extraneous peaks at the detection levels which the assay will be performed. To alter the retention time of a compound, several parameters can be manipulated. The first is the choice of column, another is the choice of mobile phase, and last is the choice in flow rate.

A sample of a known compound must be utilized in order to assure identification of the unknown compound. Identification of compounds can be assured by combining two or more detection methods. Quantification of compounds by HPLC is the process of determining the unknown concentration of a compound in a known solution. It involves injecting a series of

known concentrations of the standard compound solution onto the HPLC for detection. The chromatograph of these known concentrations will give a series of peaks that correlate to the concentration of the compound injected.

3.11: Tea Constituents

Tea contains a wide range of phenolic compounds of which the most important are briefly mentioned. Tea's polyphenols include flavanols, flavandiols, flavonoids, and phenolic acids; these compounds may account for up to 30% of the dry weight of the tea leaves according to the literature. Catechins (flavanols) are the most abundant group of phenolic compounds in fresh leaf and green tea. The major tea catechins are (-)-epigallocatechin 3 gallate (EGCG), (-)-epigallocatechin (EGC), (-)-epicatechin (EC), (-)-epicatechin 3-gallate (ECG), and (+)-catechin (CAT). Other, such as epiafzelechin and its gallate as well as acetylated catechins have also been identified.

Many attempts have been made by various researchers to correlate tea quality with its chemical composition. Black tea quality is influenced by the concentration of theaflavins (TF) and thearubigins (TR) [186,187].A very close relationship was found between TF content and broker's valuation of black tea [188,189]. Flavanol composition and caffeine content were also used as quality potential indicators of black tea [190].

Contents of amino acids and catechins were found to be correlated to tea quality assessed by professional tea tasters [191-193]. A number of efforts have been made to classify different beverages including tea using gas sensor array (E-Nose) [194-196] and electrochemical techniques such as cyclic voltametry, potentiometry and conductivity [197, 198].

3.12: Tea Sample preparation

Following studies have been carried out to study impedance behaviour of tea samples, employing non specific multi-electrode electrochemical impedance spectroscopy for classification of Indian black tea in terms of manufacturing process (CTC/Orthodox), harvest/brand variations and chemical concentrations is proposed.

Each sample has been prepared in which 4 gm of dry tea sample was added to boiling water (approx. 80 ml) allowed to boil for 2 minutes, cooled, filtered through Whatmann filter no. 42, and final volume was made 100 ml with distilled water and the same was stored for all studies. Approximately 20 ml solution was taken in a cell to carry impedance measurements. We kept this solution for a month's time to make repeated studies.

Twelve (12) Grades of Kangra Orthodox Indian Black Teas (Camellia sinensis (L.) O. Kuntze), harvested during the three flushing seasons (Early, Rains and Backend) were picked from Institute of Himalayan Bioresource Technology, Palampur (A constituent laboratory of CSIR, India).

Eight (8) grades of Assam CTC tea harvested during different flushing seasons were procured from a local market.

Taste is the ability to respond to dissolved molecules and ions called **tastants**. Humans detect taste with **taste receptor cells**. These are clustered in **taste buds** and scattered in other areas of the body. Each taste bud has a pore that opens out to the surface of the tongue enabling molecules and ions taken into the mouth to reach the receptor cells inside. There are 4 basic tastants namely sweet, sour, salty and bitter. The properties of tea and other beverages depend upon the presence of compounds which provides specific taste.

3.12.1: Sucrose

Sucrose is the organic compound commonly known as **table sugar** and sometimes called **saccharose**. The molecule is a disaccharide composed of the monosaccharides glucose and fructose with the molecular formula $C_{12}H_{22}O_{11}$.

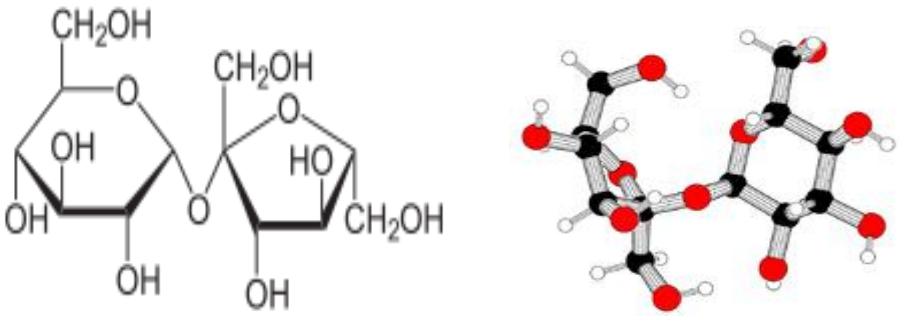

Fig. 3.26: Structure of Sucrose

25 mM of sucrose has been prepared by dissolving 8.55 gms of sucrose in 1 liltres of DI water. Sweetness, usually regarded as a pleasurable sensation, is produced by the presence of sugars and a few other substances. Sweetness is often connected to aldehydes and ketones, which contain a carbonyl group. Taste detection thresholds for sweet substances are rated relative to sucrose, which has an index of 1. The average human detection threshold for sucrose is 10 millimoles per litre.

3.12.2: Sodium chloride (NaCl)

In the crystal structure of sodium chloride each atom has six nearest neighbours, with octahedral geometry. Sodium chloride forms crystals with cubic symmetry. In these, the larger chloride ions, shown to the right as green spheres, are arranged in a cubic close-

packing, while the smaller sodium ions, shown to the right as silver spheres, fill the octahedral gaps between them. Each ion is surrounded by six ions of the other kind. This same basic structure is found in many other minerals, and is known as the halite structure. This arrangement is known as cubic close packed (ccp). It can be represented as two interpenetrating face-centred cubic (fcc) lattices, or one fcc lattice with a two atom basis. It is most commonly known as the rock salt crystal structure. It is held together with an ionic bond and electrostatic forces. Elemental chlorine is usually produced by the electrolysis of sodium chloride dissolved in water. Along with chlorine, this chlor-alkali process yields hydrogen gas and sodium hydroxide, according to the chemical equation.

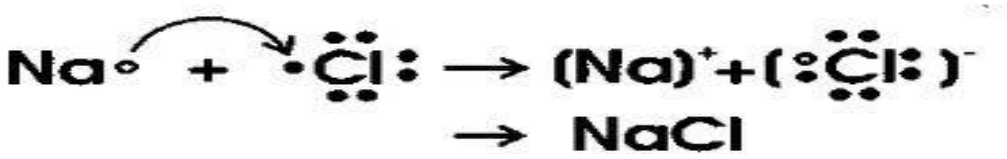

25 mM of NaCl was made by dissolving 1.45 gms in 1 litres of DI water. Saltiness is a taste produced primarily by the presence of sodium ions. Other ions of the alkali metals group also taste salty, but the further from sodium the less salty the sensation is. The size of lithium and potassium ions, most closely resemble those of sodium and thus the saltiness is most similar.

3.12.3: Quinine

Quinine, isolated originally from Cinchona succirubra, is a white crystalline alkaloid soluble in alcohol, ether, carbon disulfide, chloroform, and glycerol. It is almost insoluble in water. It

is used chiefly (usually in the form of soluble hydrochloride or sulfate salts) in the treatment of falciparum malaria resistant to other anti-malarials.

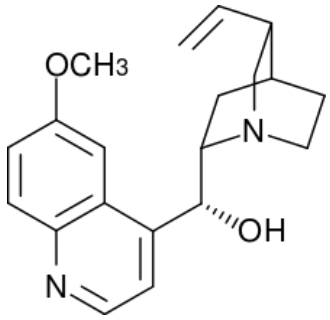

Fig. 3.27: Structure of quinine

25 mM of quinine was prepared by dissolving 8gms in 1litres of DI water. Bitterness is the most sensitive of the tastes, and many perceive it as unpleasant, sharp, or disagreeable, but it is sometimes desirable and intentionally added via various bittering agents. Common bitter foods and beverages include coffee, unsweetened cocoa, South American mate, marmalade, bitter gourd, beer (due to hops), bitters, olives, citrus peel, many plants in the Brassicaceae family, dandelion greens, wild chicory, and escarole. Quinine is also known for its bitter taste and is found in tonic water. The threshold for stimulation of bitter taste by quinine averages a concentration of 0.000008 M.

3.12.4: Citric acid

This is found in a variety of vegetables and fruits. Citric acid is a weak organic acid and a natural preservative. The acid is also an antioxidant, and is commonly used to add a sour taste to soft drinks and a variety of foods.

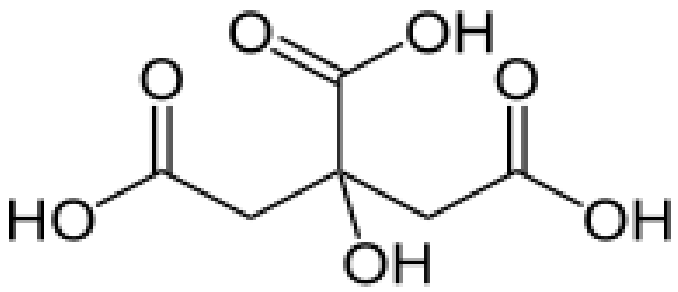

Fig. 3.28: Structure of Citric acid

25 mM of citric acid was prepared by dissolving 4.8gms of citric acid in 1 litres of DI water. citric acid a sourness index of 0.46. The most common food group that contains naturally sour foods is fruit, such as lemon, grape, orange, tamarind, and sometimes melon. Wine also usually has a sour tinge to its flavour, and if not kept correctly, milk can spoil and develop a sour taste. Sour candy is popular in North America including Cry Babies, Warheads, Lemon drops, Shock tarts and Sour Skittles and Starburst. Many of these candies contain citric acid.

CHAPTER 4.1

RESULT AND DISCUSSIONS

4.1.1 Quantification of tea constituents using HPLC and UV/VIS Spectroscopy and antioxidant capacity.

Over the past decade many scientific and medical studies have focused on green tea for its long-purported health benefits. There is convincing evidence that tea is a cup of life. It has multiple preventive and therapeutic effects. Tea is very rich in polyphenolic constituents which have high anti-inflammatory, antioxidant, and antimutagenic properties in various biological systems. Researchers indicate that tea consumption might have health-promoting properties, including the effects of reduction of cholesterol, depression of hypertension, antioxidation, antimicrobial activity, and protection against cardiovascular disease and cancer [199-203].

During the past decade, more and more chromatographic methods were used for the quality control of teas and classification of different kinds of teas. These chromatographic methods included high performance thin layer chromatography (HPTLC), high performance liquid chromatography (HPLC), ultra performance liquid chromatography (UPLC), capillary electrophoresis (CE), gas chromatography (GC), and their combination with mass spectrometry (MS). Because of high resolution and high efficiency, high performance liquid chromatography (HPLC) has been widely used in tea analysis for measuring numerous compounds, such as catechins, alkaloids, and amino acids. Based on the content of chemical components in tea samples, the HPLC method was reported for the quality control of tea samples with different grades.

Tea is particularly rich in polyphenols, including catechins, theaflavins and thearubigins, which are thought to contribute to the health benefits of tea [204].

Tea polyphenols act as antioxidants in vitro by scavenging reactive oxygen and nitrogen species and chelating redox-active transition metal ions. Antioxidant compounds in food play an important role as a health-protecting factor. Scientific evidence suggests that antioxidants reduce the risk for chronic diseases including cancer and heart disease [205]. In this chapter quantification of tea compounds i.e. EGC, CAF, EC, EGCG and ECG has been carried using HPLC and UV-VIS spectrophotometer. The HPLC study for standard compounds of tea has been carried and the same has been carried for Kangra and CTC tea samples. The UV-VIS studies were also carried for both Kangra as well as CTC Assam tea samples. Further PCA has been carried for the same tea samples and classification based on different flushes as well as different region has been possible to make. Tea tasters score has also been shown in this chapter.

4.1.2 HPLC analysis of Indian black teas

4.1.2.1 HPLC study for catechins

Twelve tea samples were analyzed for catechins according to the method described by Sharma et al. [206] on Waters HPLC using a C-18 reverse phase 250 × 4.0 mm, 5 μm column, fitted with a C-18 guard column (shown in Table 4.1.1). Infusion was centrifuged at 4000 rpm at 4°C for 10 min. Supernatant was collected and passed through Millipore filter (0.45 μm) prior to injection in HPLC. The mobile phase finally adopted was (B) acetonitrile/ (A) 0.1% ortho-phosphoric acid in water (w/v) with a flow rate of 1 mL/min at 280 nm. The HPLC

elution program is given in Table 4.1.1. For identification and quantification of EC, ECG, EGC and EGCG, the area and retention time of each analyte peak were matched with the corresponding reference standard chromatographed under similar conditions. Standard curves were prepared by plotting concentration versus area for each reference standard.

Table 4.1.1: Gradient program in HPLC

Time	A (0.1% ortho-phosphoric acid in water)	B (acetonitrile)
0	90	10
10	90	10
12	80	20
15	65	35
18	64	36
20	64	36
24	70	30
28	80	20
30	90	10

4.1.3 Spectrophotometric analysis for theaflavins (TFs) and thearubigins (TRs)

A rapid procedure for estimating theaflavins and thearubigins of black tea was adopted by Ullah, 1986 [207].

The absorbance was measured on a UV-VIS-3450 spectrophotometer, Shimadzu. Each tea sample of 9g added to 375ml of boiling water in a conical flask and boiling continued for 10

min using an air condenser on a water bath. The tea infusion was filtered through cotton cloth and cooled to room temperature.

The infusion (6 ml) was mixed with 6 ml of 1% (w/v) aqueous solution of anhydrous disodium hydrogen phosphate and the mixture extracted with 10 ml of ethyl acetate by quick repeated inversion for 1 min. The separated bottom layer drained, remaining was the ethyl acetate layer (the TF fraction) and diluted with 5 ml ethyl acetate. Optical densities, E_1, E_2, E_3; were obtained on extracts prepared as follows: 10 ml of TF extract were diluted to 25 ml with methanol (E_1) and to 1 ml of infusion was added 1 ml of aqueous oxalic acid (10% w/v (E_2), Optical densities of E_1 and E_2.

At 380 nm, % TF =2.25 x E_1

% TR =7.06 (4 E_2 - E_1)

4.1.4 DPPH free-radical scavenging assay

The antioxidant activity was determined by using Turkmen et al., method with slight modification [208].

50 µL of each tea extract was mixed with an aliquot of 1950 µL of DPPH radical in ethanol (100 µM). Ethanol was used as a control. The reaction mixture was vortex- mixed. Reaction tubes were wrapped in aluminum foil and let to stand at 25ºC in the dark for 30 min. All measurements were done under dim light. Spectrophotometric measurements were done at 517nm using Shimadzu UV-2450 UV-VIS Spectrophotometer. Antioxidant activity (AA) was

expressed as percentage inhibition of the DPPH radical and was determined by the following equation:

$$\text{AOA} \quad (\%) = \frac{\text{Abs}_{\text{control}} - \text{Abs}_{\text{sample}}}{\text{Abs}_{\text{control}}} \times 100$$

Where AOA=Antioxidant activity

$\text{Abs}_{\text{control}}$ = Absorbance Control

$\text{Abs}_{\text{sample}}$ = Absorbance Sample

4.1.5 Standard of gallic acid, caffeine and catechins on HPLC

Each standard was mixed in 70% methanol (mg/ml) stock solution and injected into HPLC. Chromatograms showed the retention time of each standard. Retention time of each standard was compared with retention time of each sample of orthodox black tea.

4.1.6 HPLC Results of Kangra Tea samples

Fig. 4.1.1 shows the HPLC chromatogram of standard tea compounds (EGC, CAF, EC, EGCG and ECG).

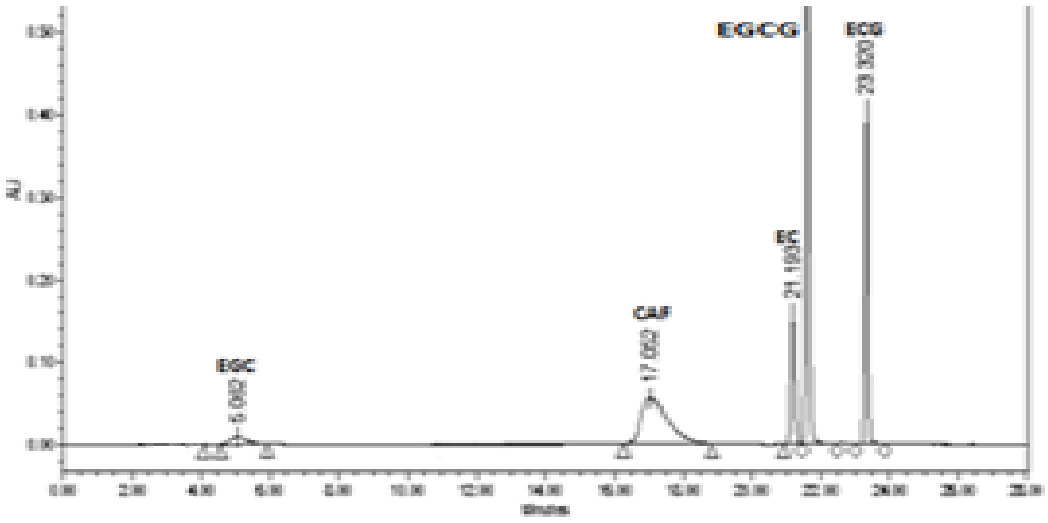

Fig. 4.1.1: HPLC chromatogram of standard mixture of catechins and caffeine

The RT for EGC can be seen at 5, CAF comes at 17, EC is evident at 21, EGCG at around 21.7 and ECG at 23.5 minutes.

Fig. 4.1.2 shows HPLC chromatogram of Kangra black tea with various peaks corresponding to the different compounds present in tea.

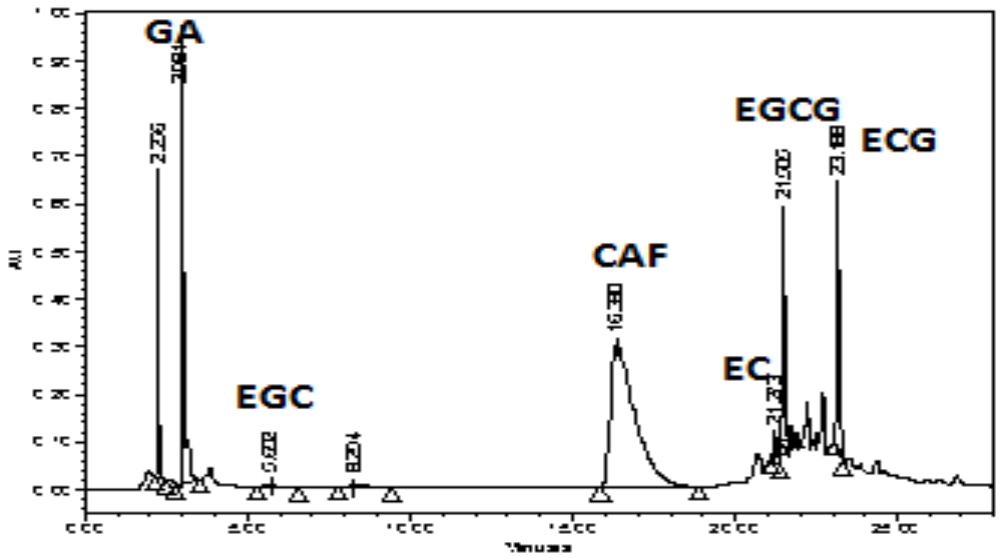

Fig. 4.1.2: HPLC chromatogram for Kangra black tea

The chromatogram of standard compounds in Fig 4.1.1 has been compared with the chromatogram of Kangra black tea in Fig. 4.1.2.

Table 4.1.2: RT of standard and Kangra tea samples (in minutes)

Compound	RT in standard (mins.)	RT in Kangra tea sample (mins.)
EGC	**5.0**	**5.0**
CAF	**17.0**	**16.3**
EC	**21.0**	**21.0**
EGCG	**21.5**	**21.0**
ECG	**23.7**	**24.0**

The average results obtained on peak area calculations are shown in Table 4.1.3.

Table 4.1.3: Mean chemical concentrations in Kangra tea samples as measured in (% weight by weight) by HPLC

S.No.	EGC*	Cat*	EC*	EGCG*	ECG*	CAF*
1	0.050 ±0.002	0.110 ±0.01	0.060± 0.002	1.390 ±0.02	0.390 ±0.02	0.830 ± 0.02
2	0.040 ±0.001	0.100 ±0.01	0.050 ±0.001	1.140 ± 0.02	0.310 ±0.03	0.640 ±0.01
3	0.050 ±0.002	0.090 ±0.002	0.059 ±0.002	1.500 ±0.02	0.470 ±0.02	0.800 ± 0.02
4	0.058 ±0.001	0.090 ±0.001	0.050 ±0.002	1.340 ±0.11	0.390 ±0.04	0.520 ± 0.01
5	0.060 ±0.002	0.100 ±0.01	0.060 ±0.001	1.920 ±0.01	0.560 ±0.03	0.830 ± 0.01
6	0.050 ±0.001	0.100 ±0.02	0.060 ±0.003	1.810 ±0.01	0.460 ±0.02	0.940 ± 0.01
7	0.130 ±0.01	0.090 ±0.001	0.060 ±0.002	0.880 ±0.02	0.320 ±0.01	0.550 ± 0.02
8	0.020 ±0.003	0.100 ±0.002	0.042 ±0.001	0.740 ±0.01	0.260 ±0.01	0.410 ±0.02

9	0.030 ± 0.002	0.090 ±0.002	0.040 ±0.002	0.560 ±0.03	0.125 ±0.02	0.370 ±0.02
10	0.100 ± 0.010	0.098 ±0.001	0.060 ±0.003	0.960 ±0.01	0.210 ±0.02	0.500 ±0.02
11	0.120 ± 0.010	0.100± 0.001	0.060 ±0.002	1.240 ±0.02	0.430 ±0.03	0.650 ±0.01
12	0.070 ± 0.001	0.100 ±0.002	0.050 ±0.001	0.850 ±0.01	0.250 ±0.01	0.430 ±0.01

**Note: An average of three mean values; values with ± represents standard deviation (SD)*

In tea, catechins or flavan-3-ol dominates the total polyphenols present in the tea. Flavan-3-ols in all types of teas comprises of mainly six catechins i.e. catechin (CAT), epicatechin (EC), epicatechin gallate (ECG), epigallocatechin (EGC), catechin gallate (CG) and epigallocatechin gallate (EGCG) [209].

Kangra valley tea samples are taken from 3 different flush seasons depending upon different manufacturing conditions i.e. early flush, rains flush and backend flush. Samples 1-4 are taken from early flush, 5-8 from rains flush and 9-12 belongs to backend flush. Table 4.1.3 shows the mean chemical concentrations in Kangra tea samples as measured by HPLC**.** Comparatively EGCG is found to be higher in all Kangra tea samples used in this study. An amount of EGCG lies between 0.560-1.920, whereas EGC (%) falls in the range 0.020-0.130. 0.090-0.110 is CAT (%) range, EC lies in 0.042-0.060, ECG (%) lies 0.125 - 0.560, CAF (%) 0.370-0.940.

The rainy flush tea samples shows highest amount of catechins which indicates, that this flush of tea samples are best in quality as compared to other flush tea samples.

4.1.7 HPLC analysis of CTC Assam tea samples

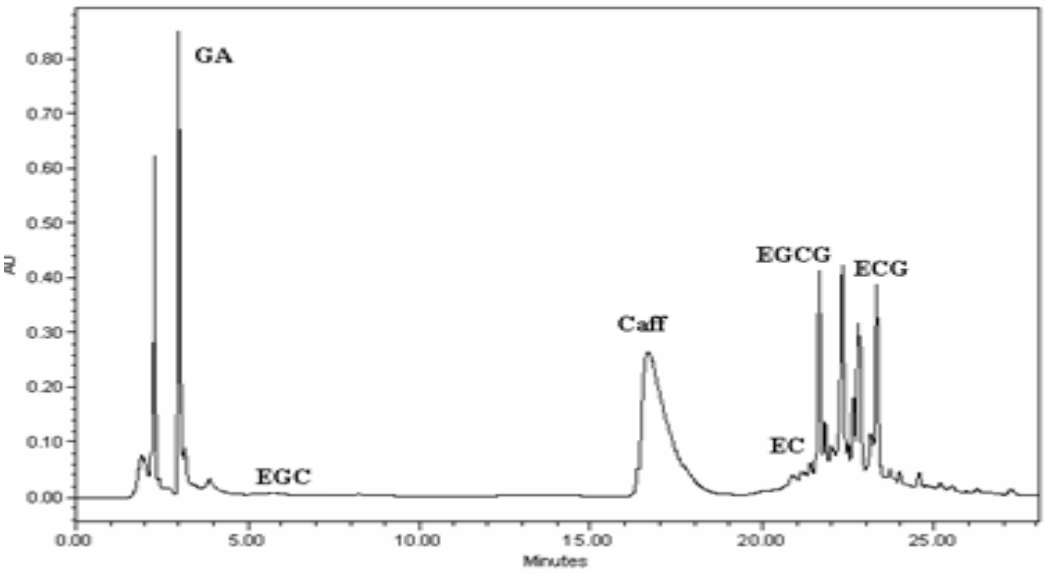

Fig. 4.1.3: HPLC chromatogram for CTC tea samples

The chromatogram in Fig. 4.1.3 of CTC Assam black tea is also compared to the chromatogram of standard tea compounds and the results are shown in table below.

Table 4.1.4: RT of standard and CTC Assam tea (in minutes)

Compounds	RT of standard (mins.)	RT of CTC Assam tea (mins.)
EGC	**5.0**	**5.0**
CAF	**17.0**	**17.0**
EC	**21.0**	**20.8**
EGCG	**21.5**	**21.2**
ECG	**23.7**	**23.6**

Tea manufacturing is normally carried out in two ways, (i) CTC and (ii) orthodox; CTC refers to the Crush Tear and Curl process where the withered green leaves are passed in-between two rollers rotating in opposite directions. CTC contains higher TF and TR than orthodox teas due to during manufacturing larger surface area in CTC which increases fermentation process. It means larger conversion of catechins into TF and TR.

Table 4.1.5: Mean chemical concentrations in CTC tea samples as measured (in % weight by weight) by HPLC

Samples	**EGC***	**CAT***	**EC***	**EGCG***	**ECG***	**Caffeine***
1	0.025 ±0.003	0.024±0.002	0.320±0.001	2.342±0.003	0.320±0.004	0.250±0.002
2	0.035 ±0.001	0.035±0.001	0.210±0.002	1.250±0.004	0.450±0.003	0.365±0.001
3	0.048±0.002	0.042±0.002	0.450±0.003	1.345±0.002	0.250±0.001	0.546±0.003
4	0.051±0.002	0.042±0.004	0.250±0.001	2.354±0.001	0.450±0.002	0.876±0.002
5	0.062±0.002	0.074±0.003	0.210±0.002	2.451±0.001	0.710±0.002	0.452±0.004
6	0.042±0.001	0.065±0.002	0.350±0.002	1.254±0.002	0.460±0.002	0.648±0.001
7	0.013±0.003	0.054±0.003	0.210±0.001	1.236±0.001	0.380±0.003	0.475±0.002
8	0.042±0.001	0.036±0.001	0.420±0.004	1.253±0.001	0.230±0.001	0.623±0.003

**Note: An average of three mean values; values with ± represents standard deviation (SD)*

CTC Assam tea samples divided into 1,2,3,4,5,6,7 and 8 are Jan-Feb, March-April, May-June, July, Aug, Sept, Oct, Nov-Dec respectively obtained during different flush seasons. Table 4.1.5 shows mean chemical concentrations in CTC tea samples as measured by HPLC. The EGC concentrations in Assam tea were found lower in comparison to Kangra tea samples and ranged from 0.013 to 0.062. Catechin concentration lies in 0.024 to 0.074 and was higher in case of Kangra tea samples and lower for CTC Assam tea sample. EC range lies from 0.210 to 0.450 and was high for Kangra tea and lower for CTC Assam tea samples. EGCG was high

for CTC Assam tea samples and less for Kangra tea samples and lay in range 1.236 to 2.451. ECG lay in the range 0.230 to 0.710 and was higher for CTC Assam tea samples than Kangra tea samples. Caffeine ranged from 0.250 to 0.876 and was higher for Kangra tea samples than CTC Assam tea samples.

4.1.8 UV-Vis studies of Kangra and CTC Assam tea samples

Mean chemical concentrations of TF and TR for Kangra tea samples have been shown in Table 4.1.6 carried out using UV-VIS technique.

Table 4.1.6: Mean chemical concentrations of TF and TR **(% weight by weight)** in Kangra tea samples Using UV-VIS *(p>0.05)*

Samples	**TF**	**TR**
1	0.860 ±0.01	6.304 ±0.3
2	0.894 ±0.03	6.529 ±0.02
3	0.924 ±0.02	6.929 ±0.04
4	0.836 ±0.02	6.727 ±0.02
5	0.936 ±0.02	7.289 ±0.02
6	0.902 ±0.03	7.732 ±0.03
7	0.884 ±0.02	6.234 ±0.02
8	0.892 ±0.04	6.436 ±0.03
9	0.845 ±0.03	6.104 ±0.02
10	0.912 ±0.03	7.123 ±0.04
11	0.902 ±0.02	7.203 ±0.03
12	0.882 ±0.02	6.543 ±0.03

Note: An average of three mean values; values with ± represents standard deviation (SD)

Catechins are the major biochemical constituents present in tea leaves and are oxidized to form theaflavins (TFs) and thearubigins (TR) during fermentation [210].

Theaflavins are composed of simple theaflavin (TF), theaflavin-3-gallate (TF-3-G), theaflavin-3'-gallate (TF 3'-G) and theaflavin-3,3'-digallate (TF-3,3'-DG) . In our teas TF lies in 0.882 - 0.924 and TR lies in the range 6.104 - 7.732 as given in Table 4.1.6. Theaflavins and thearubigin imparts yellow and orange colour to tea infusion.

Table 4.1.7: Mean chemical concentrations in CTC tea samples (in % weight by weight) as measured by UV-VIS *(p>0.05)*

Samples	**TF**	**TR**
1	1.351 ±0.02	7.256 ±0.02
2	1.451 ±0.03	8.354 ±0.04
3	1.484 ±0.02	8.000±0.03
4	1.253±0.02	6.341 ±0.02
5	1.240±0.01	7.325 ±0.03
6	1.243 ±0.01	6.235 ±0.02
7	1.352 ±0.02	7.325 ±0.02
8	1.250 ±0.02	6.325 ±0.01

Note: An average of three mean values; values with ± represents standard deviation (SD)

Table 4.1.7 gives the mean chemical concentrations in CTC tea samples as measured by UV-VIS. TF ranged from 1.2 to 1.4 and found higher in CTC Assam tea samples than Kangra tea samples. TR lies in the range 6.2 to 8.3 and can be observed almost in the same range for Kangra tea samples.

4.1.9 Antioxidant activity study of Kangra and CTC tea samples

The antioxidant activity of Kangra and CTC Assam tea is shown in Table 4.1.8 and Table 4.1.9 respectively.

Table 4.1.8: Antioxidant activity for all Kangra tea samples *(p>0.05)*

Sample	**% Inhibition**
1	88.300 ±0.1
2	87.100 ±0.2
3	88.200 ±0.3
4	89.700 ±0.3
5	89.400 ±0.4
6	88.000 ±0.3
7	89.700 ±0.2
8	88.500 ±0.2
9	88.300 ±0.4
10	89.400 ±0.3
11	86.800 ±0.2
12	88.600 ±0.2

Note: An average of three mean values; values with ± represents standard deviation (SD)

Antioxidant activity for all Kangra tea samples is presented in Table 4.1.8 which shows the antioxidant activity was minimum in tea sample 11 which represents for tea sample from 3rd flush, whereas it was maximum for tea samples 4th and 7th which stand for tea samples of 1st and 2nd flush respectively. Antioxidant activity of tea is primarily due to phenolics viz.

catechins, theaflavins, thearubigins etc. present in tea which constitutes a large number of –OH groups. These compounds are also responsible for strength, taste and colour to tea.

Maximum amount of TF and TR are found in CTC Assam tea samples as compared with Kangra tea samples. In Kangra tea samples higher amount of CAT, EC, EGCG, ECG and CAF can be seen for tea samples of Rainy flush among tea samples from 1st flush and 3rd flush tea samples. Minimum amount of catechins can be seen for last flush tea samples reason being the quality of tea deteriorates in the last flush.

Table 4.1.9: Antioxidant activity for all CTC tea samples *(p>0.05)*

Samples	**% Inhibition**
1	89.200 ±0.4
2	83.640 ±0.2
3	87.360 ±0.3
4	91.230 ±0.4
5	90.140 ±0.2
6	90.670 ±0.3
7	86.460 ±0.3
8	84.360 ±0.4

Note: An average of three mean values; values with ± represents standard deviation (SD)

In general the Antioxidant activity was found higher of CTC Assam tea samples in comparison to Kangra tea samples. This is evident from Table 4.1.9 which compared the antioxidant activities for all CTC tea samples.

Conclusion: The HPLC study of tea samples suggested that tea samples of Kangra and CTC Assam tea can be classified based on seasonal variations. From HPLC and UV-VIS study we can make out that the tea samples from rainy flush are efficiently good in chemical composition among tea samples from early rains and after rains.

CHAPTER 4.2

RESULT AND DISCUSSIONS

Impedance measurement were done at -1,0 +1 V amplitude (DC bias) at 0.005 V peak amplitude for 60 seconds in frequency range from 1 to 100 K Hz, at 20 ± 2 ºC. For each study 10 ml of working solution (tea liquor) was taken in electrochemical cell and dissolved oxygen was removed by bubbling nitrogen gas. Impedance data for each tea sample with specific tastant solution was studied employing all the five sensing electrodes as an array. The measurements was carried out as DI water as blank sample followed by tea liquor sample K1-K12 prepared in the same blank DI water, followed by various tastant solutions.

The measurements were carried out on each solution under similar experimental conditions using the six electrodes. Studies were also conducted on various beverages by mixing it with tea, milk and other compounds to generate various tastants. All the measurements were made continuously over 30 days for each sample using 6 set of sensing electrodes. The RSD value of about ±2% was observed. Each electrode was washed with distilled water and dried in nitrogen before use every day.

No significant difference in the impedance spectra at -1, 0 and +1V DC bias was observed. Hence, all measurements were carried out at +1V DC bias voltage. At still higher frequencies, the impedance converges to a single value independent of the sensor composition and only relates to the conductivity of the system whereas at lower frequencies, high variance in the readings for the same sample was observed due to the ambient noise. To ensure best discrimination, the impedance at 100 Hz was selected, but in our studies we have taken the

data 1 Hz-100 KHz to make the system more comprehensive and analyze in best practical mode.

The impedance response of working electrodes can be analyzed by an electrical equivalent circuit describing the electrical behaviour of the electrode-electrolyte interface [211-213]. Generally, an electrode-electrolyte interface is presented by a parallel combination of capacitance and resistance, taking into account the electrolyte impedance. The low frequency region in such studies are dominated by double layer effect, for the region between 10^2 Hz to 10^5 Hz the dominant effect comes from the surface coating, whereas for frequencies higher than 10^5 Hz the impedance behaviour of the system is dominated by the geometric capacitance [212, 214].

The sensitivity depends upon the combined effect of the impedance spectra of different sensing surfaces. The overall analysis is quite complicated due to high number of attributes, thus the figure of merit depends upon the type of sensing electrode, concentration of the solution and type of molecules. Therefore, in order to reduce the input dimensionality and to give a percipient graphical description, a statistical technique called Principal Component Analysis (PCA) was used.

Therefore, all the results were discussed in the mid frequency region of 1 Hz-100 KHz. The response of each sensing electrode was checked by measuring the impedance value of DI water before and after the measurement in various tea liquor samples and other tastants. The observed difference in the impedance behaviour of different sensors for DI water and tea liquors and other tastants might be attributed to electrical interaction at the sensing surface. Impedance behaviour of Au, Pt and Glassy Carbon electrode for each solution gives a specific pattern due to conducting nature of sensing surface. Contribution from surface film resistance

like oxide film, also play some role but in above case this value is minimum. Thus impedance values are nearly equal to solution resistance between metal and reference electrode. Similar results on some metal electrodes were also reported earlier.

4.2.1 Impedance study of tea liquor samples using GC electrode

The impedance studies were carried out using 3 cell electrode with Pt wire as counter electrode, Ag/AgCl as reference electrode and **GC as a working/sensing electrode**. The behaviour of DI water using GC electrode is shown in Fig. 4.2.1 which shows the impedance response of GC electrode in the frequency range 1 Hz to 100 KHz with amplitude 0.005 V. Deionization is the removal of ions – positive (cation) and negative (anion) – from the water. Since DI water has no dissolved solids, water will seek equilibrium with whatever it contacts. It will react under certain conditions with anything it comes in contact with, especially metals and alloys like calcium, magnesium, copper, brass.

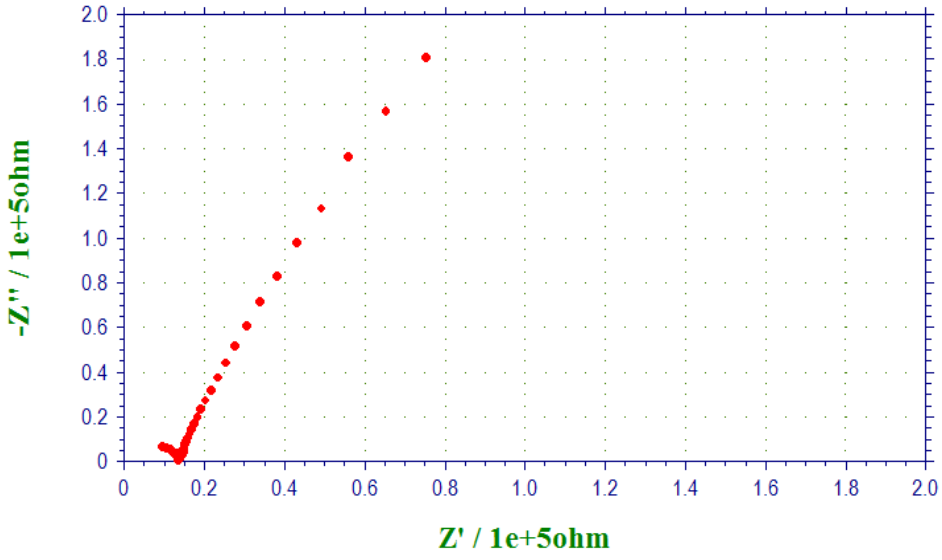

Fig. 4.2.1: Nyquist plot for DI water using GC electrode

The fitting of the impedance plot in figure above to the electrical equivalent circuit follows the Fig. 4.2.1 (a) circuit model. Semicircular arc was observed from Nyquist plot, as well as 45^0 straight line to the Z real axis. These semicircle represent charge transfer resistance while the 45^0 line represent Warburg impedance. Warburg Impedance is associated with diffusion [215]. Diffusion starts at almost the same frequency for all electrode lengths (L) in the low frequency region. The DI water is an ion free liquid that attempts to bring the solution to equilibrium when it comes in contact with the metal electrode by collecting ions from the solid, after which diffusion starts. Due to the slowness of the process, diffusion occurs only in the low frequency region.

Solution resistance is higher in case of DI water. The impedance values are of the order of 10^4 ohms indicating that the system is more resistive and after sometime there is a diffusion which may be due to some dissolved compounds from air and atmosphere or container by keeping the DI water stored for some time. The electronic equivalent circuit responsible for GC behaviour is given in Fig. 4.2.1 (a) [215].

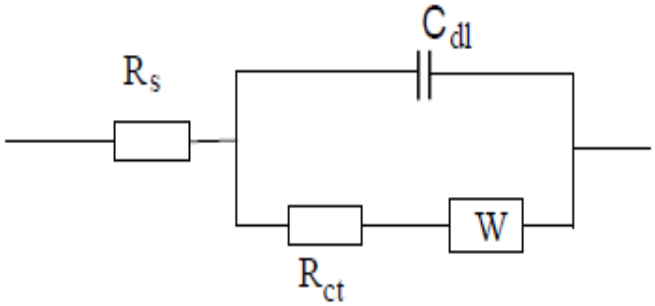

Fig. 4.2.1 (a): Equivalent circuit model for GC electrode

The physical model explaining this phenomenon is shown in Fig. 4.2.1 (a) electrical equivalent circuit model. This behaviour can be attributed to the polarization which is due to

the combination of kinetics and diffusion processes. The impedance data were simulated in terms of the Randle's equivalent circuit consisting of a parallel combination of the double layer capacitance (Cdl) and charge transfer resistance of redox electrochemical reactions (Rct) at equilibrium, since the over potential is very low in series with the resistivity of water as an electrolyte (Rs) [216].

The diffusion phenomenon occurs at the solution–electrode interface, as there is no stirring of solution and is represented by Warburg impedance (W) [217-218].

The fitting of impedance plots in Fig. 4.2.1 to the equivalent circuit has indicated a good agreement between the circuit model and the real experimental data, especially at the high frequency values. Similar response in DI water was observed for GC, Pt sensing electrodes.

Some of the experimental results of the real/virtual impedance, total impedance and phase shift for DI water using GC electrode are given in Table 4.2.1.

Table 4.2.1: Impedance data for DI water using GC electrode

Freq/Hz	Z'/ohm	Z"/ohm	Z/ohm	Phase/deg
9.668×10^4	9.723×10^3	-6.275×10^3	1.157×10^4	-32.8
5.469×10^4	1.204×10^4	-4.560×10^3	1.287×10^4	-20.7
1.758×10^4	1.372×10^4	-1.857×10^3	1.385×10^4	-7.7
9.668×10^3	1.359×10^4	-9.329×10^2	1.362×10^4	-3.9
4.590×10^2	1.388×10^4	-1.465×10^3	1.396×10^4	-6.0
2.148×10^2	1.431×10^4	-2.603×10^3	1.454×10^4	-10.3
1.758×10^2	1.44×10^4	-3.035×10^3	1.478×10^4	-11.9
97.66	1.461×10^4	-4.754×10^3	1.536×10^4	-18.0
8.071	2.346×10^4	-3.732×10^4	4.408×10^4	-57.9
1.184	7.540×10^4	-1.807×10^5	1.958×10^5	-67.4

The impedance value in the whole range lies nearly same in the order of 10^4 - 10^5 ohm with a variable phase angle, indicating that the electrode can operate with stability and not much variation in the resistivity/impedance values. The Z' lies in the range 9723 to 75400 ohm and Z'' lies in the range -6275 to -18070 ohm for DI water. Similar behaviour was observed for Pt and Au sensing surfaces.

The electrochemical impedance data is presented in the form of Bode plots in which logarithm of the impedance modulus |Z| and the phase angle Ø are plotted versus log of frequency (f) of the applied AC signal to relate the electrical elements.

The impedance spectra measured for the cathode (working electrode here is GC) in Fig. 4.2.2 shows the one time constant model (OTCM) in which solution resistance Rs is in series with the parallel combination of the capacitance of the electrode and its polarization resistance Rct. This was kept as a reference point, further studies of beverages and other tastants compounds was carried keeping frequency parameters like potential scale etc is kept constant. The Bode plot format helps in identifying the frequency break points associated with each limiting step.

The Bode plot provides a clearer description of the electrochemical system's frequency-dependent behaviour than does the Nyquist plot, in which frequency values are implicit rather than explicit.

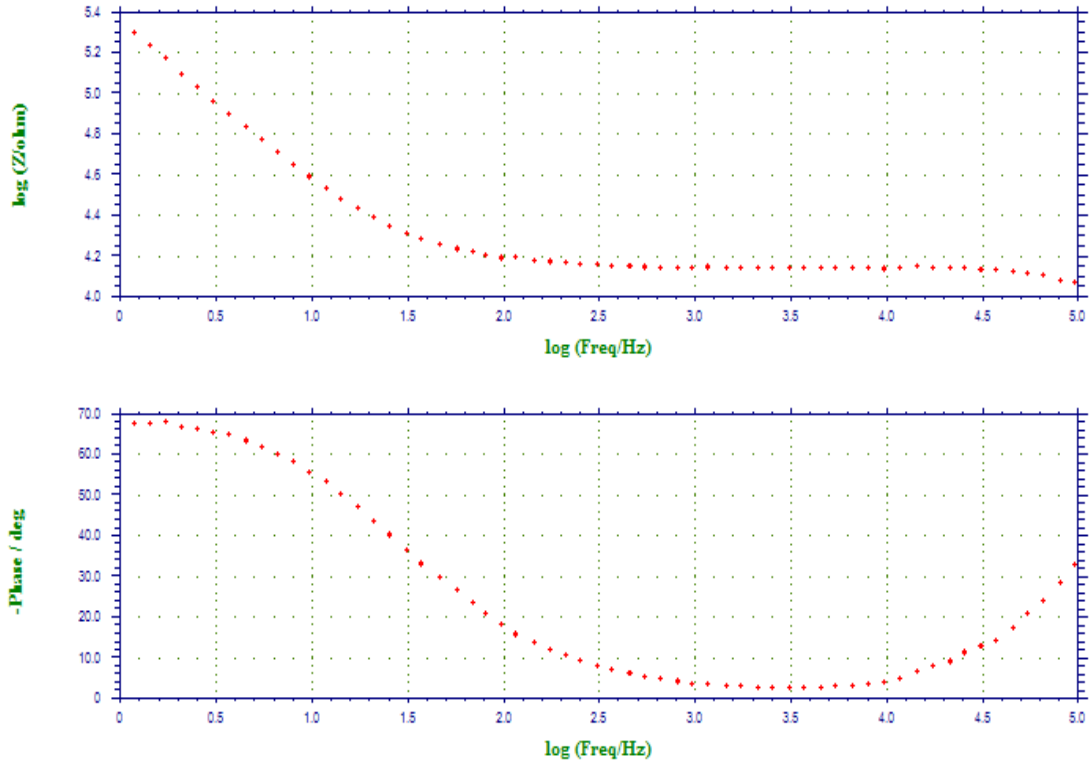

Fig. 4.2.2: Bode plot for DI water using GC electrode

Bode plot for GC electrode is shown in figure 4.2.2**.** Bode plot is a useful method for estimating the amplitude and phase response of the 2 port networks using straight line segments or asymmetric line segment. However, we have examined in our study the behaviour by considering two extreme ends of frequency about 1 or less where it behaves as DC circuit and other end of high frequency in our case 10^5 Hz for maximum reactance values.

It can be seen from the figure of Bode plot that the frequency dependence of Φ in low freq region of the spectra indicates that the polarization resistance of the GC electrode is quite high and starts decreasing in a continuous manner and becomes nearly constant between 100- 1000 Hz, showing that the oxygen reduction is much faster in water at low frequency. Moreover

from the spectra higher value of the capacitance of the GC is due to higher active surface area of this electrode.

The tea samples from Kangra valley were prepared as described in chapter III (Experimental section). The tea liquor samples were taken in the same set up and the parameters were kept constant as reported for DI water. In this impedance study 12 different samples of Kangra tea liquor were studied, however individual data of K1 and K7 tea liquor sample with GC electrode is shown in Fig. 4.2.3 and Fig. 4.2.4 and clubbed impedance data for all 12 tea samples is given in Fig. 4.2.7.

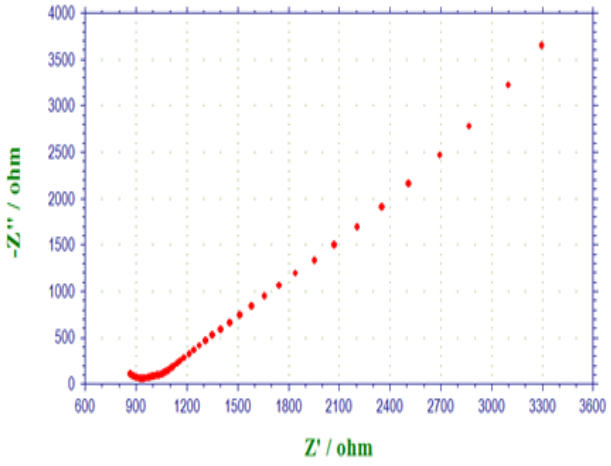

Fig. 4.2.3: Nyquist plot for K1 tea using GC

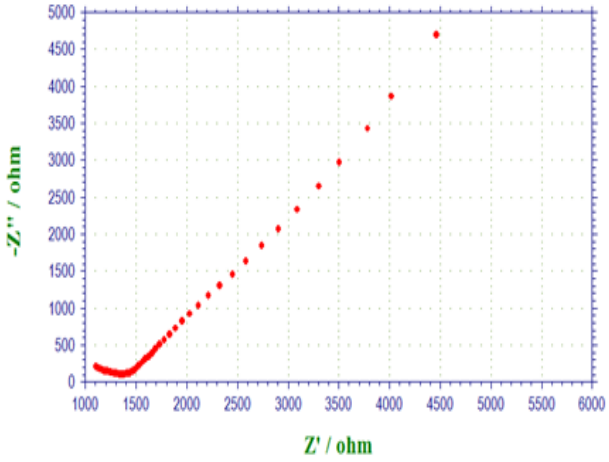

Fig. 4.2.4: Nyquist plot for K7 tea using GC

The nyquist plots for tea sample 1 of kangra valley and tea sample 7 of Kangra valley shows the impedance variations in the order of around 1000 Ohm. This variation is quite different than the GC electrode response for DI water as the impedance values are of the order of 10^4

ohm, since DI water is the purest form of water whereas tea liquor has soluble contents of chemical compounds e.g. polysaccharides, volatile oils, vitamins, minerals, purines, alkaloids (eg.caffeine), polyphenols (catechins and flavonoids) and tannins etc due to the presence of these ions/molecules the nyquist plot shows a change in impedance values.

Table 4.2.2 shows the actual values of the real/virtual impedance, total impedance and phase shift for K1 tea sample using GC electrode.

Table 4.2.2: Impedance data for K1 tea using GC sensing electrode

Freq/Hz	Z'/ohm	Z"/ohm	Z/ohm	Phase/deg
9.668×10^4	8.693×10^2	-1.031×10^2	8.754×10^2	-6.8
1.172×10^4	9.336×10^2	- 59.55	9.355×10^2	-3.6
9.668×10^3	9.444×10^2	-59.33	9.462×10^2	-3.6
4.590×10^3	9.679×10^2	-64.88	9.701×10^2	-3.8
1.758×10^3	1.005×10^3	- 81.32	1.008×10^3	-4.6
9.668×10^2	1.036×10^3	-91.23	1.040×10^3	-5.0
1.172×10^2	1.184×10^3	-2.807×10^2	1.217×10^3	-13.3
57.44	1.311×10^3	-4.628×10^2	1.390×10^3	-19.4
9.766	1.956×10^3	-1.331×10^3	2.366×10^3	-34.2
1.184	4.104×10^3	-5.782×10^3	7.091×10^3	-54.6

The impedance values in the whole range lies in the order of $10^2 – 10^3$ ohm with a variable phase angle. Bode plots shows one time constant model for this type of impedance response.

The Z' value for DI water comes at 9.723 x 10^3 ohm whereas for K1 tea sample is 8.693 x 10^2 ohm, Z" is -6.275 x 10^3 ohm for DI water and -1.031 x 10^2 ohm for K1 tea sample. Z lies at 1.157 x 10^4 ohm and 8.754 x 10^2 ohm for K1 tea sample. Phase/deg is -32.8 for DI water, whereas for K1 tea sample it is -6.8.

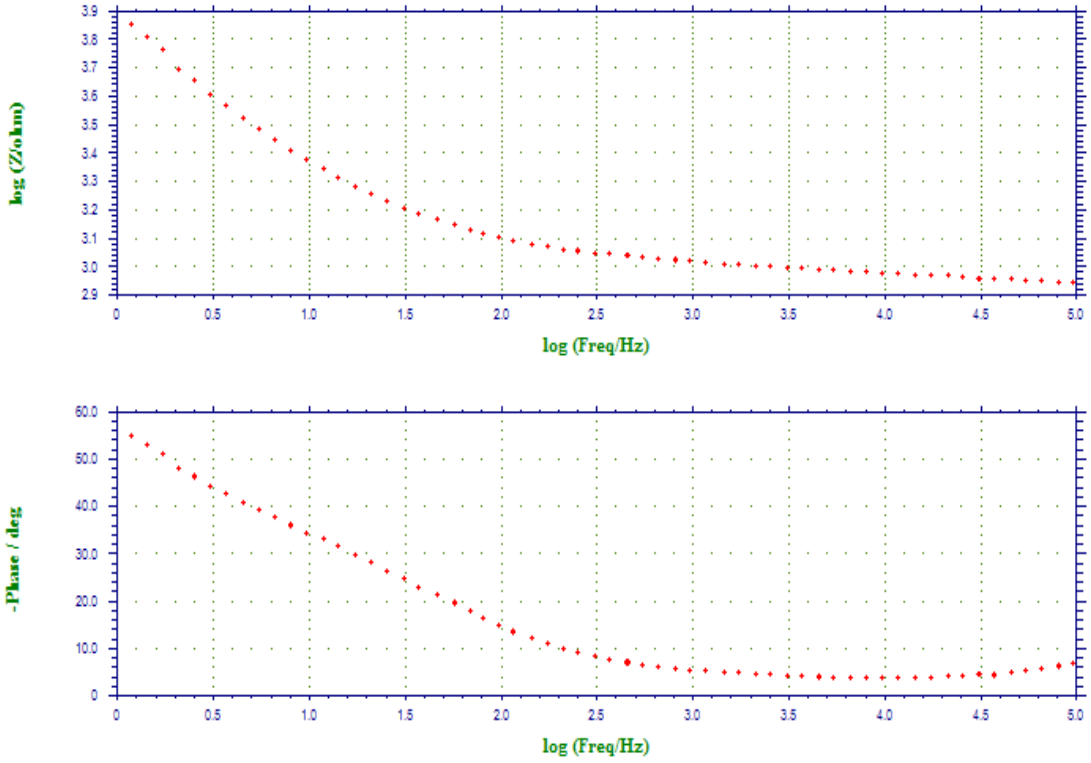

Fig. 4.2.5: Bode plot for K1 tea sample using GC electrode

Bode plot for K1 shows that the polarization resistance of the GC sensing electrode was found high and it tends to decrease in a continuous manner and becomes nearly constant between 100- 1000 Hz. With the increase in frequency, impedance tends to decrease. The phase angle of Warburg impedance is 45˚. Here Bode plot illustrate the differences in the slope of the magnitude and in the phase between the capacitor and the Warburg impedance. The Bode plot is segmented into two parts to provide more clarity in observing the impedance response.

The actual values of the real/virtual impedance; total impedance and phase shift are shown in table 4.2.3 for tea sample 7 of Kangra tea (K7) using GC sensing surface. The real impedance values lies in the range 1106 to 5014 ohm and imaginary impedance value lies in the range -210 to 6015 ohm.

Table 4.2.3: Impedance data for K7 tea sample using GC electrode

Freq/Hz,	Z'/ohm	Z"/ohm	Z/ohm	Phase/deg
9.668×10^4	1.106×10^3	-2.100×10^2	1.126×10^3	-10.8
1.465×10^4	1.262×10^3	-1.245×10^2	1.268×10^3	-5.6
9.668×10^3	1.292×10^3	-1.174×10^2	1.297×10^3	-5.2
4.590×10^3	1.338×10^3	-1.066×10^2	1.343×10^3	-4.6
1.172×10^3	1.414×10^3	-1.159×10^2	1.419×10^3	-4.7
9.668×10^2	1.428×10^3	-1.103×10^2	1.432×10^3	-4.4
1.172×10^2	1.595×10^3	-3.122×10^2	1.625×10^3	-11.1
97.66	1.630×10^3	-3.443×10^2	1.666×10^3	-11.9
11.91	2.324×10^3	-1.306×10^3	2.666×10^3	-29.3
1.184	5.014×10^3	-6.015×10^3	7.830×10^3	-50.2

The impedance values for K7 in the whole range lies in the order of 10^3 ohm with a variable phase angle. The impedance spectra here displays single time constant model.

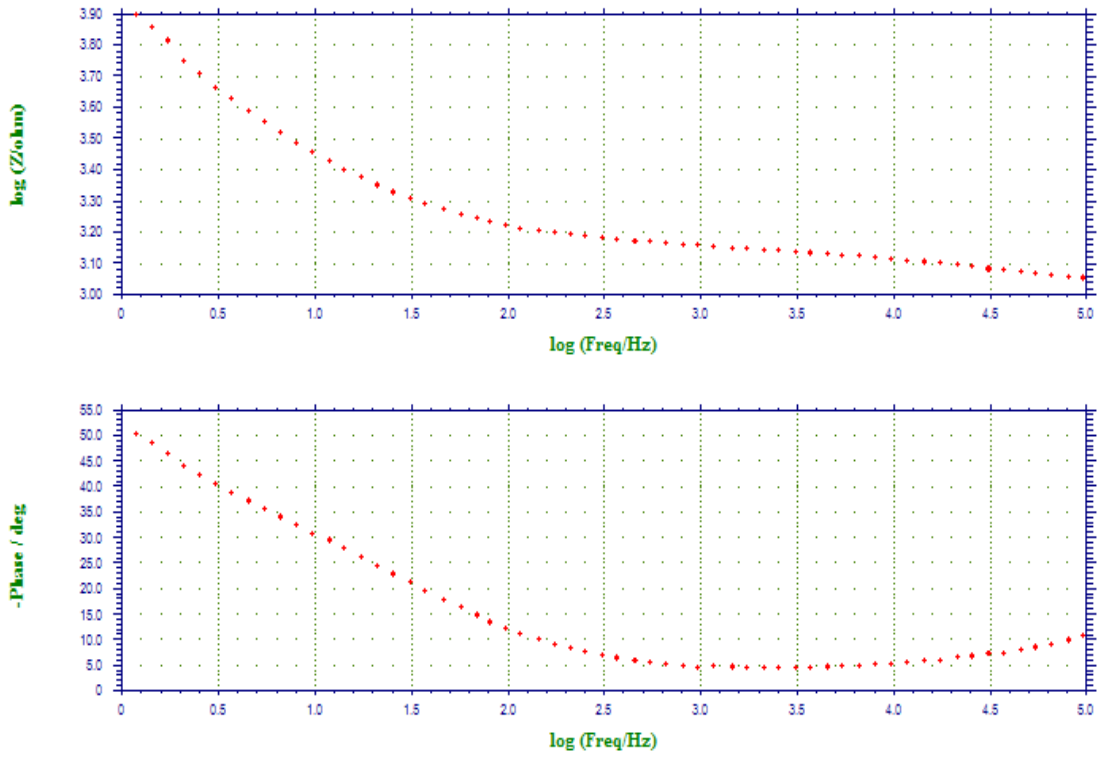

Fig. 4.2.6: Bode plot for K7 tea sample using GC electrode

It can be seen from the figure of Bode plot for K7 tea liquor sample that the behaviour of Bode plot for K1 tea sample resembles the Bode behaviour of K7 tea sample and follows one time constant model of electrical equivalent circuit in which the solution resistance is in series with a parallel combination of the polarization resistance and the electrode capacitance.

The rate of an electrochemical reaction can be strongly influenced by diffusion of a reactance towards or a product away from the electrode surface. This is often the case when a solution species must diffuse through the electrode surface. This situation is apparent in this case as the solution components got adsorbed on the surface of electrode, as the diffusion effects completely dominates the electrochemical reaction mechanism, the impedance becomes Warburg [219].

The straight line represents a faster mass-transfer limited process at lower frequencies whereas the semi-circular portion describes a relatively slower charge transfer limited process at higher frequencies. The model predicts the fitting of impedance plots in fig. 4.2.3 and fig. 4.2.4 to the equivalent circuit of fig. 4.2.1 (a) [220] which is same in case of DI water.

Fig. 4.2.7 shows the Nyquist plots for all the 12 different tea samples of Kangra valley, in a single impedance plot by overlaying the readings to one another. The parameters were kept constant throughout the study.

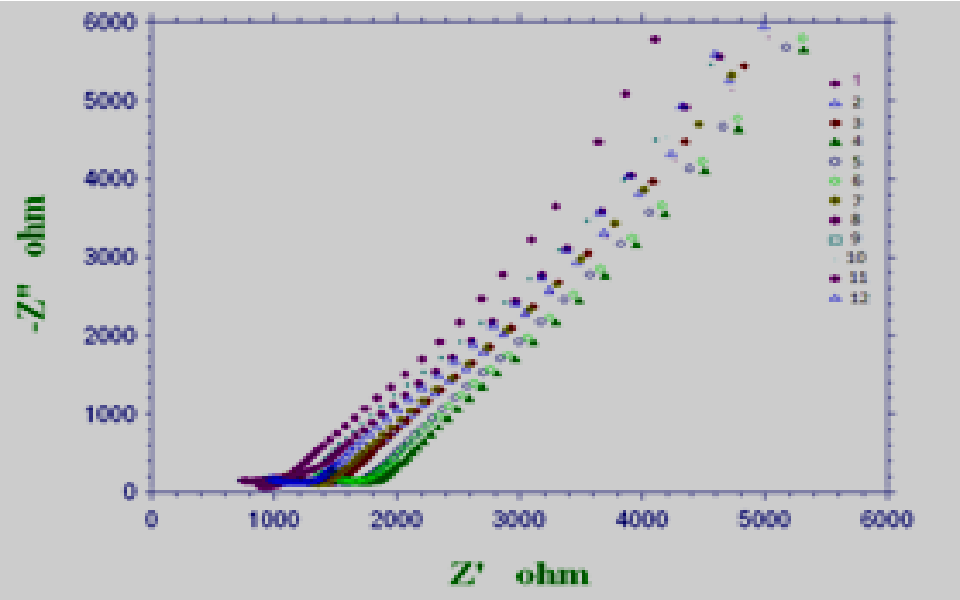

Fig. 4.2.7: Impedance plot of GC electrode for all the 12 Kangra valley tea liquor samples

All these impedance response show almost similar behaviour as impedance circuit is plotted in the complex plane. A small semi-circle combined with a straight line at an angle of 45° to the real axis can be seen, which may be due to Warburg impedance representing Randle's equivalent circuit in Fig. 4.2.1(a) with Warburg impedance element [221].

These oblique lines 45° lines represent the double layer behaviour of electrode and electrolyte. The response of these tea samples at low frequencies revered a linear impedance locus with an angle of 45 to the real axis which amounts to low frequency Warburg response. However, at high frequency the impedance response of all tea samples showed a small semi circle. The impedance behaviour was studied in the same pattern as that of DI water where 10 ml of mixture and individual catechins was used. The standard preparation has been discussed in chapter 3.

4.2.2 Impedance study of tea polyphenol standards using GC electrode

Impedance spectra of each compound of Caffiene (CAF), Gallic Acid (GA), Epigallocatechin gallate (EGCG), Epicatechin gallate (ECG), Epigallocatechin (EGC), Epicatechin (EC) and Catechin (CAT) and their mixture using GC electrode having strength 0.25 mM in DI water was measured in the frequency range 1Hz-100 KHz is given in Fig. 4.2.8. The compounds EGC showed a small semicircle in high frequency region followed by a partially resolved semicircle in low frequency with impedance values in order of 10^4 ohm.

CAT also showed two semicircle larger diameter in its behaviour as an impedance response values, one fully resolved semicircle and other less resolved semicircle with higher impedance. On the other hand, all other polyphenolic compounds have a small semicircle followed by 45 degree Warburg response lines. In case of a solution having all these compounds and mixture present together the response was found to be a very small semicircle near the origin followed by a straight line which indicates warburg impedance. The diffusion occurs in a sharp way as the number of different molecules are competing with each other and the phenomenon takes place at much lower frequency than the individual component alone.

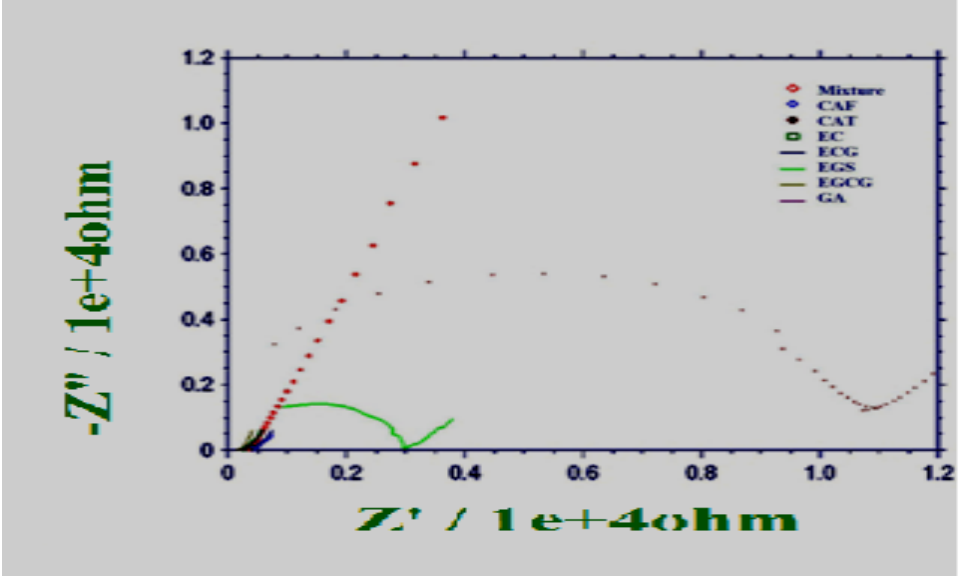

Fig. 4.2.8: Nyquist plot of some standard compounds and its mixture using GC

The values of resistance, R and capacitance, C, can be obtained by an equivalent circuit of one parallel resistance-capacitance (RC) element. On the complex plot one semicircular arc arises due to RC element, representing the grain effect. For grain the equivalent electrical equations are:

$$Z' = R + Rg/1 + (\omega RgCg)^2$$

$$Z'' = Rg[\omega RgCg/1 + (\omega RgCg)^2]$$

Rg and Cg are the grain resistance and grain capacitance respectively.

The CAT showed a semicircle both in high and low frequency corresponding to electron transfer limiting process. There is a short linear part at low frequency which may be attributed to diffusion limiting step of electrochemical process. EGC showed the first semicircle occurring in the high frequency region corresponds to the behaviour of bulk EGC compound while the second in low frequency region corresponds to electrode polarization or interfacial

interactions. The exact cause for this behaviour is not known, however it may be due to the difference in chemical structures of these compounds.

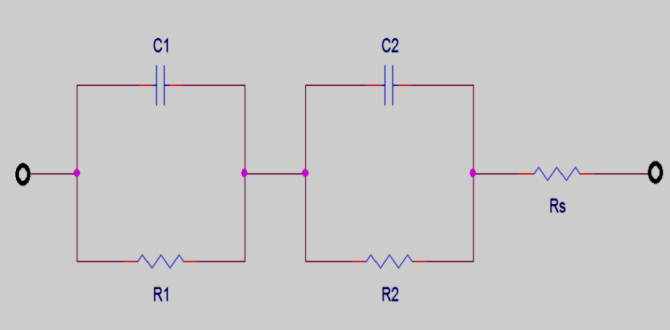

Fig. 4.2.8 (a): Bauerle's equivalent circuit

This response of CAT and EGC can be attributed to Bauerle's equivalent circuit (Fig. 4.2.8 (a). It was found that there are short linear parts at low frequencies (for CAF, GA, EGCG, ECG, EC and their mixture) resulting from the diffusion limiting step of the electrochemical process. The respective semicircles diameters at the high frequencies correspond to the charge transfer resistance at the electrode surface. The mixture of these compounds showed a straight line at an angle of 45°, whereas the semicircular behaviour has disappeared in this case which may be due to the domination of other (CAF, GA, EGCG, ECG, EC) antioxidant compounds over CAT and EGC.

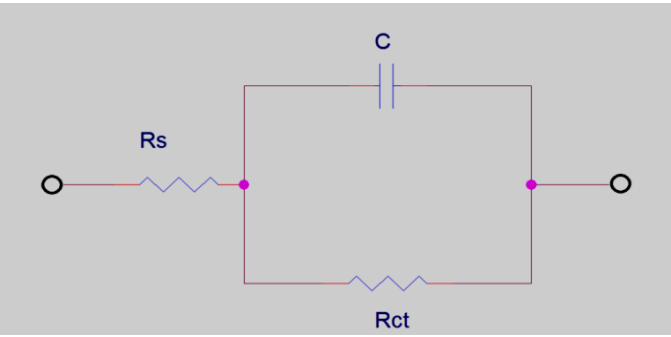

Fig. 4.2.8 (b): Randle's equivalent electrical circuit

When the impedance is plotted in the complex plane, we obtained a semicircle combined with a straight line at an angle of 45° to the real axis, arising due to Warburg impedance. The physical model explaining this phenomenon is Randle's equivalent electrical circuit (Fig. 4.2.8 (b) and the behaviour can be attributed to diffusion phenomenon occurring at the solution–electrode interface. The impedance data were simulated using the Randle's equivalent circuit consisting of a parallel combination of the capacitance (C) and charge transfer resistance by redox reactions (Rct) in series with the supporting electrolyte resistance (Rs). The fitting of spectra to the equivalent circuit has indicated a good agreement between the circuit model and the real experimental data, especially at the high frequency values.

The actual values of the real/virtual impedance, total impedance and phase shift for GC electrode for CAT is given in Table 4.2.4. The real impedance value lies in the range -5137 to 42680 ohm and the imaginary values of impedance lies in the range -37650 to -364900 ohm. This value is much higher than the real and imaginary impedance values of tea samples of Kangra tea.

Table 4.2.4: Impedance data for CAT using GC electrode

Freq/Hz	Z'/ohm	Z"/ohm	Z/ohm	Phase/deg
9.668×10^4	-5.137×10^3	-3.765×10^4	3.800×10^4	-97.8
6.641×10^4	-2.300×10^3	-6.158×10^4	6.162×10^4	-92.1
3.711×10^4	2.654×10^4	-1.153×10^5	1.183×10^5	-77.0
9.668×10^3	2.172×10^5	-1.339×10^5	2.551×10^5	-31.7
2.539×10^3	2.877×10^5	-4.505×10^4	2.912×10^5	-8.9
6.641×10^2	2.854×10^5	-1.524×10^4	2.858×10^5	-3.1
97.66	2.740×10^5	-1.289×10^4	2.743×10^5	-2.7
17.44	2.890×10^5	-3.819×10^4	2.915×10^5	-7.5
6.643	3.092×10^5	-7.757×10^4	3.188×10^5	-14.1
1.184	4.268×10^5	-3.649×10^5	5.616×10^5	-40.5

The impedance values in the whole range lies in the order of 10^4 - 10^5 ohm with a variable phase angle in the impedance data for CAT using GC electrode as given by Table 4.2.4.

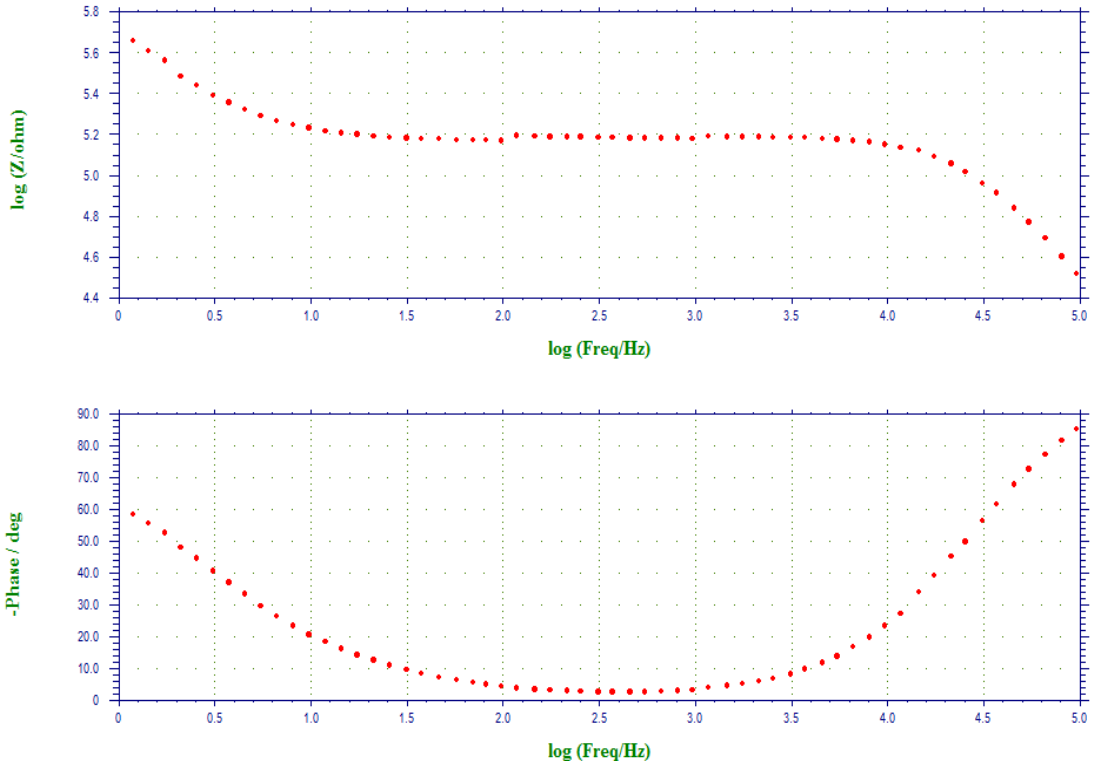

Fig. 4.2.9: Bode plot of CAT using GC electrode

The Bode plot for CAT is shown in Fig. 4.2.9 using GC sensing electrode. The Bode plot is segmented into two parts to provide more clarity in observing the impedance response. The phase angle of Warburg impedance is 45˚. Here Bode plot illustrate the differences in the slope of the magnitude and in the phase between the capacitor and the Warburg impedance.

The Bode plot shows here that the impedance is maximum at low frequency and starts decreasing with the increase in frequency and this follows two time constant model. The Bode

Response is almost similar to the response for DI water and K1 and K7 tea using GC electrode.

The actual values of the real/virtual impedance, total impedance and phase shift for GC electrode for mixture of all compounds is given in Table 4.2.5

Table 4.2.5: Impedance data for standard compound mixture using GC electrode

Freq/Hz	Z'/ohm	Z"/ohm	Z/ohm	Phase/deg
9.668×10^4	3.510×10^3	-8.966×10^2	3.623×10^3	-14.3
3.711×10^4	3.695×10^3	-3.950×10^2	3.716×10^3	-6.1
1.172×10^4	3.754×10^3	-1.985×10^2	3.759×10^3	-3.0
9.668×10^3	3.759×10^3	-1.692×10^2	3.763×10^3	-2.6
2.539×10^3	3.841×10^3	-2.752×10^2	3.851×10^3	-4.1
4.590×10^2	4.102×10^3	-8.682×10^2	4.193×10^3	-12.0
97.66	4.818×10^3	-2.869×10^3	5.607×10^3	-30.8
25.70	6.684×10^3	-8.412×10^3	1.074×10^4	-51.5
3.742	1.698×10^4	-3.933×10^4	4.284×10^4	-66.7
1.184	3.622×10^4	-1.017×10^5	1.079×10^5	-70.4

The impedance values in the whole range lies in the order of $10^3 – 10^4$ ohm with a variable phase angle whereas, for CAT the impedance value lies in the order 10^4 to 10^5 ohm with a variable phase angle. The Z’ lies in the 3510 to 36220 range and Z’’ values lie in the range 896 to -10170 ohm.

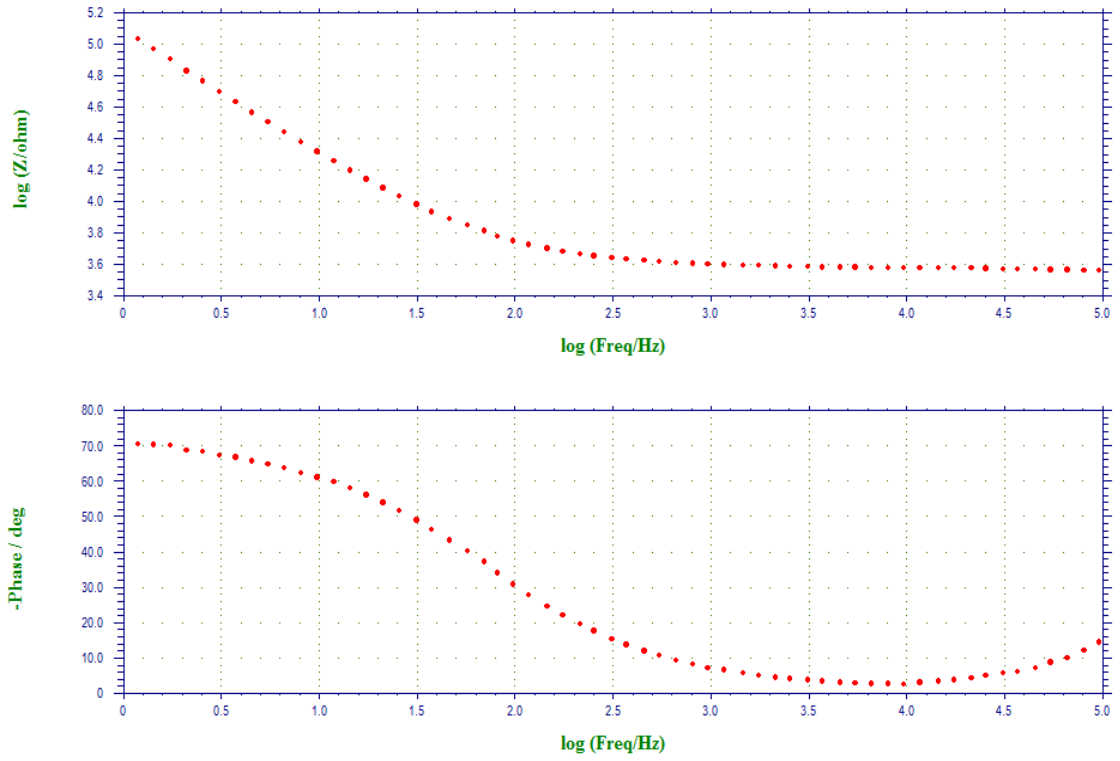

Fig. 4.2.10: Bode plot of mixture of some standard compounds using GC electrode

The Bode plot for mixture of some standard compounds is shown in figure using GC sensing electrode. The impedance spectra measured for the cathode/working electrode in Fig. 4.2.10 shows the single time constant model in which solution resistance is in series with the parallel combination of the capacitance of the electrode and its polarization resistance.

For further analysis we have stored the impedance data of 12 tea samples and standard compounds of Caffiene (CAF), Gallic Acid (GA), Epigallocatechin gallate (EGCG), Epicatechin gallate (ECG), Epigallocatechin (EGC), Epicatechin (EC) and Catechin (CAT) and their mixture with 0.25 mM concentration of each compound.

4.2.3 Impedance behaviour of Au electrode

The study was carried out using **Au sensing electrode**, keeping all the parameters and experimental conditions constant. The behaviour of DI water with Au electrode was studied using AC impedance technique keeping amplitude 0.005 V in frequency range of 1 Hz- 100 KHz.

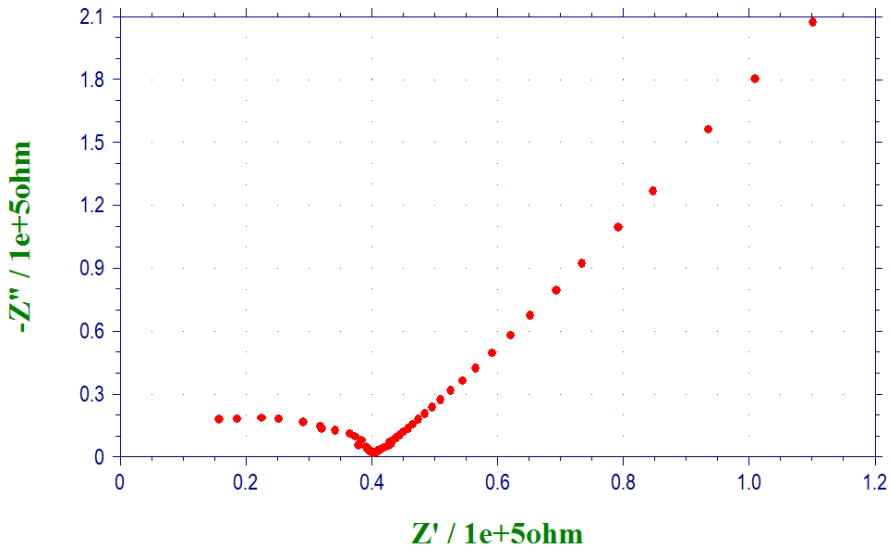

Fig. 4.2.11: Nyquist plot for DI water using Au electrode

The fitting of impedance plot in figure to the equivalent circuit follows the Fig. 4.2.1 (a) circuit model. A fully resolved semicircle at high frequency is followed by 45 degree vertical line at low frequency which arising due to Warburg impedance taking place due to diffusion. The impedance value lies in the order of 10^5 ohms indicating that the system is more resistive as this water is free from various ions and other dissolved compounds.

The physical model explaining this phenomenon is shown in Fig. 4.2.1 (a) electrical equivalent circuit model. This behaviour occurs due to polarization which is taking place as a result of combination of kinetics and diffusion processes [222].

The fitting of impedance plots in Fig. 4.2.11 to the equivalent circuit shows a good agreement between the circuit model and the real experimental data. Table 4.2.6 shows the data of frequency versus real impedance, virtual impedance, the total impedance/resistance and phase shift for Au electrode in DI water.

Table 4.2.6: Impedance data for DI water using Au electrode

Freq/Hz	Z'/ohm	Z"/ohm	Z/ohm	Phase/deg
9.668×10^4	1.575×10^4	-1.793×10^4	2.386×10^4	-48.7
2.539×10^4	3.415×10^4	-1.254×10^4	3.638×10^4	-20.2
9.668×10^3	3.909×10^4	-4.953×10^3	3.941×10^4	-7.2
4.590×10^3	3.971×10^4	-2.812×10^3	3.981×10^4	-4.1
8.105×10^2	4.049×10^4	-2.085×10^3	4.054×10^4	-2.9
1.465×10^2	4.269×10^4	-5.470×10^3	4.304×10^4	-7.3
21.23	4.847×10^4	-2.045×10^4	5.261×10^4	-22.9
3.742	6.939×10^4	-7.942×10^4	1.055×10^5	-48.9
1.738	9.356×10^4	-1.560×10^5	1.819×10^5	-59.1
1.184	1.101×10^5	-2.073×10^5	2.347×10^5	-62.0

The impedance was found to be in between 10^4 - 10^5 ohm with a variable phase angle. Real impedance values lies in the range 15750 to 110100 ohm and imaginary impedance values lie in the range -17930 to -207300 ohm.

Bode plots with Au electrode shows similar behaviour resembling the Bode behaviour of GC electrode for DI water. This indicates that both the electrodes are inert towards DI water. On the same pattern impedance study was conducted for K1 and K7 and the plots are shown in Fig. 4.2.12 and Fig. 4.2.13 respectively however Nyquist plots for all twelve tea liquor samples together are given in Fig. 4.2.14 using Au electrode.

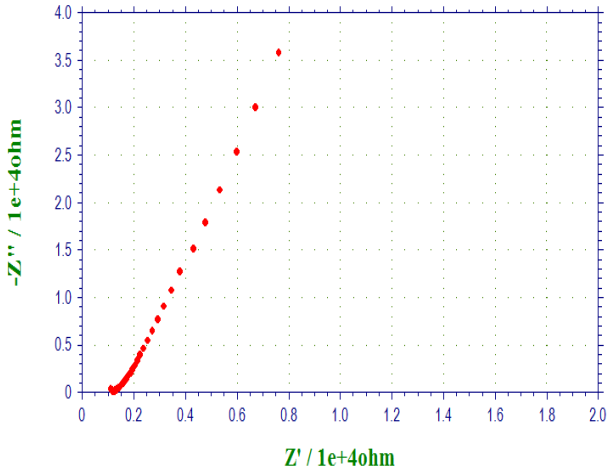

Fig. 4.2.12: Nyquist plot for K1 tea liquor sample using Au electrode

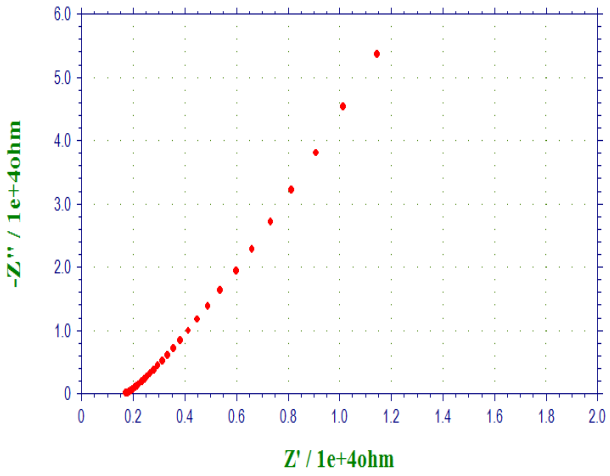

Fig. 4.2.13: Nyquist plot for K7 tea liquor sample using Au electrode

The impedance plot in Fig. 4.2.12 and Fig. 4.2.13 shows a fully resolved semicircle at high frequency is followed by a straight line of Warburg impedance at low frequency. The fitting of the above impedance plots to the electrical equivalent circuit follows Fig. 4.2.1(a). The impedance plots for both these tea liquor samples gives impedance variations in the order of Kilo Ohm. This variation is different from that of Au electrode response as shown for DI water. DI water being the purest form of water whereas tea liquor has soluble contents of many chemicals hence the presence of these ions/molecules are the reason for the change in

the nyquist plot. The impedance values in the whole range lies in the order of $10^3 – 10^4$ ohm with a variable phase angle and given in Table 4.2.7. [223]

Bode plots of tea liquor samples of K1 and K7 using Au electrode gives similar behaviour as that of other metal electrodes and follows single time constant model as shown by Bode plot behaviour of GC electrode for tea liquor samples 1 and 7 of Kangra valley.

Table 4.2.7 represents the impedance data which shows freq Z', Z'', Z and phase/degree values using Au electrode for K1 tea liquor sample. The impedance value lies in 10^3-10^4 ohm range for this tea sample. Z' falls in range 1107- 1812 ohm, Z'' lies in the range -323-1024 ohm.

Table 4.2.7: Impedance data for K1 tea sample using Au electrode

Freq/Hz	Z'/ohm	Z"/ohm	Z/ohm	Phase/deg
9.668×10^4	1.107×10^3	-3.237×10^2	1.154×10^3	-16.3
2.539×10^4	1.196×10^3	-1.237×10^2	1.202×10^3	-5.9
6.641×10^3	1.245×10^3	-1.150×10^2	1.250×10^3	-5.3
1.172×10^3	1.350×10^3	-3.070×10^2	1.385×10^3	-12.8
4.590×10^2	1.476×10^3	-5.917×10^2	1.590×10^3	-21.8
97.66	1.875×10^3	-2.023×10^3	2.759×10^3	-47.2
37.56	2.388×10^3	-4.608×10^3	5.190×10^3	-62.6
8.071	4.785×10^3	-1.788e x 10^4	1.851×10^4	-75.0
2.550	9.915×10^3	-5.068×10^4	5.164×10^4	-78.9
1.184	1.812×10^4	-1.024×10^5	1.040×10^5	-80.0

Table 4.2.8 represents the impedance data which shows freq Z', Z'', Z and phase/degree values using Au electrode for K7 Kangra valley tea liquor sample. The impedance values lies in 10^3-10^4 ohm range for K7 tea sample. The real and imaginary impedance values lies in the range 1700 to 21250 ohm and -219 to -13030 ohm respectively.

Table 4.2.8: Impedance data for K7 tea sample using Au electrode

Freq/Hz	Z'/ohm	Z''/ohm	Z/ohm	Phase/deg
9.668×10^4	1.700×10^3	-2.199×10^2	1.714×10^3	-7.4
2.539×10^4	1.724×10^3	-93.89	1.727×10^3	-3.1
1.172×10^4	1.735×10^3	-97.40	1.738×10^3	-3.2
3.711×10^3	1.787×10^3	-1.723×10^2	1.795×10^3	-5.5
3.711×10^2	2.050×10^3	-9.200×10^2	2.247×10^3	-24.2
69.75	2.799×10^3	-3.760×10^3	4.688×10^3	-53.3
11.91	5.362×10^3	-1.640×10^4	1.725×10^4	-71.9
4.542	9.093×10^3	-3.809×10^4	3.916×10^4	-76.6
2.105	1.460×10^4	-7.600×10^4	7.739×10^4	-79.1
1.184	2.125×10^4	-1.303×10^5	1.321×10^5	-80.7

Fig. 4.2.14 represents the Nyquist plot for all the twelve Kangra tea liquor samples. These tea samples represent the impedance in the complex plane, having a semicircle combined with a straight line at an angle of 45 degree to the real axis, which may be due to Warburg impedance.

The Au electrode surface get polarised in this frequency range, the surface concentration of the tea components that is being oxidized or reduced. At higher frequency, Warburg expression shows the typical 45º diffusion response in the Nyquist plot. For even lower frequencies, the influence of the resistive boundary layer increases and the diffusion tail in the Nyquist plot bends toward the real axis.

The physical model explaining this phenomenon is Randle's equivalent electrical circuit Figure 4.2.1(a) and the behaviour can be attributed to diffusion phenomenon occurring at the solution-electrode interface.

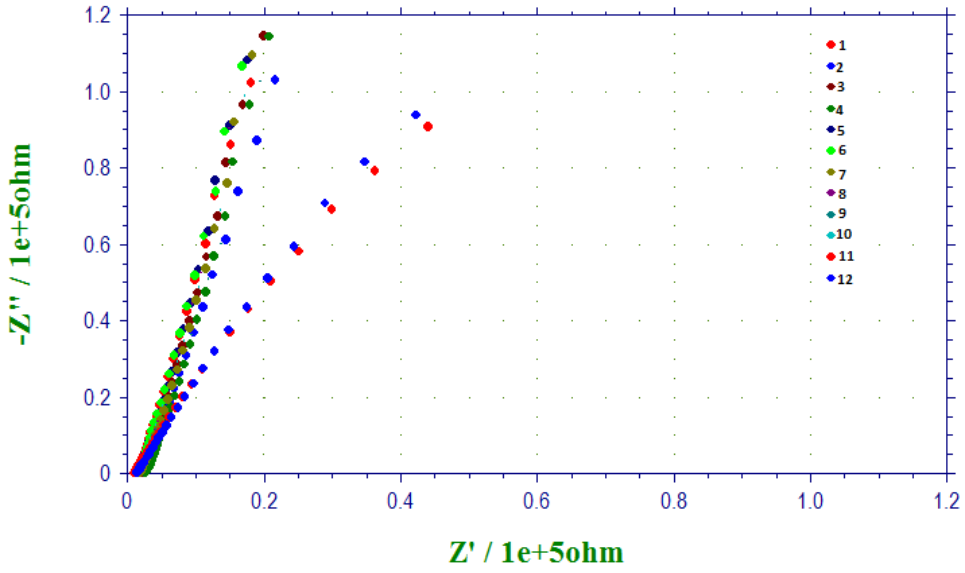

Fig. 4.2.14: Nyquist plot for all the Kangra tea sample K1- K12 tea using Au

4.2.4 Impedance study using Pt electrode for tea liquor samples

Fig. 4.2.15 shows the behaviour of **Pt electrode** and the parameters were kept constant throughout the study.

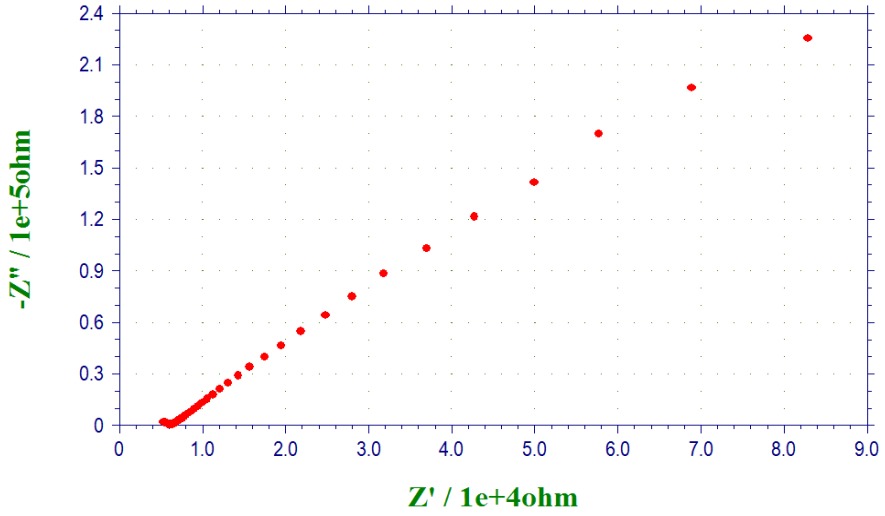

Fig. 4.2.15: Nyquist plot for DI water using Pt electrode

The impedance plot in Fig. 4.2.15 fits to the electrical equivalent circuit of Fig. 4.2.1(a). The plot shows that there is a small semicircle at high frequency and the response at low frequencies reveal a linear impedance locus with an angle of 45° to the real axis which amounts to low frequency Warburg response because DI water has negligible resistance. The impedance value lies in the order of 10^5 ohm. The total impedance lies in the range of 10^3-10^4 ohm. Bode plot for Pt electrode displays the similar response as already shown for GC electrode in Fig. 4.2.2.

The electrochemical impedance study was also carried out to check the impedance behaviour of two tea liquor samples of Kangra valley keeping the parameters constant as done for GC electrode. Fig. 4.2.16 and Fig. 4.2.17 shows the impedance plots using Pt electrode for these two tea liquor samples respectively.

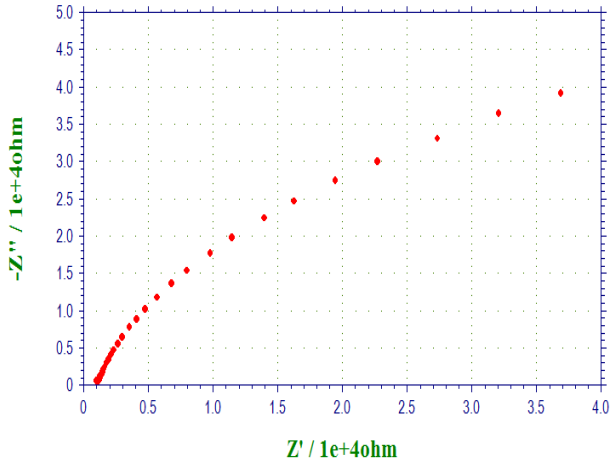

Fig. 4.2.16: Nyquist plot for K1 tea using Pt electrode

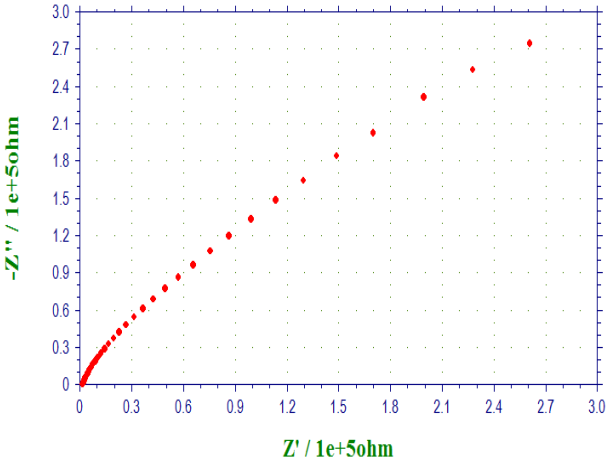

Fig. 4.2.17: Nyquist plot for K7 tea using Pt electrode

The impedance plots above gives almost similar response as that of other metal electrodes used i.e. GC and Au. These impedance plots shows a fully resolved semicircle at high frequency followed by a straight line indicating Warburg impedance taking place due to diffusion at low frequency. An impedance variation in the order of Kilo Ohm was recorded for both these tea liquor samples. The impedance depends on perturbation frequency, at high frequency a small Warburg impedance results and at low frequency higher Warburg impedance is generated. The impedance values in the whole range lies in the order of 10^3 – 10^5 ohm with a variable phase angle. For tea liquor samples Bode plots using Pt electrode gives similar response as that of Bode plot behaviour of GC and Au metal electrode for tea liquor samples 1 and 7 of Kangra valley with an increase in frequency the impedance shows a decrease and follows one time constant model.

The impedance study was carried using Pt working electrode keeping the same parameters of impedance. Nyquist plots for Kangra valley tea liquor samples is given in Fig. 4.2.18.

Virtually there is no semicircle, however an oblique around 45 degree was observed, this behaviour seems to be different than GC and Au electrodes where semicircle was seen near the origin and sharp oblique line at 45 degree was observed. Fig.4.2.1 (a) electrical equivalent circuit agrees to this type of impedance response.

The disapperance of small semicircle indicates that there is no formation of oxide layer on Pt electrode and a sharp interaction oocur among electrode-electrolyte in this frequency region provinding such nature to the plots.

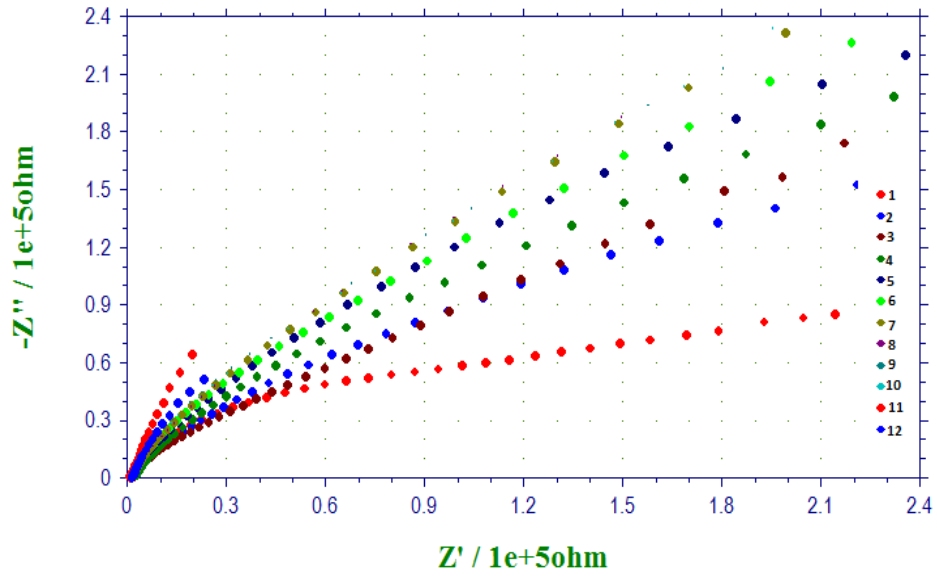

Fig. 4.2.18: Nyquist plot for all 12 Kangra tea sample using Pt electrode

The impedance response for all these 12 Kangra tea samples using Pt metal electrode in the Fig. 4.2.18 shows Warburg impedance which may have resulted from small semi circle which has disappered in this case. Fig.4.2.1 (a) electrical equivalent circuit agrees to this type of impedance response. This response is sligtly different to the impedance response of metal

electrodes of GC and Au. An important electrochemical processes and reactions could be described which may have resulted due to hydrogen and electrode reactions, metal dissolution or passivity.

4.2.5 Impedance study of tea liquors using Ag electrode

The impedance study for DI water using **Ag as a working electrode** is shown in Fig. 4.2.19. the impedance values lies in the order of 10^3 ohm.

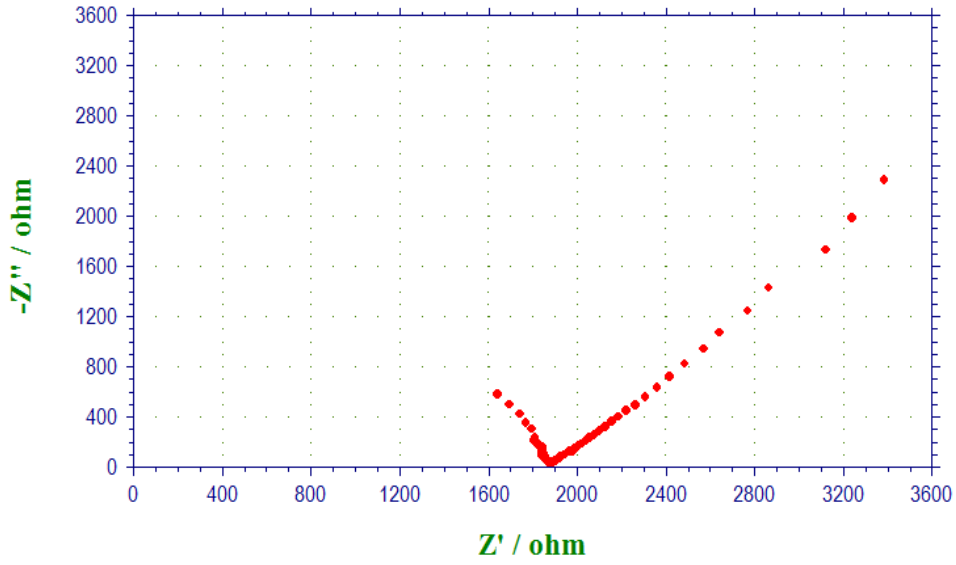

Fig. 4.2.19: Nyquist plot for DI water using Ag electrode

The electrode/electrolyte interface for Ag electrode may have quite different properties with respect to those of the metal electrodes. One remarkable difference is that the negative (RC) circuit in the low frequency region could not be detected with accuracy due to the noise in the low frequency region of the spectrum and the distortions due to non linear behaviour. Also for the silver electrode the diffusion type sub circuit presents the most pounced contribution to

the electrode impedance. The electrical equivalent circuit responsible for this type of response is shown in Fig. 4.2.19 (a)

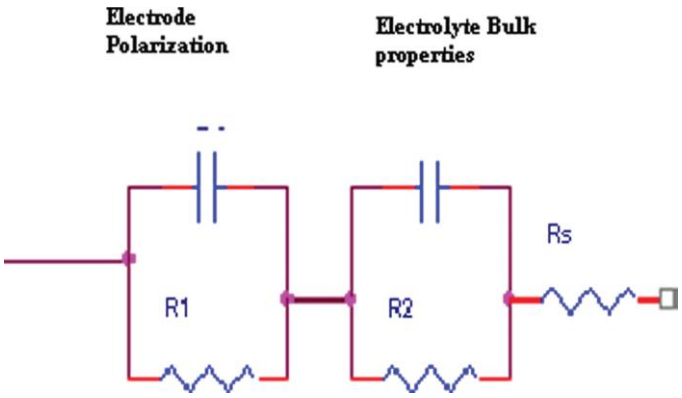

Fig. 4.2.19 (a): Equivalent circuit for Ag electrode

Table 4.2.9 represnts impedance data for DI water using Ag electrode. The total impedance lies in the range 10^4 ohm. The real impedance value lies in the range 1641 to 3384 ohm and the imaginary impedance value lies in the range -578 to -2291 ohm.

Table 4.2.9: Impedance data for DI water using Ag electrode

Freq/Hz	Z'/ohm	Z"/ohm	Z/ohm	Phase/deg
9.668×10^4	1.641×10^3	-5.786×10^2	1.740×10^3	-19.4
3.125×10^4	1.808×10^3	-2.166×10^2	1.821×10^3	-6.8
1.172×10^4	1.843×10^3	-97.27	1.845×10^3	-3.0
4.590×10^3	1.864×10^3	-52.56	1.865×10^3	-1.6
6.64×10^2	1.896×10^3	-46.50	1.897×10^3	-1.4
1.17×10^2	1.965×10^3	-1.239×10^2	1.969×10^3	-3.6
97.66	1.977×10^3	-1.300×10^2	1.981×10^3	-3.8
17.44	2.155×10^3	-3.616×10^2	2.185×10^3	-9.5
3.090	2.642×10^3	-1.074×10^3	2.852×10^3	-22.1
1.184	3.384×10^3	-2.291×10^3	4.086×10^3	-34.1

Fig. 4.2.20 represents the Bode plot for DI water using Ag electrode. Here the Bode plot shows atogether different response from metal electrodes which may be attributed to the oxide formation of silver for silver electrode and this response can be seen due to difference in time constant.

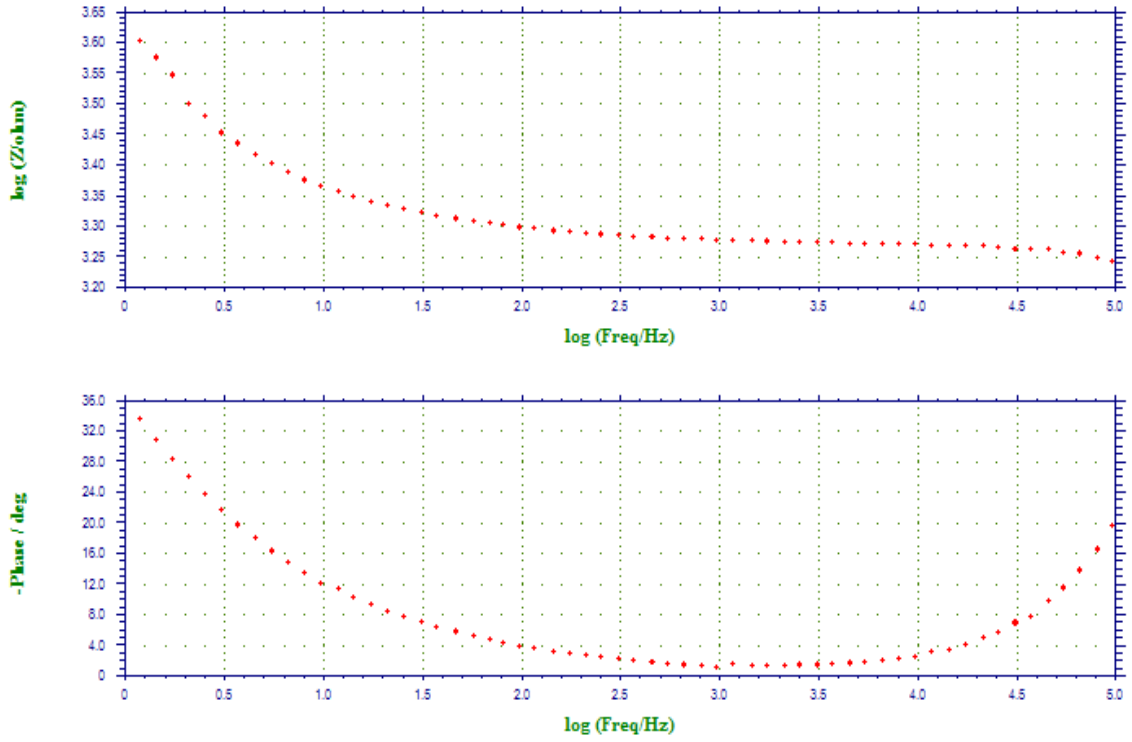

Fig. 4.2.20: The Bode plot for DI water using Ag electrode

The Bode plot using Ag sensing surface for DI water can be attributed to two time constant model.

Impedance study for tea samples K1 and K7 shown in Fig. 4.2.21 and Fig. 4.2.22 was studied using Ag as a sensing electrode. With an increase in frequency magnitude decreases and phase first decreases than starts increasing.

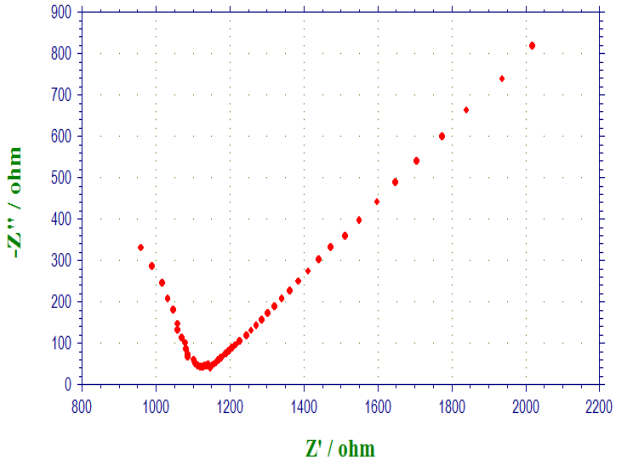

Fig. 4.2.21: Nyquist plot for K1 tea using Ag electrode

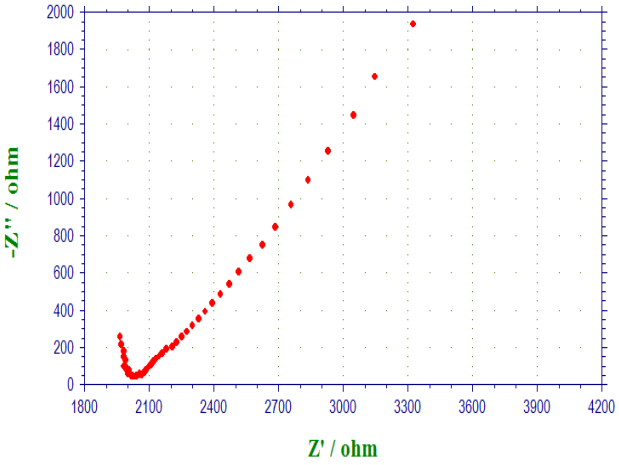

Fig. 4.2.22: Nyquist plot for K7 tea using Ag electrode

Two partially resolved semicircles can be seen here which is due to double layer effect which can be attributed to the oxide formation on the surface of Ag electrode. This behaviour of silver electrode can be complimented to the presence of well separated two time constants Figure 4.2.19 (a) in the Bauerle's equivalent electrical circuit. Such type of parallel RC combination can rise from specific adsorption occurring at electrode surface possibly associated with delayed reaction processes [224]. Usually the high frequency semi circle is related to the chemical properties of Ag sensing electrodes while the low frequency semi circle contains information about the processes related to the reaction at the electrode surface.

Table 4.2.10 represents impedance data for K1 tea samples using Ag electrode. Impedance value lies in the range 10^3 ohm. The real and imaginary values of impedance lies in the range 998 to 2542 ohm and -366 to -1274 ohm respectvely.

Table 4.2.10: Impedance data for K1 tea sample using Ag electrode

Freq/Hz	Z'/ohm	Z"/ohm	Z/ohm	Phase/deg
9.668×10^4	9.987×10^2	-3.660×10^2	1.064×10^3	-20.1
1.758×10^4	1.145×10^3	-97.92	1.149×10^3	-4.9
9.668×10^3	1.162×10^3	-69.78	1.164×10^3	-3.4
3.125×10^3	1.186×10^3	-50.37	1.187×10^3	-2.4
8.105×10^2	1.224×10^3	-51.52	1.225×10^3	-2.4
2.148×10^2	1.274×10^3	-89.62	1.278×10^3	-4.0
69.75	1.353×10^3	-1.538×10^2	1.361×10^3	-6.5
11.91	1.563×10^3	-3.571×10^2	1.603×10^3	-12.9
8.071	1.643×10^3	-4.289×10^2	1.698×10^3	-14.6
1.184	2.542×10^3	-1.274×10^3	2.844×10^3	-26.6

Table 4.2.11 represents the impedance data for K7 tea liquor sample using Ag electrode. The impedance falls in the range 10^3 ohm. The real impedance values and the imaginary impedance values lie in the range 1900 to 4060 ohm and -254 to -3685 ohm.

Table 4.2.11: Impedance data for K7 tea sample using Ag electrode

Freq/Hz	Z'/ohm	Z"/ohm	Z/ohm	Phase/deg
9.668×10^4	1.900×10^3	-2.545×10^2	1.917×10^3	-7.6
2.539×10^4	1.930×10^3	-82.34	1.932×10^3	-2.4
6.641×10^3	1.953×10^3	-43.08	1.953×10^3	-1.3
1.758×10^3	1.975×10^3	-46.12	1.975×10^3	-1.3
8.105×10^2	1.993×10^3	-53.69	1.994×10^3	-1.5
2.148×10^2	2.049×10^3	-1.271×10^2	2.053×10^3	-3.5
37.56	2.230×10^3	-3.426×10^2	2.256×10^3	-8.7
14.36	2.414×10^3	-6.003×10^2	2.487×10^3	-14.0
3.7.42	2.955×10^3	-1.468×10^3	3.300×10^3	-26.4
1.184	4.060×10^3	-3.685×10^3	5.483×10^3	-42.2

Fig. 4.2.23 represents the Bode plot for Kangra valley tea sample K1 using Ag electrode. With an increase in freqeuncy the impedance decreases. Here magnitude shows a fall with increase in frequency and phase first decreases and then shows an increase with increasing impedance. The two time constant equivalent circuit is responsible for this behaviour.

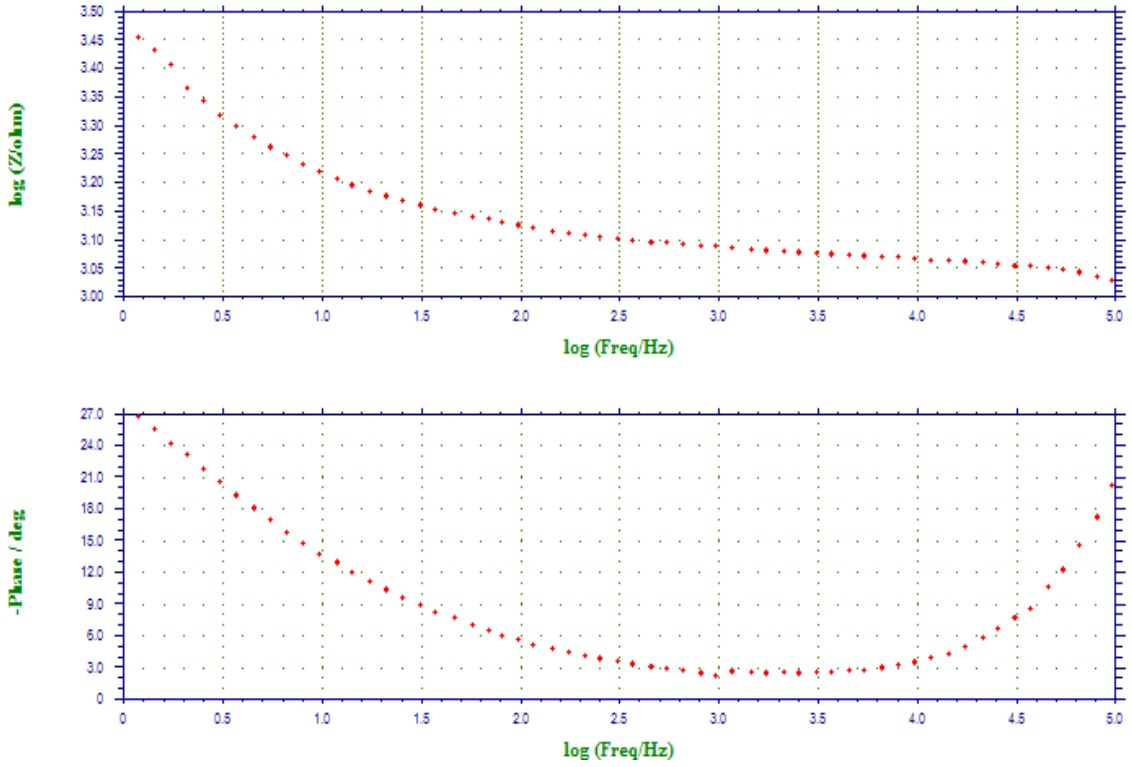

Fig. 4.2.23: Bode plot for K1 tea liquor sample using Ag electrode

The Bode plot for K7 tea liquor sample using Ag electrode is shown in Fig. 4.2.24. Magnitude shows a decrease with an increase in frequency and phase angle shows a decrease first followed by a slight increase with increasing impedance.

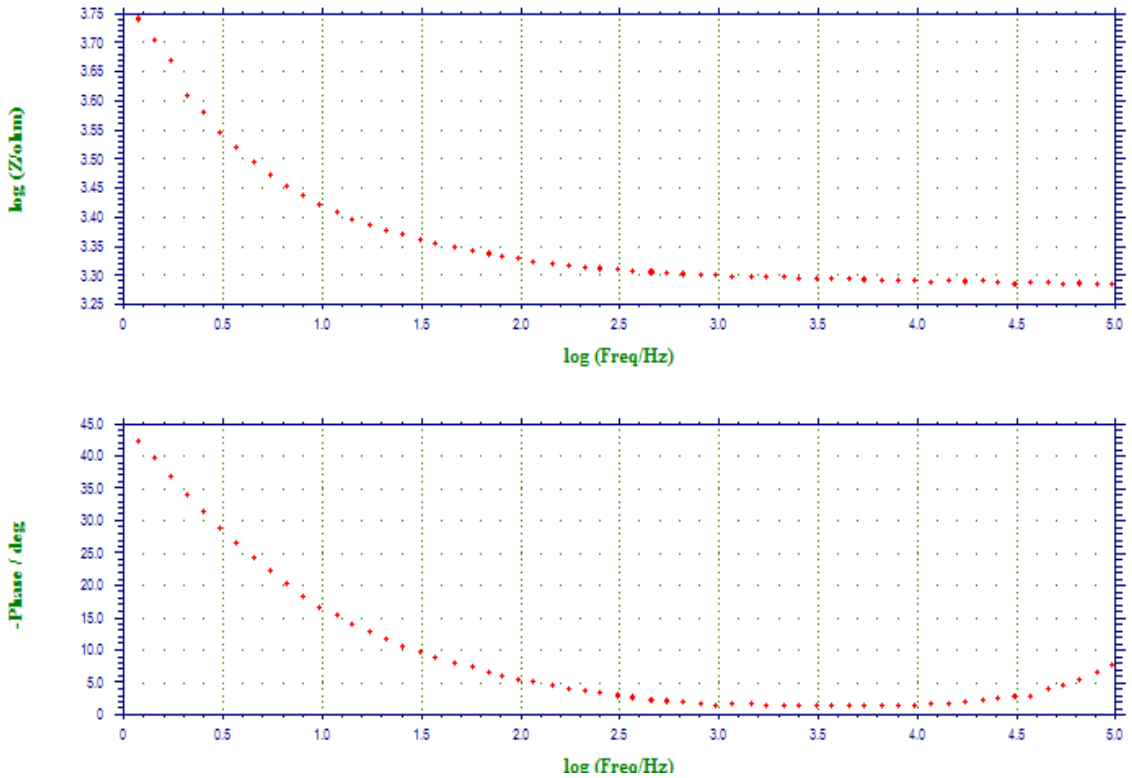

Fig. 4.2.24: Bode plot for K7 tea liquor sample using Ag electrode

The bode response of this type has arised due to electrode polarization of Ag electrode and electrolyte bulk properties which is K7 tea sample here.

The nyquist plot for all the 12 kangra valley tea samples using Ag electrode is shown in Fig. 4.2.25. A different type of impedance response is found for Ag electrode which may be attributed to the double layer effect due to oxide formation on the surface of Ag electrode. This behaviour of silver electrode can be complimented to the presence of well separated two time constants.

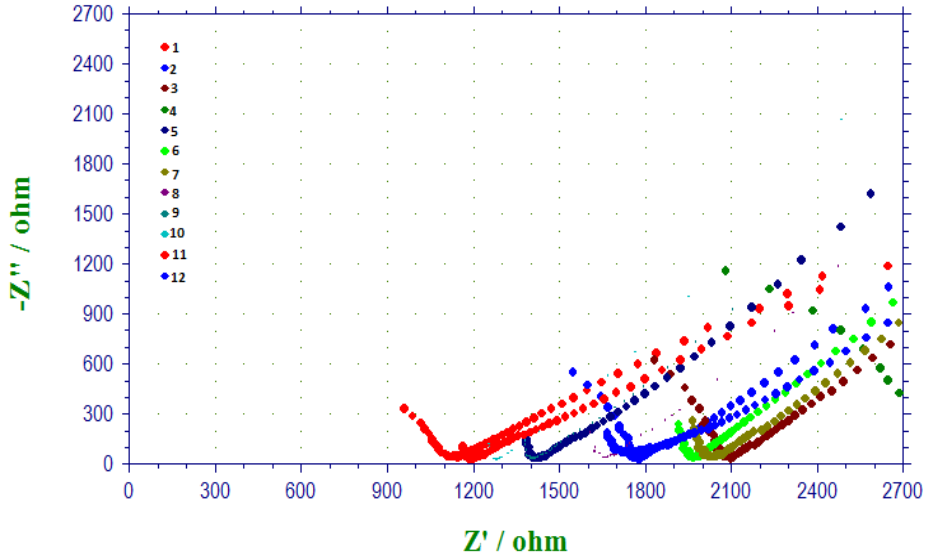

Fig. 4.2.25: Nyquist plot for all 12 Kangra valley tea samples using Ag electrode

The impedance response for 12 Kangra tea liquor samples in Fig. 4.2.25 shows two well separated time constants giving one fully and one partially resolved semi circle. This type of combination can rise from specific adsorption occurring at electrode surface possibly associated with delayed reaction processes [225].

4.2.6 Impedance study of tea liquor samples using PANI electrode

The impedance varaition of PANI film electropolymerised on ITO/glass surface is qualitatively similar for all tea liquor samples of Kangra valley. PANI film is in conducting state (oxidising form) at +1V potential, the polymer resistance is considered to be negligible compared to tea solution resistance. Thus, when the polymer is in conducting state the impedance value of tea must be equal to the solution resistance between PANI and reference electrode. similar behaviour was reported for the study of potential dependence of impedance

in electrolytes of different ionic strength electropolymerised PANI films on gold interdigitated electrodes in the frequency range of 0.1-20000 Hz and amplitude of 10 mV.

Impedance spectra of emaralidine base for chemical sensing of aqeous solution of varying pH have characteristic distinct peak frequency. Complex plane plots of PANI and metal electrodes have been observed in our studies. The other factors which affect are film thichness, porosity of film, ionic dopants also play important role in sensitivity determination. However, in the present study all parameters like monomer concentration, washing, drying was kept same for reproducible results. Keeping in view the impedance behaviour for DI water using PANI electrode is given in Fig. 4.2.26, at the frequency range 1 Hz to 100 KHz, amplitude 0.005 V.

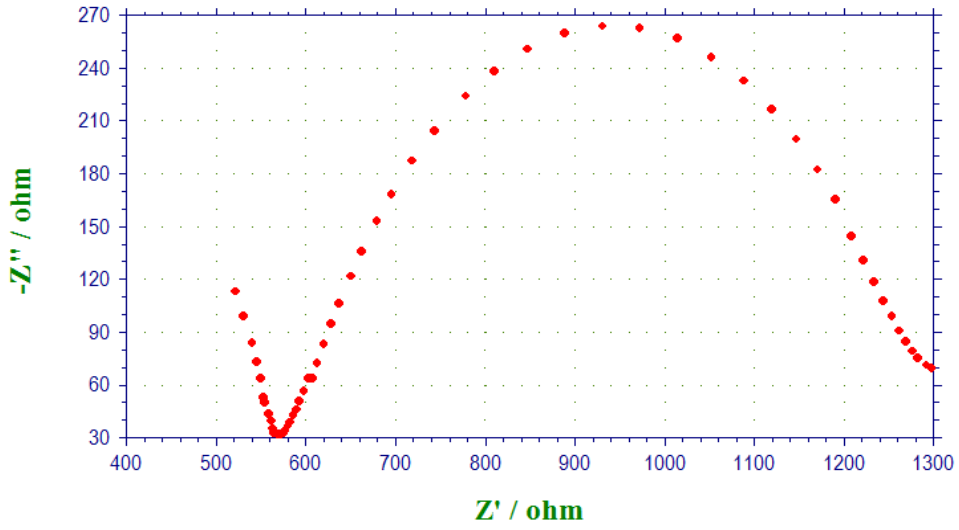

Fig. 4.2.26: Nyquist plot for DI water using PANI electrode

PANI coated on ITO surface shows two capacitive semi circles in the Nyquist plot as shown in Fig. 4.2.26. The Nyquist plot using PANI electrode shown in figure which have two partially resolved distorted semi-circles in the extending mid frequency region to the lower

frequency region. The PANI electrode shows different response than other working electrodes which may be attributed to porous surface of this electrode or might be due to the variation of the surface structure. Usually the high frequency semi circle is related to the coating properties of sensing electrodes while the low frequency semi circle contains information about the processes related to the reaction at the electrode surface.

Equivalent circuit described for the PANI surface in DI water is given in Fig. 4.2.26 (a). This circuit can be represented by the equivalent circuit where the capacitance of the intact coating is represented by Cc. Its value is much smaller than a typical double layer capacitance. Its units are pF or nF. Rpo (pore resistance) is the resistance of ion conducting paths that develop in the coating [226].

These paths may not be physical pores filled with electrolyte. On the metal side of the pore, we assume that an area of the coating has delaminated and a pocket filled with an electrolyte solution has formed. This electrolyte solution can be very different than the bulk solution outside of the coating. The interface between this pocket of solution and the bare metal is modeled as a double layer capacitance in parallel with a kinetically controlled charge transfer reaction.

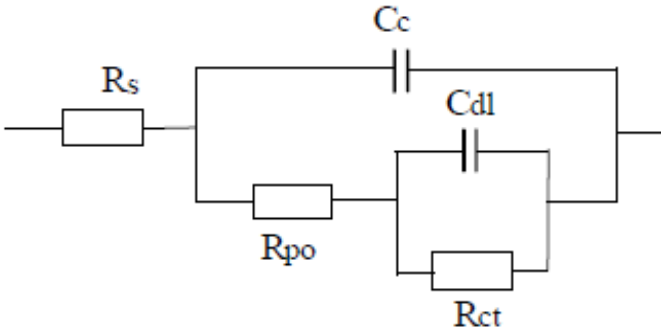

Fig. 4.2.26 (a): Equivalent circuit for PANI electrode

These paths may be physically pores filled with DI water or any other test solution one of the metal sides of the pores ITO, we assume that in area of the coating is formed. The test solution can be very different than the bulk solution outside the coating. The interface between this part of solution and ITO is modeled as double layer capacitance in parallel with a kinetically controlled charge transfer reaction. The nyquist plot for tea liquor samples K1 and K7 are given in Fig. 4.2.28 and 4.2.29 which can be compared with nyquist plot for PANI response in DI water.

Table 4.2.12 shows impedance data for DI water using PANI electrode. The total impedance lies around 10^2-10^3 ohms. The real impedance readings for DI water lies in the range of 500 to 1300 ohm, whereas imaginary impedance lies in between -113 to -69 ohm. However, in case of tea samples the impedance data is similar having Z' 600-1000 ohm and much change in Z'' i.e. -59 to -38 V. However, there has been a noticeable change in K7 sample as compared to K1 the value of Z' lies 237-774 ohm and Z'' lies in -34 to -30 ohm.

Though the Nyquist and bode behaviour is on the same pattern but overall several changes can be seen indicating that the two samples from the same region processed during different intervals of time results in variation of impedance values, which can become an excellent tool for interpretation of tea quality of the same region or of different region even with the minor changes such as plucking period, fermentation process or other processing conditions. Thus PANI electrode with different dopants can become a single electrode to interpret tea quality as a fingerprint.

Table 4.2.12: Impedance data for DI water using PANI electrode

Freq/Hz	Z'/ohm	Z''/ohm	Z/ohm	Phase/deg
9.668×10^4	5.109×10^2	-1.133×10^2	5.233×10^2	-12.5
3.125×10^4	5.468×10^2	-51.51	5.492×10^2	-5.4
9.668×10^3	5.623×10^2	-31.25	5.632×10^2	-3.2
2.148×10^2	6.852×10^2	-1.682×10^2	7.055×10^2	-13.8
97.66	7.992×10^2	-2.425×10^2	8.352×10^2	-16.9
46.50	9.670×10^2	-2.738×10^2	1.005×10^3	-15.8
8.071	1.232×10^3	-1.364×10^2	1.239×10^3	-6.3
3.742	1.272×10^3	-92.87	1.276×10^3	-4.2
2.105	1.293×10^3	-75.95	1.296×10^3	-3.4
1.184	1.313×10^3	-69.90	1.314×10^3	-3.0

Fig. 4.2.27 represents the Bode plot for DI water using PANI electrode. It shows two time constant model for this electrode. The magnitude shows a decrease with increasing impedance whereas; phase angle shows decrease followed by increase repeating the same pattern.

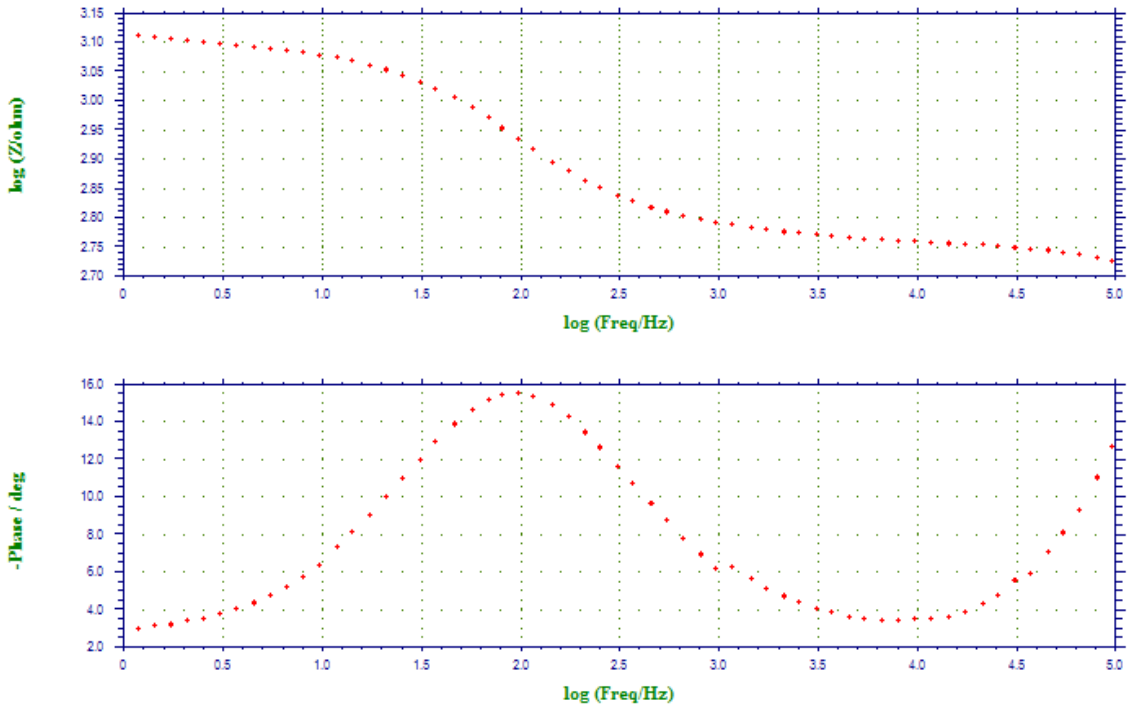

Fig. 4.2.27: The Bode plot for DI water using PANI electrode

Bode plot response here is found to be different than the Bode response of metal electrodes of GC, Pt Au and Ag. The Bode plot follows a two time constant model using PANI sensing surface.

The Nyquist plot for K1 and K7 tea liquor samples is shown in Fig. 4.2.28 and Fig. 4.2.29 respectively.

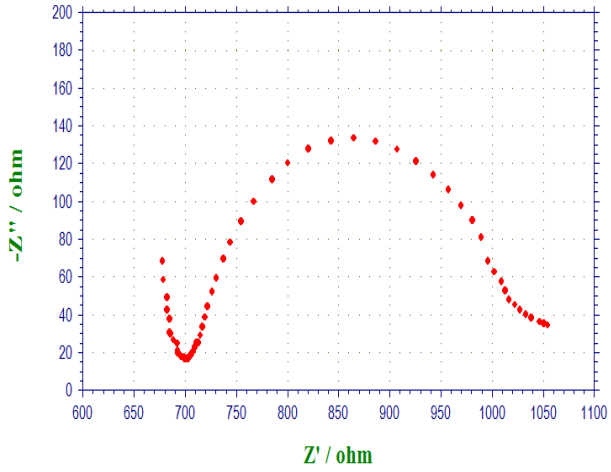

Fig. 4.2.28: Nyquist plot K1 using PANI

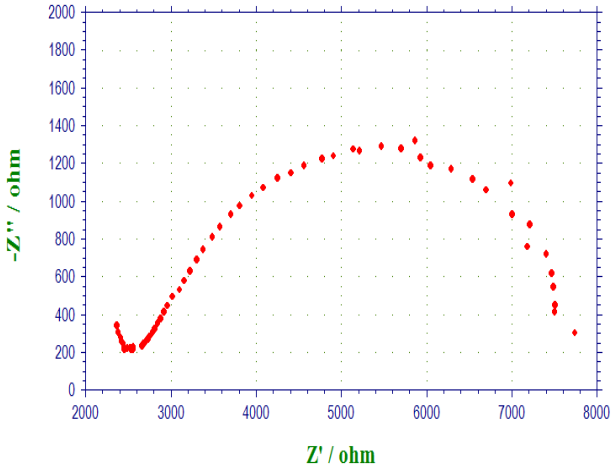

Fig. 4.2.29: Nyquist plot K7 using PANI

The Nyquist plots in Fig. 4.2.28 and Fig. 4.2.29 show that the impedance locus in both the figures takes form of one fully resolved semicircle to the left and a partially resolved semicircle to the right. This behaviour can be attributed to double layer effect involving adsorption. The shift in valley points of the impedance loci of the tea infusions (along the real as well as imaginary axis) can be attributed to charge transfer kinetics and adsorption rate. The electrical equivalent circuit is shown in Fig. 4.2.26 (a) .

Table 4.2.13 shows the actual values of the real/virtual impedance total impedance and phase shift for PANI electrode in tea sample 1 of Kangra valley.

Table 4.2.13: Impedance data for K1 tea liquor sample using PANI electrode

Freq/Hz	Z'/ohm	Z"/ohm	Z/ohm	Phase/deg
9.668×10^4	6.408×10^2	-59.55	6.436×10^2	-5.3
4.590×10^4	6.475×10^2	-32.44	6.483×10^2	-2.9
1.172×10^4	6.542×10^2	-17.35	6.544×10^2	-1.5
3.125×10^3	6.665×10^2	-14.24	6.667×10^2	-1.2
9.668×10^2	6.784×10^2	-17.12	6.786×10^2	-1.4
3.711×10^2	6.892×10^2	-45.94	6.908×10^2	-3.8
97.66	7.635×10^2	-11.60	7.723×10^2	-8.6
17.44	9.378×10^2	-10.34	9.435×10^2	-6.3
3.742	1.004×10^3	-53.60	1.006×10^3	-3.1
1.184	1.028×10^3	-38.15	1.028×10^3	-2.1

Fig. 4.2.30 shows the Bode plot for K1 tea liquor sample using PANI electrode this spectra displays two time constant model for electrical equivalent circuit. Here Bode follows a two time constant model and magnitude shows decrease in impedance whereas, phase shows increase followed by decrease which is evident by increase in impedance again.

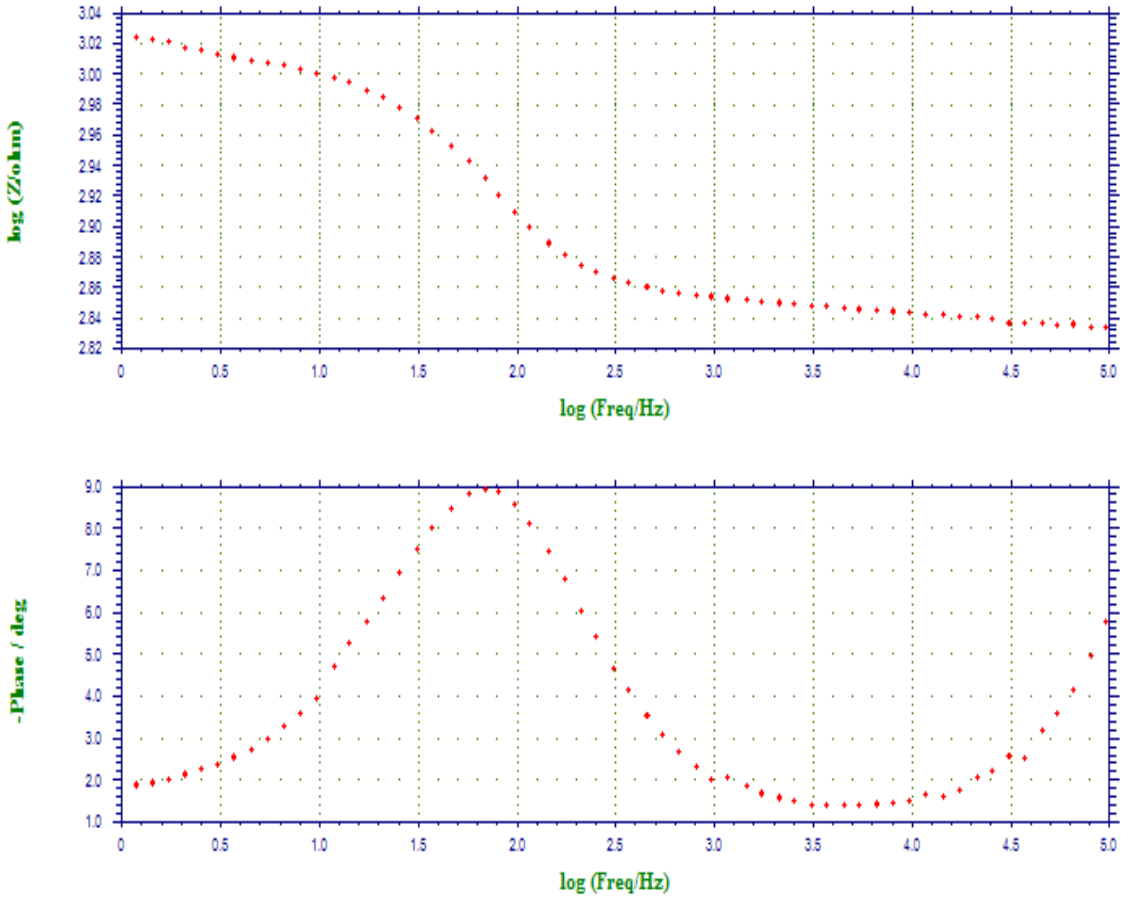

Fig. 4.2.30: Bode plot for K1 tea using PANI

The Bode Plot for K1 tea sample is shown in Fig. 4.2.30. The two time constants are not nearly as pronounced on this plot. The plot does not go sufficiently high in frequency to measure the solution resistance. In practice the solution resistance is a property of the tea liquor and the test cell geometry, not a property of the coating.

Table 4.2.14 indicates the impedance data readings for K7 tea liquor sample using PANI electrode.

Table 4.2.14: Impedance data for K7 tea liquor sample using PANI electrode

Freq/Hz	Z'/ohm	Z''/ohm	Z/ohm	Phase/deg
9.668×10^4	2.371×10^3	-3.428×10^2	2.396×10^3	-8.2
3.125×10^4	2.456×10^3	-2.247×10^2	2.467×10^3	-5.2
9.668×10^3	2.663×10^3	-2.344×10^2	2.673×10^3	-5.0
3.125×10^3	2.813×10^3	-3.236×10^2	2.832×10^3	-6.6
5.469×10^2	3.305×10^3	-6.900×10^2	3.377×10^3	-11.8
1.172×10^2	4.252×10^3	-1.123×10^3	4.398×10^3	-14.8
31.50	5.471×10^3	-1.289×10^3	5.621×10^3	-13.3
9.766	6.541×10^3	-1.114×10^3	6.636×10^3	-9.7
3.090	7.403×10^3	$-7.186e \times 10^2$	7.438×10^3	-5.5
1.184	7.740×10^3	-3.017×10^2	7.746×10^3	-2.2

Fig. 4.2.31 gives Bode plot for K7 tea liquor sample using PANI electrode. This spectrum shows two time constants arising due to two semi circles which are evident from the in Nyquist plot for PANI sensing electrode. This response can be attributed to the adsorption taking place at the PANI surface and the tea liquor. A double layer is playing an important role which is evident for ITO and PANI film and PANI sensing surface and tea solution.

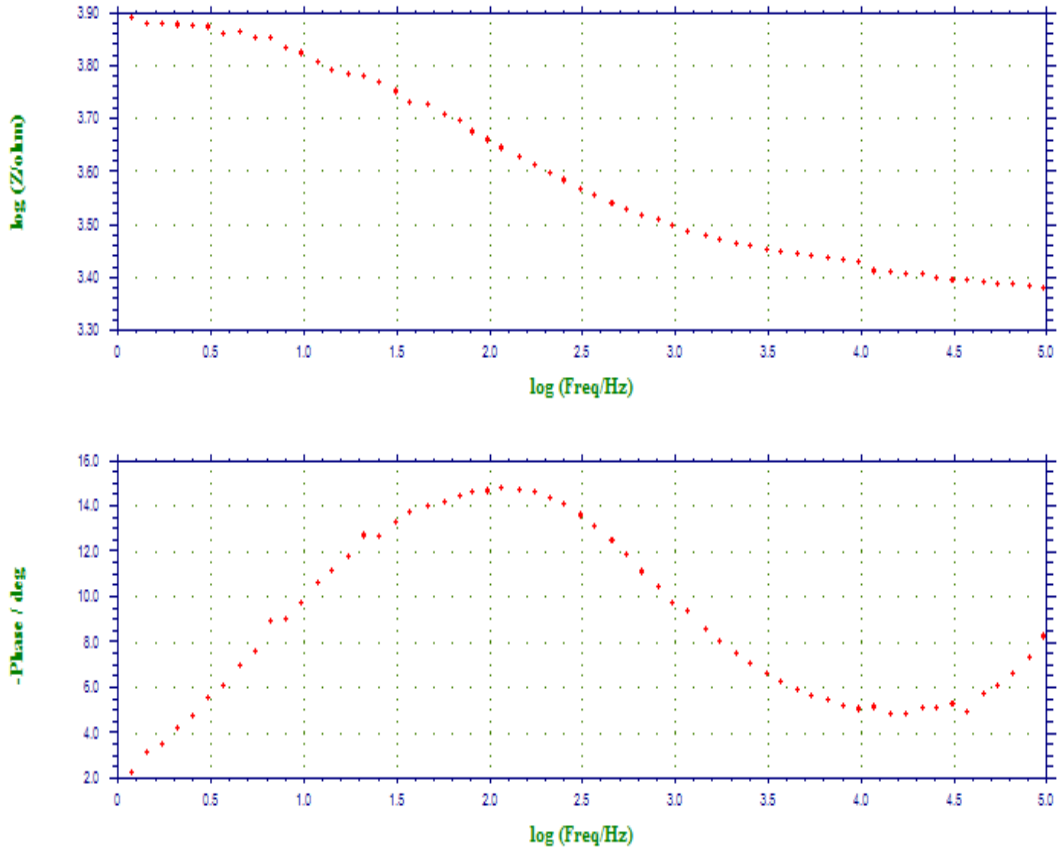

Fig. 4.2.31: Bode for K7 using PANI

The Bode response for K7 tea liquor solution is similar to the Bode behaviour of K1 tea sample**,** the reason for the similarity can be the same geographical area and similar tea grown conditions.

The Nyquist plot for all 12 Kangra tea samples is given in Fig. 4.2.32 which gives a response of two time constants.

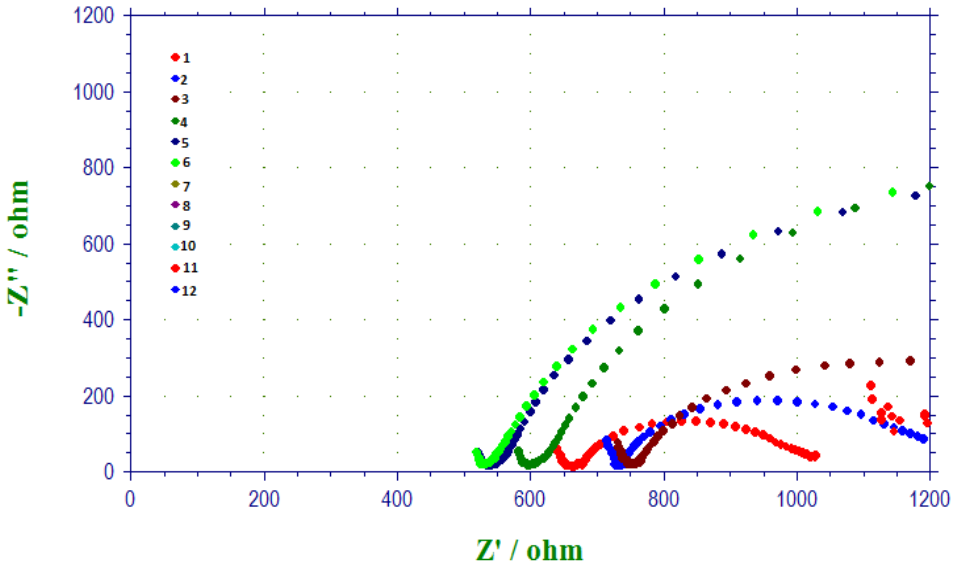

Fig. 4.2.32: Nyquist plot for all Kangra tea liquor samples using PANI

It was observed that the Nyquist plots on different tea samples shows variations from sample to sample in comparison to the metal electrodes i.e. GC Au Pt and Ag electrodes. The reason for the variation may be the porosity in the electrode surface or may be due to some variation of the surface structure of PANI by continuous dipping in various tea samples which has acidic characteristics [227].

On the same pattern as per Fig. 4.2.32 clearly indicates that the 12 samples can be classified into three or four groups.

4.2.7 Impedance study of tea liquors using PPY electrode

Each electrode coating has a specific has a special electrical response for a tea liquor and gives a distinct signal for tea samples based on seasonal variation.

Fig. 4.2.33 gives the impedance spectra for DI water using PPY electrode. This electrode has been prepared by electro deposition of pyrrole monomer on ITO surface. This electrode gives

Nyquist response in the form of two capacitive semi circles as shown in figure. The Nyquist plots shows two semicircles which are distorted in nature extending from the mid frequency region to the low frequency region. Due to the porous nature and the variation of the surface structure PPY electrode shows response different from metal electrodes. High frequency semi circle can be attributed to the coating properties of the PPY electrode, whereas, the low frequency semi circle holds the information about the processes related to the reaction at the PPY surface.

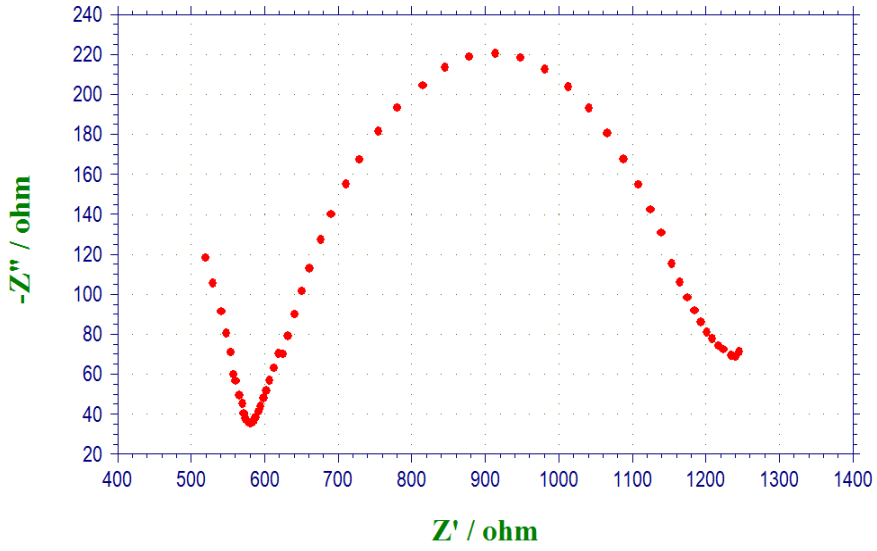

Fig. 4.2.33: Nyquist plot for DI water using PPY electrode

Nyquist plot shows two semi circles both partially resolved in Fig. 4.2.33. The electronic circuit responsible for this type of response is given in Fig. 4.2.26 (a) . The total impedance at high frequency lies in the range 10^2- 10^3 ohm. Bode plot response for DI water of PPY electrode is similar to Bode plot response of PANI electrode, both these conducting polymer electrodes displays two time constant model giving 2 time capacitive semicircles for Nyquist plots.

In this circuit the capacitance of the intact coating is represented by Cc, the value of this is much less than a typical double layer capacitance having pF or nF. The resistance of ion conducting paths that develop in the coating is Rpo (pore resistance). These paths may not be physical pores filled with electrolyte. These paths may be physically pores filled with DI water or any other test solution one of the metal sides of the pores ITO; we assume that in the area of the coating is formed. The test solution can be very different than the bulk solution outside of the coating. The interface between this part of solution and ITO is double layer capacitance in parallel with a kinetically controlled charge transfer reaction.

The Nyquist plot for both the tea liquor samples is shown in Fig. 4.2.34 and Fig. 4.2.35 respectively at 1 Hz- 100 KHz frequency range and 0.005 Amplitude.

Table 4.2.15: Impedance data for DI water using PPY electrode

Freq/Hz	Z'/ohm	Z"/ohm	Z/ohm	Phase/deg
9.668×10^4	5.194×10^2	-1.183×10^2	5.327×10^2	-12.8
4.590×10^4	5.539×10^2	-70.92	5.584×10^2	-7.3
1.758×10^4	5.717×10^2	-40.50	5.731×10^2	-4.1
4.590×10^3	5.878×10^2	-38.33	5.891×10^2	-3.7
9.668×10^2	6.249×10^2	-69.97	6.288×10^2	-6.4
1.758×10^2	7.545×10^2	-1.815×10^2	7.760×10^2	-13.5
31.50	1.041×10^3	-1.930×10^2	1.059×10^3	-10.5
8.071	1.165×10^3	-1.060×10^2	1.170×10^3	-5.2
2.550	1.217×10^3	-74.18	1.220×10^3	-3.5
1.184	1.245×10^3	-71.22	1.248×10^3	-3.3

Table 4.2.15 represents the Bode plot for DI water using PPY electrode. The real impedance value for DI water lies in the range of 519-1245 ohm, whereas the imaginary impedance value lies in between -118 to -71. However, in case of tea samples the impedance data is similar having Z' 614 to 6345 ohm, Z'' -75 to -9907 ohm for K1 tea sample and Z' lies from 625-5250 ohm, Z'' -73 to -7332 ohm for K7 tea sample. However, there are not much noticeable changes in impedance values of K1 and K7 tea samples.

Although the behaviour is on the same pattern but in total many changes are taking place which implies that the two samples from the same region processed during different intervals of time results in variation of impedance values. This can work as an unparalleled tool for the quality analysis of tea samples belonging to same region; even they vary with minor changes like, plucking period, fermentation and other processing conditions.

A two time constant model as a Bode response can be seen for this electrode. The magnitude shows a decrease with increasing impedance whereas; phase angle shows decrease followed by an increase repeating the same pattern.

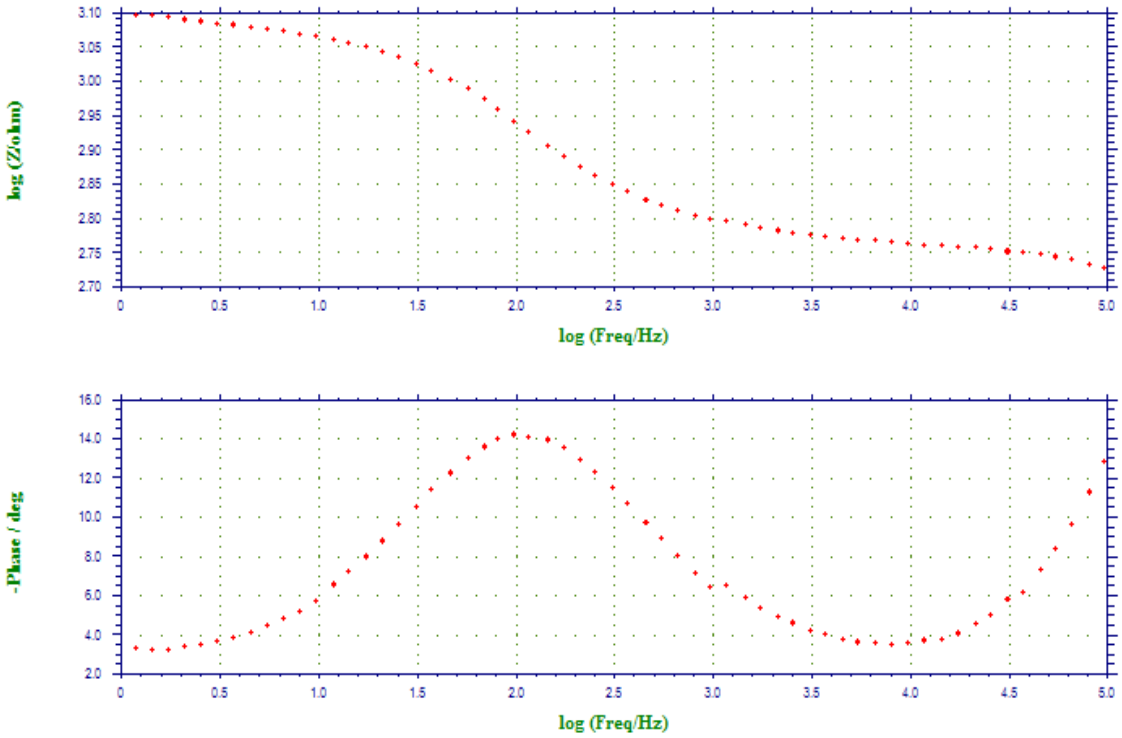

Fig. 4.2.34: Bode plot for PPY in DI water

The Bode plots presented in Fig. 4.2.34 is found to be different than that of metal electrodes of GC, Pt, Au and Ag. The Bode follows a two time constant model using PPY.

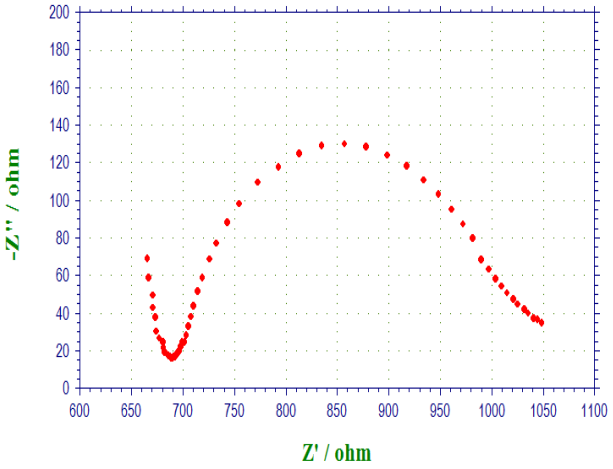

Fig. 4.2.35: Nyquist plot for K1 using PPY

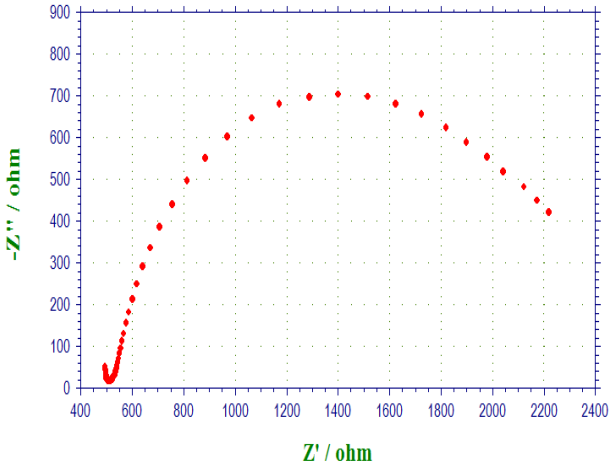

Fig. 4.2.36: Nyquist plot for K7 using PPY

The Nyquist plots for K1 and K7 tea liquor samples shown in the figure display two semicircles one towards high frequency region and the other one towards low frequency region and also shows that the Nyquist plots on different tea samples give variations from sample to sample in comparison to the metal electrodes i.e. GC, Au, Pt and Au electrodes. The reason for the variation may be the porosity in the electrode surface or may be due to some variation of the surface structure of PPY by continuous dipping in tea samples which has acidic characteristics. As shown these impedance plots appear more complex and the two semi-circles depend on the nature of the electrode material. The response for Bode plot observed is similar to the response of PANI electrode for both the tea liquor samples and follows a two time constant model for both of the conducting polymer electrodes [228-230].

Table 4.2.16: Impedance data using PPY electrode for K1 tea sample

Freq/Hz	Z'/ohm	Z"/ohm	Z/ohm	Phase/deg
9.6680	614.1	-75.40	618.7	-7.0
25390	632.5	-38.13	633.7	-3.5
5469	660.0	-38.64	661.1	-3.4
1758	682.5	-54.39	684.7	-4.6
175.8	774.6	-205.0	801.3	-14.8
25.70	1004	-885.4	1339	-41.4
5.486	1797	-3133	3612	-60.2
3.090	2653	-4959	5624	-61.9
1.738	4397	-7842	8991	-60.7
1.184	6345	-9907	11760	-57.4

The Impedance data using PPY electrode for K1 tea sample is shown in Table 4.2.16, with Z' values in the range 614 to 6345, and the imaginary values lies in the range -75 to -9907.

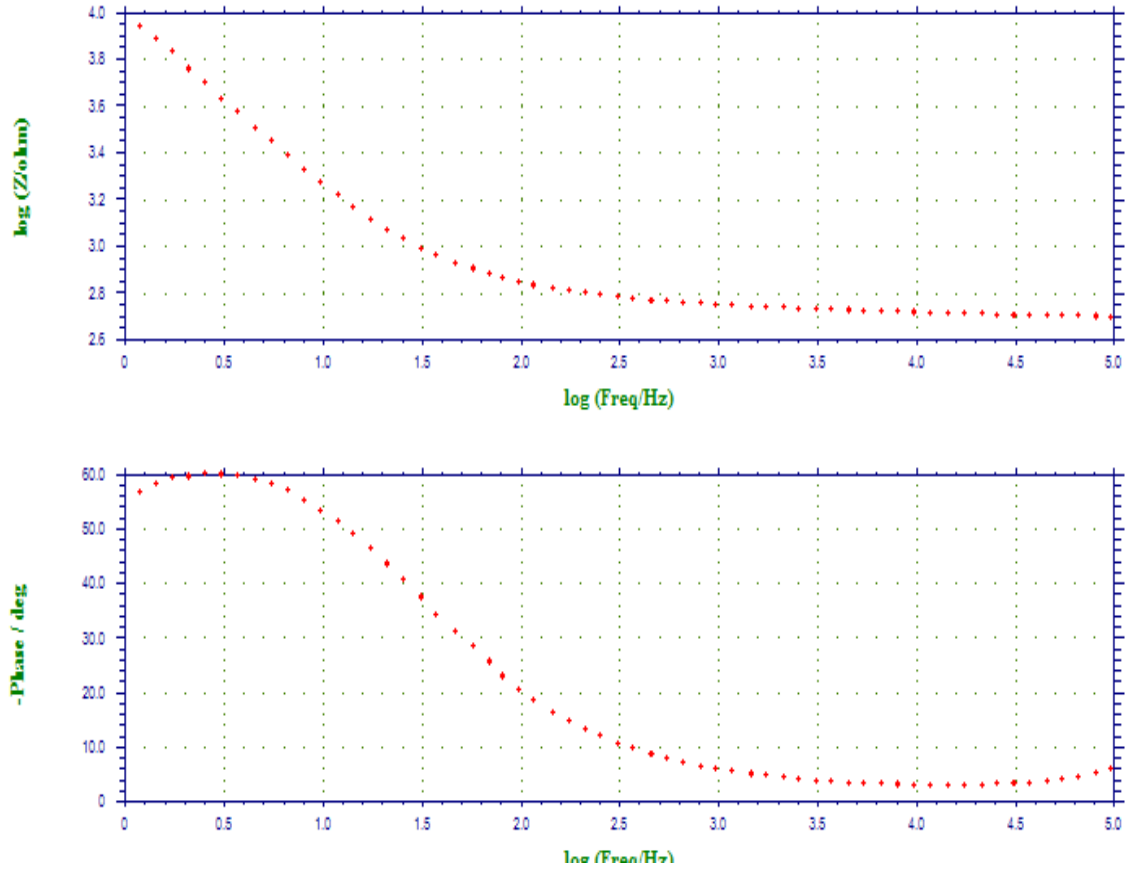

Fig. 4.2.37: Bode plot using PPY for K1 tea sample

Bode plot for K1 tea sample is given in Fig. 4.2.37 shows two time constant model and is responsible for this type of behaviour of Bode plot.

Table 4.2.17: Impedance data using PPY electrode for K7 tea sample

Freq/Hz	Z'/ohm	Z"/ohm	Z/ohm	Phase/deg
9.668×10^4	6.253×10^2	-73.52	6.296×10^2	-6.7
2.539×10^4	6.430×10^2	-34.66	6.439×10^2	-3.1
9.668×10^3	6.550×10^2	-29.93	6.557×10^2	-2.6
3.711×10^3	6.695×10^2	-35.53	6.704×10^2	-3.0
1.172×10^3	6.921×10^2	-57.43	6.945×10^2	-4.7
3.125×10^2	7.356×10^2	-1.178×10^2	7.450×10^2	-9.1
97.66	8.048×10^2	-2.573×10^2	8.450×10^2	-17.7
11.91	1.185×10^3	-1.310×10^3	1.766×10^3	-47.9
3.742	2.080×10^3	-3.298×10^3	3.899×10^3	-57.8
1.184	5.250×10^3	-7.332×10^3	9.018×10^3	-54.4

Impedance data of K7 tea sample using PPY electrode is given in Table 4.2.17 with Z’ in the range 625 to 5250 ohm and Z’’ lies in the range -73 to -7332. Compared to the impedance values of K1 tea liquor sample a small change is evident in the real as well as imaginary impedance values. The Real impedance ranged from 614 to 6345 and the imaginary values lies in the range -75 to -9907 for K1 tea sample.

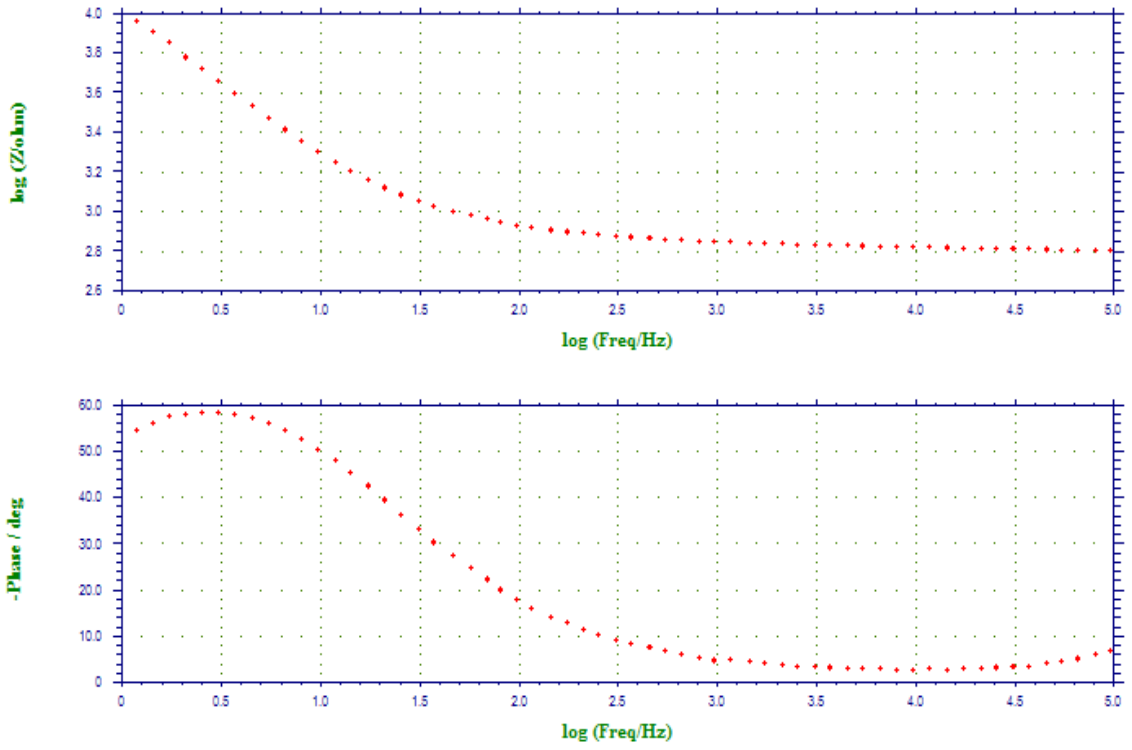

Fig. 4.2.38: Bode plot using PPY for K7 tea sample

Fig. 4.2.38 gives Bode plot for K7 tea sample which represents a two time constant model. From the plot it is evident that with an increase in impedance magnitude shows a sharp decrease whereas the phase indicates a decrease followed by a slow increase with high impedance.

Fig. 4.2.39 shows Nyquist plots for all 12 Kangra valley tea liquor samples using PPY electrode. The impedance response is similar to the impedance response of PANI conducting polymer electrode.

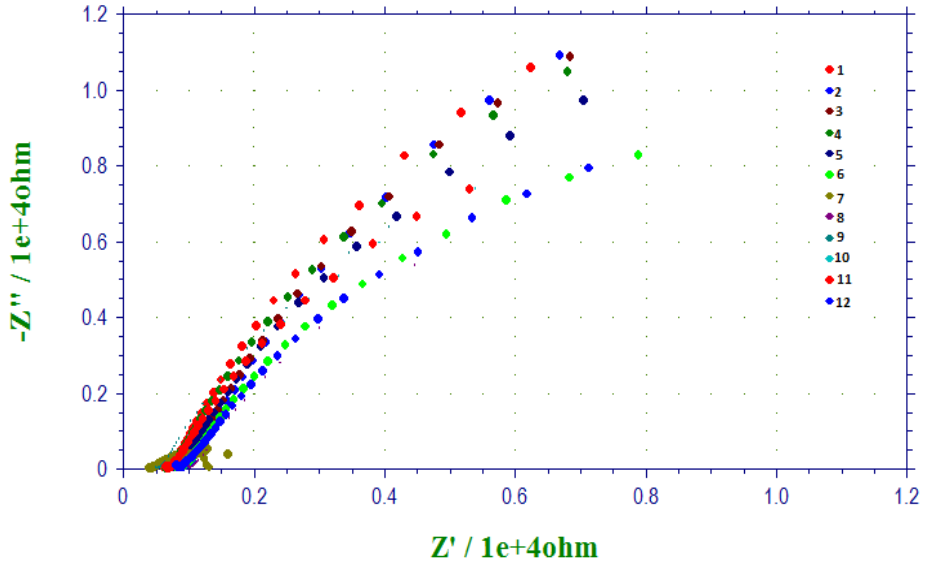

Fig. 4.2.39: Nyquist plot for all 12 Kangra tea samples using PPY electrode

The impedance locus in both the figures takes form of one fully resolved semicircle to the left and a partially resolved semicircle to the right. This behaviour can be attributed to double layer effect involving adsorption. The shift in valley points of the impedance loci of the tea infusions (along the real as well as imaginary axis) can be attributed to charge transfer kinetics and adsorption rate. The electrical equivalent circuit is shown in Fig. 4.2.26 (a).

4.2.8: PCA study for 12 Kangra tea liquor samples

PCA plots for 12 Kangra tea liquor samples using all the six sensing electrodes is given below.

4.2.8.1: PCA response of GC for Kangra tea samples

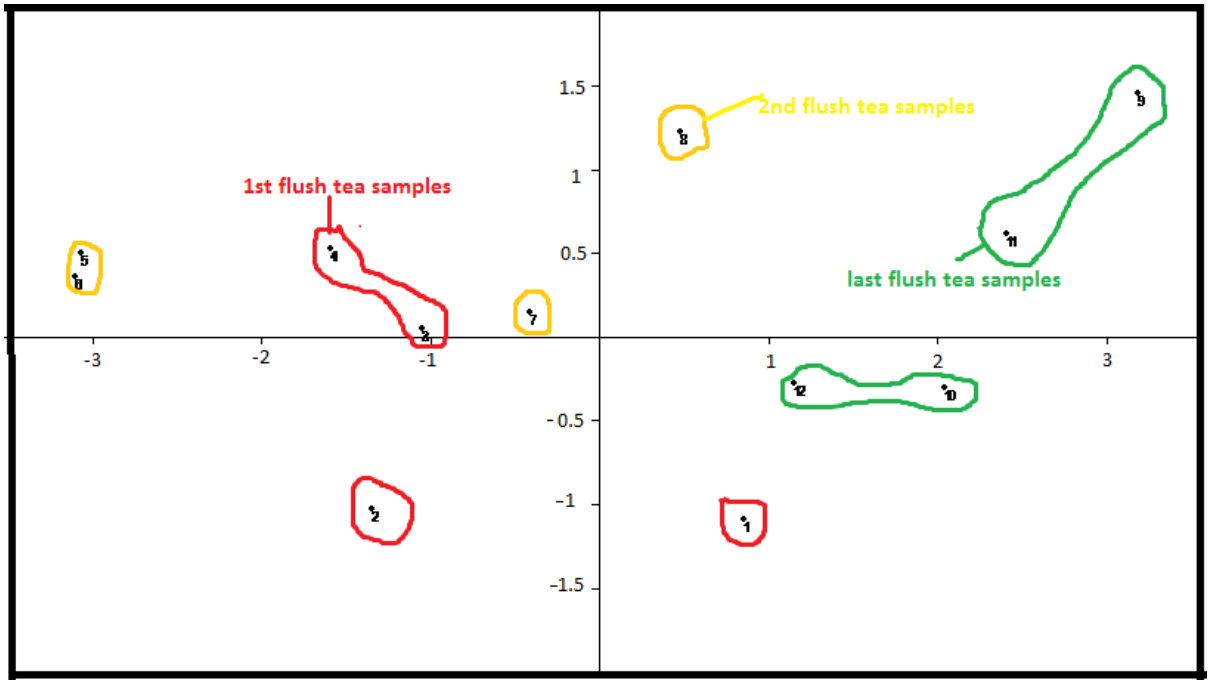

Fig.4.2.40: PCA response of GC electrode

The PCA plot of orthodox Kangra tea for 12 samples collected in various intervals has been plotted in Fig. 4.2.40. It shows the PCA score plot in the form of three groups based on seasonal variations occupy 4 regions in the variance space. More than 98% of the variation was observed with PC1 and PC2 components. From the PCA plot it has been possible to classify the same in three groups i.e. red colour represents first flush tea samples yellow colour represents rainy flush tea samples and green colour represents 3rd flush tea samples.

The tea samples from 1st and 3rd flush showed clusters spread all over the four quadrants whereas small drift in rainy flush tea samples can be seen.

From HPLC data it appears that there is not much compositional change among these tea samples since these were collected from the same source having similar geographical

location. However difference in pattern can be seen with GC which can help in classification of tea on geographical basis.

4.2.8.2 PCA response of Pt for Kangra tea samples

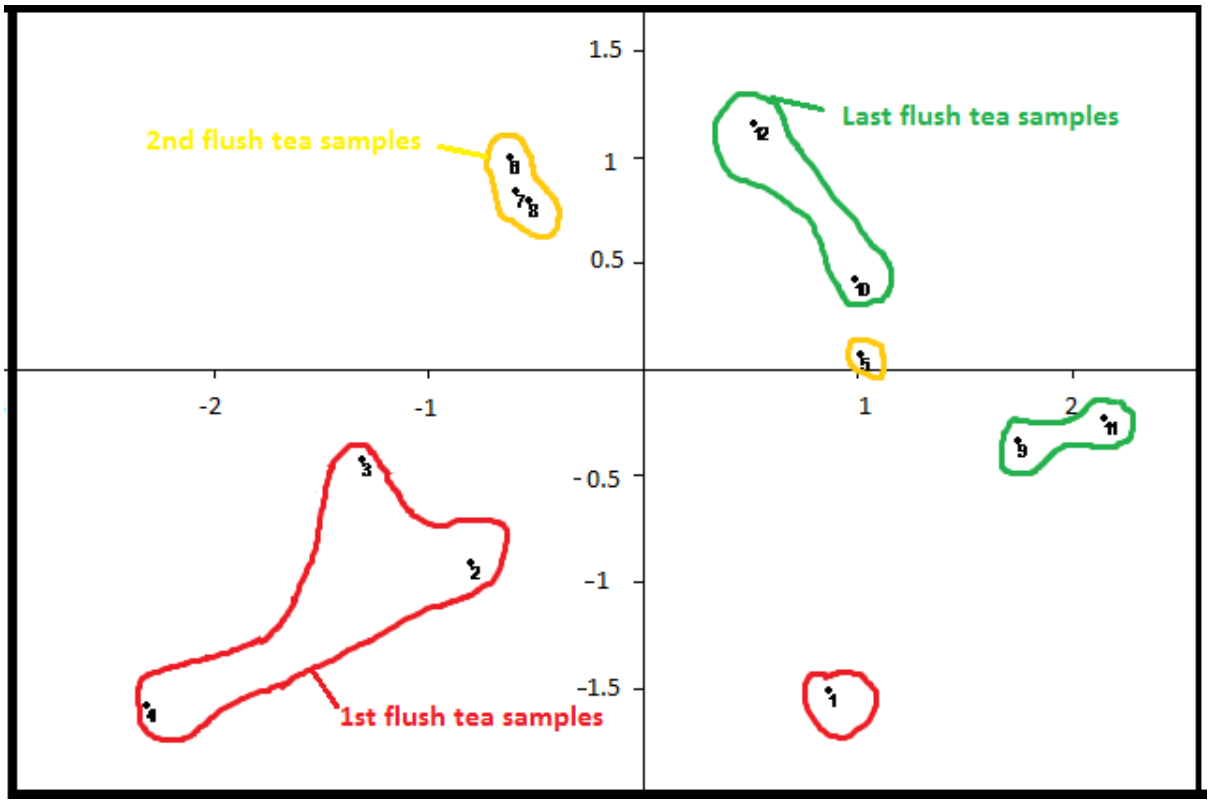

Fig. 4.2.41: PCA response of Pt electrode

Fig. 4.2.41 represents PCA response using Pt electrode for tea samples of Kangra valley. Three different clusters are evident which might have resulted due to slight difference in chemical constituents of tea samples. Almost 99% of the variation is noticed from both the principal components. The 12 different tea samples from three different flush seasons occupy all the four quadrants in the variance space of PCA plot. Using this electrode again it can be noticed that there is slight drift in the cluster of rainy flush tea samples whereas 1st and last flush tea samples shows a visibly evident change compared to the PCA response of GC

electrode. The HPLC results gave very less variation in chemical composition of these tea samples which may be due to the fact these tea samples are plucked from same tea grown site with the same processing conditions.

4.2.8.3: PCA response of Au for Kangra tea samples

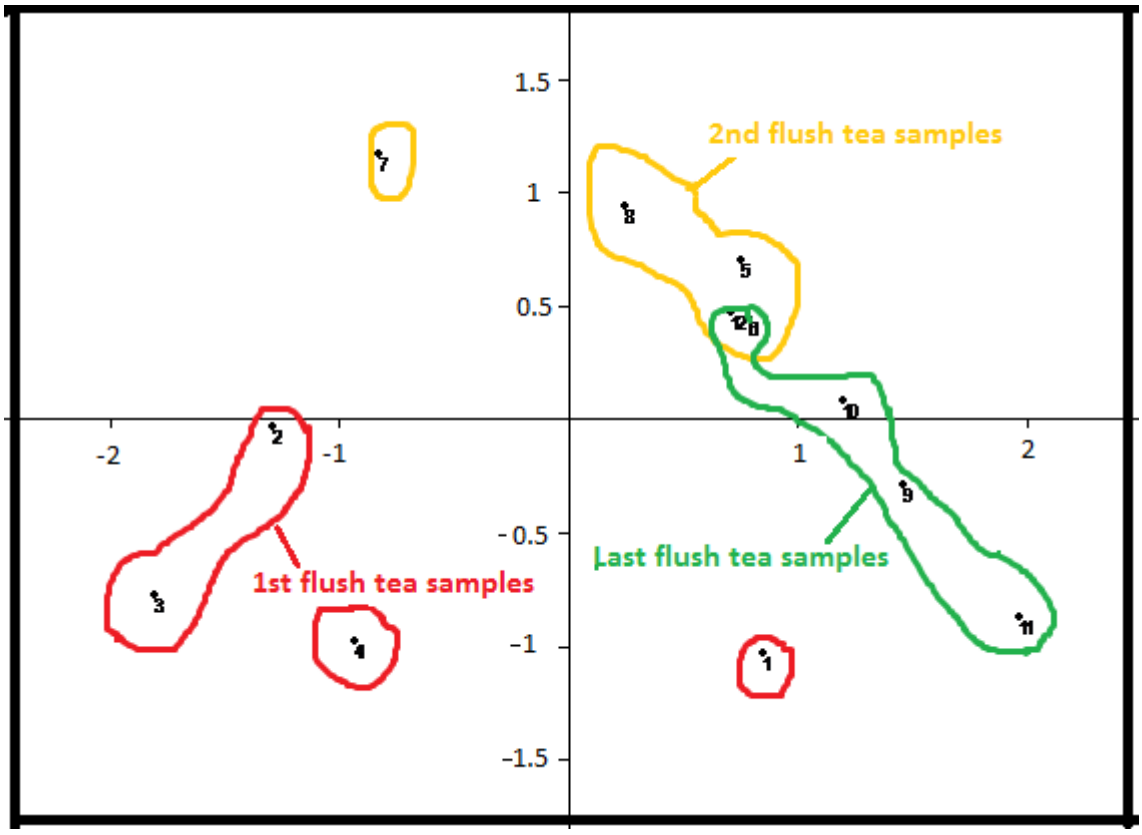

Fig. 4.2.42: PCA response of Au electrode

The PCA pattern for Au electrode can be seen in Fig. 4.2.42. Two principal components PC1 and PC2 accounted for 99% of the variance in the dataset. It is evident that the tea samples are linearly correlated. Since a reasonable co-relation exists between different categories of tea samples; it can be assumed that the categories established by PCA are consistent with the tea samples belonging to 3 different flush seasons. The response of this electrode is different from

GC and Pt electrode still a very less variation in position of Rainy flush tea samples and Au also helped in differentiating tea liquor samples based on seasonal variations.

From PCA it can also be observed that the Kangra valley tea samples are found close in the variance perhaps reflecting the fact that they are obtained from geographically the closest regions and their climatic conditions are similar as well. The PCA data analysis suggests there is considerable spread in the data. This spread may be due to a drifting in the Au electrode response.

4.2.8.4: PCA response of Ag for Kangra tea samples

Fig. 4.2.43: PCA response of Ag electrode

The PCA plot for Ag electrode has been shown in Fig. 4.2.43 this PCA behaviour classifies the 3 clusters of seasonal variations based tea samples with PC1 and PC2 contributing 99% of the variance. The PCA score plot in this approach shows that the 2nd and 3rd flush tea samples are positively correlated the primary reasons may be tea has a very complex botany and the data used in PCA included all the information acquired and a lot of them were either redundant or non-critical. A clear separation of tea samples based on seasonal variations is evident though they are grown in similar geographical and climatic conditions. The data from PCA plot could be of use as a tool in the tea industry for discriminating between different types of tea samples and also as a monitoring tool within the processing of tea.

4.2.8.5: PCA response of PANI for Kangra tea samples

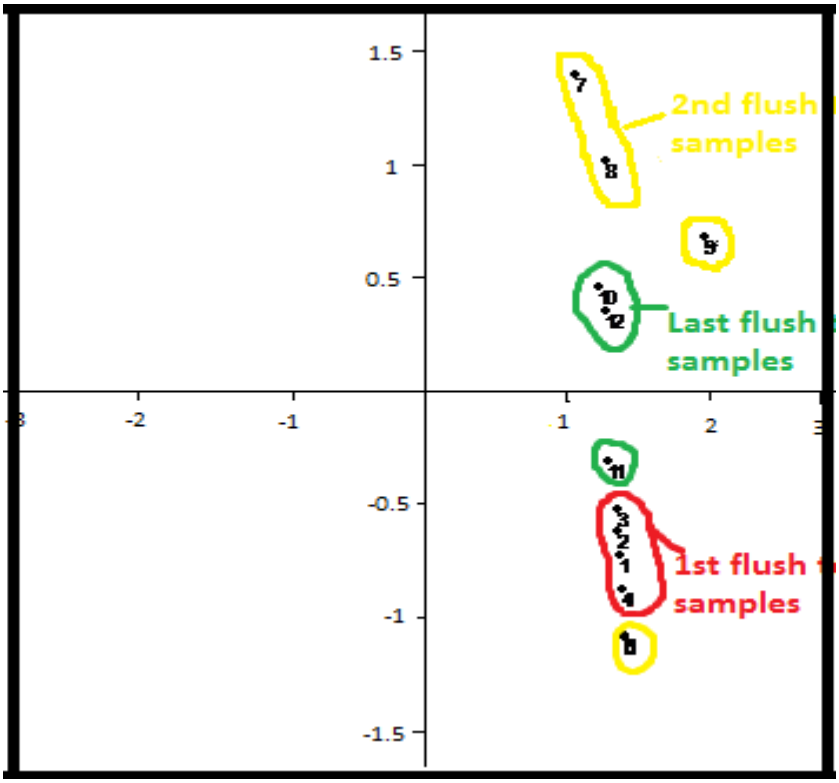

Fig. 4.2.44: PCA response of PANI electrode

Fig. 4.2.44 shows the PCA behaviour for PANI with 99% of the variance observed from PC1 and PC2 coordinates. The PCA response clearly differentiates tea samples from different seasons lie on PC1 and PC2 positive coordinates as well as PC2 negative coordinate. The tea samples from the 1st flush and 3rd flush lie close to each other as both these tea samples share almost similar chemical composition (as shown by HPLC results) and grown under similar geographical location hence these tea samples are positively correlated. PCA score plots for all the tea samples from different flush seasons occupy two regions within the variance space. It is clearly evident from the figure that the different Kangra tea samples sufficiently separate among them.

4.2.8.6: PCA response of PPY for Kangra tea samples

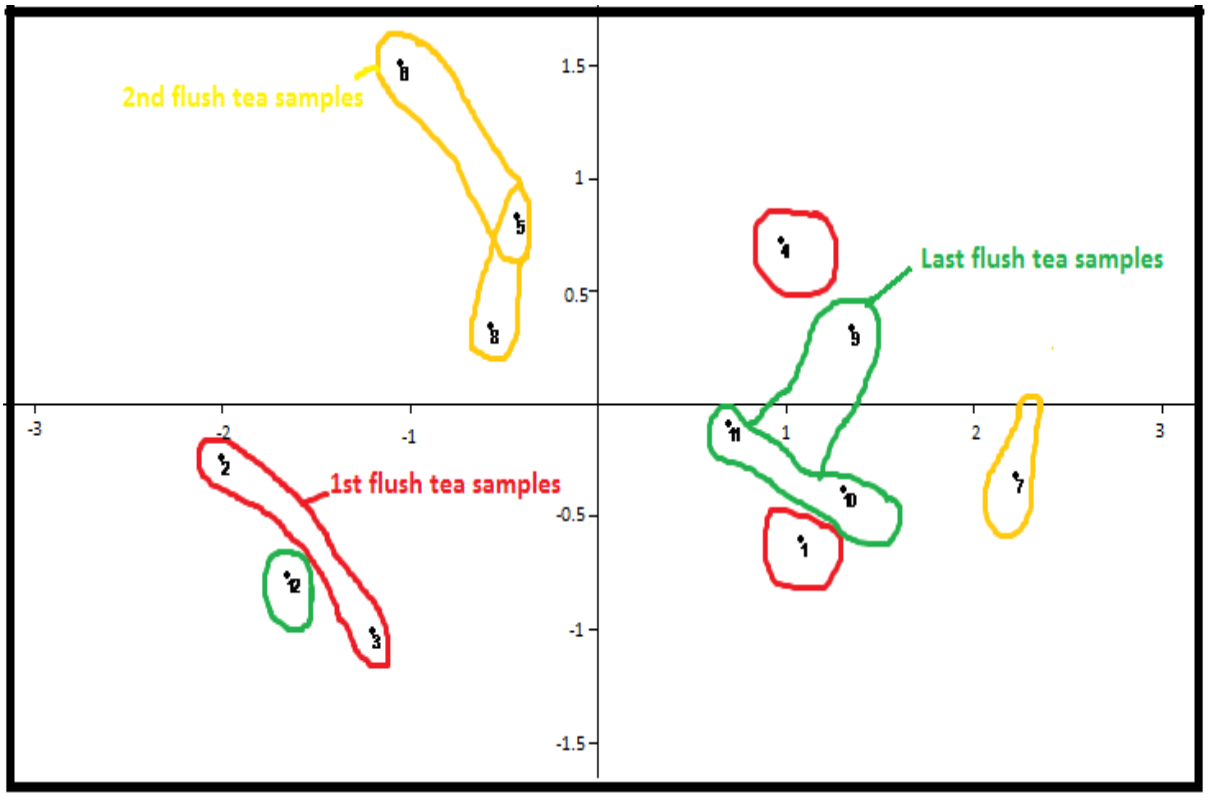

Fig. 4.2.45: PCA response of PPY electrode

The PCA response of PPY electrode can be seen in Fig. 4.2.45 nearly 98% of the variance has been contributed by PC1 and PC2 coordinates. The tea samples from the 1st flush and last flush lie close and are positively correlated. These different seasons occupy the 4 score regions in the variance space of the PCA plot. A small variation is found by HPLC data for these 12 tea samples of Kangra region since these tea samples were collected from the same source having similar geographical location and processed under similar processing conditions. However each electrode helped in classifying the tea samples based on the seasonal variation.

4.2.9: PCA results for Kangra and CTC Assam tea samples

The PCA results for 12 Kangra tea liquor samples and 2 CTC Assam tea samples are discussed below.

4.2.9.1: PCA for Kangra and CTC using GC electrode

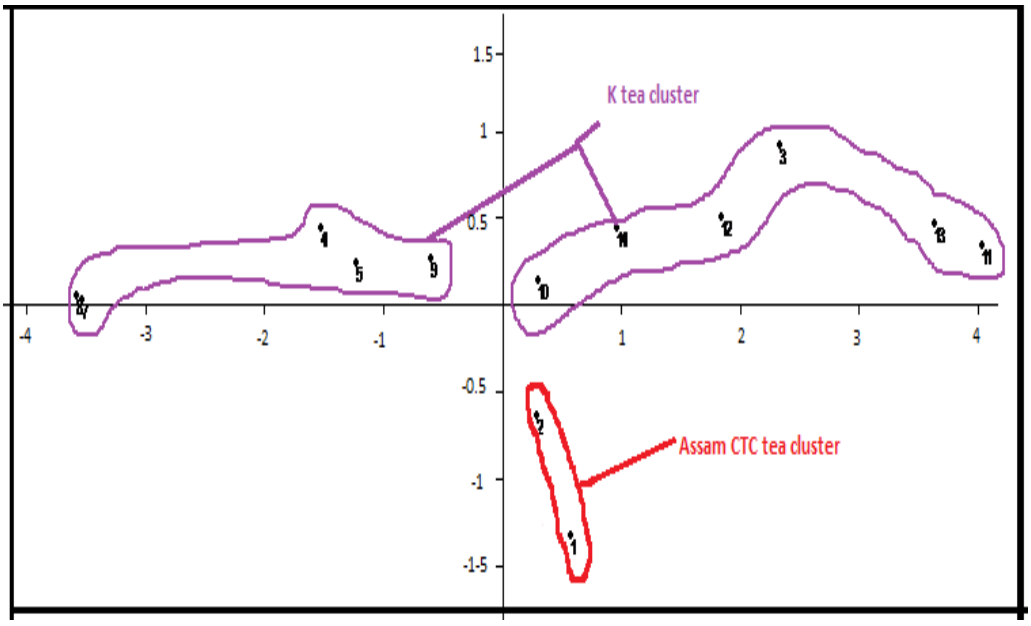

Fig. 4.2.46: Kangra and Assam CTC tea sample PCA using GC electrode

The PCA plot of 12 Kangra tea samples and 2 samples of Assam CTC tea collected at various intervals using GC metal electrode has been plotted in Fig. 4.2.46. This PCA gives almost 98% of the total variance from PC1 and PC2 coordinates. It shows the PCA scores plot in the form of two different clusters of Kangra and CTC Assam tea samples. The GC metal electrode shows a clear distinction among Kangra and CTC tea samples which might have resulted due to the difference in geographical region tea growing site and one of the major reasons is the difference in the processing methods of both these tea samples.

4.2.9.2: PCA for Kangra and CTC using PANI electrode

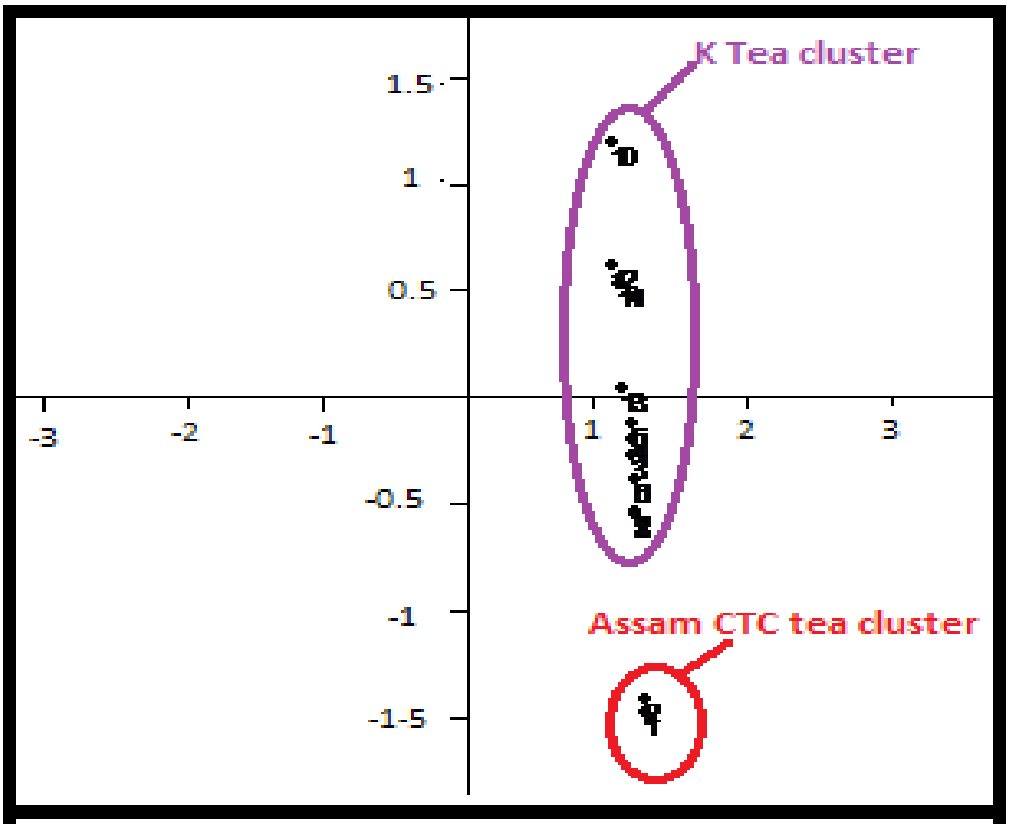

Fig. 4.2.47: Kangra and Assam CTC tea sample PCA using PANI

The PCA plot for both Kangra and CTC Assam tea samples using PANI electrode is shown in Fig. 4.2.47 which represents different clusters of Kangra tea and CTC Assam tea samples. Almost 98% of the variation is observed using both the principal components i.e. PC1 and PC2. It is evident from this PCA plot that PANI electrode also helped in classification of tea samples belonging to different regions efficiently and both the cluster lies in almost a straight line in which CTC tea sample lies far from Kangra tea samples. Hence using both metal as well as conducting polymer electrodes we can classify the tea samples of different regions. Even a minor difference in variation can be traced using sensing surfaces of conducting polymers as well as metals. This technique can work as a fingerprint for quality analysis using both impedance and PCA.

4.2.10: Tea tasters score for Kangra tea and CTC samples

The tea taster's score for both Kangra as well as CTC Assam tea samples is discussed in below mentioned sections.

4.2.10.1: Tea Tasters Score for Kangra Tea Samples

The tea tasters score for the 12 samples of Kangra valley tea has been shown in Table 4.2.18. The score is based on 9-point hedonics scale.

Table 4.2.18: Tea tasters score for Kangra tea samples

Teas	**Appearance (0-9)**	**Infusion color (0-9)**	**Taste (0-9)**	**Aroma (0-9)**	**Shape of infused leaves (0-9)**	**Total score (0-9)**
KI	7.3 ± 0.1	6.5 ± 0.3	8.3 ± 0.1	8.1 ± 0.2	6.6 ± 0.1	7.5 ± 0.1
K2	7.5 ± 0.2	6.6 ± 0.2	8.5 ± 0.2	8.3 ± 0.1	6.5 ± 0.2	7.4 ± 0.1
K3	7.4 ± 0.2	6.7 ± 0.2	8.6 ± 0.3	8.6 ± 0.2	6.8 ± 0.3	7.6 ± 0.02
K4	7.5 ± 0.3	6.5 ± 0.1	8.2 ± 0.3	8.1 ± 0.3	6.6 ± 0.1	7.3± 0.02
K5	7.6 ± 0.2	6.8 ± 0.1	8.7 ± 0.2	8.8 ± 0.3	6.7 ± 0.2	7.7± 0.02
K6	7.8 ± 0.3	6.7 ± 0.1	8.8 ± 0.1	8.7 ± 0.2	6.9 ± 0.2	7.7 ± 0.1
K7	7.3 ± 0.2	6.6 ± 0.3	8.2 ± 0.2	8.3 ± 0.2	6.5 ± 0.3	7.3 ± 0.02
K8	7.4 ± 0.1	6.4 ± 0.3	8.2 ± 0.1	8.1 ± 0.1	6.4 ± 0.3	7.3 ± 0.1
K9	7.4 ± 0.2	6.5 ± 0.2	8.3 ± 0.2	8.2 ± 0.2	6.6 ± 0.1	7.4 ± 0.1
K10	7.7 ± 0.1	6.6 ± 0.1	8.4 ± 0.2	8.1 ± 0.1	6.5 ± 0.3	7.4 ± 0.1
K11	7.6 ± 0.3	6.6 ± 0.1	8.5 ± 0.3	8.3 ± 0.2	6.7 ± 0.2	7.5 ± 0.02
K12	7.5 ± 0.2	6.5 ± 0.2	8.2 ± 0.2	8.1 ± 0.3	6.4 ± 0.2	7.3 ± 0.02

The total scores after combining the five attributes (appearance aroma infusion colour taste and infused leaves) given by the tea-tasting panel ranged from 7.3± 0.1 to 7.7± 0.1 and averaged 7.4 ± 0.1 for Kangra tea samples. Looking at the score of tea tasters we can say tea samples K5 K6 and K3 were adjudged best which can be attributed to high level of catechins present in these tea samples.

4.2.10.2: Tea Tasters Score for CTC Tea Samples

The tea taster's score for CTC Assam tea samples has been given in Table 4.2.19.

Table 4.2.19: Tea tasters score for CTC Assam tea samples

Teas CTC Assam	**Appearance (0-9)**	**Infusion color (0-9)**	**Taste (0-9)**	**Aroma (0-9)**	**Shape of infused leaves (0-9)**	**Total score (0-9)**
1	7.4 ± 0.2	6.6 ± 0.1	8.4 ± 0.3	8.4 ± 0.1	6.6 ± 0.2	7.4 ± 0.1
2	7.4 ± 0.2	6.5 ± 0.1	8.5 ± 0.2	8.3 ± 0.2	6.5 ± 0.2	7.4 ± 0.1
3	7.5 ± 0.1	6.6 ± 0.2	8.5 ± 0.2	8.4 ± 0.3	6.6 ± 0.2	7.5 ± 0.02
4	7.6 ± 0.3	6.7 ± 0.2	8.6 ± 0.2	8.5 ± 0.3	6.7 ± 0.1	7.6 ± 0.02
5	7.7 ± 0.3	6.8 ± 0.3	8.7 ± 0.3	8.7 ± 0.3	6.7 ± 0.3	7.7 ± 0.02
6	7.6 ± 0.3	6.7 ± 0.2	8.7 ± 0.2	8.6 ± 0.3	6.7 ± 0.2	7.6 ± 0.02
7	7.5 ± 0.2	6.5 ± 0.1	8.5 ± 0.1	8.4 ± 0.2	6.6 ± 0.2	7.5 ± 0.1
8	7.4 ± 0.1	6.5 ± 0.1	8.5 ± 0.2	8.4 ± 0.2	6.5 ± 0.2	7.4 ± 0.1

The total scores after combining the five attributes (appearance aroma infusion color taste and infused leaves) given by the tea-tasting panel shown in Table 4.2.19 ranged from 7.4 ± 0.1 to

7.7 ± 0.02 and averaged 7.5 ± 0.02 for CTC Assam tea samples. The tea samples from the rainy flush i.e. 4 5 and 6 were adjudged best among other CTC tea samples.

Conclusion: The AC impedance study suggests that the GC and PANI electrode response comes efficient among these sensing electrodes. PANI/PPY electrodes and metal electrodes give surface behavior in terms of electrical equivalent circuit based on geographical region sample variability such as harvest interval manufacturing process. Every sensing surface gave a unique response to each tea sample. Even a minor difference in variation can work as a fingerprint using impedometric technique.

CHAPTER 4.3

RESULT AND DISCUSSIONS

Taste recognition is the least understood process; probably due to the variety of perception mechanisms involved. In general biological system cannot recognize each chemical substance present in a beverage or food stuff. Instead the gustatory system plays a major role in differentiating the patterns of different tastes and their quality [231-236]. In order to mimic human perception of taste artificial sensors are being used to distinguish four basic tastes (sweetness saltiness sourness and bitterness). These multi-array sensing systems are comprised of number of non-specific and low selectivity sensors; which have high stability and cross-sensitivity towards distinct tastes.

4.3.1 Behaviour of metal and PANI for detection of threshold level of sucrose and citric acid in impedance mode

The substances were classified with different taste modalities i.e. the sweet and sour tastants at threshold level and related to the tastants in fresh citrus fruit juice and sweet tea liquor. Two different tastants i.e. sucrose and citric acid were prepared in concentrations ranging from 5- 100 mM and scanned for optimum frequency from 1 Hz-100 KHz at 0.1 V using three different sensing surfaces made from GC Au and PANI (emeraldine salt) and electrochemical cell for about 30 days keeping all the experimental parameters constant [237]

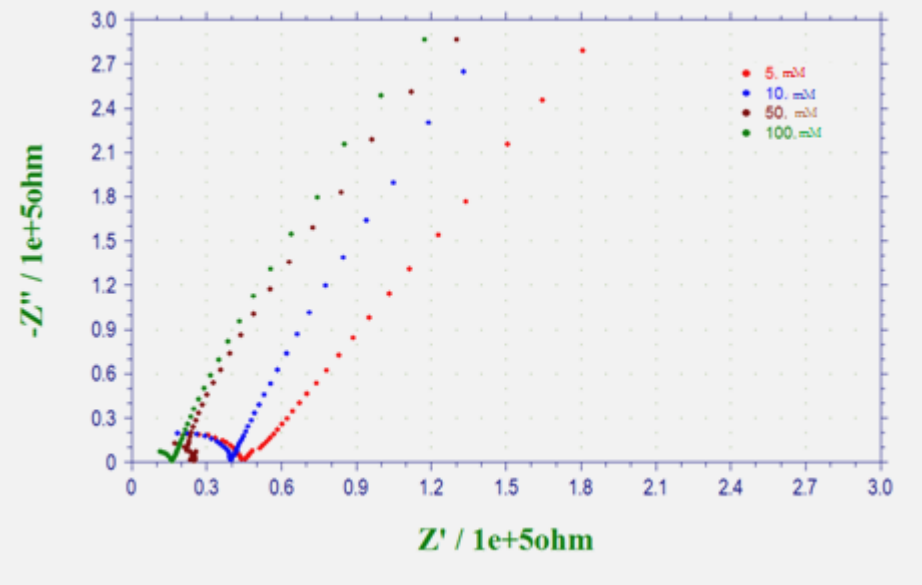

Fig.4.3.1: Nyquist plot of sucrose using GC

The Nyquist plots in Fig. 4.3.1 for sucrose using GC electrode observed are semicircular in nature having maximum radii for 5 mM and minimum radii for 100 mM indicating that the solutions having large semicircle area has maximum impedance whereas semicircle with lower radii has minimum impedance values.

Each semicircular Nyquist plot is followed by 45 º oblique lines which represents Warburg impedance behaviour in terms of Randle's equivalent circuit [Fig.4.3.2] where *Cdl* is the double layer capacitance *Rs* is the bulk sample solution resistance *Rc* is the charge-transfer resistance associated with the double layer [238].

These results indicate that it may be possible to predict the concentration of different varieties of sugars in the impedance mode using appropriate number of known samples.

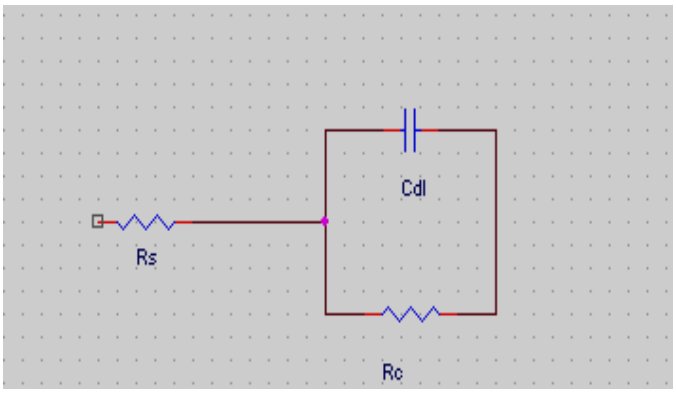

Fig.4.3.2: Randle's Equivalent circuit

Fig.4.3.3 represents Nyquist plot for Au for sucrose solution. Nyquist plots in Fig.4.3.3 shows almost fully resolved semicircle towards left followed by oblique lines at right side for 5 mM concentration solutions whereas other three concentration solutions have a very small semicircle close to the origin at high frequency followed by semicircular 45° lines whose pattern changes but not their shape [239-240].

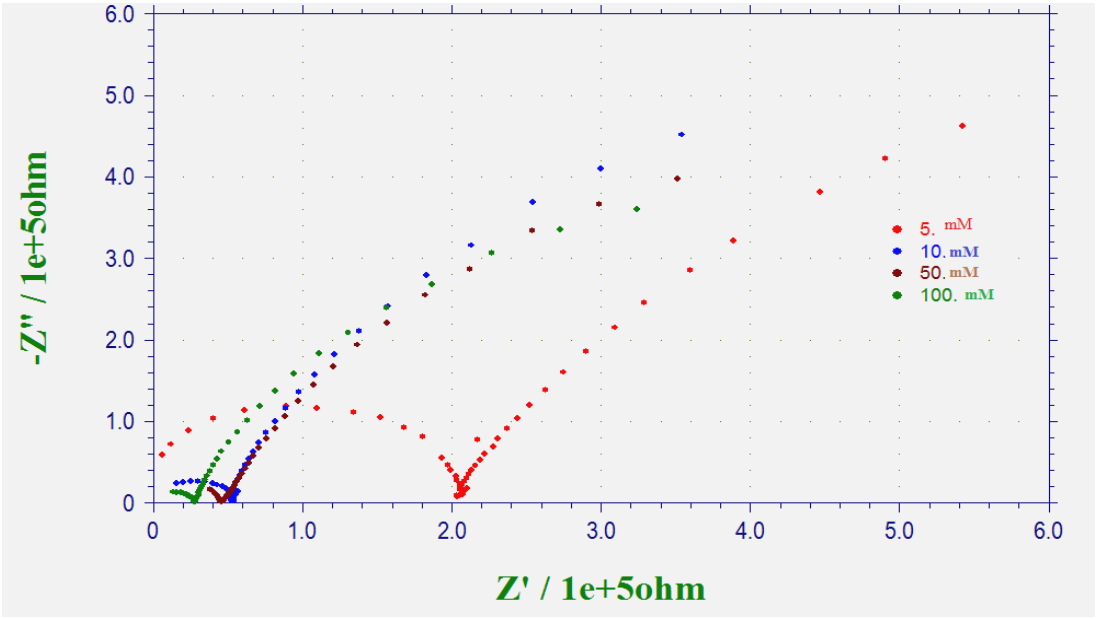

Fig.4.3.3: Nyquist plot of sucrose using Au

The impedance behaviour indicates that it is well possible to differentiate the threshold level sweet taste with Au electrode in comparison to higher concentration solutions. The reason for the same may be that a very thin layer of oxides of gold may occur with higher concentrations which are giving rise to similar impedance behaviour for 10 mM concentration onwards. The physical model appropriate for the observed impedance response is simple Randle's equivalent circuit [Fig. 4.3.2]

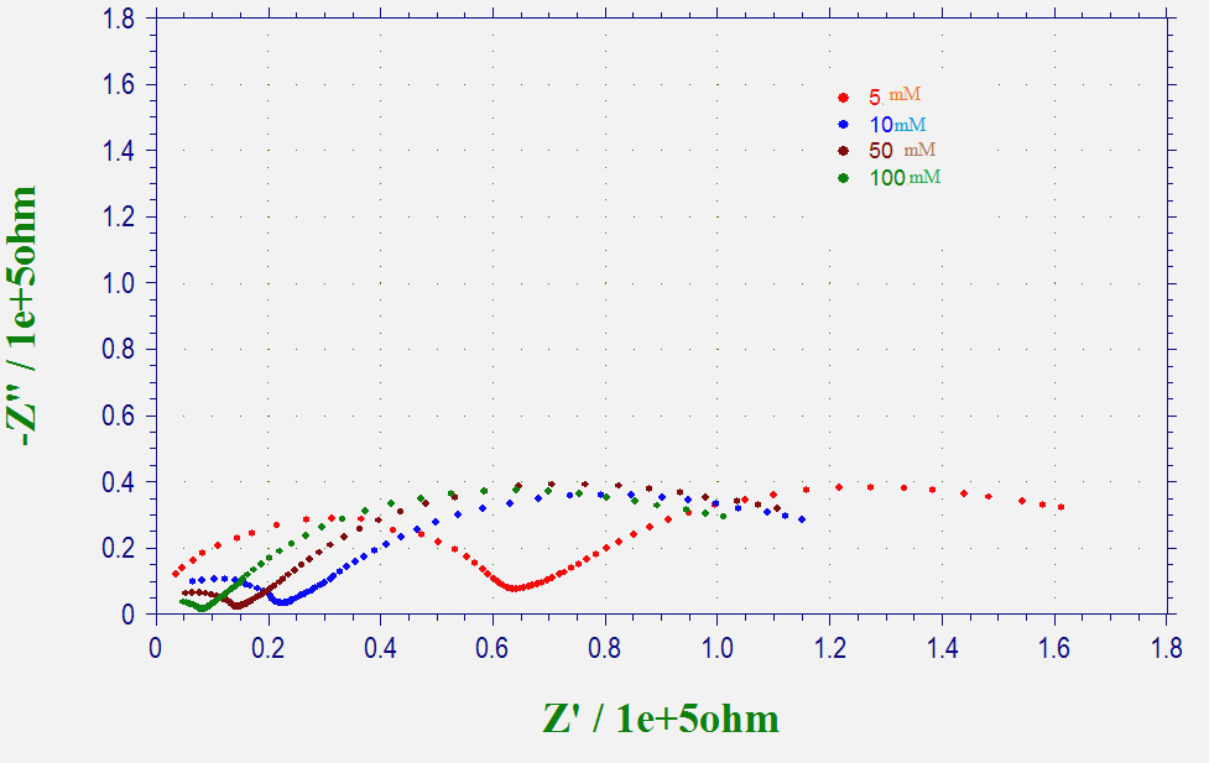

Fig.4.3.4: Nyquist plot of sucrose using PANI

Figure 4.3.4 represents the impedance plots where two semicircles were obtained using PANI working electrode a fully resolved semicircular arc can be seen on the left side of the plot and partially resolved semicircle obtained on the right side of the Nyquist plots. Conduction may

be low for dilute solutions in comparison to higher concentration solution. This behaviour occurred possibly due to the adsorption of the sucrose molecule at the surface of the PANI electrode giving rise to double layer affect. This result can be modelled by two RC-parallel circuits in series. Each parallel combination of resistance *R* and capacitance *C* results in a semi-circle in the impedance plot. Distorted nature of the semicircle attributes to the variation of the morphology of the PANI electrode resulting in change in conduction mechanism at the interface.

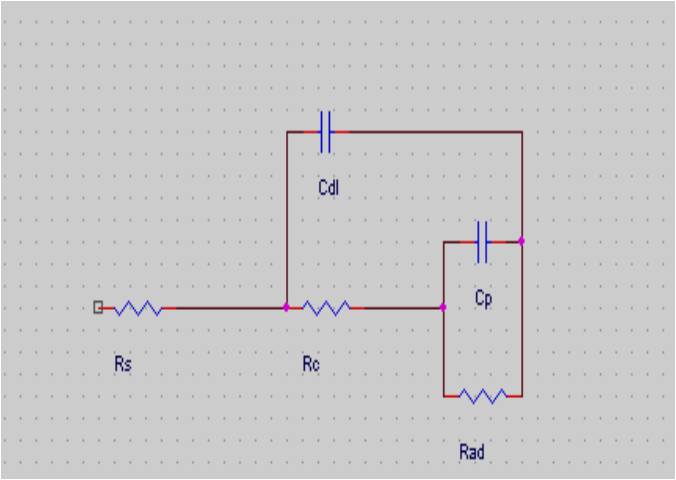

Fig.4.3.5: Equivalent circuit for adsorption

The equivalent circuit corresponding to adsorption describes the response for PANI electrode [Fig.4.3.5]. In this equivalent circuit for adsorption *Rs* is the bulk sample solution resistance *Rc* is the charge-transfer resistance associated with the double layer *Cdl* is the double-layer capacitance *Rad* is the resistance of the adsorption layer *Cp* is the passivative capacitance associated with the adsorption layer.

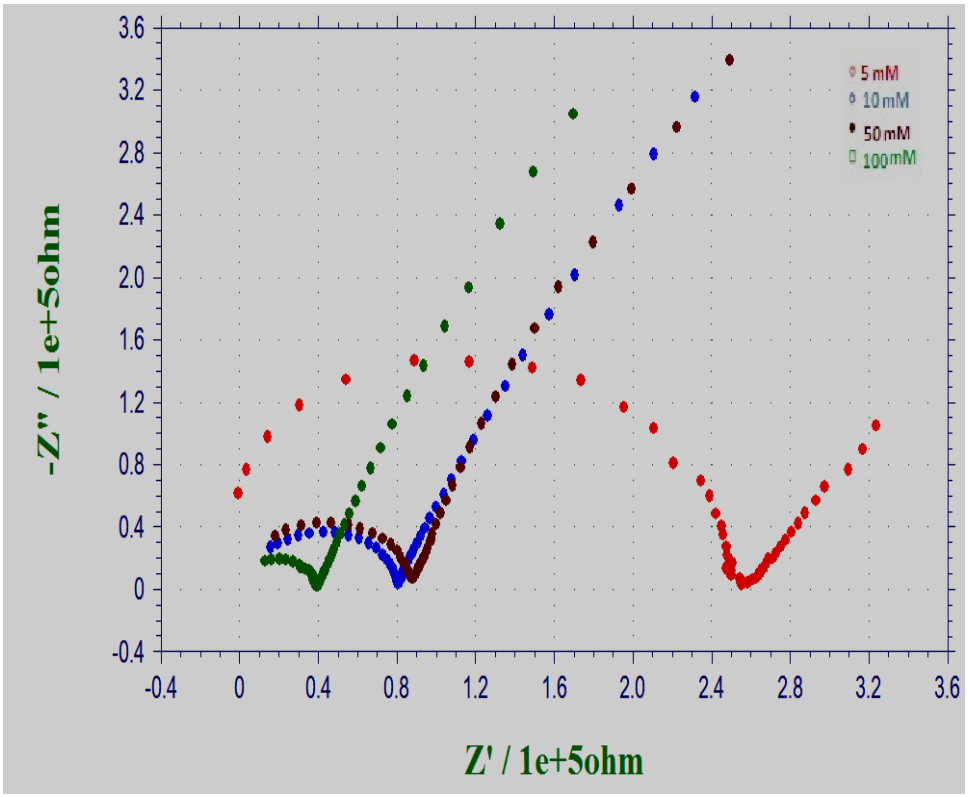

Fig.4.3.6: Nyquist plot of citric acid using GC

Fig.4.3.6 represents a linear impedance locus with an angle of 45^0 to the real axis which amounts to low frequency Warburg response [Fig.4.3.2] due to diffusion. However at high frequencies the citric acid solution shows converge with null imaginary impedance small semicircle. With the increasing concentration of solution, area under the semicircular arc decreases. The smaller semicircular part corresponds to the faradaic oxidation reaction whereas part of the large diameter semicircle is associated with charge transfer process.

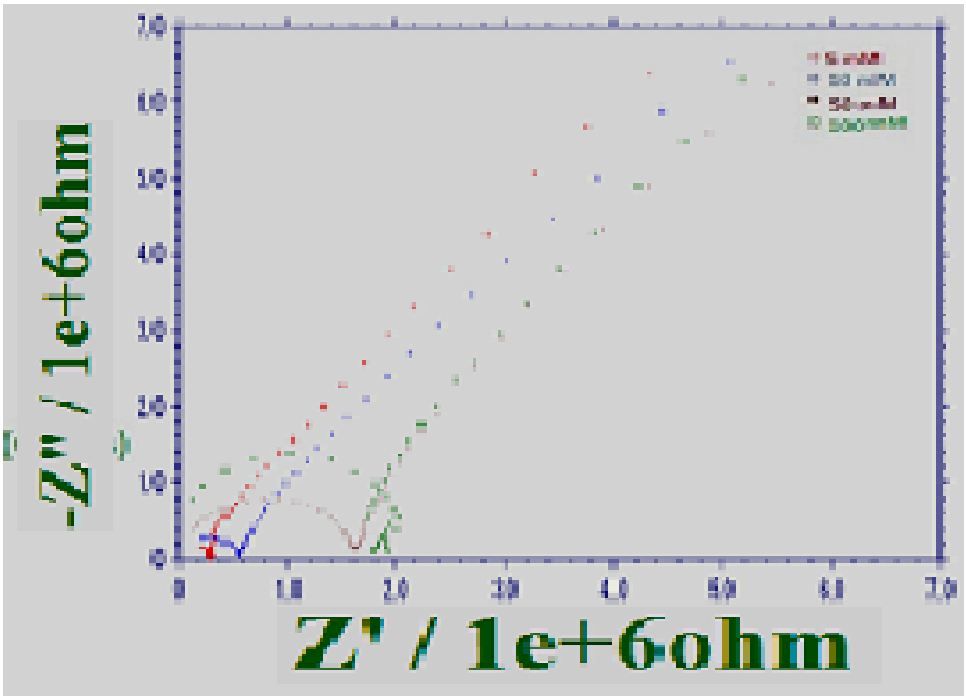

Fig.4.3.7: Nyquist plot of citric acid using Au

Figure 4.3.7 shows a small semicircular Nyquist plots for citric acid using Au surface which corresponds to the bulk electrode resistance in parallel with the capacitance. This near vertical lines with 45º trend is due to the charge transport impedance originates from non-uniform concentration profiles of charged species on the electrode [241].

This 45º line arises due to the diffusion phenomenon which leads to Warburg impedance. The physical model explaining this phenomenon is Randle's equivalent circuit [Fig. 4.3.2].

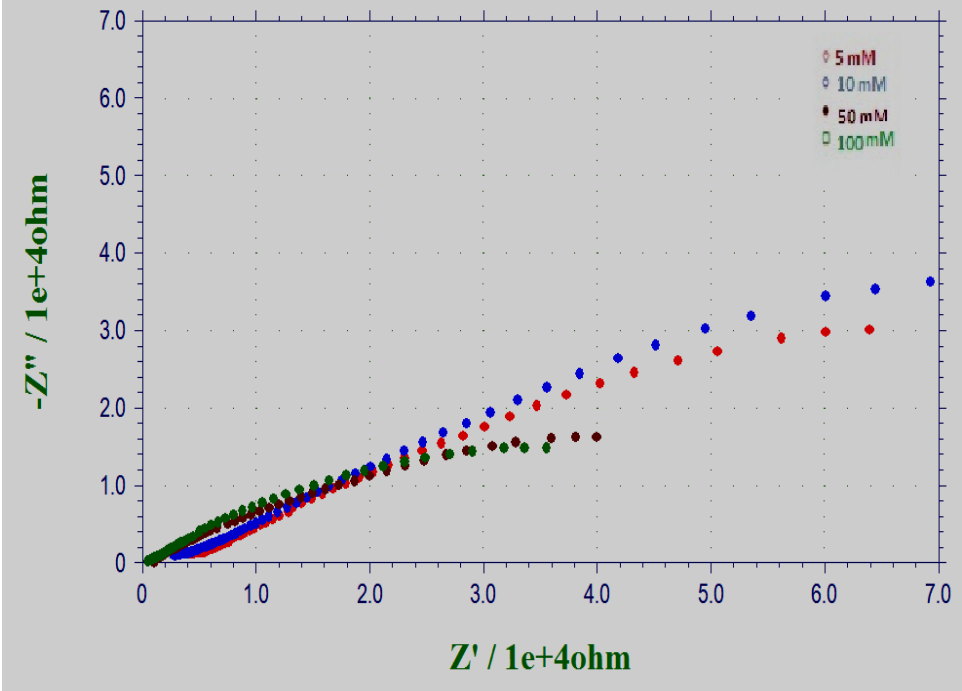

Fig.4.3.8: Nyquist plot of citric acid using PANI

Impedance response of Figure 4.3.8 shows two semicircles left fully resolved semicircle and right partially resolved semicircle for various citric acid concentrations on PANI. A capacitance dispersion effect represented by distorted semicircles can be observed for PANI electrode. This behaviour is commonly observed in case of non-homogeneous surfaces displaying surface defects for instance porosity. At open circuit potential state the PANI film is in its emeraldine form in the emeraldine state of PANI the oxidized and reduced units of the polymer are almost equal and a result the PANI film exhibits a maximum conductivity. The shift in valley points of the impedance loci of the citric acid solution (along the real as well as imaginary axis) can be attributed to charge transfer kinetics and adsorption rate. The equivalent circuit corresponding to adsorption describes the response for PANI electrode [Fig. 4.3.5].

4.3.2 PCA Study for metal and PANI for detection of threshold level of sucrose and citric acid in impedance mode

For PCA study Unscrambler9.7 has been used. The first principal component (PC1) maps the maximum variance and information of the input data followed by the other principal components (PC2 PC3 and so on) in descending order of the variance. Generally a good discrimination is mapped by the first two principal components i.e. PC1 and PC2.

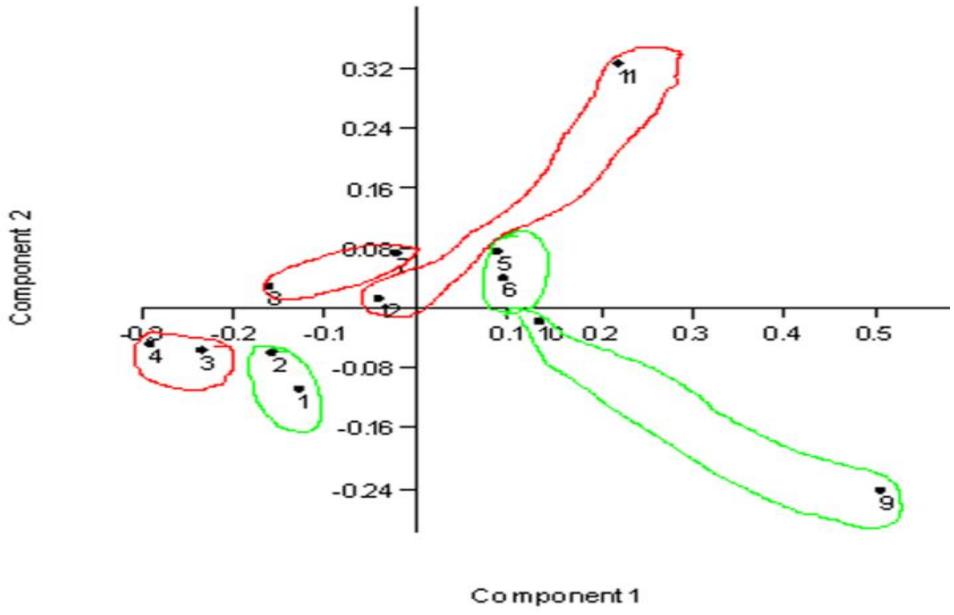

Fig.4.3.9: PCA of sucrose using PANI GC and Au

The PCA plots for sucrose and Citric acid at four different concentrations (5 10 50 and 100 mM) with GC Au and PANI working electrodes are represented in Figures 4.3.9 and 4.3.10 respectively. The data is plotted in a two dimensional plane formed by the first two PCs with

PC1 showing 73.09% and PC2 showing 26.69% data variance in Figure 4.3. 9. All the points for four different concentration solutions of sucrose lie on same quadrant i.e. 3rd quadrant (negative values). This shows PANI electrode gives nearly a common cluster for both low and high concentration solutions. The 5 and 10 mM concentration (low concentration solutions) lie close by in the 1st quadrant using GC electrode while 50 and 100 Mm concentration solutions lie on the 2nd quadrant (negative values) and can be seen near to each other. Hence GC electrode helps in classifying low and high concentration solutions clearly. The low concentration (5 and 10 mM) solutions lie together in the 4th quadrant using Au electrode. While 50 and 100 mM solutions (high concentration solutions) lie at different quadrant. This indicates Au electrodes helps in distinguishing low concentration solutions steadily [242].

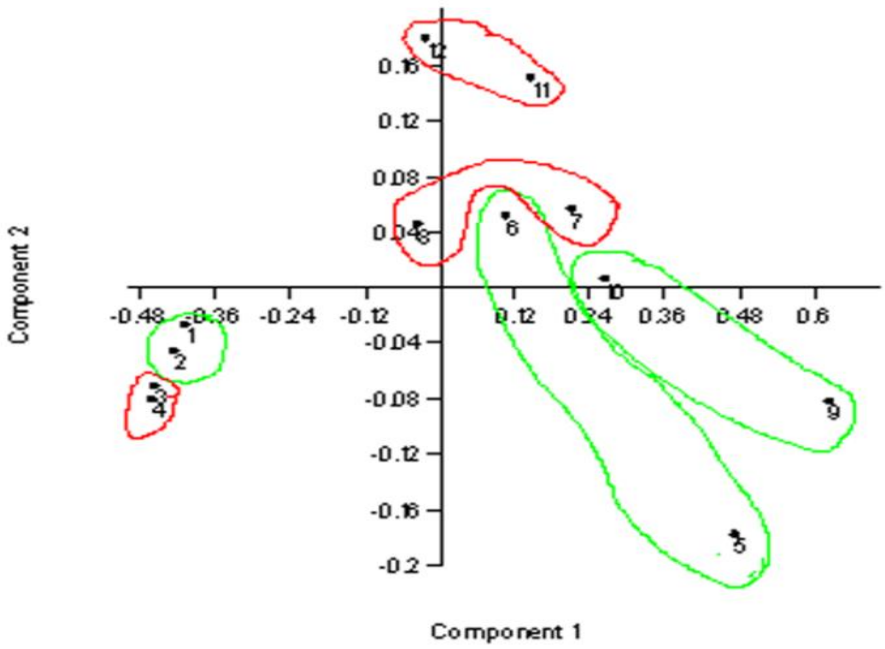

Fig. 4.3.10: PCA of Citric acid using PANI GC and Au

Fig. 4.3.10 shows the data plotted in a two dimensional plane formed by the first two PCs PC1 (horizontal) axis with an explained variance of 92.88% and PC2 showing 7.03% data variance. A cluster for both low and high concentration solutions was observed using PANI electrode i.e. in 3rd quadrant. The use of GC electrode all the four concentrations lay separately from PANI electrode whereas 10 50 and 100 mM lay close to each other indicating a positive correlation. With Au electrode both low concentrations (5 and 10 mM) and high concentrations (50 and 100 mM) were found close to each other. Hence GC metal electrode provided a good classification for both high and low concentrations solutions of citric acid.

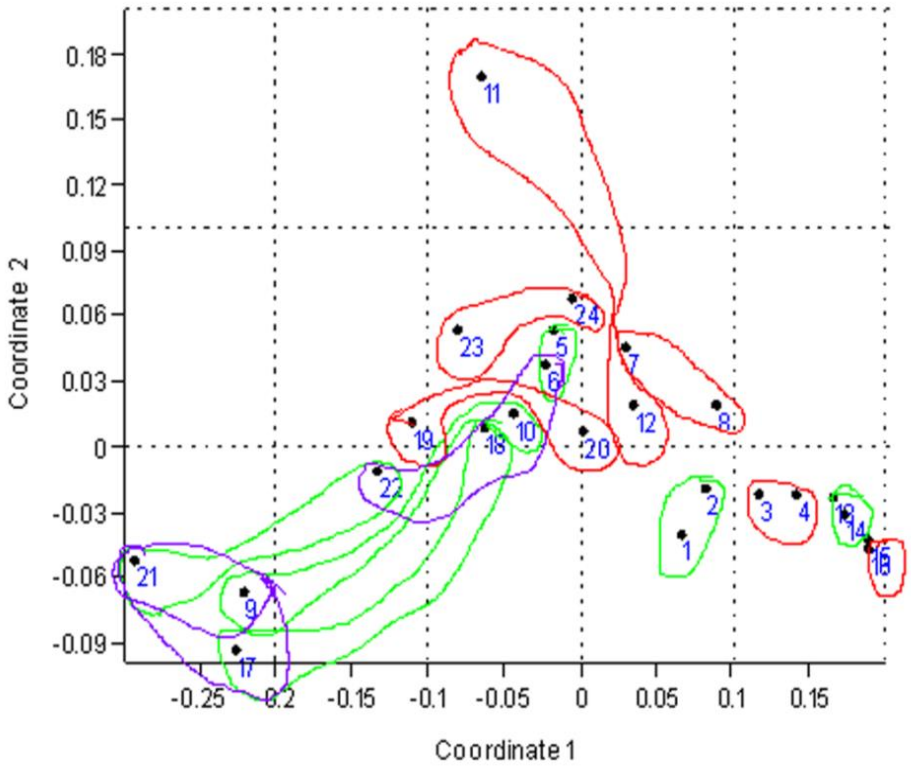

Fig.4.3.11: PCA of Sucrose and Citric acid using PANI GC and Au

Fig. 4.3.11 gives PCA plot for both the sucrose and citric acid solutions at four concentrations namely 5 10 50 and 100 mM with PANI GC and Au working electrodes PC1 gives an explained variance of 85.79% and PC2 gives 14% of data variance. All the points at four concentrations using PANI electrode for sucrose and citric acid shows a very good classification. These entire points lie closer hence PANI electrode accounted for efficient classification among intra frequency as well as intra electrode class for both the sweet and sour compounds (sucrose and citric acid). GC electrode also played a significant role in classifying low concentration as well as high concentration solutions of both sucrose and citric acid. Therefore GC and Au electrodes were important in classifying both low concentration solutions and high concentration solutions.

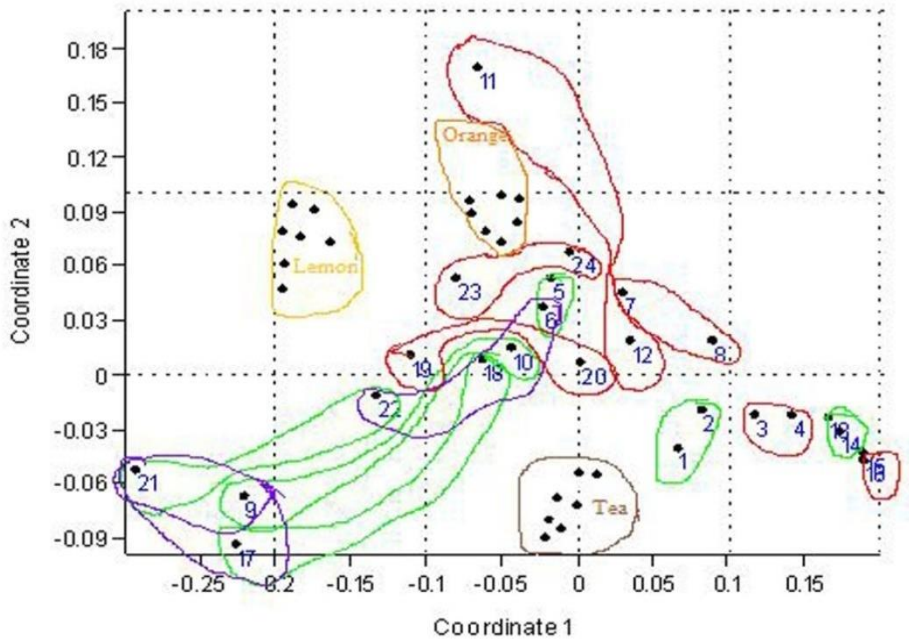

Fig. 4.3.12: PCA of Sucrose Citric acid juices and tea using PANI GC and Au

Fig. 4.3.12 gives PCA plot for sucrose citric acid freshly prepared fruit juices and sweet tea liquor at four concentrations (5 10 50 and 100 mM) with GC Au and PANI working electrodes corresponding to seven days data. More than 99% significant information is available with the first two principal components (PC1 and PC2).The lemon juice lies close to the low concentration solution of citric acid which may be due to more amounts of acidic compounds present in lemon. The orange juice gives a random response lying closer to low concentration solutions of both metal electrodes and shows some correlation with high concentration solutions of citric acid. Whereas the sweet tea liquor in sucrose falls close to low concentration solutions of sucrose with the use of PANI GC and Au working electrodes. Based on the above data it may be inferred that with the present study it may not be possible to classify the taste quality of the fruit juices and further behavioural studies in impedance mode for analyzing levels of different sugars salts and organic acids as tastants need to be carried out.

4.3.3 Impedance study of tea with added taste compounds using conducting polymer and metal electrodes

Electrochemical impedance was measured by applying an AC potential to an electrochemical cell containing the sample solution and measuring the current through the cell using small excitation signals.

4.3.4 Impedance Study of Tea Liquor Samples for tea liquor sample with sucrose

The impedance response of four electrodes (Au Pt Ag and GC) and two conducting polymer electrodes (ITO-PANI and ITO-PPY) for tea liquor sample with sucrose in the frequency

range of 1 Hz–100 KHz with a potential of 0.1 V are given in Figures 4.3.13 and 4.3.14 respectively [243].

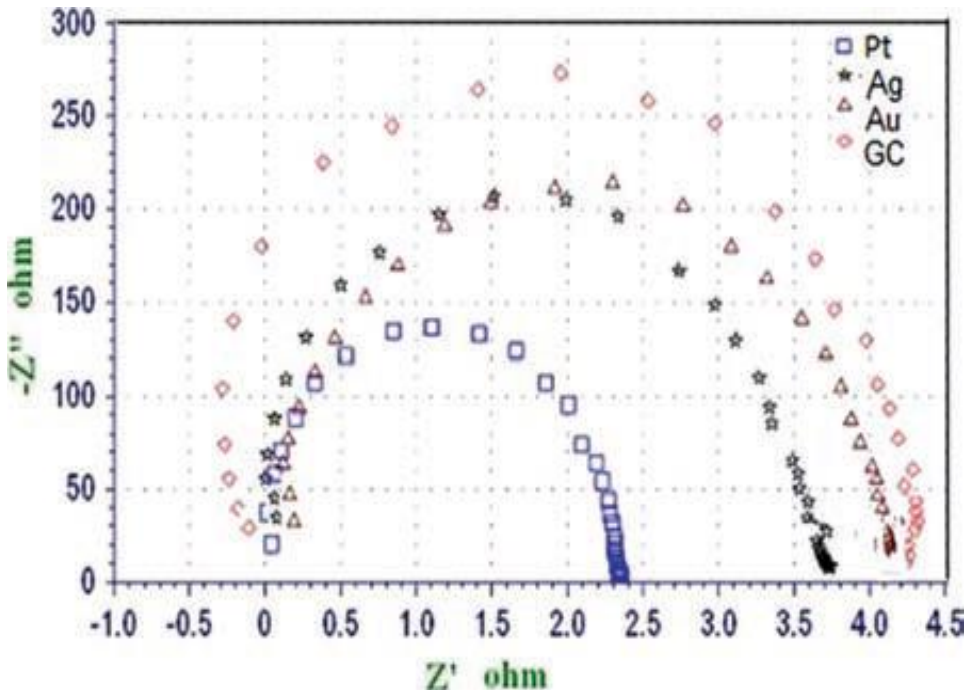

Fig. 4.3.13: Nyquist plot for tea liquor with sucrose using four metal electrodes (Pt Ag Au and GC)

Fig. 4.3.13 shows the Nyquist plots for metal electrodes for tea liquor sample with sucrose. In these impedance plots each electrode surface represents the response for tea liquor sample with sucrose. The impedance study was carried out with the open circuit potential (*E*ocp). *E*ocp of every sample was observed for 10 minutes over a frequency range of 1 Hz to 100 KHz. When the impedance is plotted in the complex plane we obtained a semicircle combined with a straight line at an angle of 45º to the real axis which may be due to Warburg impedance.

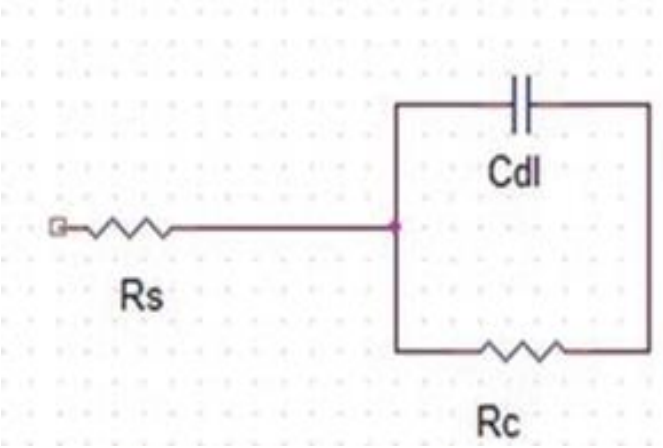

Fig. 4.3.13: (a) Randle's equivalent circuit

The physical model explaining this phenomenon is Randle's equivalent electrical circuit Fig. 4.3.13 (a). This behaviour can be attributed to diffusion phenomenon occurring at the solution–electrode interface. The impedance data were simulated using the Randle's equivalent circuit Fig. 4.3.13 (a) consisting of a parallel combination of the capacitance (*C*) and charge transfer resistance by redox reactions (*R*ct) in series with the electrolytic resistance (*Rs*). The fitting of spectra's to the equivalent circuit has indicated a good agreement between the circuit model and the real experimental data especially at the high frequency values.

Nyquist plots for PANI and PPY are shown by Fig. 4.3.14 can be described as a partially resolved semi-circle near the origin at (low frequency) followed by partially resolved semi-circles (towards high frequency). These conducting polymers of PANI and PPY show variation in comparison to the metal electrodes of Pt Ag Au and GC. The reason for the variation may be the porosity in the electrode surface or may be due to some variation of the surface structure of PANI by continuous dipping in tea liquor sample with sucrose. As shown

these impedance plots appear more complex and the two semi-circles depend on the nature of the electrode material.

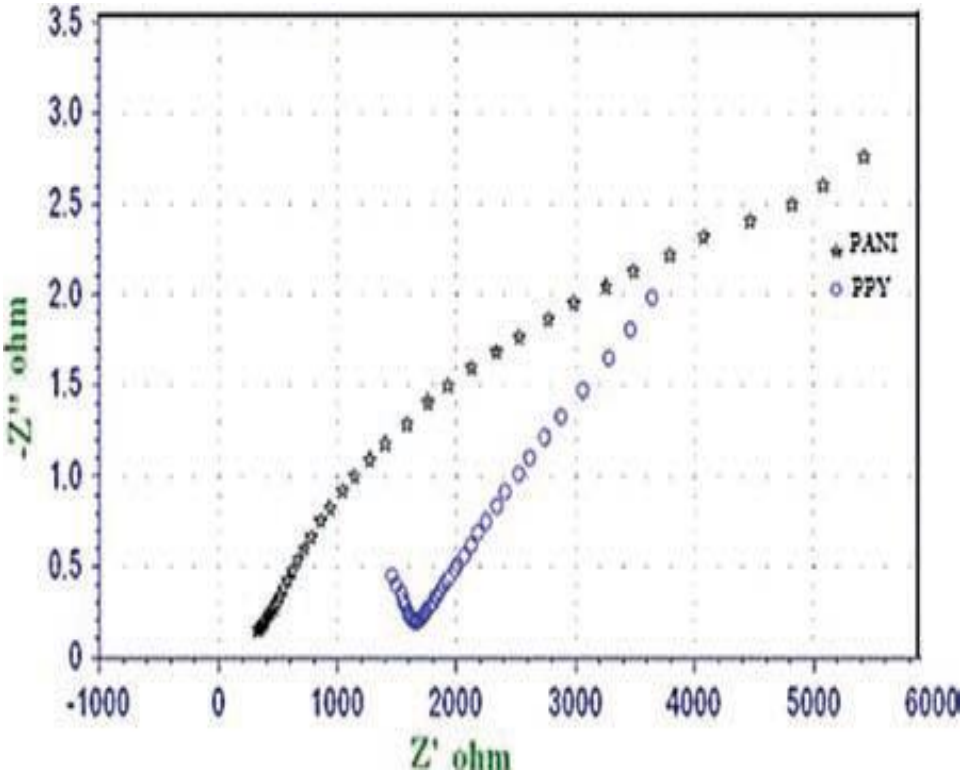

Fig. 4.3.14: Nyquist plot for conducting polymer electrodes ITO-PANI and ITO-PPY for tea liquor with sucrose

The electrical equivalent circuit responsible for PANI and PPY graphs is an equivalent circuit due to adsorption shown in Fig. 4.3.14 (a). In this equivalent circuit for adsorption *Rs* is the bulk sample solution resistance *Rc* is the charge-transfer resistance associated with the double layer Cdl is the double layer capacitance *R*ad is the resistance of the adsorption layer *C*p is the passivative capacitance associated with the adsorption layer.

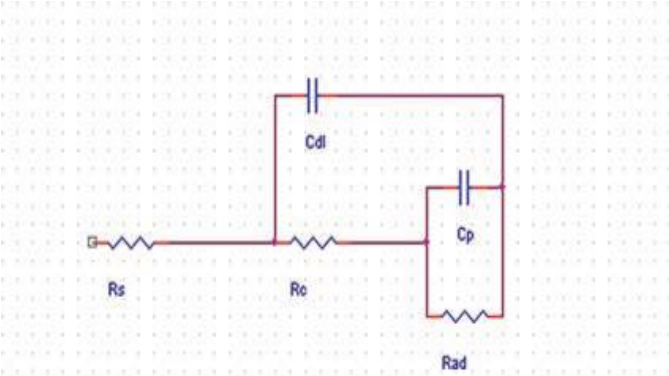

Fig. 4.3.14 (a): Equivalent circuit for PANI and PPY

These responses may be attributed to the change of the morphology and the conductivity of the electrode/electrolyte interface. The average impedance observations of six working electrodes for tea liquor with sucrose are given in Fig. 4.3.15 these observations indicates that Au and GC electrodes are highly sensitive.

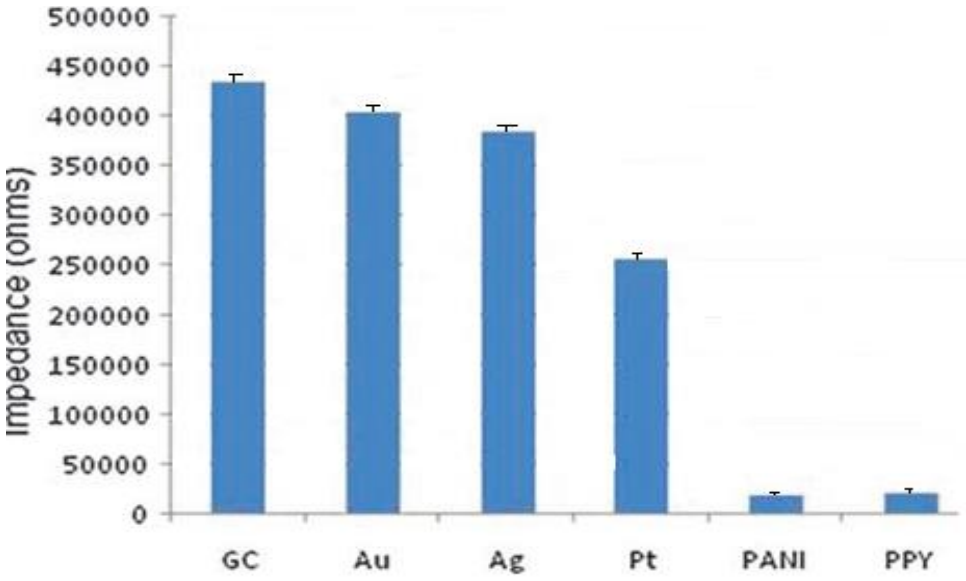

Fig. 4.3.15: An impedance of tea liquor sample with sucrose with impedance values for six different electrodes GC Au Ag Pt PANI PPY (Left to Right)

The impedance of six tea samples: A, B, C, D, E and F (Table 4.3.1) are represented in Figure 4.3.16 using all the six working electrodes.

Table 4.3.1: Nomenclature of black tea with added compounds

S. No.	Composition	Name
1	Black tea liquor + raw milk from local dairy	A
2	Black tea liquor + sweet clove syrup	B
3	Black tea liquor + sweet ginger syrup	C
4	Black tea liquor + sweet cardamom syrup	D
5	Black tea liquor + sweet chocolate syrup	E
6	Black tea liquor + vanilla flavoured milk without sugar	F

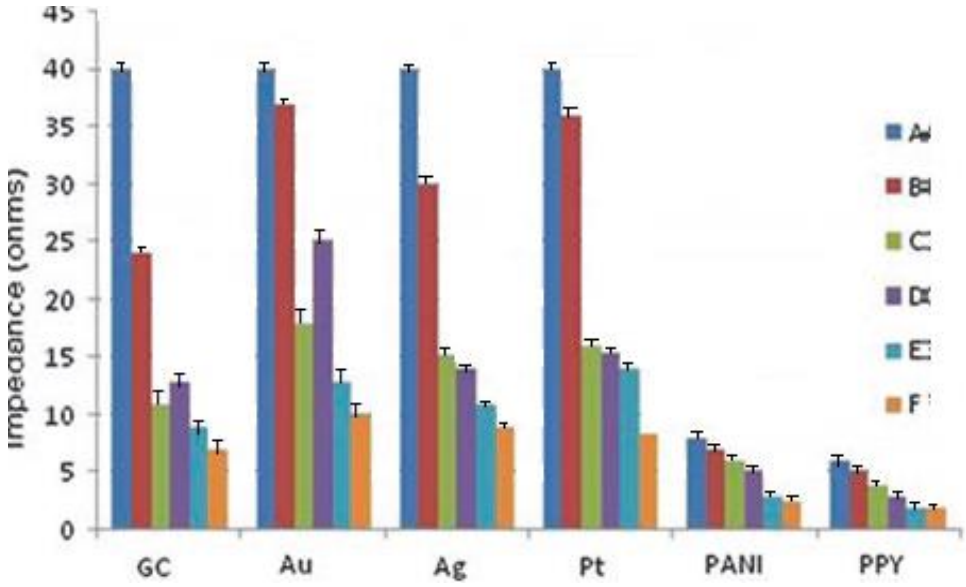

Fig. 4.3.16: An impedance of six tea liquor samples using all the six working electrodes: A, B, C, D, E and F

Fig. 4.3.16 represents the impedance of tea samples with six different added taste compounds. Sample A shows higher impedance values with all the three metal electrodes GC electrode as well as with conducting polymer electrodes tested indicating that this tea sample may contain more amounts of antioxidants/ions hence shows a flattened circle on a complex plane plot. Sample B represents almost similar values with not much significant impedance changes in Au or Pt whereas the impedance of the Ag and GC electrodes were of the order of 75% and 50% approximately to that of the Au and Pt electrodes. The B, C, D, E and other black tea liquor samples A and F have lower impedance output for GC Ag Au and Pt electrodes. The impedance behaviour of Au electrode with sample D showed somewhat higher impedance values in comparison to other metal electrodes while conducting polymer electrodes have low impedance output. Thus impedance data explained that Au electrode and sample D were related at higher impedance which may be due to dissolved minerals present that can be seen from the values of impedance. Impedance measurements of all the black tea liquor samples on the polymer electrode show charge-transfer resistance polymer thin-film interference the ion diffusion co-efficient into the polymer and the redox capacitance as an important parameter of electrochemically conducting polymers.

4.3.5 PCA Study of Tea Liquor Samples with different tastants

The assessment of sensors was carried out using impedance data with the combination of sensing electrodes for different types of tea liquor samples in PCA. In PCA results first principal component provided most of the information and presents the highest variance.

Sensing system with three metal electrodes and GC efficiently classified the data in various groups in Fig. 4.3.17.

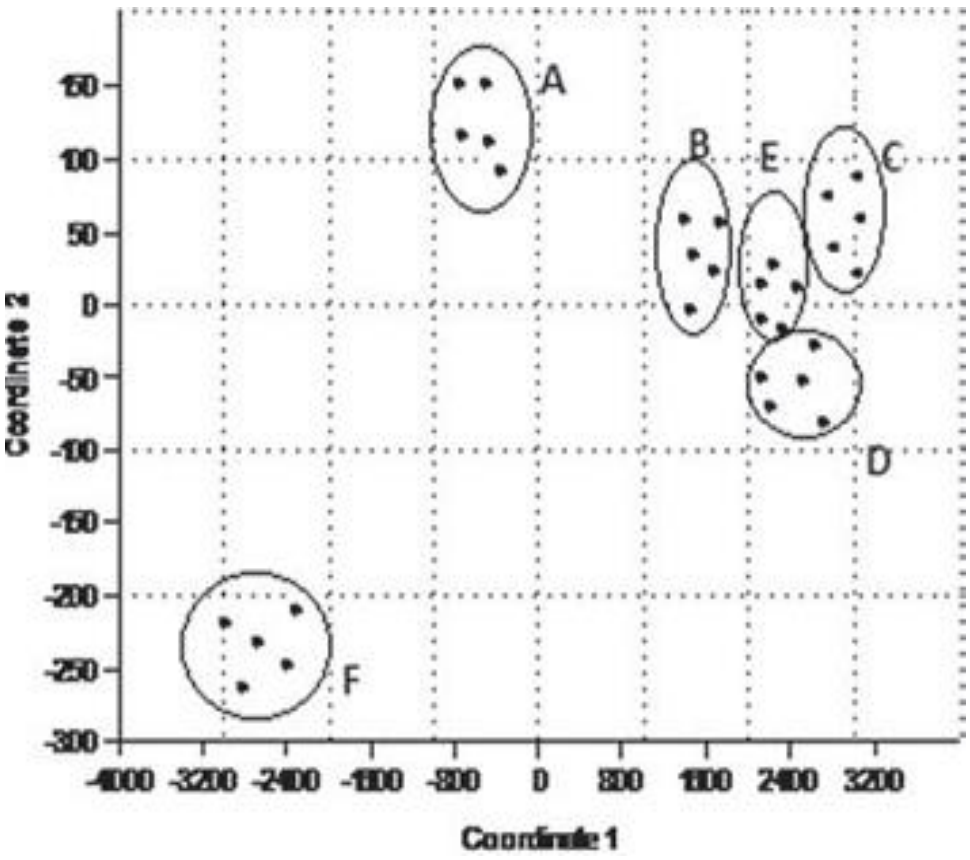

Fig. 4.3.17: PCA plot of tea liquor samples with four electrodes (Pt Au Ag and GC)

The group A depicted the top in the centre left classified the tastants class as mild sweet which represents tea liquor with cow milk. It is mild sweet in taste due to lactose contents present in it. Another class which is present downward in the extreme left represents a class with a fruity taste without any sugar. All the four classes B, C, D and E were strong and bitter spices fall close to each other towards the right side of the plot. However tea liquor with sweetened clove is considered as most spicy among these classes hence it is somewhat

separated from the other three classes i.e. C, E and D. From this data it can be interpreted that all six complex liquors can be classified into four classes i.e. mild sweet fruity most bitter and bitter spicy.

In Figure 4.3.18 PCA classification results with two conducting polymer electrodes of PANI and PPY has also efficiently classified all the six tea liquor samples into four classes.

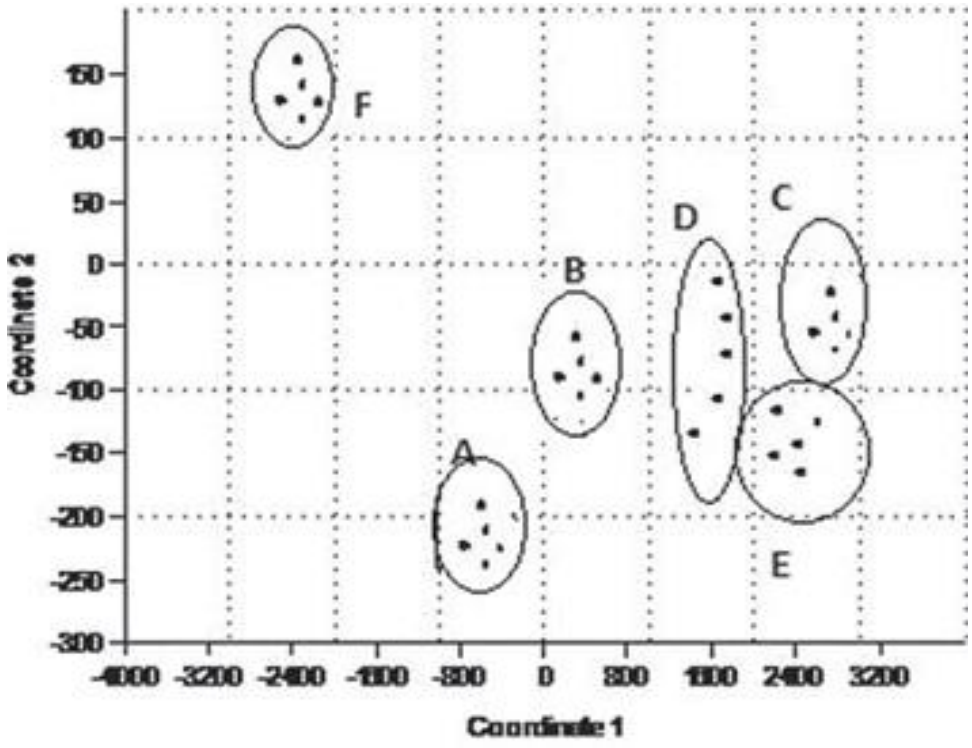

Fig. 4.3.18: PCA plot of milk samples with conducting polymer electrodes (ITO-PANI ITO-PPY)

However mild sweetened tea liquor lie at the bottom of the middle of the PCA plot whereas tea liquor with vanilla lies at the extreme top of the left corner efficiently distinguishing the

two classes. Out of all four bitter spicy compounds B, C, D and E again class B which is most bitter spicy is clearly separated from the other three C, D and E which lies close to each other.

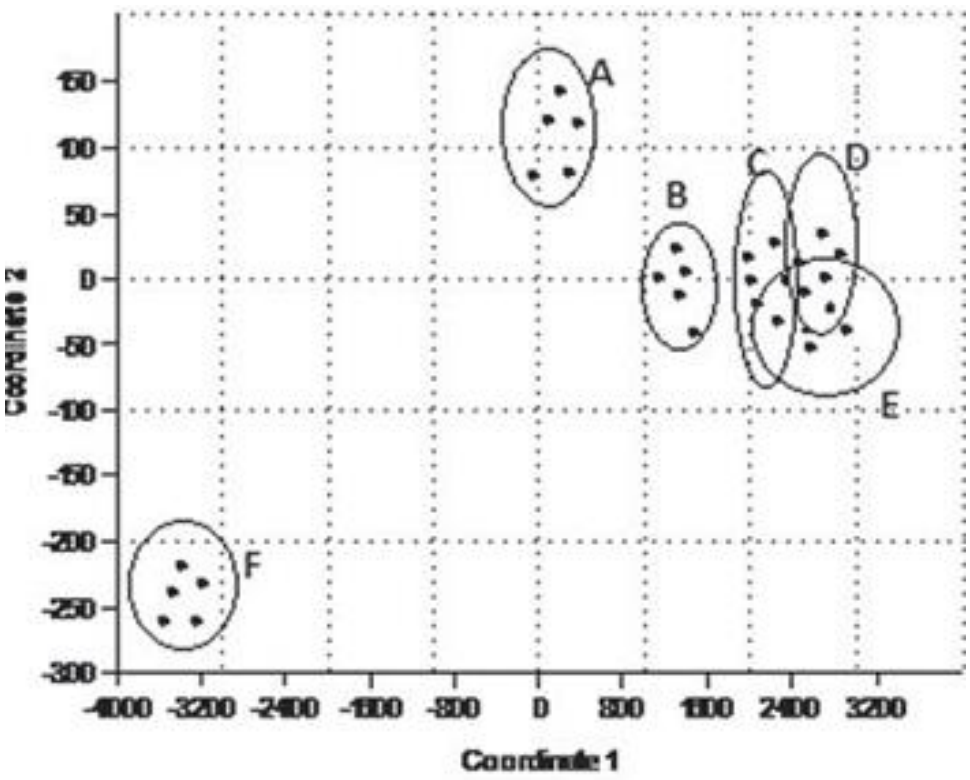

Fig.4.3.19: PCA plot of milk samples with the combination of metal and conducting polymer electrodes (Pt Au Ag GC ITO-PANI ITO-PPY)

Fig. 4.3.19 represents the classification from the data of six electrodes together which classifies very clearly into four groups which are mild sweet fruity most bitter spicy and bitter spicy. Therefore it may be concluded that the sensing system with metal electrodes or conducting polymer electrodes alone was able to classify these tastants into four distinct classes [244-247].

Conclusion: The use of sensing surfaces of metal and conducting polymers of PANI/PPY in frequency range 1 Hz-100 KHz was able to classify different types of tea liquor/samples. PCA analysis successfully analyzed the sensing signals by segregating both sweet and sour tastants into different groups according to its own unique characteristics and etablished the sensitivity of the sensing electrode. In all cases it is possible to establish correlation between the response of the sensing electrodes and PCA More detailed study in impedance mode are being carried out for the further quantification of beverages and tastant quality.

CHAPTER 5

CONCLUSIONS

In the present study addressed the problem of Quality analysis of Indian Black tea. The quality of tea is based on flavor and appearance and is key determinants of the price of tea in relation to market conditions. Conventionally tea tasters determine the quality of tea organoleptically. Any effort to increase the quality of tea and the price of tea is highly desired. The main aim of this research was to assist tea industry in improving the quality of the tea samples using Impedometric techniques.

An impedance measurement is an analytical system that mimics the sense of taste using an array of sensors and advanced signal-processing methods. Where classical analytical chemistry involves the identification of individual chemical species an impedance technique creates a fingerprint using multiple signals from its sensor array. This is useful for looking at tea beverages in which the species responsible for specific tastes are often unknown. AC impedance was used successfully to analyze tea liquor sample by assembling a set of six impedometric sensors each with different sensing surface – metal surfaces and conducting polymer surfaces. Every sensor gave a unique response to each tea liquor sample. These responses were then combined and treated with data-processing tool PCA before the system was 'trained' to classify tea liquor samples using a set of human-evaluated samples as a reference. Impedance analysis using sensory electrodes has been possible to differentiate the tea samples of the same geographical region produced in different seasons, different environment and using different tea processing methods.

Salient findings of the present study are given below:

- GC and PANI electrode response was highly efficient among other sensing electrodes; PANI/PPY electrodes and metal electrodes surface behavior in terms of electrical equivalent circuit based on geographical region sample variability such as harvest interval manufacturing process.
- Even a minor difference in variation can be used as a fingerprint using impedometric technique and PCA.
- Both sensory evaluation and existing analytical methods such as HPLC UV-VIS was exploited to analyze different sensing surfaces. These were used to investigate the quality of a tea samples on a certain scale the threshold level of various tastants (or additives) such as sweet salty sour and bitter were identified in tea liquor samples by the addition of known compounds or as such tea samples since tea has been used in the form of beverages drinks chocolates and other pharmaceutical products. This study may help generate a definite pattern of a produce by the industry using single or multi -sensor in a variable range.
- It was possible to classify different tea samples of Kangra and CTC Assam tea using Taster's score given by tea tasters. The HPLC and UV-VIS results were in good agreement with the tea taster's score.
- Principal component analysis successfully analyzed the sensed signals by segregating each tea into different regions according to its own unique characteristics and established the sensitivity of the sensing electrode. This method opens up new avenues in taste sensing and can be successfully implemented in the future to distinguish various classes of tea.

- The outcomes of this study imply an extended scope of impedance behavioral study using number type frequency variation voltage change and other reaction conditions to monitor the quality of drinking water beverages sea water and pharmaceutical products.

References

1. Wang Ni., A Comparison of Chinese and British Tea Culture, Asian Culture and History. 2011, 3 (2).
2. Fernandes S C, Osorio RE-H M B, dos Anjos A, Neves A, Micke G A, Vieira I C., Determination of catechin in green tea using catechol oxidase biomimetic sensor. The Brazilian Chemical Society, 2008, 19 (6), 1215–1223.
3. Roberts E. A. H., Wight W., Wood D. J., Paper Chromatography as an aid to the taxonomy of thea camellias, New Phytologist, 2006, 57 (2), 211-225.
4. Williams C N, Chew W Y, Rajaratnam J A., Tree and field crops of the wetter regions of the tropics. Wing Tai Cheung, 1982, 68 -74.
5. Sharma M, Thomas E V., Electronic vision study of tea grains color during Infusion. International Journal of Engineering Science Invention, 2013, 2 (4), 52-58.
6. Yemane M, Chandravanshi B S, Wondimu T., Levels of essential and non-essential metals in leaves of the tea plant (camellia sinensis) and soils of wushwush farms, Ethiopia. Food Chemistry, 2008, 107 (3), 1236-1243.
7. Hamid F S, Amin R, Ahmad N, Waheed A., Responses of increasing level of nitrogen on the yield of tea. Pakistan Journal of Agricultural Research, 2002. 17 (1), 33 -35.
8. Mudau F N, Soundy P, du Toit E S., Effects of Nitrogen, Phosphorus, and Potassium Nutrition on Total Polyphenol Content of Bush Tea (Athrixia phylicoides L.) Leaves in Shaded Nursery Environment. Hortscience 2007, 42 (2), 334–338.
9. Mohd Nasir N B., Determination of Tea Polyphenols, Thearubigins (TR), Theaflavins (TF) and Theabrownins (TB) in Teabag and Process Tea Leaves in Malaysian Market , Bachelor of science (hons.) Project, 2012.

10. Sharma V K, Bhattacharya A, Kumar A, Sharma H K., Health Benefits of Tea Consumption. Tropical Journal of Pharmaceutical Research, 2007, 6 (3), 785-792.
11. Woldegebriel D., Levels of Essential and Non-Essential Metals in Commercially Available Ethiopian Black Tea. MSc. dissertation, Addis Ababa University, Ethiopia, 2007.
12. Adam V, Mikelova R, Hubalek J, Hanustiak P, Beklova M, Hodek P, Horna A, Trnokova L, Stiborova M, Zaman L., Kizek R., Utilizing of square wave voltammetry to detect flavonoids in the presence of human urine. Sensors. 2007, 7 (10), 2402-2418.
13. Hollman P C, Van Het Hof K H, Tijburg L B, Katan M B., Addition of milk does not affect the absorption of flavonols from tea in man. Free Radical Research, 2001, 34(3),297-300.
14. du Toit R, Volsteedt Y, Apostolides Z., Comparison of the antioxidant content of fruits, vegetables and teas measured as vitamin C equivalents. Toxicology, 2001, 166 (1-2), 63-69.
15. Chang S S, Gudnason G V., Effect of addition of aluminum salts on the quality of black tea. Journal of Agricultural and Food Chemistry, 1982, 30 (5), 940-943.
16. Chitpan M., Monitoring the Binding Processes of Black Tea Polyphenols to Bovine Serum Albumin Surface using Quartz Crystal Microbalance with Dissipation Monitoring, 2009.
17. Valera P, Pablos F, Gustavo González A., Classification of tea samples by their chemical composition using discriminant analysis, Talanta, 1996, 43 (3), 415-419.

18. Togari N, Kobayashi A, Aishima T., Pattern recognition applied to gas chromatographic profiles of volatile components in three tea categories. Food Research International, 1995, 28 (5), 495-502.
19. Ghosh A, Tamuly P, Bhattacharyya N, Tudu B, Gogoi N, Bandyopadhyay R., Estimation of theflavin content in black tea using electronic tongue. Journal od Food Engineering, 2012, 110 (1), 71-79.
20. Fernández P L, Pablos F, Martín M J, González A G., Multi-element analysis of tea beverages by inductively coupled plasma atomic emission spectrometry. Food Chemistry, 2002, 76 (4), 483–489.
21. Legin A, Rudnitskaya A, Vlasov Y, Natale C D, Davide F, D'Amico A., Comparison of a voltametric electronic tongue and a lipid membrane taste sensor. Sensors and Actuators B: Chemical, 1997, 449 (1-2), 291–296.
22. Kumar P V S, Basheer S, Ravi R, Thakur M S., Comparative assessment of tea quality by various analytical and sensory methods with emphasis on tea polyphenols. Journal of Food Science and Technology, 2011, 48 (4), 440–446.
23. Wang K, Liu F, Liu Z, Huang J, Xu Z, Li Y, Chen J, Gong Y, Yang X, Analysis of chemical components in oolong tea in relation to perceived quality. International Journal of Food Science and Technology 2010, 45, 913–920.
24. Soto J, Campos I, Martínez-Máñez R, Monitoring Wastewater Treatment Using Voltammetric Electronic Tongues. Smart Sensors, Measurement and Instrumentation 2013, 65-103.

25. Liang Y R, Lu J L, Zhang L Y, Wu S, Wu Y., Estimation of black tea quality by analysis of chemical composition and color difference of tea infusions. Food Chemistry, 2003, 80 (2), 283–290.
26. Plutowska B, Wardencki W., Application of gas chromatography–olfactometry (GC–O) in analysis and quality assessment of alcoholic beverages – A review. Food Chemistry, 2008, 107 (1), 449-463.
27. Garruti D S, Franco M R B, A.P da Silva M A, Janzantti N S, Alves G L., Assessment of aroma impact compounds in a cashew apple-based alcoholic beverage by GC-MS and GC-olfactometry. LWT-Food Science and Technology, 2006, 39 (4), 372-377.
28. Toko K, Taste sensor, Sensors and Actuators B: Chemical, 2000, 64 (1-3), 205-215.
29. Kumar S, Panchariya P C, Bhanu Prasad P, Sharma A L.,Non Destructive Classification of Himalayan Orthodox Black Teas. In proceeding of: Sensors & Transducers Journal, 2012, 145 (10), 77-85.
30. Lvova L, Kim S S, Legin A, Vlasov Y, Yang J S, Cha G S, Nam H., All-solid-state electronic tongue and its application for beverage analysis, Analytica Chimica Acta , 2002, 468 (2), 303-314.
31. Lvova L, Legin A, Vlasov Y, Cha G S, Nam H., Multicomponent analysis of Korean green tea by means of disposable all-solid-state potentiometric electronic tongue microsystem. Sensors and Actuators B: Chemical, 2003, 95 (1-3), 391-399.
32. Zeravik J, Hlavacek A, LacinaK, Petr Skla´dal, State of the Art in the Field of Electronic and Bioelectronic Tongues – Towards the Analysis of Wines. Electroanalysis, 2009, 21 (23), 2509–2520.

33. Wu L, Ogawa Y, Tagawa A, Electrical impedance spectroscopy analysis of eggplant pulp tissue and effects of drying and freezing-thawing processes on its impedance characteristics, Journal of Food Engineering, 2008, 87 (2), 274-280.
34. Hollaender J., Rapid assessment of food/package interactions by electrochemical impedance spectroscopy (EIS). Food Additives and Contaminants, 1997, 14 (6-7), 617-626.
35. Ahmed R, Reifsnider K, Study of Influence of Electrode Geometry on Impedance Spectroscopy. International Journal of Electrochemical Science, 2011, 6, 1159 – 1174.
36. Scully, Silverman, Kendig, Electrochemical Impedance: Analysis and Interpretation, Books & Journals / ASTM Store, 1993, p 484.
37. Gabrielle C., Identification of Electrochemical Processes by Frequency Response Analysis, Technical Report, Solartron Instrumentation Group, Solartron Schlumberger, Farnborough, U.K, 1980.
38. Shirakawa H., The discovery of polyacetylene film: The dawning of an era of conducting polymers (Nobel lecture). Angewandte Chemie, 2001, 40 (14), 2575-2580.
39. Huang T, Murray R W, Quenching of $[Ru(bpy)_3]^{2+}$ Fluorescence by Binding to Au Nanoparticles. Langmuir, 2002, 18 (18), 7077-7081.
40. Carotenuto G, Nicolais L, Size controlled synthesis of thoil derivatized gold clusters. Journal of Materials Chemistry, 2003, 13, 1038–1041.
41. Fruend M S, Deore B, Self doped conducting polymers, Wiley: Chichester, 2007, p 338.

42. Shirakawa H, Louis E J, Macdiarmid A G, Chiang C K, Heeger A J., Synthesis of electrically conducting organic polymers - halogen derivatives of polyacetylene, $(CH)_x$. Journal of the Chemical Society-Chemical Communications, 1977, 578-580.
43. Wilcoxon J P, Provencio P P., Heterogeneous growth of metal clusters from solutions of seed nanoparticles. Journal of the American Chemical Society, 2004, 126 (20):6402-6408.
44. Mafune F, Kohno J, Takeda Y, Kondow T, Sawabe H., Formation of Gold nanoparticles by laser ablation in aqueous solution of surfactant. Journal of Physical Chemistry B., 2001, 105 (22), 5114-5120.
45. Bruchez M Jr, Moronne M, Gin P, Weiss S, Alivisatos A P., Semiconductor nanocrystals as fluorescent biological labels. Science, 1998, 281(5385) 2013-2016.
46. Chan W C W, Nie S M., Quantum dot bioconjugates for ultrasensitive nonisotopic detection. Science, 1998, 281, 2016-2018.
47. Esbensen K H., Multivariate Data Analysis- in practice, 5th ed., CAMO Process AS, 2002.
48. Anderson E, Bai Z, Bischof C, Blackford S, Demmel J, Dongarra J, Du Croz J, Greenbaum A, Hammarling S, McKenney A, Sorensen D., LAPACK Users' Guide. Society for Industrial and Applied Mathematics, Philadelphia, PA, third edition, 1999.
49. Jolliffe I T., Principal Component Analysis. Springer, second edition, 2002, p 489.
50. Francis F J., Tea. Wiley Encyclopedia of Food Science and Technology, Second Edition, 2000, 4, 2294 - 2304.
51. Caballero B, Trugo C L, Finglas P M., Tea. Encyclopedia of Food Science and Nutrition, Second Edition, 2003, 9, 5737 - 5755.

52. Graham H N., Green Tea Composition, Consumption and Polyphenol Chemistry. Preventive Medicine, 1992, 21, 334- 350.
53. Lu C H, Hwang L S., Polyphenol contents of Pu-Erh teas and their abilities to inhibit cholesterol biosynthesis in Hep G2 cell line. Food Chemistry, 2008, 111, 67–71.
54. Abourashed E A, Mossa J S., HPTLC determination of caffeine in stimulant herbal products. Journal of pharmaceutical and Biomedical analysis 2004, 36 (3), 617-620.
55. Dalluge J J, Nelson B C, Thomas J B, Sander L C., Selection of column and gradient elution system for the separation of catechins in green tea using high-performance liquid chromatography. Journal of chromatography A, 1998, 793 (2), 265-274.
56. Campanella L , Bonanni A, Tomassetti M., Determination of the antioxidant capacity of samples of different types of tea, or of beverages based on tea or other herbal products, using a superoxide dimutase biosensor. Journal of Pharmaceutical and Biomedical analysis, 2003, 32 (4-5), 725-736.
57. Carmen C, Rafael G, Lopez C M., Determination of Tea components with antioxidant activity. Journal of agricultural and food chemistry, 2003, 51 (15), 4427-4435.
58. Pineiro Z, Palma M, Barroso C G., Determination of catechins by means of extraction with pressurized liquid. Journal of chromatography A, 2004, 1026 (1-2), 19-23.
59. Pan X, Niu G, Liu H., Microwave assisted extraction of tea polyphenols and tea caffeine from green tea leaves. Chemical engineering and processing, 2003, 42 (2), 129-133.
60. Mandal V, Mohan Y, Hemlatha S., Microwave assisted extraction - An innovative and promising extraction tool for medicinal plant research. Pharmacognosy Review, 2007, 1(1), 7-18.

61. Chu K O, Wang C C, Rogers M S, Choy K W, Pang C P., Determination of catechins and catechin gallates in biological fluids by HPLC with colourimetric array detection and solid phase extraction. Analytica Chimica Acta, 2004, 510 (1), 69-76.

62. Vovk I, Simonovska B, Vourela H., Separation of eight selected flavan-3-ols on cellulose thin-layer chromatographic plates. Journal of Chromatography A, 2005, 1077 (2), 188-194.

63. Bronner W E, Beecher G R., Method for determining the content of catechins in tea infusions by high performance liquid chromatography. Journal of chromatography A, 1998, 805 (1-2), 137-142.

64. Rodrigues C I, Marta L, Maia R, Miranda M, Riberinho M, Maguas C., Application of solid phase extraction to brewed coffee caffeine and organic acids determination by UV/HPLC. Journal of food composition and analysis, 2007, 20 (5), 440-448.

65. Dawidowicz A L, Wianowska D., PLE in the analysis of plant compounds Part-I. The application of PLE for HPLC analysis of caffeine in green tea leaves. Journal of pharmaceutical and biomedical analysis, 2005, 37 (5), 1155-1159.

66. Goto T, Yoshida Y, Kiso M, Nagashima H., Simultaneous analysis of individual catechins and caffeine in green tea. Journal of Chromatography A, 1996, 749 (1-2), 295-299.

67. Mizukami Y, Sawai Y, Yamaguchi Y. , Simultaneous analysis of catechins, gallic acid, strictinin, and purine alkaloids in green tea by using catechol as an internal standard. Journal of Agricultural and Food Chemistry, 2007, 55 (13), 4957-64.

68. Liu J, Zhao G, Yuan Y, Chen F, Hu X., Quantitative analysis of acrylamide in tea by liquid chromatography coupled with electrospray ionization tandem mass spectrometry. Food Chemistry, 2008, 108, 760–767.

69. Horie H, Kohata K., Analysis of tea components by high-performance liquid chromatography and high-performance capillary electrophoresis. Journal of Chromatography A, 2000, 881 (1-2), 425-38.

70. Uysal U D, Aturki Z, Raggi M A, Fanali S., Separation of catechins and methylxanthines in tea samples by capillary electrochromatography. Journal of Separation Science, 2009, 32 (7), 1002-10.

71. Zuo Y, Chen H, Deng Y., Simultaneous determination of catechins, caffeine and gallic acids in green, Oolong, black and pu-erh teas using HPLC with a photodiode array detector. Talanta, 2002, 57 (2), 307-16.

72. K Y, Lin C L, Huang H C, Lin J K., Determination of theanine, GABA, and other amino acids in green, oolong, black, and Pu-erh teas with dabsylation and high-performance liquid chromatography. Journal of Agricultural and Food Chemistry, 2008, 56(17), 7637-7643.

73. el-Hady DA, el-Maali NA, Determination of catechin isomers in human plasma subsequent to green tea ingestion using chiral capillary electrophoresis with a high-sensitivity cell. Talanta, 2008, 76 (1), 138-45.

74. Yamauchi Y, Nakamura A, Kohno I, Kitai M, Hatanaka K, Tanimoto T., Simple and rapid UV spectrophotometry of caffeine in tea coupled with sample pre-treatment using a cartridge column filled with polyvinylpolypyrrolidone (PVPP). Chemical and pharmaceutical bulletin, 2008, 56 (2), 185-8.

75. Yamauchi Y, Nakamura A, Kohno I, Hatanaka K, Kitai M, Tanimoto T., Quasi-flow injection analysis for rapid determination of caffeine in tea using the sample pre-treatment method with a cartridge column filled with polyvinylpolypyrrolidone. Journal of Chromatography A, 2008, 1177 (1), 190-4.
76. Nakakuki H, Horie H, Yamauchi Y, Kohata K., Rapid analysis of methylated xanthines in teas by an improved high-performance liquid chromatographic method using a polyvinylpolypyrroridone pre-column. Journal of Chromatography A, 1999, 848 (1-2), 523-7.
77. Horie H, Mukai T, Kohata K., Simultaneous determination of qualitative important components in green tea infusion using capillary electrophoresis. Journal of Chromatography A, 1997, 758 (2), 332–335.
78. Arce L, Rios A, Valcarcel M., Determination of anticarcinogenic polyphenols present in green tea using capillary electrophoresis coupled to a flow injection system. Journal of Chromatography A., 1998, 827 (1), 113–120.
79. Horie H., Kohata K., Application of capillary electrophoresis to tea quality estimation. Journal of Chromatography A, 1998 (1), 802, 219–223.
80. Zhu Q H, Chen Z Y., Isolation and analysis of green tea polyphenols by HPLC. Analytical Laboratory, 1999, 18, 70–72.
81. Wang H F, Helliwel K, You X., Isocratic elution system for the determination of catechins, caffeine and gallic acid in green tea using HPLC. Food Chemistry, 2000, 68 (1), 115–121.

82. Khokhar S., Mangnusdottir S G M., Total phenol, catechin, and caffeine contents of teas commonly consumed in the United Kingdom. Journal of Agricultural and Food Chemistry, 2002, 50 (3), 565–570.
83. Lin Y S, Wu S S, Lin J K., Determination of tea polyphenols and caffeine in tea flowers (Camellia sinensis) and their hydroxyl radical scavenging and nitric oxide suppressing effects. Journal of Agricultural and Food Chemistry, 2003, 51 (4), 975–980.
84. Rawat R, Gulati A, Babu G D K, Acharya R, Kaul V K, Singh B., Characterization of volatile components of Kangra orthodox black tea by gas chromatography–mass spectrometry. Food Chemistry, 2007, 105 (1), 229–235.
85. Iiyama S, Ezaki S, Toko K, Matsuno T, Yamafuji K., Study of astringency and pungency with multichannel taste sensor made of lipid membranes. Sensors & Actuators, B: Chemical , 1995, 24 (1-3), 75–9.
86. Vlasov Y, Legin A, Rudnitskaya A., Cross-sensitivity evaluation of chemical sensors for electronic tongue: Determination of heavy metal ions. Sensors & Actuators, B: Chemical, 1997, 44 (1-3), 532–537.
87. Vlasov Y, Legin A, Rudnitsaya A, Di Natale C, Amico A D'., Nonspecific sensor arrays (electronic tongue) for chemical analysis of liquids. Pure and Applied Chemistry , 2005, 77 (11), 1965–83.
88. Persaud K, Dodd G., Analysis of discrimination mechanisms in the mammalian olfactory system using a model nose. Nature, 1982, 299, 352–355.

89. Legin A, Rudnitskaya A, Di Natale C, Mazzone E, Amico A D'., Application of electronic tongue for qualitative and quantitative analysis of complex liquid media. Sensors and Actuators B: Chemical, 2000, 65 (1-3), 232–234.
90. Deisingh A K, Stone D C, Thompson M., Applications of electronic noses and tongues in food analysis. International Journal of Food Science and Technology, 2004, 39 (6), 587–604.
91. Vlasov Y, Legin A, Rudnitskaya A., Electronic tongues and their analytical application. Analytical and Bioanalytical Chemistry, 2002, 373, 136–146.
92. Winquist F, Wide P, Lundstrom I., An electronic tongue based on voltammetry, Analytica Chimica Acta, 1997, 357 (1-2), 21–31.
93. Winquist F, Krantz-Rulcker C, Wide P, Lundstrom I., Monitoring of freshness of milk by an electronic tongue on the basis of voltammetry. Measurement Science and Technology, 1998, 9 (12), 1937–1946.
94. Legin A, Rudnitskaya A, Vlasov Y, Di Natale E, Mazzone C, D'Amico A., Application of electronic tongue for quantitative analysis of mineral water and wine. Electroanalysis, 1999, 11(10–11), 814–820.
95. Ivarsson P, Holmin S, Hojer N E., Krantz-Rulcker C, Winquist F., Discrimination of tea by means of a voltammetric electronic tongue and different applied waveforms. Sensors and Actuators B: Chemical, 2001, 76 (1-3), 449–454.
96. de Sousa H C , Riul Jr. A., Using mlp networks to classify red wines and water readings of an electronic tongue. SBRN '02 Proceedings of the VII Brazilian Symposium on Neural Networks, IEEE Computer Society Washington, DC, USA.

97. Legin A, Rudnitskaya A, Seleznev B, Vlasov Y., Recognition of liquid and flesh food using an electronic tongue. International Journal of Food Science and Technology, 2002, 37 (4), 375–385.
98. Mohanan S, Thomas Panicker P G, Iype L, Laila M, Domini I, Bindu R G, A new ultrasonic method to detect chemical additives in branded milk. Pramana, journal of physics, 2002, 59 (3), 525–529.
99. Soderstrom C, Boren H, Winquist F, Krantz-Rulcker C., Use of an electronic tongue to analyze mold growth in liquid media. International Journal of Food Microbiology, 2003, 83 (3), 253-261.
100. Ivarsson P, Holmin S, Höjer N-E, Krantz-Rülcker C, Lundström I, Winquist F., Discrimination of tea by means of a voltammetric electronic tongue and different applied potential modes. Sensors and Actuators B: Chemical, 2001, 76, 449-454.
101. Ivarsson P, Kikkawa Y, Winquist F, Krantz-Rülcker C, Höjer N-E, Hayashi K, Toko K, Lundström I., Comparison of a voltammetric electronic tongue and a lipid membrane taste sensor. Analytica Chimica Acta, 2001, 449 (1-2), 59-68.
102. Krantz-Rülcker C, Stenberg M, Winquist F, Lundström I., Electronic tongues for environmental monitoring based on sensor arrays and pattern recognition: A review. Analytica Chimica Acta, 2001, 426 (2), 217- 226.
103. Apetrei C, Apetrei I M, Nevares I, del Alamo M, Parra V, Rodríguez-Méndez M L, De Saja J A., Using an e-tongue based on voltammetric electrodes to discriminate among red wines aged in oak barrels or aged using alternative methods. Electrochimica Acta, 2007, 52 (7), 2588-94.

104. Parra V, Arrieta A, Fernández-Escudero J A, Rodríguez-Méndez M L, de Saja J A., Electronic tongue based on chemically modified electrodes and voltammetry for the detection of adulterations in wines. Sensors & Actuators, B: Chemical, 2006, 118 (1-2), 448-453.

105. Moreno-Baron L, Cartas R, Merkoci A, Alegret S, Gutierrez J, Leija L, Hernandez P, Muñoz R, del Valle M., Data Compression for a Voltammetric Electronic Tongue Modelled with Artificial Neural Networks. Analytical Letters, 2005, 38 (13), 2189-2206.

106. Moreno-Baron L, Cartas R, Merkoci A, Alegret S, del Valle M, Leija L, Hernandez P R, Muñoz R., Application of the wavelet transform coupled with artificial neural networks for quantification purposes in a voltammetric electronic tongue. Sensors & Actuators, B: Chemical, 2006, 113 (1), 487-499.

107. Tian SY, Deng S P, Chen Z X., Multifrequency large amplitude pulse voltammetry: A novel electrochemical method for electronic tongue. Sensors & Actuators, B: Chemical, 2007, 123 (2), 1049-1056.

108. Martina V, Ionescu K, Pigani L, Terzi F, Ulrici A, Zanardi C, Seeber R., Development of an electronic tongue based on a PEDOT-modified voltammetric sensor. Analytical and Bioanalytical Chemistry, 2007, 387 (6), 2101-2110.

109. Wu J, Liu J, Fu M, Li G, Lou Z., Classification of Chinese yellow wines by chemometric analysis of cyclic voltammogram of copper electrode. Sensors, 2005, 5, 529-536.

110. Winquist F, Holmin S, Krantz-Rülcker C, Wide P, Lundström I., A hybrid electronic tongue. Analytica Chimica Acta, 2000, 406 (2), 157-161.

111. Men H, Zou S, Li Y, Wang Y, Ye X, Wang P., A novel electronic tongue combined MLAPS with stripping voltammetry for environmental detection. Sensors and Actuators B: Chemical, 2005, 110 (2), 350-357.

112. Winquist F, Rydberg E, Holmin S, Krantz-Rülcker C, Lundström I., Flow injection analysis applied to a voltammetric electronic tongue. Analytica Chimica Acta, 2002, 471 (2), 159-172.

113. Gutes A, Cespedes F, del Valle M, Louthander D, Krantz-Rülcker C, Winquist F., A flow injection voltammetric electronic tongue applied to paper mill industrial waters. Sensors and Actuators B: Chemical, 2006, 115 (1), 390-395.

114. Gutes A, Ibañez A B, del Valle M, Cespedes F., Automated SIA e-tongue employing a voltammetric biosensor array for the simultaneous determination of glucose and ascorbic acid. Electroanalysis, 2006, 18 (1), 82-88.

115. Gutes A, Calvo D, Céspedes F, del Valle M., Automatic sequential injection analysis electronic tongue with integrated reference electrode for the determination of ascorbic acid, uric acid and paracetamol. Microchimica Acta, 2007, 157 (1-2), 1-6.

116. Olsson J, Winquist F, Lundstrom I., A self polishing electronic tongue, Sensors and Actuators B: Chemical, 2006, 118 (1-2), 461-465.

117. Rodriguez-Mendez M L, de Saja J., Voltammetric sensors as sensing units of an electronic tongue. Trends in Electrochemistry and Corrosion at the Beginning of the 21st Century, 2004, p 475.

118. Jain V K, Kumar P, Bhandari D, Vijay Y K., Growth and characterization of transparent conducting nanostructured zinc indium oxide thin films. Thin Solid Films, 2010, 519 (3), 1082-1086.

119. Joshi R, Sood S, Dogra P, Mahendru M, Kumar D, Bhangalia S, Pal H C, Kumar N, Bhushan S, Gulati A, Saxena A K, Gulati A., In vitro cytotoxicity, antimicrobial, and metal-chelating activity of triterpene saponins from tea seed grown in Kangra valley, India. Medicinal Chemistry Research, 2012, 22 (8), 4030-4038.

120. Kohli K S, Rai D V, Kumar P, Jindal V K, Goyal N., Impedance of a goat eye Lens. Medical & Biological Engineering & Computing, 1997, 35 (4), 348–353.

121. Singh S, Jain D V S, Singla M L., One step electrochemical synthesis of gold-nanoparticles–polypyrrole composite for application in catechin electrochemical biosensor. Analytical Methods, 2013, 5 (4), 1024-1032.

122. Kehwar T S., Analytical approach to estimate normal tissue complication probability using best fit of normal tissue tolerance doses into the NTCP equation of the linear quadratic model. J Can Res Ther., 2005, 1 (3), 168-79.

123. Lvova L, Martinelli E, Dini F, Bergamini A, Paolesse R, Di Natale C, D'Amico A., Clinical analysis of human urine by means of potentiometric electronic tongue. Talanta, 2009; 77 (3), 1097–104.

124. Legin A, Rudnitskaya A, Lvova L, Vlasov Yu, Natale C Di, Amico A D'., Evaluation of Italian wine by the electronic tongue: Recognition, quantitative analysis and correlation with human sensory perception. Analytica Chimica Acta, 2003, 484 (1), 33–44.

125. Lvova L, Roberto P, Natale C Di, Amico A D'., Detection of alcohols in beverages: An application of porphyrin-based Electronic tongue. Sensors and Actuators B: Chemical, 2006, 118 (1-2), 439–47.

126. Toko K, Iiyama S, Yahiro M., Quantitative sensing of mineral water with multichannel taste sensors. Sensors and Materials, 1995, 7, 191–201.

127. Ciosek P, Wroblewski W, Brzozka Z., Classification of beverages using a reduced sensor array. Sensors and Actuators B: Chemical, 2004, 103, 76–83.

128. Sim M Y, Shya T J, Ahmad M N, Shakaff A V, Othman A R, Hitam M S., Monitoring of milk quality with disposable taste sensors. Sensors, 2003, 3 (9), 340–349.

129. Fukunaga T, Toko K, Mori S, Nakabayashi Y, Kanda M., Quantification of taste of coffee using sensor with global selectivity. Sensors and Materials, 1996, 8 (1), 47–56.

130. Miyanaga Y, Tanigake A, Nakamura T, Kobayashi Y, Ikezaki H, Taniguchi A, Matsuyama K, Uchida T., Prediction of the bitterness of single, binary- and multiple-component amino acid solutions using a taste sensor. International Journal of Pharmaceutics, 2002, 248 (1-2), 207–18.

131. Habara M, Ikezaki H, Toko K., Study of sweet taste evaluation using taste sensors with lipid/polymer membrane. Biosensors and Bioelectronics , 2004, 19 (12), 1559–63.

132. Koichi T, Kazumi K, Yoshinobu N, Hidekazu I., Measurement of solid food using multi channel taste receptors. The Japanese Journal of Taste and Smell Research, 2009, 16, 505–8.

133. Naito Y, Ikezaki H, Taniguchi A, Toko K., New method to detect a trace amount of organic substances using a lipid membrane. IEEJ Transaction on Sensors and Micro machine, 2001, 121 (2), 65–69.

134. Anjiki N, Hosoe J, Fuchino H, Kiuchi F, Sekita S, Ikezaki H, Mikage M, Kawahara N, Goda Y., Evaluation of the taste of crude drug and Kampo formula by a taste-sensing system. Journal of Natural Medicines, 2011, 65 (2), 293-300.

135. Bhondekar A P, Dhiman M, Sharma A, Bhakta A, Ganguli A, Bari S S, Vig R, Kapur P, Singla M L., A Novel iTongue For Indian Black Tea Discrimination. Sensors and Actuators B: Chemical, 2011, 148 (2), 601-609.

136. Joshi V K, Singh R S., Food Biotechnology: Principles and Practices, (eds.),IK International Pvt. Ltd., New Delhi, India, 2012, 1-37.

137. Graham D C., The Electrical Double Layer and the Theory of Electrocapillarity, Chemical Reviews, 1947, 41 (3), 441-501.

138. Parsons R., Modern Aspects of Electrochemistry, (ed. J.O'M. Bockris), Butterworths, London, 1954, 1, p. 103

139. Delahay P., Double Layer and Electrode Kinetics, Wiley-Interscience, New York, 1965.

140. Mohilner D M., The Electrical Double Layer. Electroanalytical Chemistry. (Ed: A.J. Bard) Marcel Dekker, New York, 1966, 1, 241-409.

141. Breyer B, Bauer H H., Alternating Current Polarography and Tensammetry, Chemical Analysis Series (XIII), Wiley-Interscience, New York, 1963.

142. Smith D E., Electroanalytical Chemistry, Bard A J., Ed., Dekker, New York, 1966, Vol. 1.

143. Bond A M., Modern Polarographic Techniques in Analytical Chemistry, Dekker, New York, 1980. p: 341.

144. Delahay P., New Instrumental Methods in Electrochemistry, Interscience, New York, 1954, p 214, chap 8.

145. Vetter K J., Electrochemical Kinetics, Academic Press, New York, 1967, p 732.

146. Macdonald D.D., Transient Techniques in Electrochemistry, Plenum Press, New York, 1977, p 119.

147. Icier F, Ilicali C., The effects of concentration on electrical conductivity of orange juice concentrates during ohmic heating. European Journal of Food Research Technology, 2005, 220, 406-414.

148. Southampton Electrochemistry group, Instrumental Methods in Electrochemistry, Ellis Horwood, Chichester, 1985.

149. Gileadi E., Electrode Kinetics for Chemists, Engineers, and Material Scientists, VCH, New York, Weinheim, 1993, p 420.

150. Brett C M A, Brett A M O, Electrochemistry, Principles, Methods, and Applications, Oxford University Press, 1993.

151. Galus Z., Fundamentals of Electrochemical Analysis, 2 nd edition, Ellis Horwood, polish scientific publishers, PWN, New York, 1994, p 278.

152. Oldham H B, Myland J C., Fundamentals of Electrochemical Science, Academic Press, San Diego, 1994, p 233.

153. Ward M D, In: Physical Electrochemistry, Principles, Methods, and Applications, Rubinstein I. (ed), Marcel Dekker, New York, 1995, Chap 7, 293-338.

154. Macdonald J R. (ed), Impedance Spectroscopy Emphasizing Solid Materials and Systems, Wiley, New York, 1987.

155. Stoynov Z B, Grafov B M, Savova-Stoynova B S, Elkin V V, Damaskin B B., Electrochemical Impedance, Nauka, Moscow, 1991.

156. Orazem M E, Tribollet B., Electrochemical Impedance Spectroscopy, John Wiley & Sons, Hoboken, New Jersey, 2008, p 554.

157. Loveday D, Peterson P, Rodgers B., Evaluation of Organic Coatings with Electrochemical Impedance Spectroscopy. Part 1: Fundamentals of Electrochemical Impedance Spectroscopy. JCT Coatings Tech, 2004, p 46-52.

158. Makharia R, Mathias M F, Baker D R., Measurement of Catalyst Layer Electrolyte Resistance in PEFCs Using Electrochemical Impedance Spectroscopy. Journal of Electrochemical Society, 2005, 152 (5), A970-A977.

159. Bard A J, Faulkner L R., Electrochemical Methods; Fundamentals and Applications, Wiley Interscience Publications, 2000.

160. Agarwal P, Orazem M E, Garc´ıa Rubio L H., Application of the Kramers Kronig Relations in Electrochemical Impedance Spectroscopy, Electrochemical Impedance: Analysis and Interpretation, ASTM STP 1188, Scully J, Silverman D, Kendig M., Editors, American Society for Testing and Materials, Philadelphia, 1993, 115-139.

161. Geenen F., Characterization of Organic Coatings with Impedance Measurements; A study of Coating Structure, Adhesion and Underfilm Corrosion, Ph-D thesis, TU-Delft 1990.

162. Yeager E, Bockris J O'M, Conway B E, Sarangapani S., Comprehensive Treatise of Electrochemistry; Volume 9 Electrodics: Experimental Techniques; chapter 4, AC Techniques, M. Sluyters-Rehbach, J.H. Sluyters, Plenum Press 1984.

163. Walter G.W., A review of impedance plot methods used for corrosion performance analysis of painted metals. Corrosion Science, 1986, 26 (9), 681-703.

164. Gabrielli C., Use and Applications of Electrochemical Impedance Techniques, England, Schlumberger Technical Report 1990.

165. Kendig M, Scully J., Basic aspects of electrochemical impedance application for the life prediction of organic coatings on metals. Corrosion, 1990, 46, 22-29.

166. Fletcher S., Tables of Degenerate Electrical Networks for Use in the Equivalent-Circuit Analysis of Electrochemical Systems. Journal of the Electrochemical Society, 1994, 141 (7), 1823.

167. Fasshauer G E, Schumaker L L, O B K, Sung J P, Almøy T., A simulation study on comparison of prediction models when only a few components are relevant. Computational Statistics and Data Analysis, 1996, 21, 87–107.

168. Gutierrez-Osuna R., Pattern analysis for machine olfaction: A review, IEEE Sensors Journal, 2002, 2 (3), 189–202.

169. Pearce T C, Schiffman S S, Nagle H T, Gardner J W., Handbook of Machine Olfaction. Electronic nose technology, Frankfurt, Germany, Wiley-VCH, 2003.

170. Dhiman M, Joshi R, Gulati A, Kapur P, Ganguli A, Singla M L., Interpretation of Indian Orthodox Tea Using Multi-Sensing Impedometric Technique. Journal of Nanoscience and Nanotechnology, 2013, 13, 6767-6772.

171. Van der Linden W E, Dieker J W., Glassy carbon as electrode material in electro-analytical chemistry. Analytica Chimica Acta, 1980, 119 (1), 1–24.

172. Dhiman M, Kapur P, Ganguli A, Singla M L., Behaviour of Metal and Emeraldine Salt for Detection of Threshold Level of Sucrose and Citric Acid in Impedance Mode. Sensor letters, 2012, 11 (3), 459-465.

173. Awasthi S, Srivastava A, Singla M L., Voltammetric determination of citric acid and quinine hydrochloride using polypyrrole–pentacyanonitrosylferrate/platinum electrode. Synthetic Metals, 2011, 161 (15-16), 1707-1712.

174. Wei Y, Hsueh K F, Jang G W., A Study of Leucoemeraldine and Effect of Redox Reactions on Molecular Weight of Chemically Prepared Polyaniline. Macromolecules, 1994, 27 (2), 518-525.

175. Singla M L, Awasthi S, Srivastava A., Humidity sensing; using polyaniline/Mn_3O_4 composite doped with organic/inorganic acids. Sensors and Actuators B: Chemical, 2007, 127 (2), 580-585.

176. Pouget J P, Jozefowicz M E, Epstein A J , Tang X, MacDiarmid A G., X-ray structure of polyaniline, Macromolecules, 24, 1991,779-789

177. Randles J E B., A cathode ray polarograph. Transactions of the Faraday Society, 1948, 44, 322-327.

178. Gileadi E, Kirowa-Eisner E, Penciner J., Interfacial Chemistry: An Experimental Approach, Addison-Wesley, U.S.A, 1975.

179. Bard A J, Faulkner L R., Bulk electrolysis methods in: Electrochemical Methods: Fundamentals and Applications, A.J. Bard and L.R. Faulkner (eds.), John Wiley & Sons, Inc., New York, 1980. p 370–428.

180. Fernandez C L., Electro-Catalytic Reactions, Ph.D thesis, The University Of Hull, 2009.

181. Bockris J, Khan S U M., Surface Electrochemistry: A Molecular Level Approach, Plenum Press, New York and London 1993.

182. Parsons R, Electrical double layer: Recent experimental and theoretical developments. Chemical Reviews, 1990, 90, 813–826.

183. Majid K, Awasthi S, Singla M L., Low temperature sensing capability of polyaniline and Mn3O4 composite as NTC material. Sensors & Actuators A: Physical, 2007, 135 (1), 113-118.

184. Kondawar S B, Anwane S W, Nandanwar D V, Dhakate S R., Carbon nanotubes reinforced conducting polyaniline and its derivative poly(o-anisidine) composites. Advanced Materials Letters, 2013, 4 (1), 35-38.

185. Vishnuvardhan T K, Kulkarni V R, Basavaraja C, Raghavendra S C, Synthesis, characterization and a.c. conductivity of polypyrrole/Y2O3 composites. Bulletin of Material Science, 2006, 29 (1), 77–83.

186. Roberts E A H, Smith R F., The phenolic substances of manufactured tea. IX. – the spectrophotometric evaluation of tea liquors. Journal of the Science of Food and Agriculture, 1963, 14, 689-700.

187. John B C., The effect of fermentation temperature on the quality parameters and price evaluation of Central African black teas. Journal of the Science of Food and Agriculture, 1980, 31 (9), 911-919.

188. Hilton P J, Ellis R T., Estimation of the market value of Central African tea by theaflavin analysis. Journal of the Science of Food and Agriculture, 1972, 23 (2), 227-232.

189. John B C, Rex T E., The effect of pH modification during fermentation on the quality parameters of central African black teas. Journal of the Science of Food and Agriculture, 1980, 31 (9), 924-934.

190. Martin O, Owuor P O, Taylor S J., Flavanol Composition and Caffeine Content of Green Leaf as Quality Potential Indicators of Kenyan Black Teas. Journal of the Science of Food and Agriculture, 1997, 74 (2), 209-215.

191. Wright L P, Mphangwe N I K, Nyirenda H E, Apostolides Z, Analysis of caffeine and flavan-3-ol composition in the fresh leaf of Camellia sinesis for predicting the quality of the black tea produced in Central and Southern Africa. Journal of the Science of Food and Agriculture, 2000, 80 (13) 1823-1830.

192. Liang Y R, Liu Z S, Xu Y R, Hu Y L., A study on chemical composition of two special green teas (Camellia sinensis). Journal of the Science of Food and Agriculture, 1990, 53 (4), 541-548.

193. Yuerong L, Jianliang L, Shuling S., Effect of Gibberellins on Chemical Composition and Quality of Tea (Camellia sinensis). Journal of the Science of Food and Agriculture, 1996, 72 (4), 411-414.

194. Bhattacharya N, Tudu B, Jana A, Ghosh D, Bandhopadhyaya R, Bhuyan M., Preemptive identification of optimum fermentation time for black tea using electronic nose. Sensors and Actuators B: Chemical, 2008, 131 (1), 110-116.

195. Bhattacharyya N, Seth S, Tudu B, Tamuly P, Jana A, Ghosh D, Bandyopadhyay R, Bhuyan M., Monitoring of black tea fermentation process using electronic nose. Journal of Food Engineering, 2007, 80 (4), 1146-1156.

196. Tudu B, Jana A, Metla A, Ghosh D, Bhattacharyya N, Bandyopadhyay R., Electronic nose for black tea quality evaluation by an incremental RBF network. Sensors and Actuators B: Chemical, 2009, 138 (1), 90-95.

197. Švorc Ľ., Determination of Caffeine: A Comprehensive Review on Electrochemical Methods. International Journal of Electrochemical Science, 2013, 8, 5755 – 5773.

198. Albareda-Sirvent M, Merkoci A, Alegret S., Pesticide determination in tap water and juice samples using disposable amperometric biosensors made using thick-film technology. Analytica Chimica Acta, 2001, 31, 35-44.

199. Wheeler D. S, Wheeler W J., The medicinal chemistry of tea. Drug Development Research, 2004, 61 (2), 45-65.

200. Weisburger J H., Tea and health: a historical perspective. Cancer Letters, 1997, 114 (1-2), 315-317.

201. Kurodo A, Hara Y., Antimutagenic and anticarcinogenic activity of tea polyphenols. Mutation Research, 1999, 436 (1), 69-97.

202. Deng Z, Tao B, Li X, He J, Chen Y., Effect of green tea and black tea on the blood glucose, the blood triglycerides, and antioxidation in aged rats. Journal of Agricultural and Food Chemistry , 1998, 46 (10), 3875- 3878.

203. Nakagawa T, Yokozawa T, Terasawa K, Shu S, Juneja L H., Protective activity of green tea against free radical- and glucose-mediated protein damage. Journal of Agricultural and Food Chemistry, 2002, 50 (8), 2418-2422.

204. Frei B, Higdon JV, Antioxidant activity of tea polyphenols in vivo: evidence from animal studies. Journal of Nutrition, 2003, 133 (10), 3275S-3284S.

205. Miller H E, Rigelhof F, Marquart L, Prakash A, Kanter M., Whole-grain products and antioxidants. Cereal Foods World, 2000, 45 (2), 59-63.

206. Sharma V, Gulati A, Ravindranath S D, Kumar V, A simple and convenient method for analysis of tea biochemicals by reverse phase HPLC. Journal of Food Composition and Analysis, 2005, 18 (6), 583–594.

207. Ullah M R., A rapid procedure for estimating theaflavins and thearubigins of black tea. Two and a Bud, 1986, 33 (1–2), 46-48.

208. Turkmen N, Poyrazoglu E S, Sari F, Velioglu Y S., Effects of cooking methods on chlorophylls, pheophytins and colour of selected green vegetables. International Journal of Food Science & Technology, 2006, 41 (3), 281–288.

209. Wang Y F, Shao S H, Xu P, Yang X Q, Qian L S., Catechin-enriched green tea extract as a safe and effective agent for antimicrobial and anti-inflammatory treatment. African Journal of Pharmacy and Pharmacology, 2011, 5 (12), 1452-1461.

210. Hampton M G, Production of black tea, In Tea: cultivation to consumption (Wilson KC and Clifford MN, Eds.,), Chapman and Hall, London, 1992; 459-512.

211. Riul Jr A, Gallardo Soto A M, Mello S V, Bone S, Taylor D M, Mattoso L H C., An electronic tongue using polypyrrole and polyaniline. Synthetic Metals, 2003, 132 (2), 109-116.

212. Taylor D M, Macdonald A G, AC admittance of the metal/insulator/electrolyte interface. Journal of Physics D: Applied Physics, 1987, 20 (10), 1277-1283.

213. Bandarenka A S., Exploring the interfaces between metal electrodes and aqueous electrolytes with electrochemical impedance spectroscopy. Analyst, July 2013.

214. Irimia-Vladu M, Fergus J W., Impedance spectroscopy of thin films of emeraldine base polyaniline and its implications for chemical sensing. Synthetic Metals, 2006, 156 (21), 1396-1400.

215. Sridharan V., Master's thesis, Measurement of Carbon Dioxide Corrosion on Carbon Steel Using Electrochemical Frequency Modulation. June 2009.

216. Lisdat F, Schäfer D., The use of electrochemical impedance spectroscopy for biosensing. Analytical and Bioanalytical Chemistry, 2008. 391 (5), 1555–1567.

217. Warburg E., Ueber das verhalten sogenannter unpolarisbarer elektroden gegen wechselstrom. Annalender Physik und Chemie, 1899, 67, 493–499.

218. Randles J E B., Kinetics of rapid electrode reactions. Discussions of the Faraday Society 1947, 1, 11–19.

219. Macdonald D D., Reflections on the history of electrochemical impedance spectroscopy. Electrochimica Acta, 2006, 51 (8-9), 1376-1388.

220. Johnson M D, Otto K J, Kipke D R., Repeated voltage biasing improves unit recordings by reducing resistive tissue impedances. IEEE Transactions on Neural Systems and Rehabilitation Engineering, 2005, 13 (2), 160–165.

221. Otto K J., Johnson M D., Kipke D R., Voltage pulses change neural interface properties and improve unit recordings with chronically implanted microelectrodes. IEEE Transactions on Biomedical Engineering, 2006, 53 (2), 333–340.

222. Zia A I, Rahman M S A, Mukhopadhyay S C., Yu P-L, Al-Bahadly I H, Gooneratne C P, Kosel J, Liao T-S, Technique for rapid detection of phthalates in water and beverages. Journal of Food Engineering, 2013, 116 (2), 515–523.

223. Wang J., Analytical Electrochemistry. Wiley-VCH. 3rd edn. 2006, Hoboken

224. Macdonald J R, Barsoukov E, Impedance Spectroscopy: Theory, Experiment, and Applications, 2nd ed., Wiley, 2005.

225. Rashwan F., The Application of Electrochemical Impedance Techniques in Analyzing the AC Response of Some Two-electron Transfer Dye Systems, American Journal of Applied Sciences 2005, 2 (12),1595-1599.

226. Abidian M R, Kim D H, Martin D C., Conducting-polymer nanotubes for controlled drug release. Advanced Materials , 2006, 18 (4), 405–409.

227. Dhiman M, Kapur P, Ganguli A, Singla M L., Impedance Study of Tea with Added Taste Compounds Using Conducting Polymer and Metal Electrodes. Journal of Nanoscience and Nanotechnology, 2012, 12 , 1-6.

228. Bisquert J, Gratzel M, Wang Q, Fabregat-Santiago F. Three-channel transmission line impedance model for mesoscopic oxide electrodes functionalized with a conductive coating. Journal of Physical Chemistry B, 2006, 110 (23), 11284–11290.

229. Grandle J A, Taylor S R., Electrochemical impedance spectroscopy of coated aluminum beverage containers .1. Determination of an optimal parameter for large-sample evaluation. Corrosion 1994, 50 (10), 792–803.

230. Liu C, Bi Q, Leyland A, Matthews A. An electrochemical impedance spectroscopy study of the corrosion behaviour of pvd coated steels in 0.5 n nacl aqueous solution: Part I. Establishment of equivalent circuits for eis data modelling. Corrosion Science 2003, 45(6), 1243–1256.

231. Caicedo A, Roper S D., Taste receptor cells that discriminate between bitter stimuli. Science. 2001, 291 (5508):1557-1560.

232. Lindermann B., Receptors and Transduction in taste. Nature 2001, 413, 219-225.

233. Rouhi A M., Unlocking the secrets of taste. Chemical & Engineering News, 2001, 79 (37), 42-46.

234. Cruz A, Green B G., Thermal stimulation of taste. Nature, 2000, 403, 889-892.

235. Schiffman S S., Taste quality and neural coding: implications from phycophysics and neurophysiology. Physiology and Behaviour, 2000, 69 (1), 147-159.

236. DeSimone J A., Rapid entry of bitter and sweet tastants into liposomes and taste cells: implications for signal transduction. American Journal of Physiology, Cell Physiol. 2000, 278 (1), C17-C25.

237. Brudzewski K, Osowski S, Markiewicz T., Classification of milk by means of an electronic nose and SVM neural network. Sensors and Actuators B: Chemical, 2004, 98 (2), 291–298.

238. Zhang S, Xie C, Zeng D, Zhang Q, Li H, Bi Z., A feature extraction method and a sampling system for fast recognition of flammable liquids with a portable E-nose. Sensors and Actuators B: Chemical, 2007, 124 (2), 437–443.

239. Behera B, Nayak P, Choudhary R N P., Impedance spectroscopy study of NaBa2V5O15 ceramic. Journal of Alloys and Compounds, 2007, 436 (1-2), 226-232.

240. Rashwan, F., Doctoral Dissertation, Freiburgi. AC voltammetrische und cyclovoltammetrische Untersuchungen an mehrstufigen redoxsystemen.Freiburgi Br. Universitt, West Germany. 1988.

241. Riul Jr A, Dos Santos Jr D S, Wohnrath K, Tommazo R, Carvalho ACPLF, Fonseca F J, Oliveira Jr O N, Taylor D M, Mattoso L H C., Artificial taste sensor: Efficient combination of sensors made from Langmuir-Blodgett films of conducting polymers

and a ruthenium complex and self-assembled films of an azobenzene-containing polymer. Langmuir 2002, 18 (1), 239–45.

242. Beebe K R, Pell R J, Seasholtz M B., Chemometrics: A Practical Guide. New York: Wiley interscience, 1998.

243. Ferloni P, Mastragostino M, Maneghello L., Impedance analysis of electronically conducting polymers. Electrochimica Acta 1996, 41 (1), 27-33.

244. Bartoshuk L M., Taste mixtures: Is mixture suppression related to compression? Physiology & Behavior, 1975, 14 (5), 643–9.

245. Breslin P A S., Interaction among salty, sour and bitter compounds. Trends in Food Science and Technology, 1996, 7 (12), 390–399.

246. Walters D E., How are bitter and sweet tastes related? Trends in Food Science and Technology, 1996, 7 (12), 399–403.

247. Bartoshuk L M, Murphy C, Cleveland C T., Sweet taste of dilute NaCl: psychophysical evidence for a sweet stimulus. Physiology & Behavior , 1978, 21 (4), 609–613.

Appendix I

The detailed list of chemicals/materials with their composition is given below in Table 1.

Chemicals used	**Supplier**	**Molecular mass**
Aniline (C_6H_7N)	M/s. Spectro Chem Pvt Ltd, India	93.13 g/mol
Hydrochloric acid (HCl)	M/s. Spectro Chem Pvt Ltd, India	98.079 g/mol
Pyrrole (C_4H_5N)	M/s. Spectro Chem Pvt Ltd, India	67.09 g/mol
Sulphuric acid (H_2S0_4)	Ranbaxy, India	98.079 g/mol
Potassium ferrocynate $K_4[Fe(CN)_6]$	M/s. Spectro Chem Pvt Ltd, India	368.35 g/mol (anhydrous) 422.388 g/mol (trihydrate)
Acetone (C_3H_6O)	Merck (Bangalore, India)	58.08 g/mol
Sodium chloride (NaCl) Pottasium chloride (KCl)	NaCl and KCL - Loba Chemie, India	NaCl: 58.44 g/mol KCl : 74.5513 $g \cdot mol^{-1}$
Quinine ($C_{20}H_{24}N_2O_2$)	Fluka, India	324.417 g/mol
Citric acid ($C_6H_8O_7$)	Merck (Bangalore, India)	192.124 g/mol (anhydrous) 210.14g/mol (monohydrate)
Methanol (CH_4O)	Merck (Bangalore, India)	32.04 g/mol
Acetonitrile (C_2H_3N)	Merck (Bangalore, India)	41.05 g/mol

Folin's ciocalteus reagent	SRL (Mumbai, India)	
Hydrochloric acid (HCl)	Loba Chemie, India	36.46094 g/mol
2,2-diphenyl-1-picrylhydrazyl (DPPH)	Sigma Aldrich (New Delhi, India)	394.32 g/mol
Ethanol (C_2H_6O)	Merck (Bangalore, India)	46.06844 g/mol
Sucrose ($C_{12}H_{22}O_{11}$)	Fluka, India	342.2965 g/mol
Lithium perchlorate ($LiCl0_4$)	Alfa Aesar, India	106.392 g/mol
Indium Tin Oxide glass plates	Sigma Aldrich Pvt. Ltd., India,	
Biochemicals used	**Supplier**	**Molecular Mass**
Caffeine ($C_8H_{10}N_4O_2$)	Sigma Chemicals Co., United States.	194.19 g/mol
Galic Acid ($C_7H_6O_5$)	Sigma Chemicals Co., United States	170.12 g/mol
(−)epigallocatechin gallate ($C_{22}H_{18}O_{11}$)	Sigma Chemicals Co., United States	458.372 g/mol
(−)-epicatechin gallate ($C_{22}H_{18}O_{10}$)	Sigma Chemicals Co., United States	442.37 g/mol
(−)epigallocatechin ($C_{15}H_{14}O_7$)	Sigma Chemicals Co., United States	306.27 g/mol

(−)-epicatechin ($C_{15}H_{14}O_6$)	Sigma Chemicals Co., United States	290.3 g/mol
Dibenzylideneacetone ($C_{17}H_{14}O$)	Sigma Chemicals Co., United States	234.29 g/mol
(+)-catechin ($C_{15}H_{14}O_6$)	Sigma Chemicals Co., United States	290.26 g/mol
HPLC grade acetonitrile (ACN)	Sigma Chemicals Co., United States	41.05 g/mol
Theaflavin ($C_{29}H_{24}O_{12}$)	Sigma Chemicals Co., United States	564.49 g/mol
Thearubigin (Tr)	Sigma Chemicals Co., United States	
Dry tea varieties used	**Brands**	**Supplier**
Kangra	12 samples each of Kangra Orthodox black tea (Camellia sinensis (L.)O. Kuntze)	Early, Rains and Backend seasons, from IHBT, Palampur
CTC	8 samples of Assam CTC tea (Camellia sinensis var. assamica)	From local market, Chandigarh

Juices/beverages	**Source**
"Packed" orange juice (Minute Maid from Coca-Cola)	From local market Chandigarh (India)
Raw milk from local dairy	From local milkman, Chandigarh (India)
Sweetened clove syrup	Procured from local market of Chandigarh (India)
Sweetened ginger syrup	Procured from local market of Chandigarh (India)
Sweetened cardamom syrup	Procured from local market of Chandigarh (India)

c

Sweet chocolate syrup	Procured from local market of Chandigarh (India)
Vanilla flavoured milk without sugar	Procured from local market of Chandigarh (India)
Fresh orange juice (Fresh squeezed)	Prepared in laboratory (used immediately)
Fresh lime juice (Fresh squeezed)	Prepared in laboratory (used immediately)

SENSOR LETTERS
Vol. 10, 1–7, 2012

Behavior of Metal and Emeraldine Salt for Detection of Threshold Level of Sucrose and Citric Acid in Impedance Mode

Mopsy Dhiman[1, 2, *], Pawan Kapur[1], Abhijit Ganguli[2], and Madan Lal Singla[1]

[1] *Central scientific Instruments Organization, CSIR, Chandigarh 160020, India*
[2] *Thapar University, P.O. Box 32, Patiala 147004, India*

(Received: 5 March 2012. Accepted: 20 May 2012)

Taste is an organoleptic quality attribute and probably most time consuming and expensive property to evaluate. In the present study sucrose and citric acid (sweet and sour tastants) was evaluated in the concentration range 5, 10, 50 and 100 mM and a frequency range of 1 Hz–100 KHz deploying Glassy Carbon, Gold and Polyaniline electrodes and the data was related with citrus fruit juices and sweet tea liquor. Nyquist plots are drawn to identify an equivalent circuit and study the interactions between electrode–electrolyte. Nyquist plots show different fully resolved semicircle followed by 45° line for each concentration using Glassy Carbon and Gold electrode whose pattern changes but not their shape, while Polyaniline (emeraldine salt) represents one fully resolved and one partially resolved semicircle. Principal Component Analysis was performed on the signals to show that the signals vary to distinguish both the threshold level concentrations of sucrose and citric acid (sweet and sour tastants) which leads to subsequent classification and able to relate the behavior of juices towards sucrose and citric acid (sweet and sour taste).

Keywords: Organoleptic, Tastants, Nyquist Plots, Impedance, Principal Component Analysis.

RESEARCH ARTICLE

1. INTRODUCTION

A very subjective quality characteristic of food products is taste. Like olfaction, it is a fundamental chemical sense, which involves the detection of stimuli dissolved in water, saliva or oil by the taste buds.[1] Humans cannot taste absolute concentrations but only taste differences in the concentration of substances, and their sensitivity to levels that are lower than those which appear in saliva is low. Several conditions in the mouth that affect taste perception are the viscosity, rate, temperature, duration and area of application of the stimulus, the chemical state of the saliva and the presence of other tastants in the solution being tasted in addition to the concentration of a taste stimulus. five gustatory perceptions describes taste, sweetness, sourness, saltiness, umami and bitterness, caused by soluble substances in the mouth.[2] The five tastes are mainly caused by the presence of respectively sugars, organic acids, salts, monosodium-glutamate, phenolics and alkaloids. The presence of sugars in a food product produces sweetness which is often connected to aldehydes and ketones, which contain a carbonyl group. 10 mM is the average human detection threshold for sucrose in water. Sourness is thus triggered by H+ ions and free acids and detects acidity. 0.09 mM is the average human detection threshold for HCl in water. The relation between titratable acidity, pH, and total acids is not clear since several authors give different statements on this subject.[3–5] Correlations of several volatile substances have been found with sourness.[6, 7] Several factors like genetics, maturity, pre and post-harvest handling cause significant changes in the taste and the content of taste compounds in a fruit can be influenced by these factors. The chemical content of fruits from different cultivars can differ substantially. The taste will change significantly by genetically manipulating the sugar/acid content of a fruit.[8]

Many vegetables and fruits are determined by their typical sour and sweet taste. To determine the sugar and acid content of plant material various techniques are used. Techniques such as high performance liquid chromatography (HPLC) or, after derivatization, gas chromatography (mass spectrometry) (GC-MS) can determined both sugars and acids. Both techniques require expensive

*Corresponding author; E-mail: mopsyd@gmail.com

apparatus and demand a considerable amount of time per measurement.[9] In the last decade, arrays of sensors which are referred to as electrochemical techniques/tongue that analyze liquids, were developed. Different detection methods have been used in these studies which include Cyclic Voltammetry, Potentiometry[10–12] and admittance measurements.[13] Recently impedance technique has been deployed for several applications in food processing industry but the technique has not been still extensively used and several groups are working on impedance based studies in bioelectrochemistry based sensors.[14–17]

The objective of this study is to classify substances with different taste modalities i.e., the sweet and sour tastants at threshold level and relate it to the tastants in fresh citrus fruit juice and sweet tea liquor. Two different tastants i.e., sucrose and citric acid are prepared in concentrations ranging from 5–100 mM and scanned for optimum frequency from 1 Hz–100 KHz at 0.1 V using three different sensing surfaces made from GC, Au and PANI (emeraldine salt) an electrochemical cell for about 30 days keeping the constant experimental parameters. Using the electrochemical responses obtained from impedance technique as departure information and performing the data treatment with PCA for their classification/pattern generation it is possible to classify the threshold level sweet and sour tastants. An impedance technique based on sensing electrodes of GC, Au and PANI is assessed as a rapid tool for the quantification of threshold level sweet and sour tastants.

RESEARCH ARTICLE

2. EXPERIMENTAL DETAILS

2.1. Materials Used

Glassy Carbon (GC), Gold (Au) and Polyaniline (PANI) working electrodes and Ag/AgCl (4 M KCl) reference electrode were supplied by CH Instruments (Austin, USA) whereas PANI working electrode was fabricated in the lab. The PANI electrode was fabricated on Indium Tin Oxide (ITO) glass slide supplied by Sigma Aldrich Pvt. Ltd., India, using aniline (C_6H_7N) supplied by M/s. Spectro Chem Pvt. Ltd., India. Both the taste solutions were prepared using Analytical grade chemicals. 100 mM solutions of sucrose/citric acid were prepared (Loba Chemie, India). Each solution was further diluted to 50, 10 and 5 mM concentration. Fresh orange and lemon were purchased daily for one week and their juice was extracted and filtered. Each juice sample was kept for about 30 minutes to study the impedance behavior. One brand of Assam CTC tea (Camellia sinensis var. assamica) was procured from local market. Impedance study for 1% Black tea solution with sucrose was carried (prepared by adding 0.5 gm of sucrose to 50 ml black tea liquor). PCA data points for Sucrose solutions using PANI electrode was named as 1 (5 mM), 2 (10 mM), 3 (50 mM) and 4 (100 mM). Similar marking has been done for GC electrode 5 (5 mM), 6 (10 mM), 7 (50 mM) and 8 (100 Mm) and for Au electrode as 9 (5 mM), 10 (10 mM), 11 (50 mM) and 12 (100 mM) respectively. The PCA data points for Citric acid for GC, Au and PANI was also marked 13–16, 17–20 and 21–24 for the above four concentrations respectively. In PCA pattern with green encircled area represents low concentrations whereas the red shows the higher concentrations. Encircled points representing lemon, orange, sweet tea liquor are shown in yellow, orange and brown colors respectively.

2.2. Electrodeposition of PANI on ITO Coated Glass Surface

An ITO coated glass of $2.5 \times 1 \times 0.1$ cm^3 was used for deposition of PANI (emaralidine salt) film on 0.8 cm^2 area. In a three electrode set up [ITO coated glass as working electrode, Pt wire as counter electrode and saturated calomel electrode (SCE) as reference electrode] at room temperature film was deposited potentiostatically at +1.2 V potential for 2 min in a glass cell containing 10 ml H_2SO_4 solution (1 M) and 0.5 ml of aniline.[18, 19] Each film were washed 2–3 times in DI water, dried and stored in vacuum desiccators for further use.

2.3. Impedance Measurements

Impedance measurements were made at room temperature in a three electrode set up using GC, Au and PANI working electrodes independently, Pt wire as counter electrode and Ag/AgCl (4 M KCl) was used as reference electrodes. GC and Au electrodes were polished with alumina powder of 0.3 followed by polishing with 0.05 μm for smoothing the electrode surface. Each electrode was washed well with DI water before use. The working electrodes for measurements were selected manually using a wire jumper arrangement. The data was recorded continuously for 30 days for standard samples and seven days with juice and sweet tea liquor. The AC-impedance parameters were kept constant at +0.1 V potential for 60 sec in the amplitude 0.005 V with a frequency range of 1 Hz to 100 KHz.[20]

2.4. Principal Component Analysis

The PCA is a common pattern recognition algorithm used to analyze data obtained.[21, 22] In particular, PCA is used to reduce the complexity of data by computing a new, much smaller set of uncorrelated variables which best represent the original data. This is done by projecting the high dimensional data set in a dimensional reduced space based on the uncorrelated and orthogonal eigenvectors of the covariance matrix computed from the instrument used. These eigenvectors were called principal components (PC) of the features and were arranged in sequence where the first principal component was the one with the greatest amount of variance, followed by the second greatest and

so on. The plot of the original data in the new space defined by the first few principal components will give visual interpretation on how the original data are scattered. In particular, the plot will show features that have small variation appear together while the features with large variation appear distant. Therefore PCA is able to expose some clusters of the data naturally. The PCA is a straightforward analysis, which is validated through conducting several experiments, measurements and testing the data.

3. RESULTS AND DISCUSSION

3.1. Impedance Study

The impedance behavior of aqueous sucrose solution for four concentrations (5, 10, 50 and 100 mM) in the frequency range 1 Hz–100 KHz scanned for their real and imaginary impedance plots are given in Figures 1–3 for GC, Au and PANI respectively. The nyquist plots in Figure 1 observed are semicircular in nature having maximum radii for 5 mM and minimum radii for 100 mM

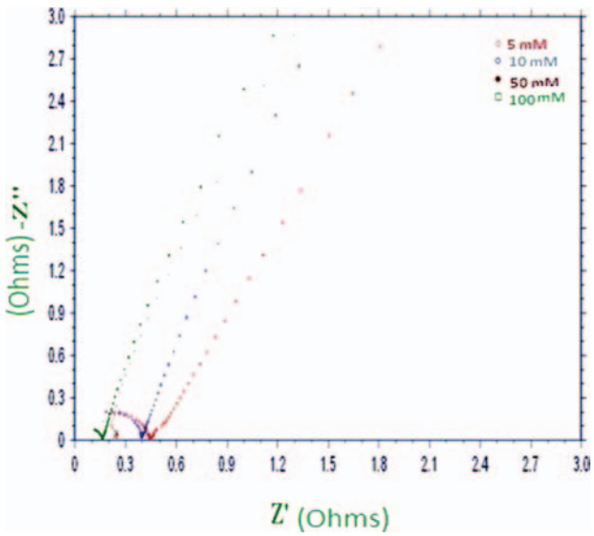

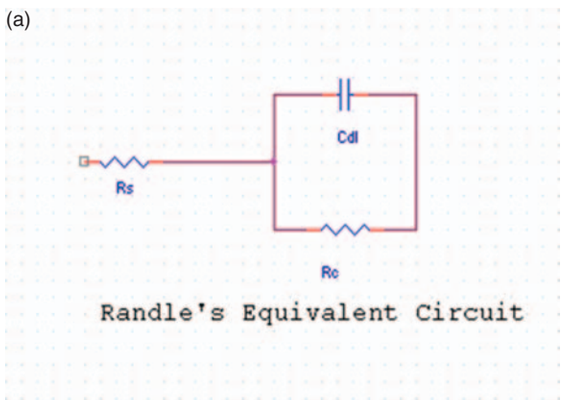

Fig. 1. Nyquist plot of sucrose using GC. (a) Randle's equivalent circuit.

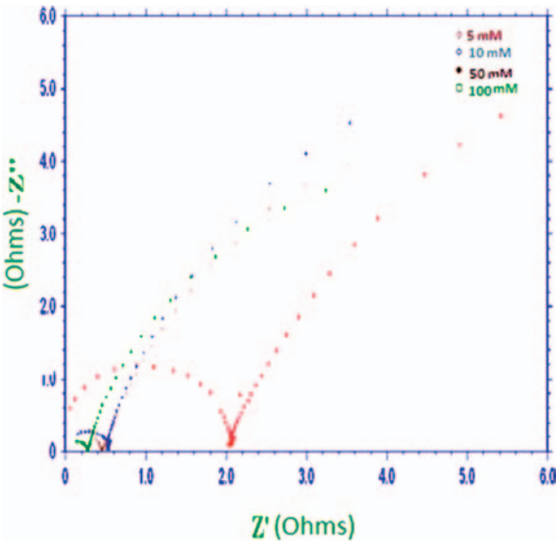

Fig. 2. Nyquist plot of sucrose using Au.

indicating that the solutions having large semicircle area has maximum impedance whereas semicircle with lower radii has minimum impedance values. Each semicircular Nyquist plot is followed by 45° oblique line which represents Warburg impedance behavior in terms of Randle's equivalent circuit [Fig. 1(a)], where C_{dl} is the double-layer capacitance, R_s is the bulk sample solution resistance, R_c is the charge-transfer resistance associated with the double layer. These results indicate that it may be possible to predict the concentration of different varieties of sugars in the impedance mode using appropriate number of known samples.

Nyquist plots in Figure 2 shows almost fully resolved semicircle towards left followed by oblique lines at right side for 5 mM concentration solutions whereas other three concentration solutions have a very small semicircle close to the origin at high frequency followed by semicircular 45° lines whose pattern changes but not their shape.[20] The impedance behavior indicates that it is well possible to differentiate the threshold level sweet taste with Au electrode in comparison to higher concentration solutions. The reason for the same may be that a very thin layer of oxides of gold may occur with higher concentrations which are giving rise to similar impedance behavior for 10 mM concentration onwards. The physical model appropriate for such impedance response is simple Randle's equivalent circuit [Fig. 1(a)].

Figure 3 represents the impedance plots where two semicircles were obtained using PANI working electrode, a fully resolved semicircular arc can be seen on the left side of the plot and partially resolved semicircle obtained on the right side of the Nyquist plots. Conduction may be low for dilute solutions in comparison to higher concentration solution. This behavior occurred may be due to the adsorption of the sucrose molecule at the surface of the PANI

RESEARCH ARTICLE

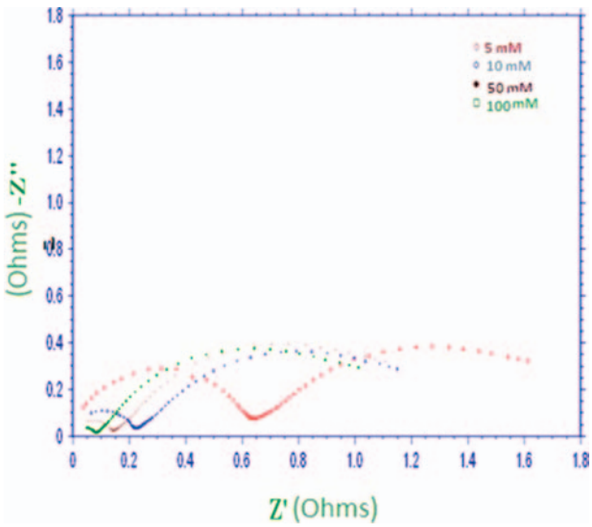

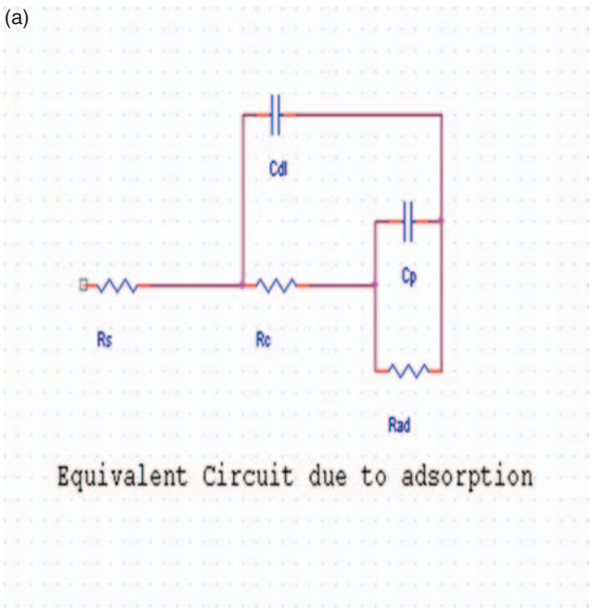

Fig. 3. Nyquist plot of sucrose using PANI. (a) Equivalent circuit for adsorption.

electrode giving rise to double layer affect. This result can be modeled by two RC-parallel circuits, in series. Each parallel combination of resistance R and capacitance C results in a semi-circle in the impedance plot.[23] Distorted nature of the semicircle attributes to the variation of the morphology of the PANI electrode resulting in change in conduction mechanism at the interface. The equivalent circuit corresponding to adsorption describes the response for PANI electrode [Fig. 3(a)]. In this equivalent circuit for adsorption, R_s is the bulk sample solution resistance, R_c is the charge-transfer resistance associated with the double layer, C_{dl} is the double-layer capacitance, R_{ad} is the resistance of the adsorption layer, C_p is the passivative capacitance associated with the adsorption layer.

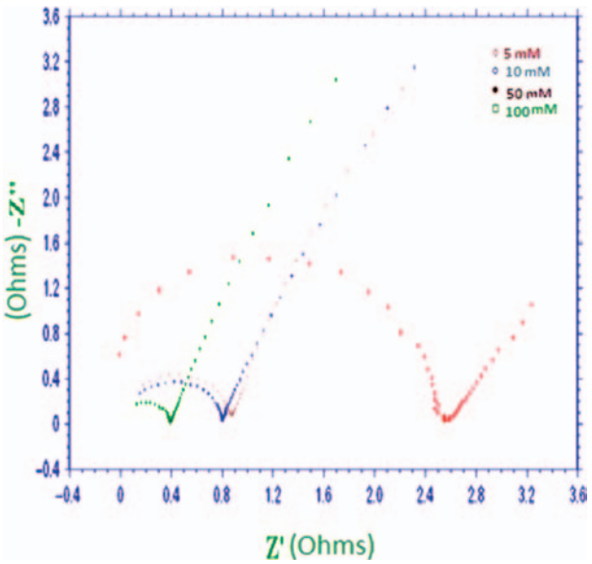

Fig. 4. Nyquist plot of citric acid using GC.

The impedance behavior/Nyquist plots for Citric acid solution in the frequency range of 1 Hz–100 KHz with four different concentrations (5, 10, 50 and 100 mM) are given in Figures 4–6 for GC, Au and PANI electrode respectively. Figure 4 represents a linear impedance locus with an angle of 45° to the real axis which amounts to low frequency Warburg response [Fig. 1(a)] due to diffusion. However at high frequencies the citric acid solution shows converge with null imaginary impedance small semicircle. With the increasing concentration of solution, area under the semicircular arc decreases. The smaller semicircular part corresponds to the faradaic oxidation reaction whereas part of the large diameter semicircle is associated with charge transfer process.

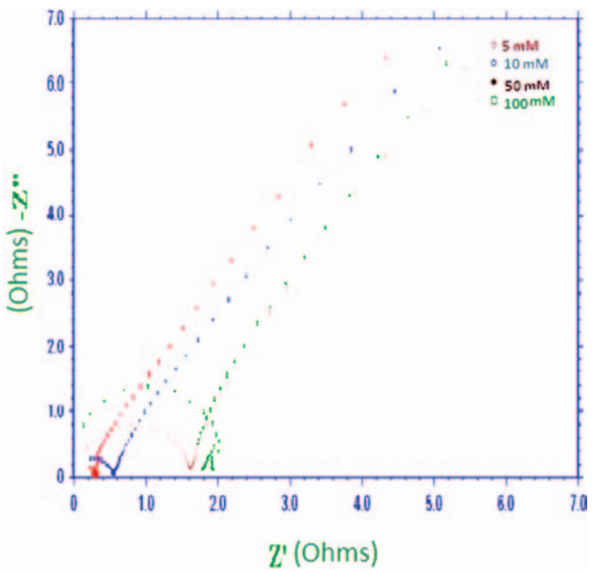

Fig. 5. Nyquist plot of citric acid using Au.

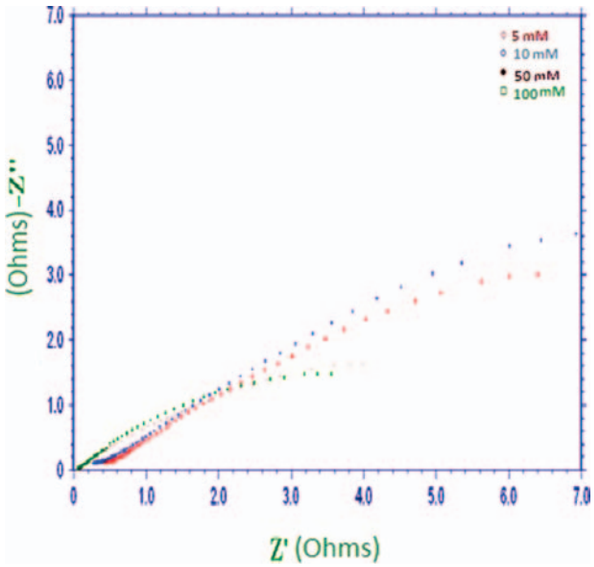

Fig. 6. Nyquist plot of citric acid using PANI.

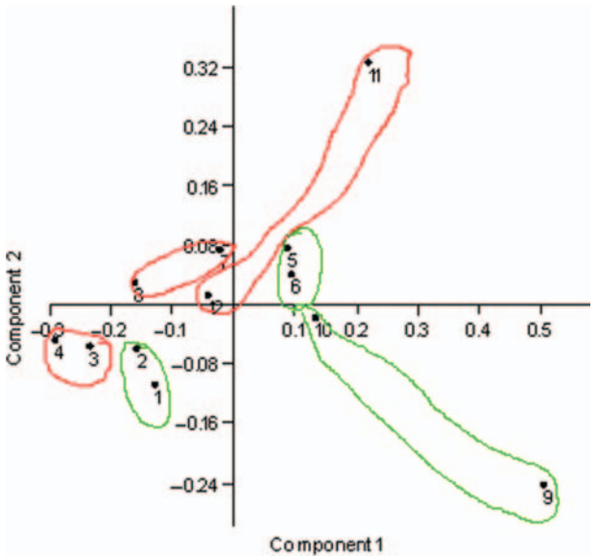

Fig. 7. PCA of sucrose using PANI, GC and Au.

Figure 5 shows a small semicircular Nyquist plots for citric acid using Au surface, which corresponds to the bulk electrode resistance in parallel with the capacitance. This near vertical lines with 45° trend is due to the charge transport impedance originates from non-uniform concentration profiles of charged species on the electrode. This 45° line arises due to the diffusion phenomenon which leads to Warburg impedance. The physical model explaining this phenomenon is Randle's equivalent circuit [Fig. 1(a)].

Impedance response of Figure 6 shows two semicircles left fully resolved semicircle and right partially resolved semicircle for various citric acid concentrations on PANI. A capacitance dispersion effect represented by distorted semicircles can be observed for PANI electrode. This behavior is commonly observed in case of inhomogeneous surfaces displaying surface defects, porosity. At open circuit potential state the PANI film is in its emeraldine form. In the emeraldine state of PANI the oxidized and reduced units of the polymer are almost equal. As a result the PANI film exhibits a maximum conductivity. The shift in valley points of the impedance loci of the citric acid solution (along the real as well as imaginary axis) can be attributed to charge transfer kinetics and adsorption rate. The equivalent circuit corresponding to adsorption describes the response for PANI electrode [Fig. 3(a)].

3.2. PCA Study

For PCA study Unscrambler9.7 has been used. The first principal component (PC1) maps the maximum variance and information of the input data followed by the other principal components (PC2, PC3 and so on) in descending order of the variance. Generally a good discrimination is mapped by the first two principal components, i.e., PC1 and PC2.

The PCA plots for sucrose and Citric acid at four different concentrations (5, 10, 50 and 100 mM), with GC Au and PANI working electrodes are represented in Figures 7 and 8 respectively. The data is plotted in a two dimensional plane formed by the first two PCs, with PC1 showing 73.09% and PC2 showing 26.69% data variance in Figure 7. All the points for four different concentration solutions of sucrose lie on same quadrant i.e., 3rd quadrant (negative values). This shows PANI electrode gives nearly a common cluster for both low and high concentration solutions. The 5 and 10 mM concentration (low concentration solutions) lie close by in the 1st quadrant using GC electrode while 50 and 100 Mm concentration solutions lie on the 2nd quadrant (negative values) and can be seen near to each other. Hence GC electrode helps in classifying low and high concentration solutions clearly. The low concentration (5 and 10 mM) solutions lie together in the 4th quadrant using Au electrode. While 50 and 100 mM solutions (high concentration solutions) lie at different quadrant. This indicates Au electrodes helps in distinguishing low concentration solutions steadily.

Figure 8 shows the data plotted in a two dimensional plane formed by the first two PCs, PC1 (horizontal) axis with an explained variance of 92.88% and PC2 showing 7.03% data variance. A cluster for both low and high concentration solutions can be seen using PANI electrode i.e., in 3rd quadrant. With the use of GC electrode all the four concentrations lay separately from PANI electrode whereas 10, 50 and 100 mM lay close to each other indicating these are positively correlated. Using Au electrode both low concentrations (5 and 10 mM) and high concentrations (50 and 100 mM) lie close to each other. Hence GC metal electrode gives a good classification for both high and low concentrations solutions of citric acid.

RESEARCH ARTICLE

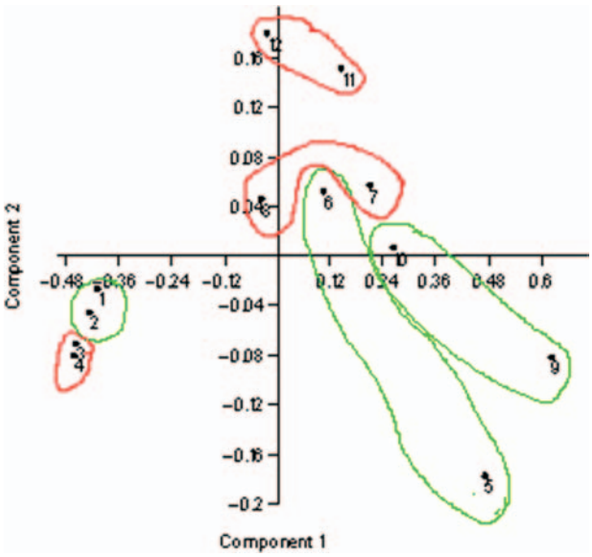

Fig. 8. PCA of citric acid using PANI, GC and Au.

Figure 9 gives PCA plot for both the sucrose and citric acid solutions at four concentrations namely 5, 10, 50 and 100 mM with PANI, GC and Au working electrodes, PC1 gives an explained variance of 85.79% and PC2 gives 14% of data variance. All the points at four concentrations using PANI electrode for sucrose and citric acid shows a very good classification. These all points lie closer hence PANI electrode helps very well in classification among intra frequency as well as intra electrode class for both the sweet and sour compounds (sucrose and citric acid). GC electrode also plays a significant role in classifying low concentration as well as high concentration solution of both sucrose and citric acid. GC and Au electrodes help in classifying both low concentration solutions and high concentration solutions.

Figure 10 gives PCA plot for sucrose, citric acid, freshly prepared fruit juices and sweet tea liquor at four

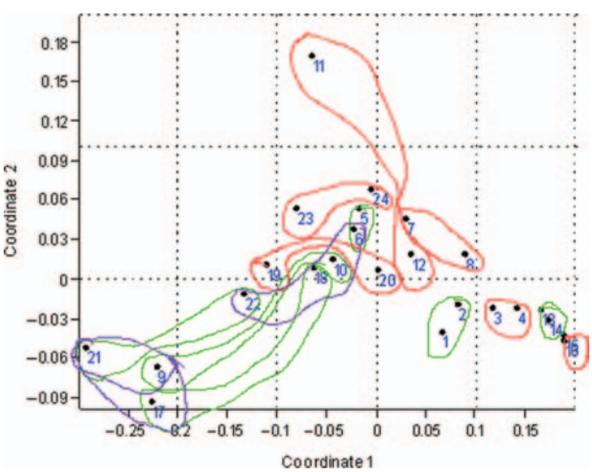

Fig. 9. PCA of sucrose and citric acid using PANI, GC and Au.

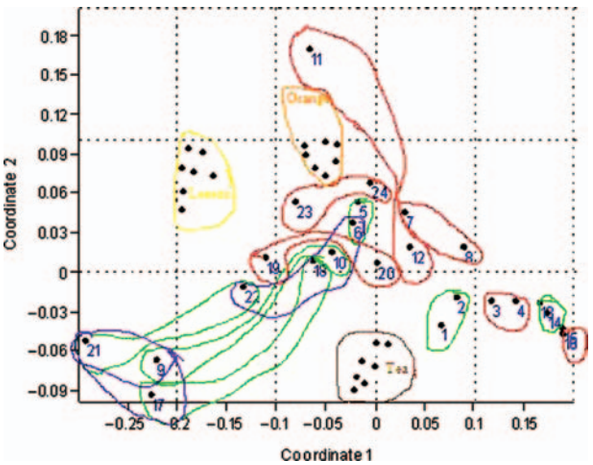

Fig. 10. PCA of sucrose, citric acid, juices and tea using PANI, GC and Au.

concentrations (5, 10, 50 and 100 mM) with GC ,Au and PANI working electrodes corresponding to seven days data. More than 99% significant information is available with the first two principal components (PC1 and PC2).

The lemon juice lies close to the low concentration solution of citric acid which may be due to more amounts of acidic compounds present in lemon. The orange juice gives a random response lying closer to low concentration solutions of both metal electrodes and shows some correlation with high concentration solutions of citric acid. Whereas the sweet tea liquor in sucrose falls close to low concentration solutions of sucrose with the use of PANI, GC and Au working electrodes. With the present study it may not be possible to classify the taste quality of the fruit juices, however further behavioral studies in impedance mode are being carried out looking the levels of different sugars, salts and organic acids as tastants.

4. SUMMARY

Impedance analysis based on three electrode system helped to distinguish both the sweet and sour tastants using impedance technique. Impedance/Nyquist plots shows a fully resolved semicircle followed by 45° line for both Au and GC, while Nyquist plots representing two semicircles (one fully resolved and one partially resolved) were observed for PANI. PCA analysis successfully analyzed the sensed signals by segregating both sweet and sour tastants into different regions according to its own unique characteristics and established the sensitivity of the sensing electrode. In PCA plots it is possible to distinguish low level concentration with GC and Au clearly however PANI electrode shows nearly a common cluster up to 100 mM. Impedance data of sucrose, citric acid and fruit juices/ sweet tea liquor in PCA shows that the lemon juice lies close to the low concentration solution of citric acid. The orange juice gives a random response lying closer to low

RESEARCH ARTICLE

concentration solutions of both metal electrodes Whereas the sweet tea liquor in sucrose falls close to low concentration solutions of sucrose with the use of PANI, GC and Au working electrodes. In all cases it is possible to establish correlation between the response of the sensing electrodes and PCA. Further studies are being carried out for better taste classification. This method opens up new avenues in taste sensing and can be successfully implemented in the future to distinguish various classes of tastants.

Acknowledgments: The authors are grateful to, Mrinmoy Misra, Vishal, Sukhwinder Singh and Ravi K. Komaravalu for their interest in this study.

References and Notes

1. A. Drewnowksi, *Nutrition Reviews* 59, 163 **(2001)**.
2. M. Meilgaard, G. Civille, and B. Carr, Sensory Evaluation Technique, 4th edn., CRC Press, Boca Raton, Florida, U.S.A **(2007)**.
3. M. Petro-Truza, *Food Reviews International* 2, 309 **(1987)**.
4. T. Malundo, R. Shewfelt, and J. Scott, *Postharvest Biology and Technology* 6, 103 **(1995)**.
5. V. Fernandez-Ruiz, M. C. Sanchez-Mata, M. Camara, M. E. Torija, C. Chaya, L. Galiana-Balaguer, S. Rosello, and F. Neuz, *Hort Science* 39, 339 **(2004)**.
6. A. Noble, *Trends in Food Science and Technology* 7, 439 **(1996)**.
7. R. Stevenson, J. Prescott, and R. Boakes, *Chemical Senses* 24, 627 **(1999)**.
8. R. Jones and S. Scott, *Euphytica* 32, 845 **(1983)**.
9. I. Molnar-Perl, *J. Chromatogr. A* 845, 181 **(1999)**.
10. C. Di Natale, R. Paolesse, A. Macagnano, A. D'Amico, M. Ubigli, A. Legin, L. Lvova, A. Rudnitskaya, and Y. Vlasov, *Sens. Actuators, B* 69, 342 **(2000)**.
11. A. Sakai, S. Liyama, and K. Toko, *Sens. Actuators, B* 66, 251 **(2000)**.
12. C. Di Natale, A. Macagnano, F. Davide, A. Damico, A. Legin, Y. Vlasov, A. Rudnitskaya, and B. Selenzenev, *Sens. Actuators, B* 44, 423 **(1997)**.
13. A. Riul, Jr, D. S. dos Santos, Jr, K. Wohnrath, R. Di Tommazo, A. C. P. L. F. Carvalho, F. J. Fonseca, O. N. Oliveira, Jr, D. M. Taylor, and L. H. C. Mattoso, *Langmuir* 18, 239 **(2002)**.
14. Y. Vlasov, A. Legin, and A. Rudnitskaya, *Analytical and Bioanalytical Chemistry* 373, 136 **(2002)**.
15. D. Zielinska and B. Pierozynski, *J. Electroanal. Chem.* 625, 149 **(2009)**.
16. P. Roy, T.-C. Tsai, C.-T. Liang, R.-J. Wu, and M. Chavali, *J. Chin. Chem. Soc.* 58, 714 **(2011)**.
17. Md. A. Rahman, P. Kumar, D.-S. Park, and Y.-B. Shim, *Sensors* 8, 118 **(2008)**.
18. K. Meral, A. Levent, and S. Mehmet, *Polym. Int.* 51, 1371 **(2002)**.
19. A. A. Arrieta, C. Apetrei, M. L. Rodríguez-Méndez, and J. A. de Saja, *Electrochim. Acta* 49, 4543 **(2004)**.
20. A. P. Bhondekar, M. Dhiman, A. Sharma, A. Bhakta, A. Ganguli, S. S. Bari, R. Vig, P. Kapur, and M. L. Singla, *Sens. Actuators, B* 148, 601 **(2010)**.
21. K. Brudzewski and J. Ulaczyk, *Sens. Actuat. B-Chem.* 140, 43 **(2009)**.
22. S. Zhang, C. Xie, D. Zeng, Q. Zhang, H. Li, et al., *Sens. Actuat. B-Chem.* 124, 437 **(2007)**.
23. B. Behera, P. Nayak, and R. N. P. Choudhary, *J. Alloys Compd.* 436, 226 **(2007)**.

RESEARCH ARTICLE

Journal of
Nanoscience and Nanotechnology
Vol. 12, 1–6, 2012

Impedance Study of Tea with Added Taste Compounds Using Conducting Polymer and Metal Electrodes

Mopsy Dhiman[1, 2, *], Pawan Kapur[1], Abhijit Ganguli[2], and Madan Lal Singla[1]

[1] *Central Scientific Instruments Organization, CSIR, Chandigarh 160020, India*
[2] *Thapar University, P.O Box 32, Patiala, 147004, India*

In this study the sensing capabilities of a combination of metals and conducting polymer sensing/working electrodes for tea liquor prepared by addition of different compounds using an impedance mode in frequency range 1 Hz–100 KHz at 0.1 V potential has been carried out. Classification of six different tea liquor samples made by dissolving various compounds (black tea liquor + raw milk from milkman), (black tea liquor + sweetened clove syrup), (black tea liquor + sweetened ginger syrup), (black tea liquor + sweetened cardamom syrup), (black tea liquor + sweet chocolate syrup) and (black tea liquor + vanilla flavoured milk without sugar) using six different working electrodes in a multi electrode setup has been studied using impedance and further its PCA has been carried out. Working electrodes of Platinum (Pt), Gold (Au), Silver (Ag), Glassy Carbon (GC) and conducting polymer electrodes of Polyaniline (PANI) and Polypyrrole (PPY) grown on an ITO surface potentiostatically have been deployed in a three electrode set up. The impedance response of these tea liquor samples using number of working electrodes shows a decrease in the real and imaginary impedance values presented on nyquist plots depending upon the nature of the electrode and amount of dissolved salts present in compounds added to tea liquor/solution. The different sensing surfaces allowed a high cross-selectivity in response to the same analyte. From Principal Component Analysis (PCA) plots it was possible to classify tea liquor in 3–4 classes using conducting polymer electrodes; however tea liquors were well separated from the PCA plots employing the impedance data of both conducting polymer and metal electrodes.

Keywords: Impedance, Sensing Electrodes, Principal Component Analysis, Conducting Polymers.

RESEARCH ARTICLE

1. INTRODUCTION

One of the most popular beverages in the world is tea. Tea was once believed as the very expensive form of the medicine that could cure the human body for a variety of symptoms. As far as taste and smell goes each type of tea leaf has its own unique characteristic. Taste sensing is the most important aspect in the food and as well as pharmaceutical industry and is applied in variety of ways e.g., optimization of taste according to the target clients, quality control during processing of tea, juices and water etc, control of ageing process of tea leaves, automatic control of taste and identification of any unpleasant taste.[1–2] Several methods have been used to quantify the quality of tea and tea beverages.[3–6]

To evaluate and distinguish between different types of taste the human sense of taste has been used for centuries but this has been largely unreliable due to its poor subjectivity, selectivity and reproducibility. So when we apply human panel to judge the taste of food substance, there is a tendency to grade the quality of tea/beverage according to his/her preference, and panel might not be able to make subtle difference in taste that might be present in the tea because of overlapping tastes which might lead to results being biased. In the last few decades new techniques have been developed to distinguish and classify different food products using taste sensors. Different tasks such as discrimination and classification, quality evaluation and control, process monitoring and quantitative analyses have been successfully performed with electronic tongues.[7–11]

Descriptive analysis and consumer affective tests are some of the sensory tests which are regularly used to study food ingredient effects, processing variables and storage changes on the perceived sensory properties of food products. Sensory analysis provides marketers with an understanding of directions for product quality, food product

*Author to whom correspondence should be addressed.

quality, profiles of competing products, and evaluations of product reformulations from a consumer perspective.[12] The technique discussed here is based on the impedance which acts as a taste sensor. It is supported by fast computer-aided computations, which allow real-time monitoring of the product quality. The sensing system is cost effective and highly reliable both in terms of measurement accuracy and speed of measurement.

This study aims at demonstrating how analytical sensory analysis can provide important information about the impedance behaviour of tea solutions at a constant voltage of 0.1 V in the frequency range from 1 Hz–100 KHz using a combination of working/sensing electrodes. The metal electrode surface area was kept constant for all the measurements. For each of the working electrode after repeated measurements of the samples over a period of 90 days were taken into consideration and used for the AC-impedance study and principal component analysis (PCA). Impedance technique has also been widely used to evaluate the quality of food, water and milk.[13–15]

2. EXPERIMENTAL DETAILS

2.1. Materials

Working electrodes of GC, Au, Pt, Ag, and reference electrode of Ag/AgCl (4MKCl) were supplied by CH Instruments (Austin, USA) whereas PANI and PPY working electrodes were fabricated in-house. The PANI and PPY electrodes were fabricated using aniline (C_6H_7N) and pyrrole (C_4H_5N) supplied by M/s. Spectro Chem Pvt. Ltd., India. All the chemicals used were of analytical grade and Deionized (DI) water was used for practical purposes. The Black tea with added compounds is labelled in Table I. All the black tea samples were procured from local market of Chandigarh (India). The chemicals used for the preparation of conducting polymer sensors are aniline and pyrrole (Spectrochem Pvt. Ltd. India), $LiClO_4$ (Alfa Aesar), H_2SO_4 (Ranbaxy, India), and Indium Tin Oxide glass plates.

2.2. Equipments Used

CH Instruments Electrochemical workstation 660C (Austin, TX, USA) was used for the impedance study. All the impedance experiments were carried out at 20 ± 2 °C using a single compartment 3 electrode cell as shown in Figure 1. Pt, Au, GC, and Ag (supplied by CHI Instruments) were used as working electrodes; ITO-PANI and ITO-PPY working electrodes were grown potentiostatically. Pt wire as the counter electrode and Ag/AgCl (4 M KCl) as the reference electrode were used. The AC-impedance parameters were +0.1 V potential for 60 sec at an amplitude of 0.005 V with a frequency range from 1 Hz–100 KHz.

Table I. Labelling of black tea with added compounds.

S. no.	Composition	Name
1	Black tea liquor + raw milk from milkman	A
2	Black tea liquor + sweetened clove syrup	B
3	Black tea liquor + sweetened ginger syrup	C
4	Black tea liquor + sweetened cardamom syrup	D
5	Black tea liquor + sweet chocolate syrup	E
6	Black tea liquor + vanilla flavoured milk without sugar	F

2.3. Impedance Measurements

2.3.1. Metal Electrode Polishing and Electro Polymerization of Conducting Polymers at ITO Coated Glass Surface

All the four metal electrodes (Pt, Au, glassy carbon, and Ag) were polished to obtain a smooth surface with alumina powder (Al_2O_3, CH Instruments, Inc., USA) of particle sizes of 1, 0.3, and 0.05 μm and washed before use. PANI and PPY films were deposited on the ITO surface (0.8 cm^2) by the electro polymerization of the respective monomers in a glass cell having a three electrode ITO coated glass as the working electrode, Pt wire as the counter electrode and Ag/AgCl as the reference electrode.

For the ITO-PPY electrode 0.1 ml of pyrrole monomer and 10 ml of 0.2 M $LiClO_4$ were taken in the glass cell and a film was grown potentiostatically at +1 V for 30 s. Similarly PANI films were grown on an ITO surface using 0.5 ml of aniline in 10 ml of 0.2 M H_2SO_4 at +1.2 V for 60 s by the potentiostatic method.[16–17] Each ITO-polymer film electrode was washed with DI water 2–3 times dried and kept in a dessicator before and after use. Each polymer electrode was observed 10 times.[18]

2.4. Principal Component Analysis

Statistical Analysis software The Unscrambler TM (CAMO, Norway) was used for performing PCA. The PCA is a common pattern recognition algorithm used to analyze data obtained.[19–20] In particular, PCA is used to reduce the complexity of data by computing a new, much smaller set of uncorrelated variables which best represent the original data. This is done by projecting the high dimensional data set in a dimensional reduced space based on the uncorrelated and orthogonal eigenvectors of the covariance matrix computed from the instrument used. These eigenvectors were called principal components (PC) of the features and were arranged in sequence where the first principal component was the one with the greatest amount of variance, followed by the second greatest and so on. The plot of the original data in the new space defined by the first few principal components will give visual interpretation on how the original data are scattered. In particular, the plot will show features that have small variation appear together while the features with large variation appear distant. Therefore PCA is able to expose some

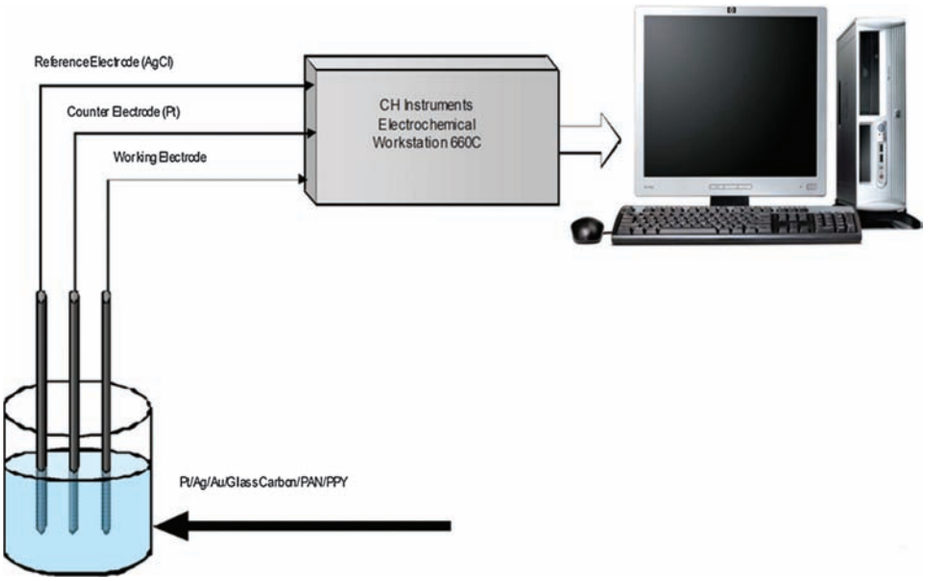

Fig. 1. Setup of electrochemical workstation.

clusters of the data naturally. The PCA is a straightforward analysis, which is validated through conducting several experiments, measurements and testing the data.

3. RESULTS AND DISCUSSION

Electrochemical impedance was measured by applying an AC potential to an electrochemical cell containing the sample solution and measuring the current through the cell using small excitation signals.

3.1. Impedance Study of Tea Liquor Samples

The response of four electrodes (Au, Pt, Ag and GC) and two conducting polymer electrodes (ITO-PANI, and ITO-PPY) for tea liquor sample with sucrose in the frequency range of 1 Hz–100 KHz with a potential of 0.1 V are given in Figures 2 and 3 respectively.

Figure 2 shows the nyquist plots for metal electrodes for tea liquor sample with sucrose. In these impedance plots, each electrode surface represents the response for tea liquor sample with sucrose. The impedance study was carried out with the open circuit potential (E_{ocp}). E_{ocp} of every sample was observed for 10 minutes over a frequency range of 1 Hz to 100 KHz. When the impedance is plotted in the complex plane, we obtained a semicircle combined with a straight line at an angle of 45° to the real axis, which may be due to Warburg impedance. The physical model explaining this phenomenon is Randle's equivalent electrical circuit Figure 2(b) and the behaviour can be attributed to diffusion phenomenon occurring at the solution–electrode interface.

The impedance data were simulated using the Randle's equivalent circuit consisting of a parallel combination of the capacitance (C) and charge transfer resistance by redox reactions (R_{ct}) in series with the supporting electrolyte resistance (R_s). The fitting of spectras to the equivalent circuit has indicated a good agreement between the circuit model and the real experimental data, especially at the high frequency values.

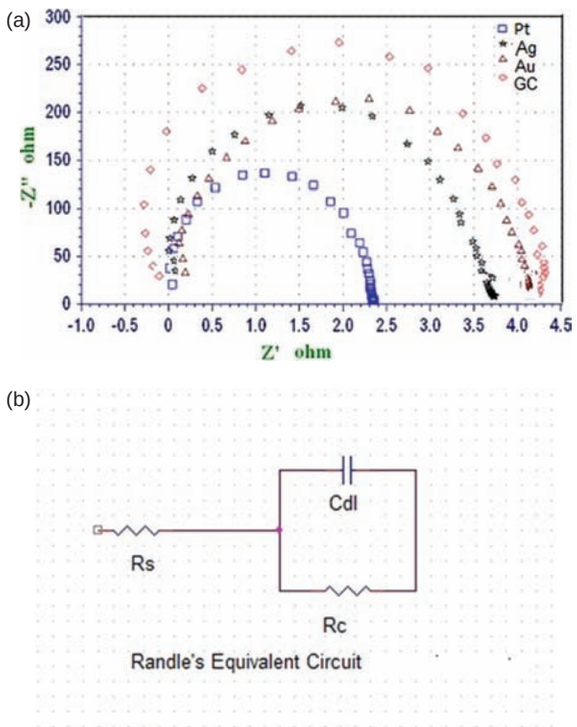

Fig. 2. (a) Nyquist plot for tea liquor with sucrose using four metal electrodes (Pt, Ag, Au, and GC). (b) Randle's equivalent circuit.

RESEARCH ARTICLE

Nyquist plots for PANI and PPY are shown by Figure 3 can be described as a partially resolved semi-circle near the origin at (low frequency) followed by partially resolved semi-circles (towards high frequency). These conducting polymers of PANI and PPY show variation in comparison to the metal electrodes of Pt, Ag, Au, and GC. The reason for the variation may be the porosity in the electrode surface or may be due to some variation of the surface structure of PANI by continuous dipping in tea liquor sample with sucrose. As shown these impedance plots appear more complex, and the two semi-circles depend on the nature of the electrode material. Circuit responsible for PANI and PPY graphs is an equivalent circuit due to adsorption shown in Figure 3(a).

In this equivalent circuit for adsorption, R_s is the bulk sample solution resistance, R_c is the charge-transfer resistance associated with the double layer, C_{dl} is the double-layer capacitance, R_{ad} is the resistance of the adsorption layer, C_p is the passivative capacitance associated with the adsorption layer. These responses may be attributed to the change of the morphology and the conductivity of the electrode/electrolyte interface.

The average impedance observations of six working electrodes for tea liquor with sucrose are given in Figure 4, these observations indicates that Au and GC electrodes are highly sensitive. The impedance of six tea samples: A, B, C, D, E and F are represented in Figure 5 using all the six working electrodes.

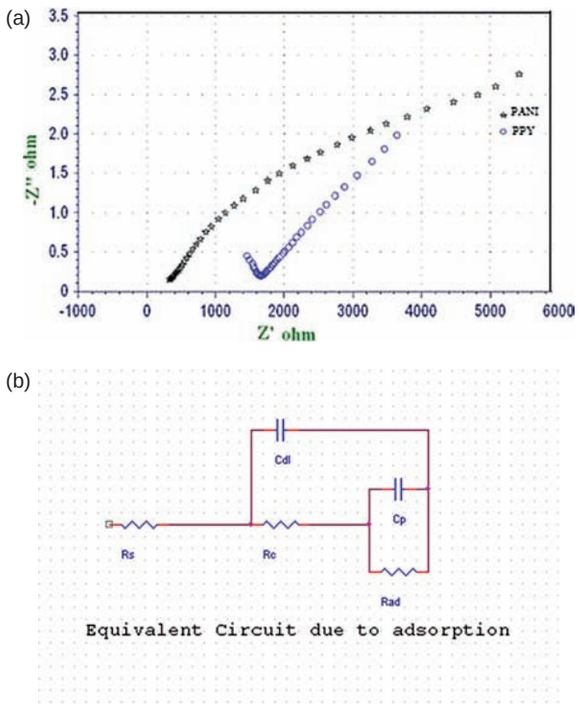

Fig. 3. (a) Nyquist plot for conducting polymer electrodes ITO-PANI and ITO-PPY for tea liquor with sucrose. (b) Equivalent circuit for PANI and PPY.

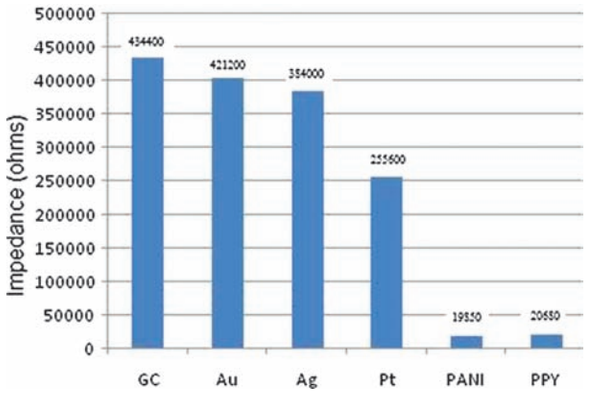

Fig. 4. An impedance of tea liquor sample with sucrose with impedance values for six different electrodes GC, Au, Ag, Pt, PANI, PPY (Left to Right).

In Figure 5 which represents the impedance of tea samples with six different added taste compounds. Sample A, shows the higher impedance values with all the three metal electrodes, GC electrode as well as with conducting polymer electrodes, indicating that this tea sample may contain more amounts of antioxidants/ions, hence shows a flattened circle on a complex plane plot. Sample B, represents almost similar values with no significant impedance changes in Au or Pt, whereas the impedance of the Ag and GC electrodes are of the order of 75% and 50% approximately to that of the Au and Pt electrodes. The B, C, D, E, and other black tea liquor samples A and F have lower impedance output for GC, Ag, Au, and Pt electrodes.

The impedance behaviour of Au electrode with sample D shows somewhat higher impedance values in comparison to other metal electrodes, while conducting polymer electrodes have low impedance output. Thus impedance data explains some relation between Au electrode and Sample D at higher impedance which may be due to dissolved minerals present that can be seen from the values of impedance. Impedance measurements of all the black tea liquor samples on the polymer electrodes show a charge-transfer resistance, polymer thin-film interference,

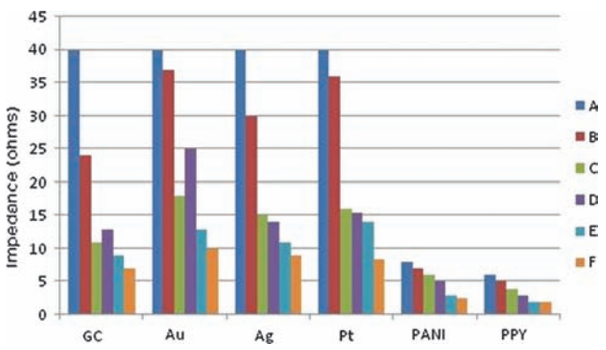

Fig. 5. An impedance of six tea liquor samples using all the six working electrodes: A, B, C, D, E and F.

RESEARCH ARTICLE

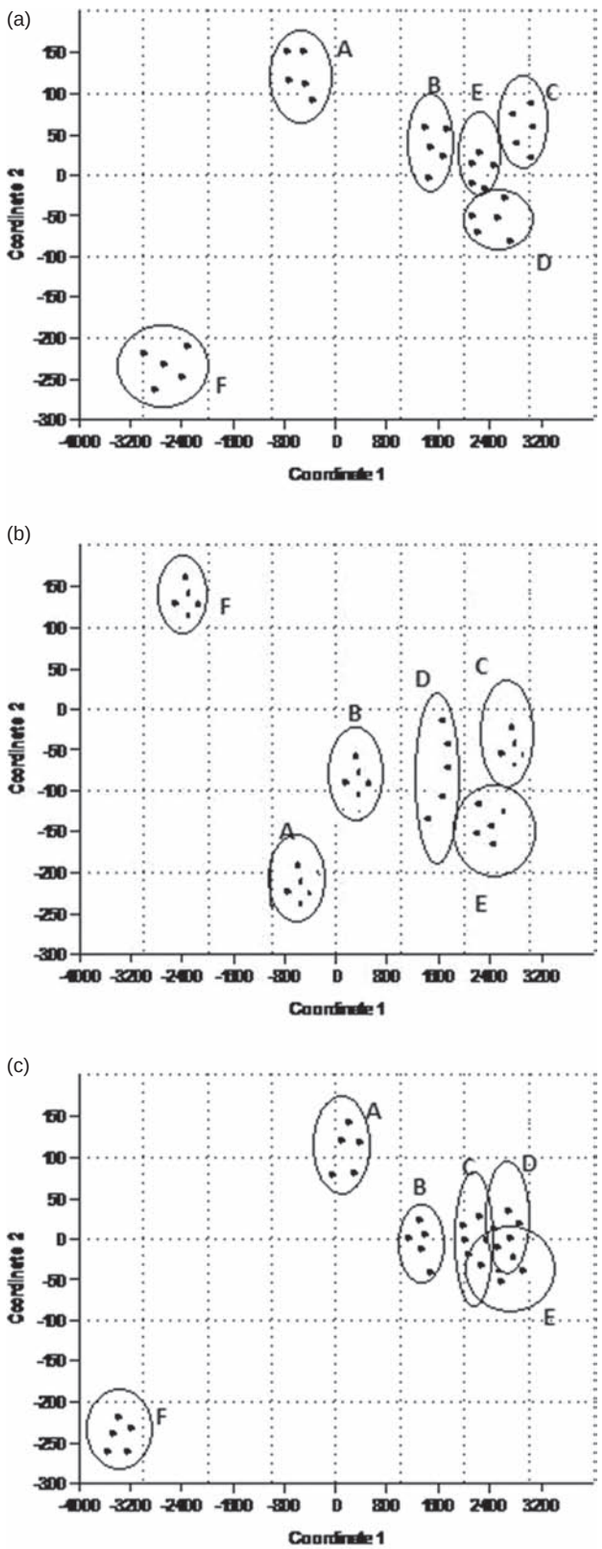

Fig. 6. (a) PCA plot of tea liquor samples with four electrodes (Pt, Au, Ag and GC). (b) PCA plot of milk samples with conducting polymer electrodes (ITO-PANI, ITO-PPY). (c) PCA plot of milk samples with the combination of metal and conducting polymer electrodes (Pt, Au, Ag, glassy carbon, ITO-PANI, ITO-PPY).

the ion-diffusion co-efficient into the polymer and the redox capacitance which is an important parameter of electrochemically conducting polymers.[21]

3.2. PCA Study of Tea Liquor Samples

The assessment of sensors has been carried out using impedance data with the combination of sensing electrodes for different types of tea liquor samples in PCA. In PCA results, first principal component provides most of the information and presents the highest variance.

Sensing system with three metal electrodes and GC well classifies the data in various groups as given in Figure 6(a). The group A which is at the top in the centre left classifies the tastants class as mild sweet, which represents tea liquor with cow milk. It is mild sweet in taste, due to lactose contents present in it. Another class which is present downward in the extreme left represents a class with a fruity taste without any sugar.

All the four classes B, C, D and E are strong and bitter spices lie close to each other, towards the right side of the plot. However tea liquor with sweetened clove is considered as most spicy among these classes, hence it is somewhat separated from the other three classes i.e., C, E and D. From this data it can be interpreted that all six complex liquors can be classified into four classes i.e., mild sweet, fruity, most bitter and bitter spicy.

In Figure 6(b) PCA classification results are due to two conducting polymer electrodes, has also well classified all the six tea liquor samples into four classes. However mild sweetened tea liquor lies at the bottom of the middle of the PCA plot, whereas tea liquor with vanilla lies at the extreme top of the left corner, well classifying the two classes. Out of all four bitter, spicy compounds B, C, D and E again class B which is most bitter spicy, is clearly separated from the other three C, D and E which lies close to each other.

Figure 6(c) represents the classification from the data of six electrodes together which classifies very clearly into four groups which are mild sweet, fruity, most bitter spicy and bitter spicy. Thus it is concluded that the sensing system with metal electrodes or conducting polymer electrodes alone can well classify these tastants into four classes.

4. CONCLUSION

The use of conducting polymer i.e., PANI and PPY electrodes in frequency range 1 Hz to 100 KHz was able to classify different types of tea liquors/samples. The impedance behaviour clearly distinguishes tea liquor samples without added sugar from other tea liquor samples with added sugars. Metal electrodes were also found to be helpful in classification of different types of tea liquors. More detailed studies in impedance mode are being carried

RESEARCH ARTICLE

out for the further quantification of beverages and tastants quality.

Acknowledgments: The authors are grateful to Mrimoy Misra, Shweta Arora of CSIO, Chandigarh for their support.

References and Notes

1. P. Roy, T. C. Tsai, C. T. Liang, R. J. Wua, and M. Chavali, *J. Chin. Chem. Soc.* 58, 3 **(2011)**.
2. Y. Kuroda and Y. Hara, *Mutat. Res.* 436, 69 **(1999)**.
3. W. Pongsuwan, T. Bamba, K. Harada, T. Yonetani, A. Kobayashi, and E. Fukusaki, *J. Agric. Food Chem.* 56, 10705 **(2008)**.
4. V. Armoskaite, K. Ramanauskiene, A. Maruska, A. Razukas, A. Dagilyte, A. Baranauskas, and V. Briedis, *Journal of Medicinal Plants Research* 5, 811 **(2011)**.
5. M. Dhiman, P. Kapur, A. Ganguli, and M. L. Singla, *International Journal of Soft Computing and Engineering* 2, 1 **(2012)**.
6. R. Rawat, A. Gulati, and R. Joshi, *Journal of Food Biochemistry* 35, 953 **(2011)**.
7. S. McDougalla, P. Murdough, W. Pankey, C. Delaney, J. Barlow, and D. Scruton, *Small Ruminant Res.* 40, 245 **(2001)**.
8. L. Yang and R. Bashir, *Biotech. Adv.* 26, 135 **(2008)**.
9. V. Parra, Á. A. Arrieta, J. A. Fernández-Escudero, H. García, C. Apetrei, M. L Rodríguez-Méndez, and J. A. De Saja, *Sens. Actuators B: Chemical* 115, 54 **(2006)**.
10. H. Xiao and J.Wang, *African Journal of Biotechnology* 8, 6985 **(2009)**.
11. W. He, X. Hu, L. Zhao, X. Liao, Y. Zhang, M. Zhang, and J. Wu, *Food Research International* 42, 1462 **(2009)**.
12. N. R. Pavon, Sensory characteristics of flavored milk candies (Thesis) **(2003)**.
13. C. Piton, A. Dasen, and I. Bardoux, *Lait* 68, 467 **(1988)**.
14. S. McDougalla, P. Murdough, W. Pankey, C. Delaney, J. Barlow, and D. Scruton, *Small Ruminant Res.* 40, 245 **(2001)**.
15. L. Yang and R. Bashir, *Biotech. Adv.* 26, 135 **(2008)**.
16. K. Meral, A. Levent, and S. Polymer, *International* 51, 1371 **(2002)**.
17. A. A. Arrieta, C. Apetrei, M. L. Rodríguez-Méndez, and J. A. de Saja, *Electrochim. Acta* 49, 4543 **(2004)**.
18. A. P. Bhondekar, M. Dhiman, A. Sharma, A. Bhakta, A. Ganguli, S. S. Bari, R. Vig, P. Kapur, and M. L. Singla, *Sen. Act. B. Chem.* 148, 601 **(2010)**.
19. K. Brudzewski and J. Ulaczyk, *Sens. Actuat. B-Chem.* 140, 43 **(2009)**.
20. S. Zhang, C. Xie, D. Zeng, Q. Zhang, H. Li, and Z. Bi, *Sens. Actuat. B-Chem.* 124, 437 **(2007)**.
21. P. Ferloni, M. Mastragostino, and L. Maneghello, *Electrochim. Acta* 41, 27 **(1996)**.

Received: 8 May 2012. Accepted: 4 June 2012

RESEARCH ARTICLE

Journal of
Nanoscience and Nanotechnology
Vol. 13, 1–6, 2013

Interpretation of Indian Orthodox Tea Using Multi-Sensing Impedometric Technique

Mopsy Dhiman[1, 3, *], Robin Joshi[2], Ashu Gulati[2], Pawan Kapur[1], Abhijit Ganguli[3], and Madan Lal Singla[1, *]

[1] *Central Scientific Instruments Organization, CSIR, Chandigarh 160020, India*
[2] *Institute of Himalyan Bioresource Technology, CSIR, Palampur 176061, India*
[3] *Thapar University, P.O. Box 32, Patiala 147004, India*

Twelve different orthodox Indian tea samples were collected from tea growing and processing sites of Kangra (Valley), India. The percentage of major chemical constituents responsible for the tea quality has been determined by HPLC and UV-vis spectrophotometer. Impedance response using Platinum (Pt), Gold (Au), Silver (Ag), Glassy Carbon (GC), Polyaniline (PANI) (emraldine salt) and Poly Pyrrole (PPY) working electrodes in tea infusions in the frequency range of 1 Hz to 100 kHz has been measured for 30 days on each tea sample. The impedance response of these working electrodes along with the determined chemical concentrations was subjected to Principal Component Analysis (PCA). It was possible to map the antioxidant levels in these tea samples with few exceptions from the score plot of PCA.

Keywords: Orthodox Teas, Antioxidant Activity, Impedance, Principal Component Analysis.

RESEARCH ARTICLE

1. INTRODUCTION

Tea (*Camellia sinensis*), originated in China, dates back several thousand years, which is rich in phenols. These are responsible for its refreshing astringent taste. These polyphenols known as Catechin (C), including epigallocatechin-3 gallate (EGCG), epigallocatechin (EGC) and epicatechins-3 gallate (ECG) make tea popular due to their biological activities.[1] Tea Catechins and other phenols have been reported to act as antioxidants *in vitro* by sequestering metal ions and by scavenging reactive oxygen and nitrogen species and affecting the activities of transcription factors and enzymes.[2] In the past several years, tea quality had been assessed using different analytical tools like, High-Performance Liquid Chromatography,[3] Gas Chromatography,[4] Capillary[5] and Plasma Atomic Emission Spectrometry.[6]

However, these methods are not able to quantify the quality of tea and results differ from sensory evaluation panel. Since tea is a complex mixture of large number of chemical compounds. Impedance technology (Voltametry, Potentiometry) is an application of multi-sensor system applied particularly to analyze liquid phase foodstuffs.[7] Different tasks such as discrimination, classification, quality control and process monitoring of beverages have been successfully performed using impedance techniques. The main method used in impedance technology is the application of the array of non-specific chemical sensors with wide sensitivity toward several components. Thus, the impedance technique output contains the overlapped information about the sample due to cross-sensitivity of sensors. Considerable results may be extracted from this overlapped information with the help of multivariate data analysis. In recent years, intensive studies have been reported out regarding the sensory activity of the individual components of food and alcoholic beverage tastes, and the dependence between the taste and the chemical composition.[8]

Further the advent of electronic tongue opened a new kind of analytical approach; it has potential applications in many different fields, such as assessment of various foodstuffs and beverages, environmental contamination monitoring and medical diagnostics etc.[9] Some chemically modified electrodes gained attention due to their wide potential use in analytical and technical applications. A substantial surface characterization technique Electrochemical Impedance Spectroscopy (EIS) is shown to be a valuable tool to investigate electrochemical reaction mechanisms, to explore the properties of porous electrodes and most importantly to investigate passive surfaces.[10] The aim of present studies is to evaluate the possibility of using a set of metal and conducting polymer working electrodes

*Authors to whom correspondence should be addressed.

in impedometric 1 Hz–100 KHz modes to classify orthodox Indian black tea in terms of chemical concentrations. Made tea samples have been taken in electrochemical cell and studies were carried out in impedance mode in frequency range of 1 Hz–100 KHz continuously using each sensing working electrode for twelve different grades of tea samples.

Impedance data was fed to Principal Component analysis. In a similar way the antioxidant level of various compounds such as Galic acid (GA), theaflavins (TFs) and thearubigins (TRs) was also determined by HPLC technique using UV-Vis as a detector. Electrochemical impedance spectroscopy was also used to characterize response of all the six working electrodes on tea samples. However this method was also able to characterize the response of six working electrodes individually. GC can be used due to its unique feature i.e., chemical resistance, compactness, mechanical stability and impermeability to fluid and gases. However, there is some deviation in the data from PANI and PPY electrodes as there seems to be some drift in the data with time.

2. MATERIALS AND METHODS

Methanol, acetone and acetonitrile were purchased from Merck (Bangalore, India). Folin's ciocalteus[11] reagent from SRL (Mumbai, India) and HCl from Rankem (Mohali, India) has been used. GA, CAF and C standards-EGC, EGCG, EC, ECG and TF were purchased from Sigma Aldrich (New Delhi, India). DPPH was purchased from Sigma Aldrich (New Delhi, India) and ethanol from E-Merck (Bangalore, India).

2.1. DPPH Free-Radical Scavenging Assay

The antioxidant activity was determined by using Turkmen, Sari and Velioglu method with slight modification. 50 μL of tea extract was mixed with an aliquot of 1950 μL of DPPH radical in ethanol (100 μM). Ethanol was used as a control. The reaction mixture was vortex-mixed. Reaction tubes were wrapped in aluminum foil and let to stand at 25 °C in the dark for 30 min. All measurements were done under dim light. Spectrophotometric measurements were done at 517 nm using Shimadzu UV-2450 UV-Vis Spectrophotometer. Antioxidant activity (AA) was expressed as percentage inhibition of the DPPH radical and was determined by the following equation:

$$AA(\%) = \frac{Abs_{control} - Abs_{sample}}{Abs_{control}} \times 100$$

Where

AA = Antioxidant activity
$Abs_{control}$ = Absorbance Control
Abs_{sample} = Absorbance Sample

2.2. High Performance Liquid Chromatography (HPLC) Analysis of Tea Catechins

Twelve tea samples were analyzed for Catechins according to the method described by Sharma et al.[12] on Water's HPLC using a C-18 reverse phase 250 × 4.0 mm, 5 μm columns, fitted with a C-18 guard column (shown in Table I). Infusion was centrifuged at 4000 rpm at 4 °C for 10 min. Supernatant was collected and passed through Millipore filter (0.45 μm) prior to inject in HPLC. The mobile phase finally adopted was acetonitrile/0.1% Ortho-phosphoric acid in water (w/v) with a flow rate of 1 mL/min. Standard solution containing Catechins was dissolved in methanol for making a concentration of mg/mL.

2.3. Catechins Were Estimated Following the Method of Singh et al.

40 μl of sample was dispensed into triplicate sets of 25 mL volumetric flasks.[13] 1 mL of diazotized sulfanilamide reagent (in acetone) followed by 1 mL HCl (30%). The mixture incubated for 1 h at ambient temperature, and absorbance taken against reference blank at 425 nm after making the volume to 25 mL with distilled water on a spectrophotometer.

2.4. Instrument Used

Electrochemical Workstation 660C has been used to study the impedance behavior of tea infusions with an inbuilt

Table I. Mean % chemical concentrations in tea samples as measured by HPLC and UV-Vis.

Samples	Inhibition	EGC	C	EC	EGCG	ECG	TF	TR	Caffeine
1	88.300	0.050	0.110	0.060	1.390	0.390	0.860	6.304	0.830
2	87.100	0.040	0.100	0.050	1.140	0.310	0.894	6.529	0.640
3	88.200	0.050	0.090	0.059	1.500	0.470	0.924	6.929	0.800
4	89.700	0.058	0.090	0.050	1.340	0.390	0.836	6.727	0.520
5	89.400	0.060	0.100	0.060	1.920	0.560	0.936	7.289	0.830
6	88.000	0.050	0.100	0.060	1.810	0.460	0.902	7.732	0.940
7	89.700	0.130	0.090	0.060	0.880	0.320	0.884	6.234	0.550
8	88.500	0.020	0.100	0.042	0.740	0.260	0.892	6.436	0.410
9	88.300	0.030	0.090	0.040	0.560	0.125	0.845	6.104	0.370
10	89.400	0.100	0.098	0.060	0.960	0.210	0.912	7.123	0.500
11	86.800	0.120	0.100	0.060	1.240	0.430	0.902	7.203	0.650
12	88.600	0.070	0.100	0.050	0.850	0.250	0.882	6.543	0.430

RESEARCH ARTICLE

frequency response analysis module. All impedance measurements were carried out in a three electrode arrangement. Impedance spectra were recorded over a frequency range of 1 Hz–100 KHz (10 points per decade) at room temperature.

2.5. Electrodes and Instrumentation for AC Impedance Measurements and Preparation of Tea Infusion

An electrochemical system and cell comprising of working electrode, reference electrode (Ag/AgCl (4M KCl)) and (Pt wire) counter electrode supplied by CH Instruments (Texas, USA) has been used throughout the study. Working electrode made from Pt, Au, Ag and GC were used as such supplied by CH Instruments (Texas, USA). The PANI and PPY electrodes were fabricated using aniline (C_6H_7N) and pyrrole (C_4H_5N) supplied by M/s. Spectro Chem. Pvt. Ltd. (Mumbai, India). PANI and PPY polymer films were deposited on Indium Tin Oxide (ITO) surface by electropolymerization from their respective monomers.[14]

All the four metal electrodes (Pt, Au, glassy Carbon, and Ag) were polished to get smooth surface with alumina powder (Al_2O_3, CH Instruments, Inc., USA) of particle sizes of 1, 0.3, and 0.05 μm and washed before use. PANI and PPY films were deposited on ITO surface (0.8 cm^2) by electropolymerization of the respective monomers in a glass cell having three electrodes ITO coated glass as working electrode, platinum wire as counter electrode and saturated calomel electrode (SCE) as reference electrode. Deionized (DI) water of TKA (Niederelbert, Stockland) was used to prepare tea infusions. 12 grades of Kangra Orthodox Indian black tea (*Camellia sinensis* (Kuntze), harvested during the three flushing seasons (Early, Rains and Backend) were picked from Institute of Himalayan Bioresource Technology, Palampur (A constituent laboratory of CSIR, India).

2.6. Preparation of Tea Infusion

0.4 gm of tea sample was added to 25 mL of boiling water in a flask and boiling was continued for 10 minutes in a water bath and maintained for 10 minutes for each sample. The reaction mixture was cooled to room temperature and the residue was filtered using Whatmann 42 (Bhondekar et al. 2010). The filtrate was treated as a tea infusion. Equal volume of each tea infusion was later used for further studies. Fresh samples of tea infusion were prepared for 12 samples continuously for 30 days. Five observations per day were recorded for each sample continuously for 30 days. The analysis was carried out after generating the mean data. Observation was carried out to check the reproducibility/deviation. All the antioxidants has been named as A (% inhibition), B (EGC), C (C), D (EC), E (EGCG), F (ECG), G (TF), H (TR) and I (CAF). Impedance data for twelve tea samples has been treated as GC sensing electrode: 1–12, Au sensing electrode: 13–24, Pt sensing electrode: 25–36, PPY sensing electrode: 37–48, PANI sensing electrode: 49–60 and Ag sensing electrode: 61–72.

2.7. Principal Component Analysis (PCA)

The PCA is a common pattern recognition algorithm used to analyze data obtained.[15, 16] In particular, PCA is used to reduce the complexity of data by computing a new, much smaller set of uncorrelated variables which best represent the original data. This is done by projecting the high dimensional data set in a dimensional reduced space based on the uncorrelated and orthogonal eigenvectors of the covariance matrix computed from the instrument used. These eigenvectors were called principal components (PC) of the features and were arranged in sequence where the first principal component was the one with the greatest amount of variance, followed by the second greatest and so on. The plot of the original data in the new space defined by the first few principal components will give visual interpretation on how the original data are scattered. In particular, the plot will show features that have small variation appear together while the features with large variation appear distant. Therefore PCA is able to expose some clusters of the data naturally. The PCA is a straight forward analysis, which is validated through conducting several experiments, measurements and testing the data.

3. RESULTS AND DISCUSSION

3.1. Impedance Response

Impedance behavior of GC, Au and Pt electrodes are shown in Figures 1(a)–(c) respectively on the tea infusions representing Nyquist plots. The electrical response of these sensing electrodes yield plots for real and imaginary components of impedance in 1 Hz–100 KHz frequency range. These plots shows almost similar behavior as impedance circuit is plotted in the complex plane. A small semi-circle combined with a straight line at an angle of 45° to the real axis which may be due to Warburg impedance represents Randle's equivalent circuit.[17] The electrical circuit responsible for behavior of these electrodes is single time constant as given in Figure 2 where Cdl is the double-layer capacitance, R_s is the bulk sample solution resistance, R_c is the charge-transfer resistance associated with the double layer.

Nyquist plots for PPY are shown by Figure 1(d) can be described as a partially resolved semi-circle near the origin at (high frequency) followed by half resolved semi-circles towards (low frequency).[18, 19] The semi-circle for this electrode is not complete in the selected frequency range. Since, it appears that the response can be extended in the higher frequency region also. This result can be modeled by two RC-parallel circuits, in series. Each parallel combination of resistance R and capacitance C results

RESEARCH ARTICLE

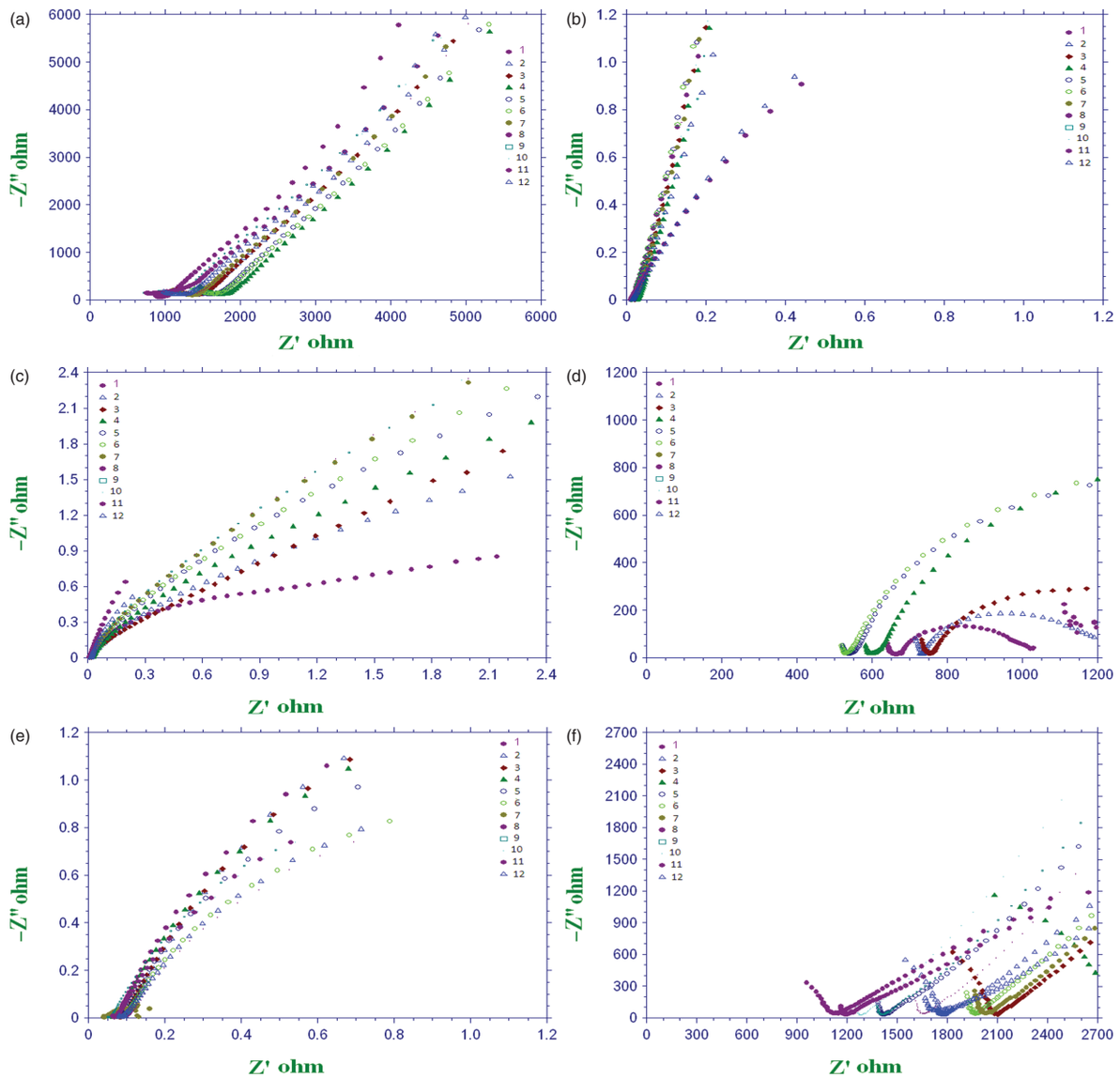

Fig. 1. (a): Impedance plot of GC electrode, (b): Impedance plot for Au electrode, (c): Impedance plot for Pt electrode, (d): Impedance plot for PPY, (e): Impedance plot for PANI electrode, (f): Impedance plot for Ag electrode.

in a semi-circle in the impedance plot. Distorted nature of the semicircle attributes to the variation of the morphology of the PPY electrode resulting in change in conduction mechanism at the interface.

Figure 1(e) shows the Nyquist plot for PANI electrode which have two partially resolved distorted semi-circles in the extending mid frequency region to the lower frequency region. It has been observed that the Nyquist plots on different tea samples shows variations from sample to sample in comparison to the metal electrodes i.e., GC, Au, PPT and PPY electrodes. The reason for the variation may be the porosity in the electrode surface or may be due to some variation of the surface structure of PANI by continuous dipping in various tea samples, which has acidic characteristics.[20, 21] As shown these impedance plots appear more complex, and the two semi-circles depend on the nature of the electrode material. Equivalent circuit responsible for PANI and PPY graphs is due to adsorption as shown in Figure 3. In this equivalent circuit for adsorption, R_s is the bulk sample solution resistance, R_c is the charge-transfer resistance associated with the double layer, Cdl is the double-layer capacitance, Rad is the resistance of the adsorption layer, C_p is the passivative capacitance associated with the adsorption layer. These responses may be attributed to the change of the morphology and the conductivity of the electrode/electrolyte interface.[22]

Figure 1(f) represents Nyquist plot of Ag electrode. The electrode/electrolyte interface for Ag electrode may have quite different properties with respect to those of the metal electrodes.[23] One remarkable difference is that the negative

RESEARCH ARTICLE

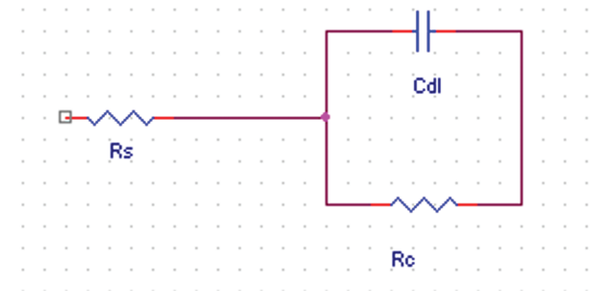

Fig. 2. Randle's equivalent circuit.

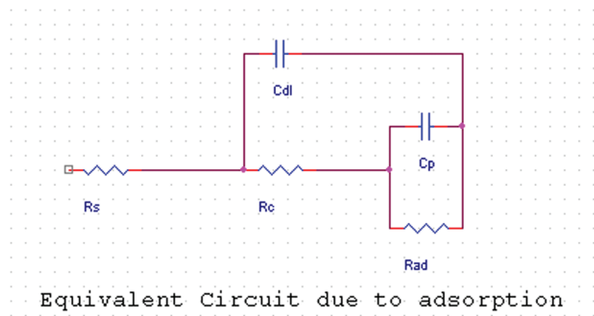

Fig. 3. Equivalent circuit for PPY and PANI electrode.

(*RC*) circuit in the low frequency region could not be detected with accuracy, due to the noise in the low frequency region of the spectrum and the distortions due to non linear behavior.[24] Also for the silver electrode the diffusion type sub circuit presents the most pounced contribution to the electrode impedance. Two partially resolved semicircles can be seen here, which is due to double layer effect which may be due to oxide formation on the surface of Ag electrode. This behavior of silver electrode can be complimented to the presence of well separated two time constants due to Randle's equivalent circuit Figure 4 in the Bauerle's equivalent electrical circuit. Such type of parallel *RC* combination can rise from specific adsorption occurring at electrode surface, possibly associated with delayed reaction processes.

3.2. PCA Study

For PCA study Unscrambler9.7 has been used. The impedance response of the six electrodes has been

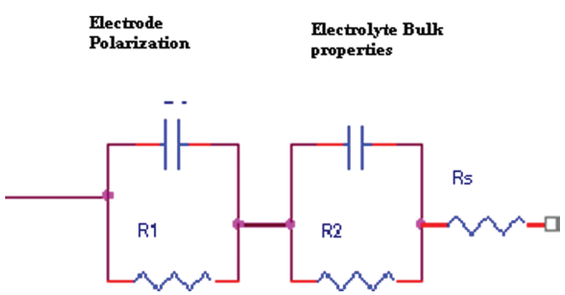

Fig. 4. Equivalent circuit for Ag electrode.

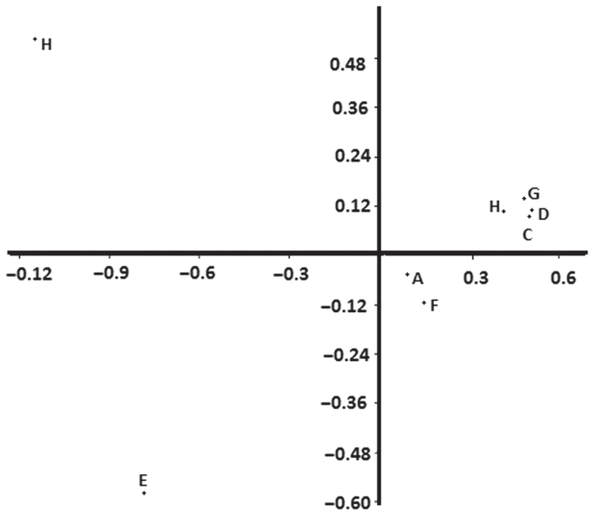

Fig. 5. PCA plot for chemical concentrations.

measured in a range of 1 Hz to 100 kHz having 60 steps for each electrode, the total number of impedance variables amounts to 360 (6×60). More than 99% significant information is available with the first two principal components (PC1 and PC2). The score plot shown in Figure 5 was obtained for nine tea antioxidants. Besides, a good discrimination between the classes was observed and the different types of antioxidants were located in different quadrants on the score plot. It can be seen that there is an overlapping of the D and C i.e., EC and C respectively, which may be due to structural similarity of these compounds. C and EC have almost same geometry hence they are laying at the same place. % inhibition and ECG are positively correlated to each other, hence lying in same quadrant near to each other. However, EGCG is negatively correlated to TFs, EGC, C and EC, thus finds a place in 3rd quadrant. TRs are found to be negatively correlated to % inhibition and ECG thus clearly visible in 2nd quadrant. From these results, it may be possible to club the antioxidant levels in various tea samples, in terms of 4 broad Categories.

In Figure 6 the score plot of PC1 versus PC2 for the tea samples is plotted using impedance and chemical concentration variables. The data is plotted in a two dimensional plane formed by the first two PCs, with PC1 showing 73.09% and PC2 showing 26.69% data variance in Figure 6. In the 1st quadrant both PC1 and PC2 are positive coordinates-TFs, EC and C are laying close to each other. The reason for the same may be geometric resemblance or they may have similar chemical behavior. 3rd and 5th tea sample using GC electrode show positive correlation with TFs, EC and C or may have maximum amount of TFs, EC and C when measurements were made using GC electrode. The 6th, 9th, 10th, 11th tea sample using gold electrode are positively correlated to each other it means these tea samples shows almost similar response with gold electrode. 9th tea sample using GC electrode and

RESEARCH ARTICLE

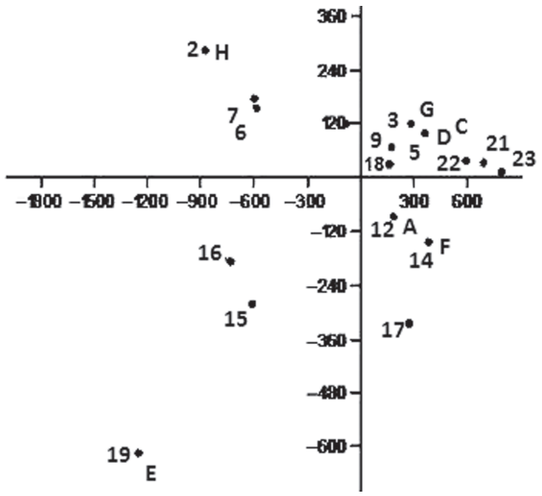

Fig. 6. PCA plot for tea samples and chemical concentrations.

6th tea sample using Au electrode shows resemblance with each other which indicates, that these tea samples have sufficient level of either of TFs or EC or C compounds.

In 2nd quadrant with PC2 positive coordinate and PC1 negative coordinate, the 2nd tea sample using GC electrode lies close to point TR, whereas 6th and 7th tea samples with GC electrode lies close to TR in the same quadrant indicating its presence. TR is negatively correlated to % inhibition and ECG. In the 3rd quadrant both PC1 and PC2 are negative coordinates. EGCG is negatively correlated to TF, EC and C. It appears that the sufficient amount of EGCG is present in 7th tea sample using Au electrode. PC1 is positive and PC2 is negative in the 4th quadrant, % inhibition and ECG lies close to 12th tea sample analyzed by GC electrode, 2nd tea sample and 5th tea samples using Au electrode indicates the higher concentration of % inhibition and ECG.

Since ECG and % Inhibition (symmetric resemblance) fall close to each other in 4th quadrant and show close relation with each other. 12th tea sample using GC electrode and 2nd tea sample using Au electrode shows positive correlation with ECG and % Inhibition. Indicating maximum amount of ECG and % Inhibition is present in 2nd and 12th tea samples, using Au and GC electrode respectively.

The behavior of other four electrodes is not much related for interpretation in this PCA, indicating that GC electrode and Au electrode individually or together may work as better sensing system for quantification of various tea and beverages, for which further studies are being carried out.

4. CONCLUSION

The purpose of this study was to ascertain whether impedance technology can discriminate in terms of antioxidant level of different tea samples from the leaves plucked on same site under different environments (12 different orthodox tea samples were considered). The electrochemical interpretation in terms of impedometric analysis using multi electrode system, have shown that the tea samples can be well differentiated through PCA tool. The study shows that the single GC electrode/single Au electrode can be used to classify the tea quality, when scanned in broad frequency range. Thus multi/single-electrode system in variable frequency domain may become a tool to classify tea quality in terms of antioxidant levels.

Acknowledgment: The authors are grateful to Poonam, Dr. Gursharan, and Sukhwinder Singh for their interest in this study.

References and Notes

1. A. Von Gadow, E. Joubert, and C. F. Hansmann, *Food Chem.* 60, 73 (**1997**).
2. C. A. Rice-Evans, N. J. Miller, and G. Paganga, *Free Rad. Bio. Med.* 20, 933 (**1996**).
3. P. Valera, F. Pablos, and A. Gustavo González, *Talant* 43, 415 (**1996**).
4. N. Togari, A. Kobayashi, and T. Aishima, *Food Res. Inter.* 28, 495 (**1995**).
5. H. Horie, T. Mukai, and K. Kohata, *J. Chrom. A.* 758, 332 (**1997**).
6. Q. Chen, J. Zhao, and H. Lin, *Spectr. Act. A: Mol. Biom. Spect.* 72, 845 (**2009**).
7. Q. Chen, J. Zhao, and S. Vittayapadung, *Food Res. Inter.* 41, 500 (**2008**).
8. B. Plutowska and W. Wardencki, *Food Chem.* 107, 449 (**2008**).
9. H. Yanxia, J. R. Nicole, M. Claude, T. Chaker, and Z. Aidong, *J. Adv. Sc*. 17, 49 (**2005**).
10. D. D. Macdonald, *Electrochimica Acta* 51, 1376 (**2006**).
11. N. Turkmen, F. Sari, and Y. S. Velioglu, *Food Chem.* 99, 835 (**2006**).
12. V. Sharma, A. Gulati, S. D. Ravindranath, and V. Kumar, *J. food composition and analysis.* 18, 583 (**2005**).
13. H. P. Singh, S. D. Ravindranath, and C. Singh, *J. Agric. Food Chem.* 47, 1041 (**1999**).
14. A. P. Bhondekar, M. Dhiman, A. Sharma, A. Bhakta, A. Ganguli, S. S. Bari, R. Vig, P. Kapur, and M. L. Singla, *Sen. Act. B: Chem.* 148, 601 (**2010**).
15. K. Brudzewski and J. Ulaczyk, *Sens. Actuat. B-Chem.* 140, 43 (**2009**).
16. S. Zhang, C. Xie, D. Zeng, Q. Zhang, H. Li, and Z. Bi, *Sens. Actuat. B: Chem.* 124, 437 (**2007**).
17. J. Macdonald, *Annals of Biomedical Engineering* 20, 289 (**1992**).
18. K. Ariga, H. Ito, J. P. Hill, and H. Tsukube T, *Chem. Soc. Rev.* 41, 5800 (**2012**).
19. Y. Z. Long, M. Yu, B. Sun, C. Z. Gu, and Z. Fan, *Chem. Soc. Rev.* 41, 4560 (**2012**).
20. K. Saha, S. S. Awasthi, C. Kim, X. Li, and V. M. Rotello, *Chem. Rev.* 112, 2739 (**2012**).
21. K. Ariga, S. Ishihara, H. Abe, M. Li, and J. P. Hill, *J. Mater. Chem.* 22, 2369 (**2012**).
22. M. Dhiman, P. Kapoor, A. Ganguli, and M. L. Singla, *J. Nanosci. Nanotechnol.* 12, 7081 (**2012**).
23. H. Jans and Q. Huo, *Chem. Soc. Rev.* 41, 2849 (**2012**).
24. G. Singh, A. Bhalla, N. Caplash, and P. Sharma, *Indian Journal of Science and Technology* 3, 48 (**2010**).

Received: 7 March 2013. Accepted: 3 April 2013.

RESEARCH ARTICLE

Sensors and Actuators B xxx (2010) xxx–xxx

Contents lists available at ScienceDirect

Sensors and Actuators B: Chemical

journal homepage: www.elsevier.com/locate/snb

A novel iTongue for Indian black tea discrimination

Amol P. Bhondekar[a,*], Mopsy Dhiman[a], Anupma Sharma[a], Arindam Bhakta[a], Abhijit Ganguli[b], S.S. Bari[c], Renu Vig[c], Pawan Kapur[a], Madan L. Singla[a]

[a] Central Scientific Instruments Organisation (CSIO), CSIR, Sector-30C, Chandigarh 160030, India
[b] Thapar University, Patiala 147004, Punjab, India
[c] Panjab University, Chandigarh 160014, India

ARTICLE INFO

Article history:
Received 29 March 2010
Received in revised form 15 May 2010
Accepted 20 May 2010
Available online xxx

Keywords:
Electrochemical impedance spectroscopy
Black tea
Classification
HPLC
UV–vis
Principal component analysis

ABSTRACT

A novel impedance-Tongue (iTongue) based on multi-electrode Electrochemical Impedance Spectroscopy is proposed for discrimination of Indian black tea. Impedance response of platinum, gold, silver, glassy carbon, polyaniline and polypyrrole working electrodes in tea infusions for a sinusoidal excitation in the frequency range of 1 Hz to 100 kHz has been measured. Also, the percentage of major chemical constituents responsible for the tea quality has been determined by HPLC and UV–vis spectrophotometer. Frequency specific impedance response of these working electrodes along with the determined chemical concentrations was subjected to Principal Component Analysis to confirm the discriminability of the proposed iTongue. The correlations between the frequency specific impedance response of working electrodes and the chemical concentrations which depend on sample variability, such as harvest interval, manufacturing process and brand type have been established. These correlations were further used for dimensionality reduction and discriminability enhancement. The results show that the frequency specific responses of working electrodes play a key role in discrimination of Indian black tea which can be enhanced by combination of working electrodes and their frequency specific responses.

1. Introduction

Tea is one of the widely consumed beverage in the world and India being the second largest producer, has its tremendous agro-commercial importance. Teas are majorly classified as black tea (fermented), green tea (unfermented), oolong tea (semi-fermented) apart from local variations in manufacturing processes. Orthodox and Cut–Tear–Curl (CTC) are the principal categories of black tea, their manufacturing techniques differ considerably and have a pronounced impact on the formative and degradative patterns of various cellular components [1]. Consumer acceptability of tea depends upon its flavour and taste, on the other hand flavour and taste depends upon spatiotemporal variability of the crop and manufacturing processes, which in turn highly influence its chemical composition, and are very critical in determining its quality [2,3]. Traditionally tea quality is assessed by tea tasters who have their own jargons to describe various quality attributes of a tea infusion. These jargons are sometimes not only difficult to comprehend by consumers but also highly subjective. It is therefore important to develop precise chemical or physical methods for the objective estimation of tea quality.

Many attempts have been made by various researchers to correlate tea quality with its chemical composition. Black tea quality is influenced by the concentration of theaflavins (TF) and thearubigins (TR) [4,5]. A very close relationship was found between TF content and broker's valuation of black tea [5–7]. Flavanol composition and caffeine content were also used as quality potential indicators of black tea [8]. Contents of amino acids and catechins were found to be correlated to tea quality assessed by professional tea tasters [9–11]. Theanine being the main amino acid component in tea, constitutes only 1–2% of the dry weight [12], whereas polyphenols account upto 30% of the dry weight [13].

A number of efforts have been made to classify different beverages including tea using gas sensor array (E-Nose) [14–16] and electrochemical techniques such as Cyclic Voltametry, Potentiometry and Conductivity [17,18]. Capillary electrophoresis and lipid membrane taste sensor have also been applied to tea quality estimation [19,20].

A novel impedance-Tongue (iTongue) employing non-specific multi-electrode Electrochemical Impedance Spectroscopy for classification of Indian black tea in terms of manufacturing process (CTC/Orthodox), harvest/brand variations and chemical concentrations is proposed. Three types of working electrodes, i.e. metal (Pt, Au and Ag), glassy carbon (GC) and conducting polymer [polyaniline (PANI), polypyrrole (PPY)] were used. Impedance response of these electrodes in tea infusions for a frequency range of 1 Hz to 100 kHz was measured using a standard electrochemical worksta-

* Corresponding author. Tel.: +91 172 2657811x489; fax: +91 172 2657820.
E-mail addresses: amol.bhondekar@gmail.com, amolbhondekar@csio.res.in (A.P. Bhondekar).

0925-4005/$ – see front matter © 2010 Elsevier B.V. All rights reserved.
doi:10.1016/j.snb.2010.05.053

tion. The impedance response of the electrodes at 1, 100 Hz, 1, 10 and 100 kHz along with the chemical concentrations of caffeine (CAF), catechins, gallic acid (GA), 3,5-dihydroxybenzoic acid (DBA), TF and TR, determined by HPLC/UV–vis, were used for Principal Component Analysis (PCA). Further, dimensionality reduction and discrimination has been done by analyzing the frequency specific impedance response of the electrodes.

The iTongue with six working electrodes based on Electrochemical Impedance Spectroscopy displayed good discrimination ability in Indian black teas. The results showed that the electrochemical interactions of working electrodes are frequency dependent and the frequency segments on the working electrode played a key role for the discrimination of the samples. Moreover, better discrimination ability can be achieved by the combination of working electrodes and specific frequency segments, and in comparison with potentiometry especially with voltammetry, the impedance measurements are advantageous because of the potential experimental simplicity and the reduction of the response times [21].

2. Experimental details

2.1. Material used

Pt, Au, Ag, GC working electrodes and Ag/AgCl (4 M KCl) reference electrode were supplied by CH Instruments (Austin, USA) whereas PANI and PPY working electrodes were fabricated in-house. The PANI and PPY electrodes were fabricated using aniline (C_6H_7N) and pyrrole (C_4H_5N) supplied by M/s. Spectro Chem Pvt. Ltd., India. All standards, viz. CAF, GA, DBA, (−)-epigallocatechin gallate (EGCG), (−)-epicatechin gallate (ECG), (−)-epigallocatechin (EGC), (−)-epicatechin (EC) and (+)-catechin (C) were purchased from Sigma Chemicals Co., St. Louis, MO, USA. HPLC grade acetonitrile (ACN) and water were used. De-ionized (DI) water was used otherwise. All other chemicals used were of analytical grade.

Three different batch samples each of two brands of Assam CTC tea (*Camellia sinensis* var. *assamica*) were procured from local market. Similarly, three samples each of Kangra Orthodox black tea (*C. sinensis* (L.) O. Kuntze), harvested during the three flushing seasons (Early, Rains and Backend) were sourced from Institute of Himalayan Bio-Resource Technology, Palampur (A constituent laboratory of CSIR, India).

2.2. Equipments used

CH Instruments, Electrochemical Workstation 660C was used to study the impedance behaviour of tea infusions. A Waters HPLC system equipped with a dual pump system, Spherisorb 5 μm ODS2 (4.6 mm × 250 mm) column, thermostatic controlled column chamber, rheodyne injection valve with a 20 μl sample loop and photo diode array detector was employed for the study. A PerkinElmer Lambda 35 UV–vis spectrometer was used for absorbance study. Statistical Analysis software The Unscrambler™ (CAMO, Norway) was used for performing PCA.

2.3. Impedance measurements

2.3.1. Sample preparation

0.4 gm of tea sample was added to 25 ml of boiling water in a flask and boiling was continued for 10 min in a water bath. Then the tea infusion was cooled down to room temperature and filtered on a Whatman Filter No. 42. The infusions were prepared in triplicates.

2.3.2. Electro-polymerization of conducting polymers on ITO coated glass surface

An ITO coated glass of dimensions 2.5 cm × 1 cm × 0.1 cm was used to deposit conducting polymer film on 0.8 cm^2 area. The conducting polymer films were deposited by electro-polymerization from their respective monomers in a glass cell with standard three electrode setup [ITO coated glass as working electrode, Pt wire as counter electrode and saturated calomel electrode (SCE) as reference electrode] at room temperature [22,23]. PPY film was grown potentiostatically applying +1 V potential for 1 min in 10 ml aqueous solution of $K_4[Fe(CN)_6]$ (0.422 g) and 129 μl of pyrrole monomer. Similarly, PANI film was grown potentiostatically applying +1.2 V potential for 2 min in 10 ml aqueous solution of H_2SO_4 (1 M) and 450 μl of aniline monomer. Each film was washed 2–3 times with DI water. After drying these electrodes were stored in vacuum desiccators before and after their use.

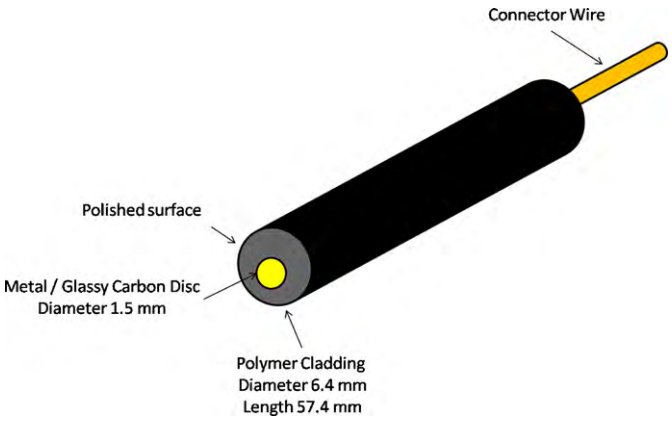

Fig. 1. Geometry of metal/glassy carbon electrodes.

2.3.3. Experimental setup

Fig. 1 shows the geometry of the Pt, Au, Ag and GC electrodes. Fig. 2 shows the geometry of the PANI and PPY electrodes deposited on ITO coated glass. Fig. 3 shows the experimental setup. All impedance measurements were carried out at room temperature. Pt, Au, Ag and GC working electrodes were polished with alumina powder of particle size of 1.0, 0.3, and 0.05 μm stepwise to get smooth surface. Each electrode was washed well with DI water. The working electrodes for measurements were selected manually using a wire jumper arrangement. The data was recorded and displayed by the software provided with the electrochemical workstation which communicates with a personal computer using a RS232 link. Pt, Au, Ag, GC, PANI and PPY were used as working electrodes. Pt wire and Ag/AgCl (4 M KCl) were used as counter and reference electrodes, respectively. Five readings per sample were taken and their mean was used for further analysis.

2.4. HPLC study

2.4.1. Sample preparation

Tea samples of 0.2 g were grounded and extracted once with 4 ml of 80% ACN solution and stirred for 10 min on a magnetic stirrer at 500 rpm followed by centrifugation for 2 min at 1400 rpm. The process was then repeated twice by adding 3 ml of 80% ACN to

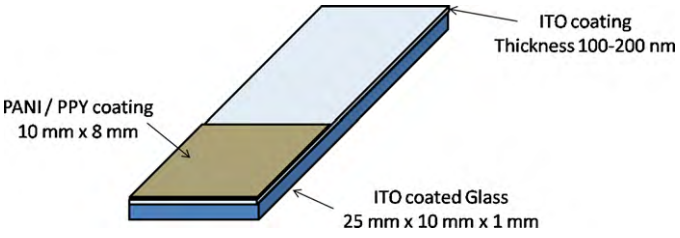

Fig. 2. Geometry of PANI/PPY electrodes.

Please cite this article in press as: A.P. Bhondekar, et al., A novel iTongue for Indian black tea discrimination, Sens. Actuators B: Chem. (2010), doi:10.1016/j.snb.2010.05.053

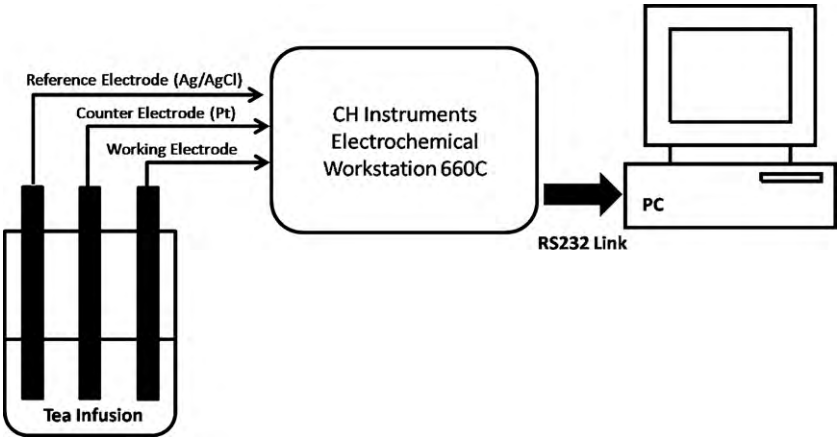

Fig. 3. Experimental setup for impedance measurement.

the residues. The extracts so obtained were combined and filtered through 0.45 μm filter. The samples were prepared in triplicates. Each sample was then analyzed with the Waters HPLC system having column temperature 30 °C.

2.4.2. Experimental setup

A simple and fast HPLC method [24] using a photodiode array detector (PDA) for simultaneous determination of catechins, CAF, GA, and DBA was used with mobile phase combination comprising of 3% acetic acid solution & ACN. All the solvents were filtered through 0.22 μm Millipore filter and degassed prior to their use in HPLC. Calibration curves were obtained at a detection wavelength of 280 nm for the catechins, CAF, GA and DBA using a series of standard solutions (prepared in 80% ACN). The mean of percentage concentrations of these compounds are listed in Table 1. However, the concentrations of EGC and EC were found to be below the detection threshold in the samples and hence not listed in Table 1.

2.4.3. UV–vis study

A rapid procedure for estimating TF and TR of black tea was adopted [25].

3. Results and discussions

3.1. Impedance response

The impedance response of working electrodes can be analyzed by an electrical equivalent circuit describing the electrical behaviour of the electrode–electrolyte interface [26–28]. Generally, an electrode–electrolyte interface is presented by a parallel combination of capacitance and resistance, taking into account the electrolyte impedance. The low frequency region in such studies are dominated by double layer effect, for the region between 10^2 and 10^5 Hz the dominant effect comes from the surface coating, whereas for frequencies higher than 10^5 Hz the impedance behaviour of the system is dominated by the geometric capacitance [27,29].

Fig. 4 presents the normalized Nyquist plots (real vs. imaginary impedance) of working electrodes. Fig. 4(a) shows impedance response of GC electrode for all the tea infusions. The responses of CTC as well as Orthodox tea at low frequencies reveal a linear impedance locus with an angle of 45° to the real axis which amounts to low frequency Warburg response. However, at high frequencies the Orthodox tea responses converge with null imaginary impedance, whereas the CTC responses show a small semicircle.

The physical model appropriate for this case is the simple Randle's equivalent electrical circuit [Fig. 5(a)] and the behaviour can be attributed to diffusion phenomenon occurring at the solution–electrode interface [30]. Similar behaviour is observed for Au and Pt electrodes for which the normalized Nyquist plots are presented in Fig. 4(b) and (c), respectively. The Nyquist plot of Ag electrode is presented in Fig. 4(d). Here, the impedance locus takes the form of two partially resolved semicircles and appears dominated by double layer effect. The difference in charge transfer kinetics of tea infusions is evident from the shift in valley points (along the real axis) of their corresponding impedance loci. This behaviour can be attributed to the presence of well separated time constants in the Bauerle's equivalent electrical circuit as shown in Fig. 5(b). Such type of parallel RC combination can rise from specific adsorption occurring at electrode surface, possibly associated with delayed reaction processes. The high frequency semicircle [the one on the left of Fig. 4(d)] can be ascribed to bulk electrolyte behaviour, while the low frequency semicircle [on the right in Fig. 4(d)] corresponds to electrode polarization [31]. Fig. 4(e) and (f) are normalized Nyquist plots of PANI and PPY electrodes, respectively. The impedance locus in both the figures takes form of one fully resolved semicircle to the left and a partially resolved semicircle to the right. This behaviour can be attributed to double layer effect involving adsorption [30,32]. The shift in valley points of the impedance loci of the tea infusions (along the real as well as imaginary axis) can be attributed to charge transfer kinetics and adsorption rate. The electrical equivalent circuit is shown in Fig. 5(c).

The species specific frequency dependent interactions in the tea infusions is a matter of investigation. However, recently Zielinska and Pierozynski [33] have studied the GC–quercetin (flavonoid) electrochemical interactions.

3.2. Data analysis (PCA)

PCA is a statistical technique for the reduction of input data dimension and is largely used for feature extraction. It captures the relevant information in a set of input data providing a lower dimension, but informative representation of the original data. It sequentially creates a set of principal components from the original data. The first principal component (PC1) maps the maximum variance and information of the input data followed by the other principal components (PC2, PC3 and so on) in descending order of the variance. Generally a good discrimination is mapped by the first two principal components, i.e. PC1 and PC2. Statistical software The Unscrambler 9.7 has been used for the PCA. Since the impedance response of the six electrodes was measured for a range of 1 Hz to 100 kHz having 60 steps, the total number of impedance variables amounts to 360 (6 × 60). In order to reduce the

Please cite this article in press as: A.P. Bhondekar, et al., A novel iTongue for Indian black tea discrimination, Sens. Actuators B: Chem. (2010), doi:10.1016/j.snb.2010.05.053

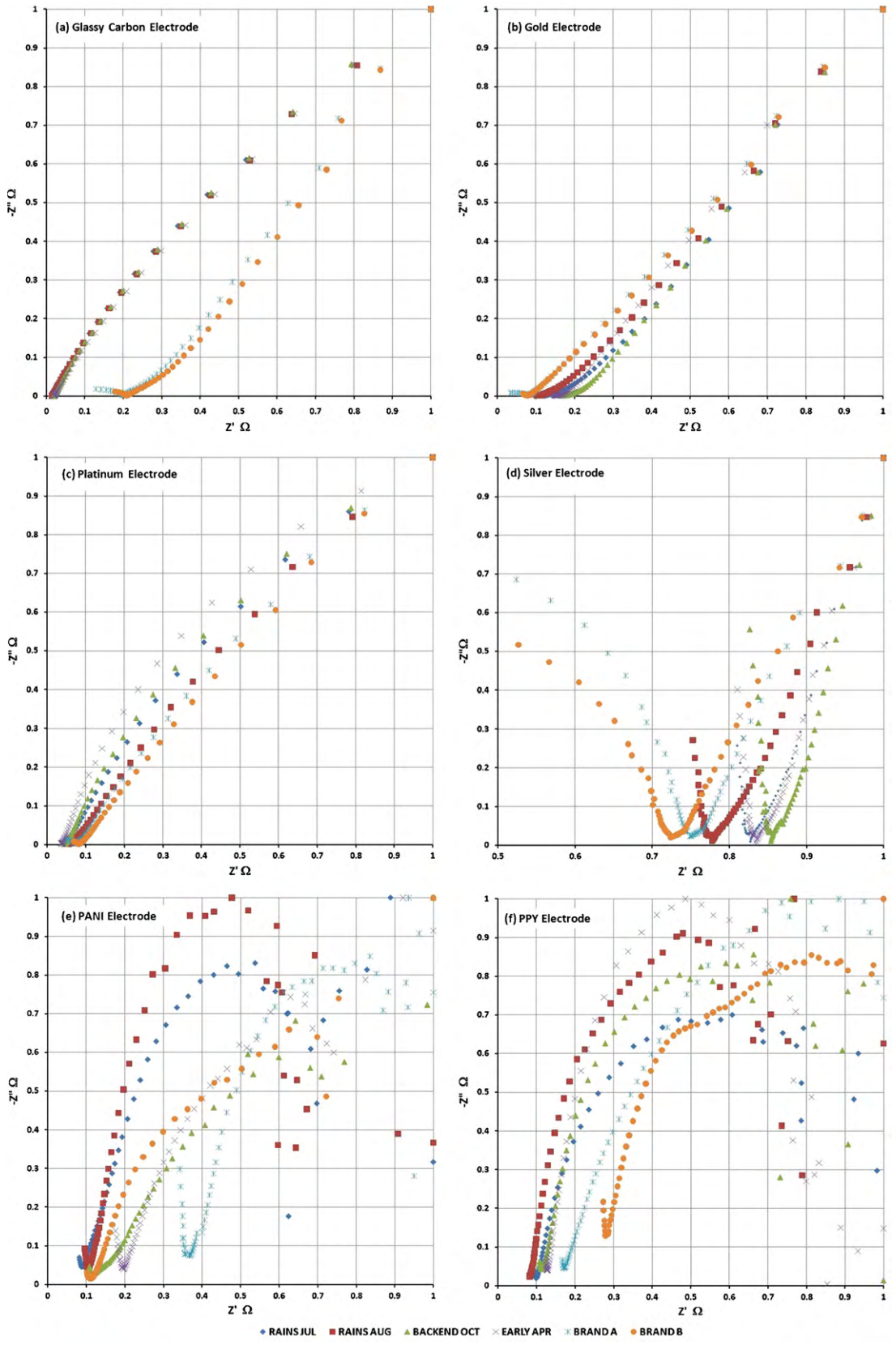

Fig. 4. Normalized Nyquist plots of (a) glassy carbon, (b) gold, (c) platinum, (d) silver, (e) PANI and (f) PPY electrodes.

Please cite this article in press as: A.P. Bhondekar, et al., A novel iTongue for Indian black tea discrimination, Sens. Actuators B: Chem. (2010), doi:10.1016/j.snb.2010.05.053

Table 1
Mean % chemical concentrations in tea samples as measured by HPLC and UV–VIS.

	DBA	GA	C	EGCG	ECG	CAF	TF	TR
Early April	0.378	1.317	0.472	10.527	2.387	5.297	0.194	7.990
Rains July	0.487	0.848	0.491	6.010	1.337	3.130	0.147	5.050
Rains August	0.382	0.594	0.468	10.157	1.473	2.827	0.108	5.033
Backend October	0.375	0.567	0.414	9.677	1.477	2.733	0.115	5.089
Brand A	0.451	0.760	0.436	1.593	0.684	4.277	0.622	12.647
Brand B	0.451	0.760	0.436	1.593	0.684	4.277	0.622	12.647

number of impedance variables, only five fiducial frequency points were selected based on previous work [18,34–36]. Therefore the impedance response of electrodes at 1, 100 Hz, 1, 10 and 100 kHz along with the percentage chemical concentrations (Table 1) as measured by HPLC and UV–vis spectroscopy was subjected to PCA. The data was arranged in a 18 × 38 matrix, standardized (i.e. mean centred and multiplied by inverse standard deviation) and subjected to PCA, wherein the rows represent samples (tea infusions) and the first 30 columns [6 electrodes × 5 frequencies (1, 100 Hz, 1, 10 and 100 kHz)] contain the modulus of impedance of an electrode at a specific frequency, the next eight columns contain percentage chemical concentrations namely TF, TR, CAF, GA, ECG, C, EGCG and DBA.

In Fig. 6 the score plot of PC1 vs. PC2 for the tea samples is plotted using 30 impedance and 8 chemical concentration variables. A score plot is simply any two pair of score vectors plotted against each other which correspond to plotting the objects (samples) in a pertinent PC sub-space. A wide separation is observed between the two broad classes of tea samples, i.e. CTC and Orthodox along the PC1 (horizontal) axis with an explained variance of 63%. Two clusters of CTC samples are observed on the left hand side of the plot; these samples are of two different commercial brands of CTC tea. Whereas, on the right hand side (1st and 4th quadrant), four distinct clusters of Orthodox tea samples are noticed. Amongst these four clusters, two are close to each other due to the fact that both have been harvested during the Rains Flush, i.e. July and August.

The cluster of samples appearing distinct on the top right corner (1st quadrant) have been harvested during Early Flush, i.e. April. The Early Flush spans for 3 months namely April, May and June. The samples of the cluster close to the origin have been harvested during October, i.e. the Backend Flush which spans for 2 months namely September and October. The PC2 (vertical) axis primarily maps the separation among these Orthodox tea clusters and accounts for 20% of total explained variance. Together, PC1 and PC2 account for 83% of total explained variance. However, it would be particularly convenient if the relationships between the samples and variables could be displayed. This could be achieved on a two-dimensional bi-plot (Figs. 7–9). In this way, the loadings for each variable can be presented as vectors, superimposed upon the scores plot for the same PCs. Longer the loading vector, more significant the corresponding variable is.

The angles between the vectors show the relationships between the variables themselves, and the vector direction is indicative of the correlations between variables and samples. Variables close to each other, situated out towards the periphery of the plots, covary strongly, proportionally to the degree distanced from the PC-origin. If the variables lie on the same side of the origin, they covary in a positive sense, i.e. they have positive correlation. If they lie on opposite sides of the origin, more or less along a straight line through the PC-origin, they are negatively correlated. The loading vectors which are perpendicular to each other through the origin are independent. Loadings close to the PC axis are significant only to that PC and variables with a large loading on both the PCs are significant to them [37].

Thus, in Fig. 7, only the vector loadings of chemical variables have been superimposed. In this, the variance along the PC1 axis can be attributed to the difference in chemical composition of CTC and Orthodox tea. This is majorly due to the difference in the manufacturing processes. However, some effect of geographical origins and species cannot be ruled out [3,38]. CTC tea is manufactured by passing the withered tea leaves in-between two rollers rotating in opposite directions, resulting in their complete maceration. Whereas, Orthodox tea is manufactured by rolling the withered tea leaves on specially designed Orthodox rollers which twist and crush the leaves, thereby rupturing their cells. Rupture of the cells leads to enzymatic action resulting in the initiation of a series of biochemical reactions with the uptake of atmospheric oxygen, forming TF and TR. The maceration is more in CTC processing, leading to more enzymatic actions. Therefore, TF and TR concentrations are high in CTC tea and are negatively correlated with Orthodox tea. This is also evident from the directions of loading vectors of chemical variables, particularly TF, TR, EGCG, C and ECG. The variance along the vertical axis is majorly due to the CAF and GA concentrations, and is evident from the fact that the early flush samples have higher CAF and GA concentrations. Due to the high values of CAF and GA in early flush samples their clusters appear distinct on the scores plot.

Further, the impedance loadings of six different electrodes at five different frequencies have also been superimposed in Fig. 8. The low frequency impedance loading vectors (i.e. 1 and 100 Hz) of GC electrode are close to the PC1 axis, EGCG and C vectors, suggesting positive correlation with catechins and negative correlation

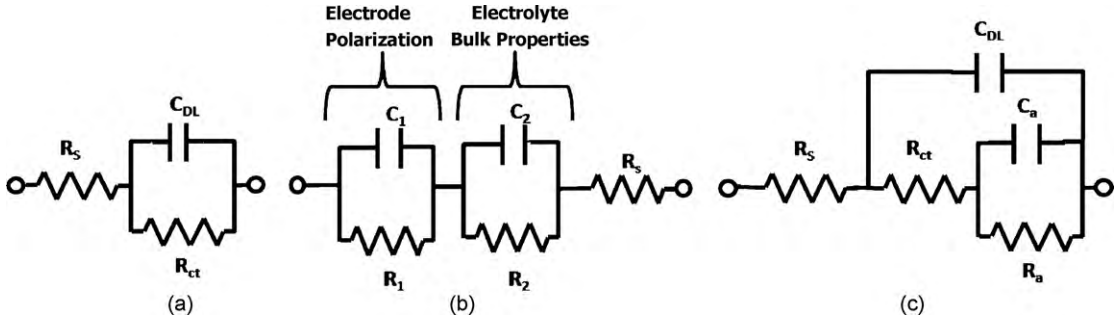

Fig. 5. (a) Randell's equivalent circuit, (b) Bauerle's equivalent circuit and (c) equivalent circuit corresponding to adsorption.

Please cite this article in press as: A.P. Bhondekar, et al., A novel iTongue for Indian black tea discrimination, Sens. Actuators B: Chem. (2010), doi:10.1016/j.snb.2010.05.053

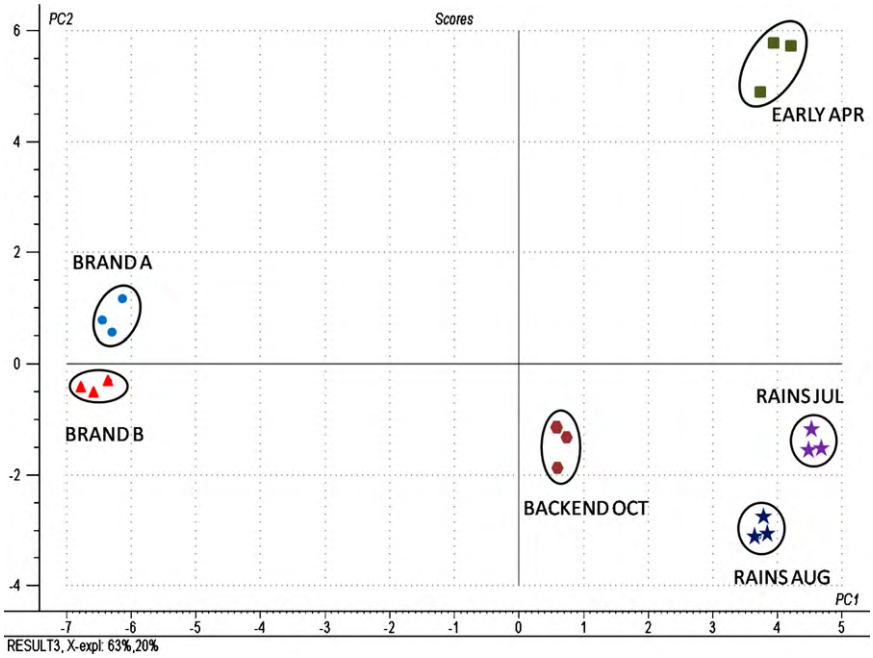

Fig. 6. PCA score plot of CTC and Orthodox teas.

with TF and TR. Interestingly, the impedance loading vectors above 100 Hz (i.e. 1, 10 and 100 kHz) of GC electrode show a positive correlation with TF and TR, and negative correlation with catechins. This suggests that the low and high frequency responses of GC electrode are equally important in mapping the variance along the PC1 axis, in other words they are one of the major loadings in differentiating the CTC and Orthodox tea.

The impedance loading vector of Pt electrode at 1 Hz is one of the major loadings responsible for variance along the PC2 axis, suggesting a negative correlation with CAF and GA. The impedance loading vectors of Pt electrode at 100 Hz, 1, 10 and 100 kHz are positively correlated with the TF and TR, and are equally important for the variance along the PC1 and PC2 axes.

The impedance loading vectors of Au electrode at 1, 100 Hz, 1 and 10 kHz, are positively correlated with the TF and TR, and are one of the significant loadings responsible for variance along PC1 axis and have a strong negative correlation with EGCG. However, the impedance loading vector of Au electrode at 100 kHz is less significant being closest to the origin.

The impedance loading vectors of Ag electrode at all the frequencies are cluttered together, which may be attributed to the symmetry between the modulus of polarization impedance and electrolyte bulk impedance about the valley points as shown in Fig. 4(d). However, the overall response of Ag electrode is observed to be positively correlated to TF and TR.

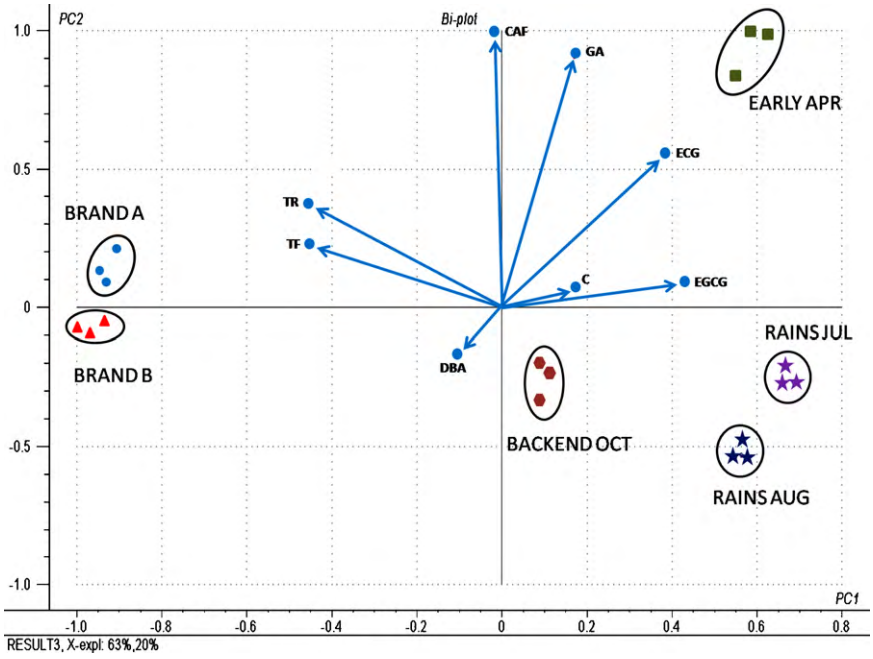

Fig. 7. PCA bi-plot with chemical concentration loadings.

Please cite this article in press as: A.P. Bhondekar, et al., A novel iTongue for Indian black tea discrimination, Sens. Actuators B: Chem. (2010), doi:10.1016/j.snb.2010.05.053

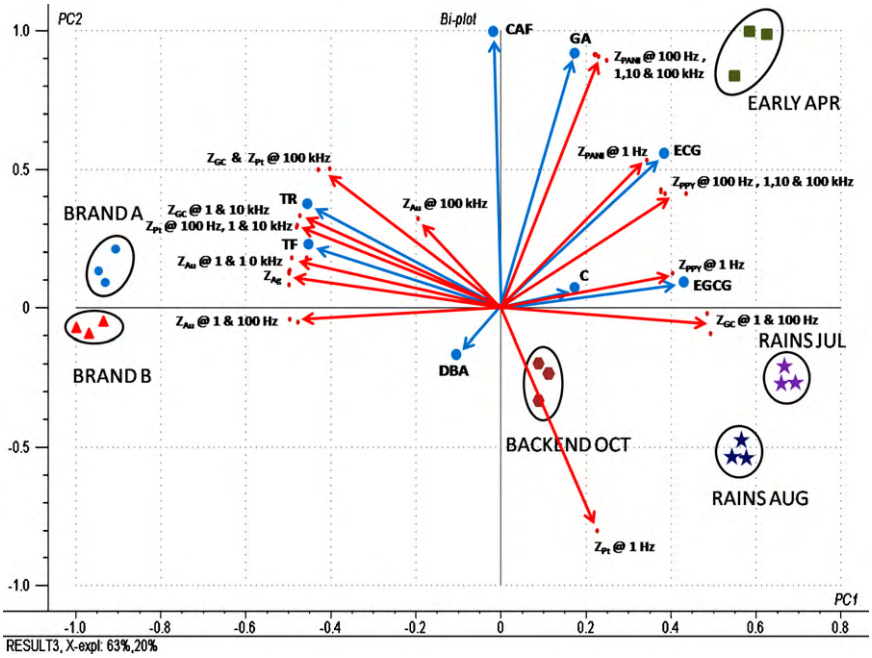

Fig. 8. PCA bi-plot with chemical and impedance loadings.

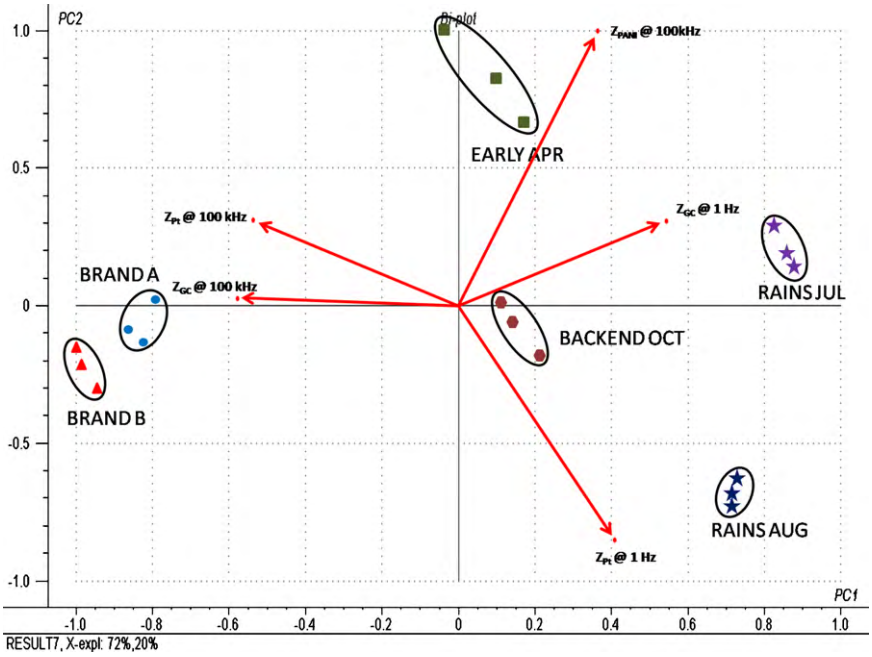

Fig. 9. PCA bi-plot with impedance loading vectors of Pt (1 Hz and 100 kHz), GC (1 Hz and 100 kHz) and PANI (100 kHz).

The impedance loading vector of PPY electrode at 1 Hz is very close to EGCG vector suggesting a strong positive correlation and its significance in variance along the PC1 axis. However, its impedance loading vectors above 1 Hz are placed together and are close to ECG vector, suggesting a positive correlation with ECG and a strong negative correlation with DBA. Also, these are equally significant for variance along both the axes. The impedance loading vector of PANI electrode at 1 Hz is very close to ECG vector suggesting a strong positive correlation and has equal significance in variance along both the axes. However, its impedance loading vectors above 1 Hz are placed together and are close to the GA vector, suggesting a strong positive correlation. These vectors are also significant for variance along the PC2 axis.

Based on the correlations of various impedance loading vectors, a few significant loading vectors were chosen to discriminate the samples. These impedance loading vectors are Pt (1 Hz and 100 kHz), GC (1 Hz and 100 kHz) and PANI (100 kHz). Fig. 9 shows the clustering of the samples using these few loadings. The total explained variance using these five loadings is 92% whereas the total explained variance using 38 loadings (Fig. 6) is 83%. However, the intra-class variance of the samples has increased.

4. Conclusion

In this work a novel iTongue was introduced for classification of Indian black tea. The results show that the frequency

Please cite this article in press as: A.P. Bhondekar, et al., A novel iTongue for Indian black tea discrimination, Sens. Actuators B: Chem. (2010), doi:10.1016/j.snb.2010.05.053

specific impedance response of a multi-electrode system can be used for discrimination of Indian black tea. This work can be extended for classification based on tea tasters score and other quality attributes apart from classification of other beverages. It may find applications in offline/handheld and online process control instrumentation. This work is of great importance to the tea manufacturing wherein this technique may be suitably modified and applied for monitoring and controlling the tea fermentation process. Further investigation is being pursued for selection and optimization of frequency/electrode specific impedance responses to minimize intra-class variance and maximize inter-class variance. Optimization techniques such as Genetic Algorithms, Simulated Annealing, Particle Swarm Optimization, Ant Colony Optimization, etc. might be helpful. This work is of great importance for dimensionality reduction in classification techniques such as Artificial Neural Network.

Acknowledgements

The authors are thankful to the scientists of Institute of Himalayan Bioresource Technology (Palampur, Himachal Pradesh, INDIA) and especially to Dr. Ashu Gulati for providing the tea samples and valuable discussions on tea chemistry. The authors are also thankful to Monika Singla, Amit Bhole, Sajeela Awasthi and Jagvir Singh for their valuable inputs and suggestions.

References

[1] P. Mahanta, Biochemical analysis as a measure of dynamic equilibrium in genomic setup during processing of tea, Journal of Biosciences 13 (1988) 343–350.
[2] K.I. Tomlins, A. Mashingaidze, Influence of withering, including leaf handling, on the manufacturing and quality of black teas—a review, Food Chemistry 60 (1997) 573–580.
[3] P.L Fernandez, F. Pablos, M.J. Martin, A.G. Gonzalez, Study of catechin and xanthine tea profiles as geographical tracers, Journal of Agricultural and Food Chemistry 50 (2002) 1833–1839.
[4] E.A.H. Roberts, R.F. Smith, The phenolic substances of manufactured tea. IX. The spectrophotometric evaluation of tea liquors, Journal of the Science of Food and Agriculture 14 (1963) 689–700.
[5] B.C. John, The effect of fermentation temperature on the quality parameters and price evaluation of Central African black teas, Journal of the Science of Food and Agriculture 31 (1980) 911–919.
[6] P.J. Hilton, R.T. Ellis, Estimation of the market value of Central African tea by theaflavin analysis, Journal of the Science of Food and Agriculture 23 (1972) 227–232.
[7] B.C. John, T.E. Rex, The effect of pH modification during fermentation on the quality parameters of central African black teas, Journal of the Science of Food and Agriculture 31 (1980) 924–934.
[8] O. Martin, P.O. Owuor, J.T. Sarah, Flavanol composition and caffeine content of green leaf as quality potential indicators of Kenyan black teas, Journal of the Science of Food and Agriculture 74 (1997) 209–215.
[9] P.W. Louwrance, K.M. Nicholas I, E.N. Hastings, A. Zeno, Analysis of caffeine and flavan-3-ol composition in the fresh leaf of *Camellia sinesis* for predicting the quality of the black tea produced in Central and Southern Africa, Journal of the Science of Food and Agriculture 80 (2000) 1823–1830.
[10] Y.R. Liang, Z.S. Liu, Y.R. Xu, Y.L. Hu, A study on chemical composition of two special green teas (*Camellia sinensis*), Journal of the Science of Food and Agriculture 53 (1990) 541–548.
[11] L. Yuerong, L. Jianliang, S. Shuling, Effect of gibberellins on chemical composition and quality of tea (*Camellia sinensis* L.), Journal of the Science of Food and Agriculture 72 (1996) 411–414.
[12] K.H. Ekborg-Ott, A. Taylor, D.W. Armstrong, Varietal differences in the total and enantiomeric composition of theanine in tea, Journal of Agricultural and Food Chemistry 45 (1997) 353–363.
[13] Y.-S. Lin, Y.-J. Tsai, J.-S. Tsay, J.-K. Lin, Factors affecting the levels of tea polyphenols and caffeine in tea leaves, Journal of Agricultural and Food Chemistry 51 (2003) 1864–1873.
[14] N. Bhattacharya, B. Tudu, A. Jana, D. Ghosh, R. Bandhopadhyaya, M. Bhuyan, Preemptive identification of optimum fermentation time for black tea using electronic nose, Sensors and Actuators B: Chemical 131 (2008) 110– 116.
[15] N. Bhattacharyya, S. Seth, B. Tudu, P. Tamuly, A. Jana, D. Ghosh, R. Bandyopadhyay, M. Bhuyan, Monitoring of black tea fermentation process using electronic nose, Journal of Food Engineering 80 (2007) 1146– 1156.
[16] B. Tudu, A. Jana, A. Metla, D. Ghosh, N. Bhattacharyya, R. Bandyopadhyay, Electronic nose for black tea quality evaluation by an incremental RBF network, Sensors and Actuators B: Chemical 138 (2009) 90–95.
[17] P. Ivarsson, S. Holmin, N.-E. Höjer, C. Krantz-Rülcker, F. Winquist, Discrimination of tea by means of a voltammetric electronic tongue and different applied waveforms, Sensors and Actuators B: Chemical 76 (2001) 449–454.
[18] S.-Y. Tian, S.-P. Deng, Z.-X. Chen, Multifrequency large amplitude pulse voltammetry: a novel electrochemical method for electronic tongue, Sensors and Actuators B: Chemical 123 (2007) 1049–1056.
[19] H. Horie, K. Kohata, Application of capillary electrophoresis to tea quality estimation, Journal of Chromatography A 802 (1998) 219–223.
[20] P. Ivarsson, Y. Kikkawa, F. Winquist, C. Krantz-Rülcker, N.-E. Höjer, K. Hayashi, K. Toko, I. Lundström, Comparison of a voltammetric electronic tongue and a lipid membrane taste sensor, Analytica Chimica Acta 449 (2001) 59–68.
[21] A. Riul, H.C. de Sousa, R.R. Malmegrim, D.S. dos Santos, A.C.P.L.F. Carvalho, F.J. Fonseca, O.N. Oliveira, L.H.C. Mattoso, Wine classification by taste sensors made from ultra-thin films and using neural networks, Sensors and Actuators B: Chemical 98 (2004) 77–82.
[22] K. Meral, A. Levent, S. Mehmet, Polypyrrole/polyaniline conductive films obtained electrochemically on polycarbonate-coated platinum electrodes, Polymer International 51 (2002) 1371–1377.
[23] A.A. Arrieta, C. Apetrei, M.L. Rodríguez-Méndez, J.A. de Saja, Voltammetric sensor array based on conducting polymer-modified electrodes for the discrimination of liquids, Electrochimica Acta 49 (2004) 4543–4551.
[24] V. Sharma, A. Gulati, S.D. Ravindranath, V. Kumar, A simple and convenient method for analysis of tea biochemicals by reverse phase HPLC, Journal of Food Composition and Analysis 18 (2005) 583–594.
[25] M.R. Ullah, A rapid procedure for estimating theaflavins and thearubigins of black tea, Two and a Bud 18 (1986) 583–594.
[26] A. Riul, A.M. Gallardo Soto, S.V. Mello, S. Bone, D.M. Taylor, L.H.C. Mattoso, An electronic tongue using polypyrrole and polyaniline, Synthetic Metals 132 (2003) 109–116.
[27] D.M. Taylor, A.G. Macdonald, AC admittance of the metal/insulator/electrolyte interface, Journal of Physics D: Applied Physics 20 (1987) 1277– 1283.
[28] P. Ferloni, M. Mastragostino, L. Meneghello, Impedance analysis of electronically conducting polymers, Electrochimica Acta 41 (1996) 27– 33.
[29] M. Irimia-Vladu, J.W. Fergus, Impedance spectroscopy of thin films of emeraldine base polyaniline and its implications for chemical sensing, Synthetic Metals 156 (2006) 1396–1400.
[30] D.D. Macdonald, Reflections on the history of electrochemical impedance spectroscopy, Electrochimica Acta 51 (2006) 1376–1388.
[31] J.R.M. Evgenij Barsoukov, Impedance Spectroscopy: Theory, Experiment, and Applications, 2nd ed., Wiley, 2005.
[32] F. Rashwan, The application of electrochemical impedance techniques in analyzing the AC response of some two-electron transfer dye systems, American Journal of Applied Sciences 2 (2005) 1595–1599.
[33] D. Zielinska, B. Pierozynski, Electrooxidation of quercetin at glassy carbon electrode studied by a.c. impedance spectroscopy, Journal of Electroanalytical Chemistry 625 (2009) 149–155.
[34] A. Riul, D.S. dos Santos, K. Wohnrath, R. Di Tommazo, A.C.P.L.F. Carvalho, F.J. Fonseca, O.N. Oliveira, D.M. Taylor, L.H.C. Mattoso, Artificial taste sensor: efficient combination of sensors made from Langmuirâ'Blodgett films of conducting polymers and a ruthenium complex and self-assembled films of an azobenzene-containing polymer, Langmuir 18 (2002) 239–245.
[35] R.E.G. Bruno Barreto Bergamo, José Alberto Giacometti, SLEad: electronic tongue data analysis system, Info Comp Journal of Computer Science 7 (2007) 69–78.
[36] M.R.K. Maria Jamal, S.A. Imam, Electronic tongue and their analytical application using artificial neural network approach: a review, MASAUM Journal of Reviews and Surveys 1 (2009) 130–137.
[37] K.H. Esbensen, Multivariate Data Analysis—In Practice, 5th ed., CAMO Process AS, 2004.
[38] G. Ashu, S.D. Ravindranath, Seasonal variations in quality of Kangra tea (*Camellia sinensis* (L.) O. Kuntze) in Himachal Pradesh, Journal of the Science of Food and Agriculture 71 (1996) 231–236.

Biographies

Amol P. Bhondekar is M.Tech in Electronics and currently working as a Scientist at CSIO, Chandigarh. His research interests are in computational instrumentation and performance enhancement of artificial organoleptic systems.

Mopsy Dhiman is MSc in Bio-Physics (Hons.). She is a research scholar at CSIO, Chandigarh. Her research interests are in food biotechnology and biosensors.

Anupma Sharma is MSc in chemistry. She is presently working in the area of chromatography and tea chemistry.

Arindam Bhakta is pursuing his M.Tech in Mechatronics and Robotics and currently doing his thesis at CSIO, Chandigarh. His research interests are in computational instrumentation and robotics.

Abhijit Ganguli is Doctorate in Bio-Technology and currently working as assistant professor at Thapar University. His research interests are in microbial ecology and food safety.

Please cite this article in press as: A.P. Bhondekar, et al., A novel iTongue for Indian black tea discrimination, Sens. Actuators B: Chem. (2010), doi:10.1016/j.snb.2010.05.053

S.S. Bari is a Doctorate in Chemistry. He is presently a professor at the Department of Chemistry, and also holds the post of the Registrar at Panjab University. His research interests are in organic synthesis.

Renu Vig is a Doctorate in computer sciences and currently is the Director of University Institute of Engineering and Technology, Panjab University, Chandigarh. Her research interests are in fuzzy systems and artificial intelligence.

Pawan Kapur is a Doctorate in Bio-medical engineering and is the Director of CSIO. His research interests are in intelligent instrumentation, process automation and soft computing.

Madan L. Singla is a Doctorate in Chemistry and is senior scientist at CSIO, Chandigarh. His research interests are in nano-particle synthesis, nano-biosensors development.

Please cite this article in press as: A.P. Bhondekar, et al., A novel iTongue for Indian black tea discrimination, Sens. Actuators B: Chem. (2010), doi:10.1016/j.snb.2010.05.053